ISSN 0957-798X

The Paton WELDING JOURNAL

SEPTEMBER
OCTOBER 2000

«WELDED STRUCTURES»

International Conference,
10–12 October, 2000, Kyiv, Ukraine

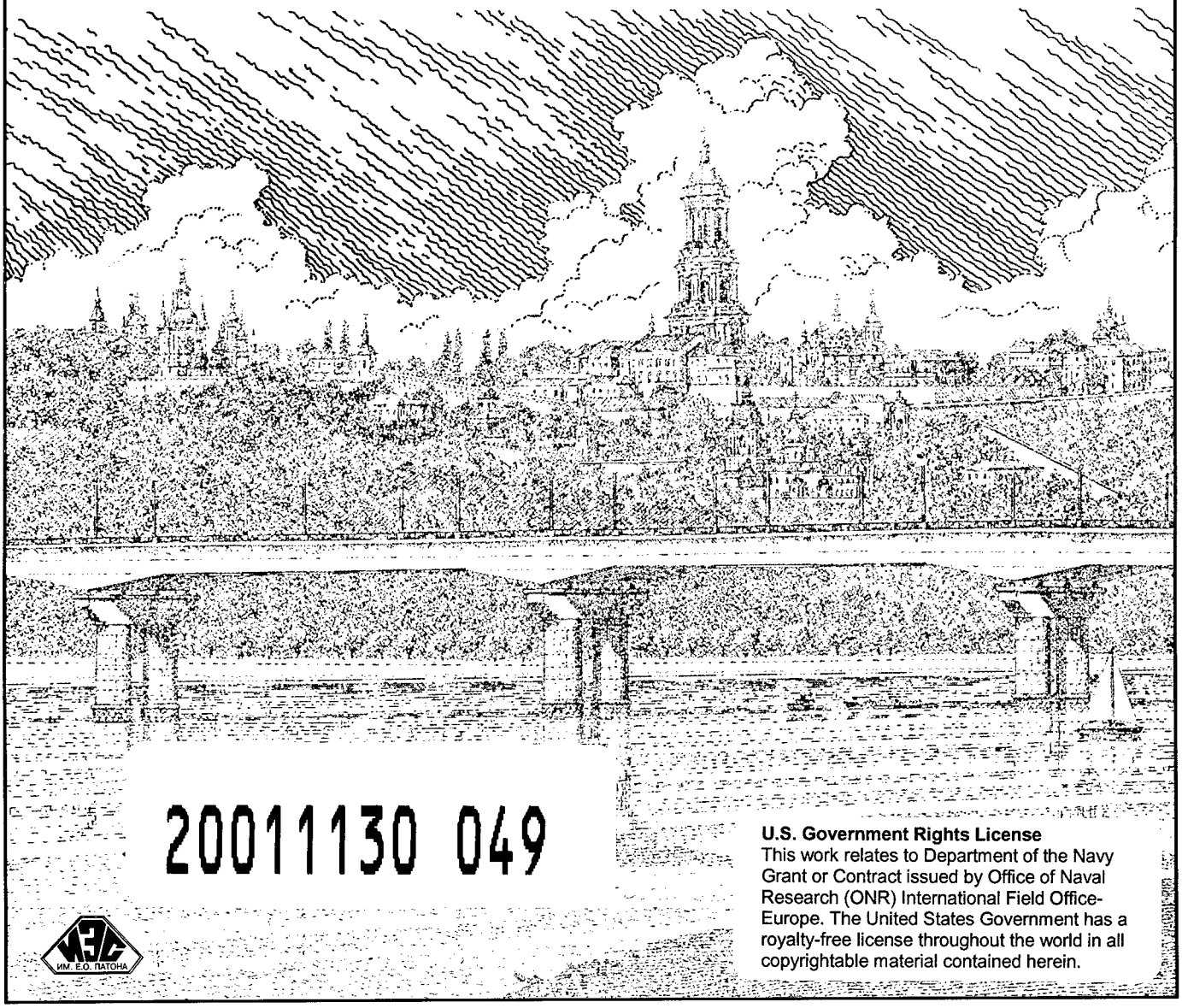

ИМ. Е.О. ПАТОНА

Our International Conference is dedicated to celebration of 130 years since the birth of Evgeny O.Paton, the prominent scientist and engineer, whose creative work led to a radical change in the attitude to welding as "the science of making barrels without rivets", and to realization that this technology could be a key factor ensuring technical progress in all industries which use metal as the basic structural material.

Anticipating a great future of welding, seventy years ago Evgeny Paton founded a specialized scientific institution in the system of the Academy of Sciences of Ukraine with a mission of carrying out integrated research at an interdisciplinary level, as well as development and implementation of welding technologies, equipment and materials. With time this institution has evolved into a world-largest scientific-and-technical complex bearing proudly the name of its founder.

A welded structure is a purport and purpose, alpha and omega of welding technologies. The acme of creation of academician E.O.Paton is the bridge across the Dnipro river in Kyiv, a grand, one-and-a-half-kilometer long all-welded structure, which has been in use for almost half a century and embodied the most daring dreams and results of the inspired labour of its founder and team of scientists, designers, engineers and workers guided by him.

"Welded Structures" — this is a laconic title of our Conference, which will include sessions and discussions of papers to be presented by experts from many countries all over the world, focusing on the most important science and technology results obtained lately in the field of welding fabrication. As to their subject matter, the papers will cover a very wide range of the problems, including:

- new types of welded structures, application of advanced structural materials, optimization of structures, automation of their computation and design methods;
- strength of welded joints and structures, theoretical and experimental studies of their stress-strain states, methods for regulation of welding stresses and strains;
- technical diagnostics and estimation of residual life of welded structures, methods for improving reliability and extending service life of welded structures;
- technologies and equipment for welding structures, automation of fabrication and improvement of manufacture precision and quality;
- certification of the welding industry products, training and attestation of specialists.

I am sure that the comprehensive exchange of the most recent information on the latest achievements in the field of welding fabrication will strengthen the international scientific-and-technical cooperation and progress, stimulate creative search, yield novel results and allow the new and beneficial scientific and business contacts to be established.

I wish all participants of the International Conference "Welded Structures" the intensive and fruitful work.

B. E. Paton

REPORT DOCUMENTATION PAGE

Form Approved OMB No. 0704-0188

1. AGENCY USE ONLY (Leave blank)	2. REPORT DATE	3. REPORT TYPE AND DATES COVERED
	2001	June 25-28, 2001 Conference Proceedings - Final Report

4. TITLE AND SUBTITLE
International Conference "Welded Structures" Held in Kyiv, Ukraine, 10-12 October, 2000. Papers of Plenary Sessions.

5. FUNDING NUMBERS

6. AUTHOR(S)
B.E. Paton, Editor

7. PERFORMING ORGANIZATION NAME(S) AND ADDRESS(ES)
8.
National Academy of Sciences of Ukraine
Paton Welding Institute (PWI)
Department 51
11, Bozhenko str.
03680, Kyiv, Ukraine

8. PERFORMING ORGANIZATION REPORT NUMBER

ISSN 0957-798x

9. SPONSORING/MONITORING AGENCY NAME(S) AND ADDRESS(ES)

Office of Naval Research,
European Office
PSC 802 Box 39
FPO AE 09499-0039

10. SPONSORING/MONITORING AGENCY REPORT NUMBER

11. SUPPLEMENTARY NOTES
Published the Paton Welding Journal, No. 9-10, Sep-Oct 2000. Published by PWI, Department 51, 11, Bozhenko str., 03680, Kyiv, Ukraine. This work relates to Department of the Navy Grant issued by the Office of Naval Research International Field Office. The United States has a royalty free license throughout the world in all copyrightable material contained herein. See http://www.nas.gov.ua/pwj

12a. DISTRIBUTION/AVAILABILITY STATEMENT

Approved for Public Release; Distribution Unlimited.

12b. DISTRIBUTION CODE

A

12. ABSTRACT (Maximum 200 words)
Conference papers discuss new types of welded structures, applications of advanced structural materials, optimization of structures, automated computation and design methods, theoretical and experimental studies of stress-strain states, methods for improving reliability and extending service life and more.

13. SUBJECT TERMS
ONRIFO, Foreign reports, Conference Proceedings, Welded structures

15. NUMBER OF PAGES

16. PRICE CODE

17. SECURITY CLASSIFICATION OF REPORT	18. SECURITY CLASSIFICATION OF THIS PAGE	19, SECURITY CLASSIFICATION OF ABSTRACT	20. LIMITATION OF ABSTRACT
UNCLASSIFIED	UNCLASSIFIED	UNCLASSIFIED	UL

The Paton WELDING JOURNAL

September – October 2000 # 9 – 10

English translation of the monthly «Avtomaticheskaya Svarka» journal published in Russian since 1948

«The Paton Welding Journal» monthly is published by the PWI and International Association «Welding»

Promotion group
V.N.Lipodaev, V.I.Lokteva
A.T.Zelnichenko (Exec. director)

Translators
S.A.Fomina, I.N.Kutianova, T.K.Vasilenko

Editor
N.A.Dmitrieva

Editorial and advertising offices are located at PWI, Dept. 51, 11, Bozhenko str., 03680, Kyiv, Ukraine.
Tel.: (38044) 227 67 57
Fax: (38044) 268 04 86
E-mail: paton@i.kiev.ua

Subscriptions: 12 issues $460, postage included

«The Paton Welding Journal» Website: http://www.nas.gov.ua/pwj

International Conference «Welded Structures»

Papers of Plenary Sessions

Sponsors of the Conference

Ministry of Education and Science of Ukraine, Presidium of the National Academy of Sciences of Ukraine, Office of Naval Research International Field Office (UK), USAF European Office of Aerospace Research and Development

AQ F02-02-0292

MODERN TRENDS TOWARD INCREASE IN STRENGTH AND LIFE OF WELDED STRUCTURES

B.E. PATON
The E.O. Paton Electric Welding Institute, NASU, Kyiv, Ukraine

ABSTRACT

The set of topical problems associated with fabrication of high-efficiency welded structures, increase in their strength and reliability and extension of their life is presented. The importance of improvement of scientific approaches to design of welded joints is shown. Consideration is given to issues related to evaluation of performance of main and process pipelines and effect of plastic deformation on fracture toughness of pipe steels. Results of investigations aimed at development of methods for improvement of fatigue resistance of welded joints and fatigue crack arresting are presented. The demand for a wider application of high-strength steels is noted. Capabilities of the acoustic emission and optical holography methods in terms of using them for diagnostics of welded structures are considered.

Key words: *welded structures, design, fabrication, strength, operation, safety factor for reliability, fatigue life.*

The part played by welded structures, which are extensively used in construction, power engineering, transport, ship building and other industries, is increasing in importance. They work on Earth, under water, in space, at normal, high and cryogenic temperatures, in aggressive environments an under conditions of heavy radiation. This leads to progressively increasing requirements to their quality, reliability and life, which generates the need for finding new design-technology solutions, improvement of the design methods, comprehensive investigation of strength of welded joints and optimization of technologies used for the fabrication of structures.

Historically, the majority of critical structures in use in many countries are approaching their critical age. Entire industries, such as power engineering and transport, turn out to be in a difficult situation. Of special concern is technical state of bridge structures. The state of main gas and oil pipelines is also disturbing. An increasing share of old pipelines which have exhausted their assigned life is one of the main causes of an increased number of accidents. The problems of residual life of power generating equipment at heat and nuclear power stations (NPS), petrochemical equipment and railway transport rolling stock become more and more pressing. The situation is complicated also by the fact that there are cases where the regulatory-technical documents required for ensuring reliable and safe operation of industrial and utility facilities get out of date or are unavailable at all.

Therefore, the problem of development of scientific-and-technical approaches to evaluation and extension of life of welded structures is extremely pressing. Such approaches should be based on a comprehensive analysis of all stages of the life cycle of structures, including design, fabrication and operation. To obtain reliable information on their technical state, it is necessary to make use of the up-to-date means of technical diagnostics.

Mass fraction of weld metal in welded structures rarely exceeds 1 %. However, the role it plays in ensuring safe operation of a structure is very important. As proved by statistics, 70 – 80 % of all failures registered in structures is related to welded joints. Therefore, the challenge now is to improve quality of design of welded joints on the basis of current requirements. The problem of design has many aspects. Some of them are considered below.

Aspect one is associated with the necessity for the in-depth investigation into behaviour of different zones of welded joints in advanced structural materials under actual service conditions, especially in their long-time operation under extraordinary conditions. This can be illustrated by an example of the well-known case of sensitization of austenitic steels of the 18-10 type (AISI 304), i.e. susceptibility of the weld zone of welded joints in such steels to formation and development of intercrystalline stress corrosion cracks. Similar failures were detected in pipes of power units of the BWR type at some of the US NPS approximately 30 years ago. About 25 % of joints in pipes had such defects. So, that required cardinal measures to be taken and high costs to be incurred. At NPS with the RBMK type units the main process pipings with a nominal diameter D_n 300 in the multiple forced circulation systems were made allowing for the US experience. Steel of the 08Kh18N9T grade is characterized by a higher resistance to the above failures. Nevertheless, the level of this resistance was obviously insufficient for actual service conditions, which was

evidenced by the results of inspection conducted at the Leningrad, Kursk, Smolensk and Chernobyl NPS. Steel 08Kh18N9T has a relatively high content of carbon, and its titanium stabilization is insufficient to suppress formation of chromium carbides in the weld metal zone of the welded joints. However, this circumstance was ignored at the stage of design.

It should be noted that the technology for butt welding of pipings used by the manufacturer provided a sufficiently high labour productivity. The level of residual transverse stresses on the internal surface of the pipes was close to yield strength of a material, which also contributed to formation and propagation of stress intercrystalline corrosion cracks in the HAZ. This can be avoided to a considerable degree by modifying the welding technology, i.e. by increasing the number of passes and decreasing the welding heat input.

Making welded joints in casings of the WWER type nuclear reactors is also a well-known problem. Service life of NPS with this type of reactors is determined primarily by the radiation life of the reactor casing, which in turn depends upon brittle fracture resistance of the casing material. In this case the basic and limiting parameter for the WWER type reactors is the critical brittle temperature of the weld metal located in front of the active section of the reactor and thus subjected to the maximum neutron radiation. Unfortunately, a high content of harmful impurities in the weld metal (such as phosphorus, copper, etc.) enhances embrittlement and leads to the need of using special expensive measures for its elimination.

The second aspect of the problem of design of welded joints, which requires special consideration, is the use of advanced approaches of fracture mechanics for evaluation of limiting states of welded joints under different loading conditions. The explanation is that the traditional way of eliminating fracture of welded structures, which is based primarily on limitation of sizes and quantity of defects, decrease in stress concentration, avoidance of crack-like defects and ensuring the required level of metal toughness by results of testing of standard samples, does not always guarantee high reliability of the structures. The concept which makes allowance for existence of crack-like defects in welded structures, not revealed by the NDT methods employed, and which is termed as the «the fitness for purpose» gains an increasing international acceptance, as it is based not only on the empirical method but also on the quantitative calculation methods. Despite significant theoretical advances in this area achieved also in Ukraine, practical application of modern methods of fracture mechanics for design of welded joints is restricted by the absence of the appropriate regulatory base. Meanwhile, as far back as in 1990 the IIW issued the

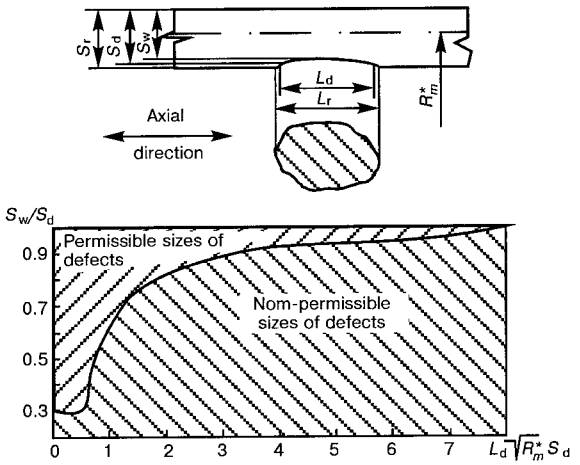

Figure 1. Diagram of maximum permissible sizes of the damaged zone versus erosion-corrosion wear of piping (S_r, S_d and S_w — rated, design and wear zone thickness of the pipe wall, respectively; L_r and L_d — length of the wear zone corresponding to the rated and design wall thickness, respectively; R_m^* — mean radius of the pipe in the wear zones)

document «The Fitness for Purpose of Welded Structures» (IIW/IIS-1157–90), giving a detailed description of the procedure for applying the above approaches for design of welded joints, which is well-suitable to be the basis for development of the corresponding national regulatory documents.

One of the causes of emergency situations at nuclear and heat power stations is erosion-corrosion wear of internal surfaces of pipes that transport working medium under conditions of high pressures, temperatures and velocities. The regulatory documents in force in the CIS countries, which specify rejection of sections of pipes with such a damage, fail to objectively estimate their serviceability. The only criterion of permissibility of their further operation as specified in these documents is wall thickness of piping within the zone of local wear. Investigations conducted at the E.O.Paton Electric Welding Institute resulted in development of a cardinally new approach to evaluation of strength of pipe sections with erosion-corrosion wear and prediction of their residual life. The approach is based on theoretical and experimental dependencies characterized by such relationships of limiting values of depth and length of the damaged zone which ensure the design strength of a piping to persist for its entire service life (Figure 1).

Estimation of operational state and residual life of main pipelines takes a special place. There is no need to note that main pipelines in their significance, length and environmental impact are of paramount importance among other engineering structures. Recent investigations show that despite the efficient, as they seem, methods of corrosion protection, main pipelines are prone to formation of numerous defects of both corrosion and mechanical origin. When the point is to reveal the most dangerous service defects, consideration is usually

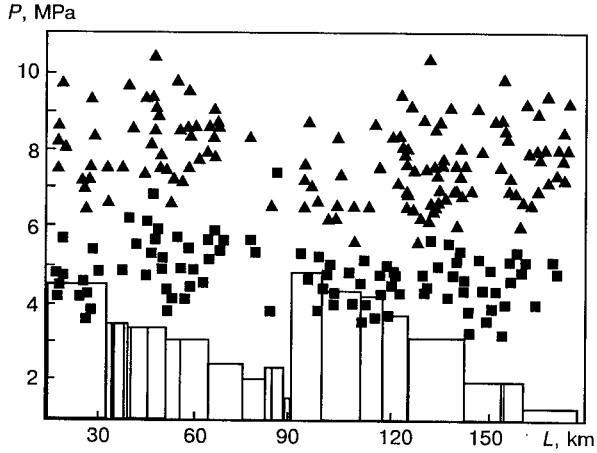

Figure 2. Operational, as well as critical (▲ and tolerable (■ pressures calculated with allowance for corrosion damage in two sections of oil pipelines neighbouring the compressor plants: P — pressure, L — length of the pipeline section

given to two approaches: pressure testing and in-pipe diagnostics.

It should be admitted that the use of the first approach does not ensure the desirable performance of a pipeline. This is associated with the fact that along with revealing the most dangerous zones, it contributes to development of the less dangerous defects the effect of which on strength can show up later with time. At the same time, in-pipe diagnostics enables volumetric corrosion damage to be detected and wall thickness of a pipe to be measured at a high degree of accuracy and reliability. However, detection of plane defects in welded joints involves certain difficulties. This makes it necessary to use a more precise method to estimate condition of a pipeline by the data of selective inspection of individual, most critical locations, i.e. hot zones. Diagnostics of these zones is a separate scientific-and-technical challenge. It involves a number of problems associated with substantiation of the method for determination of the pitting locations, as well as other external NDT methods. Importance of such problems is illustrated in Figure 2, which gives an idea of the quantity and degree of danger of corrosion defects in one of the oil pipelines.

Problems associated with diagnostics of main pipelines are not limited just to results of in-pipe NDT. There are some aspects which are related both to estimation of permissible defects and optimization of repair of main pipelines. It should be noted that existing standards and literature data have substantial differences regarding determination of sizes of permissible defects. In addition, conditions causing growth of technological defects with time require further investigations. In particular, apart from the corrosion impact, it is necessary to establish the exact conditions which cause propagation of fatigue cracks from conventional technological defects.

In evaluation of serviceability of pipelines it is necessary to take into account probable degradation of service properties of metal as a result of its ageing with time (e.g. general and local changes in fracture toughness associated with peculiarities of hydraulic and mechanical expansion of pipes, forming, etc.). Ignoring these peculiarities may lead to formation of inadmissible errors in estimation of crack resistance of pipelines.

As proved by practice, conditions of operation of pipelines differing from the normal ones can cause a fundamental change in mechanical properties of metal. In this case the important factors are the stressed-strained state and environment. It should be noted that under the effect of these factors embrittlement of metal occurs in local zones, and it should not spread to all metal of the pipeline.

Properties of metals are greatly affected by plastic deformation. It can occur in zones of design stress raisers (zones of welding of T-joints or branch pipes to pipelines), different types of defects (cracks, zones of lack of penetration or lack of fusion, dents, scratches, tool marks) and changes of pipe geometry. Results of investigation of the effect exerted by the level of plastic deformation of tension ε_1 and compression ε_2 on fracture toughness are shown in Table 1. Plastic deformation causes a substantial decrease in fracture toughness. Thus, at a value of plastic deformation equal to 20 %, resistance of steel of the 17G1S grade to initiation of tough fracture decreases almost to the level of the brittle state. The lowest values of fracture toughness were fixed on samples simulating typical mechanical damage of metal of the pipes, i.e. dents with shallow surface tears (cracks).

Since most of welded structures operate under conditions of repeated-alternating loading, their fatigue is a very important problem. It determines

Table 1. Fracture toughness of pipe metal (δ_i — at the stage of initiation of tough crack, δ_t at the stage of its transition to unstable condition) depending upon the level of plastic deformation of tension ε_1 and compression ε_2

Steel grade	δ_c, *mm*	ε_1, %				ε_2, %		
		0	*5*	*10*	*15*	*0*	*10*	*20*
17G1S	δ_i	0.13	0.11	0.09	0.08	0.20	0.11	0.04
	δ_t	0.38	0.23	0.11	0.09	0.25	0.21	0.08
10G2BT	δ_i	0.24	0.15	0.10	0.09	0.23	0.21	0.09
	δ_t	0.34	0.21	0.17	0.17	0.31	0.25	0.12

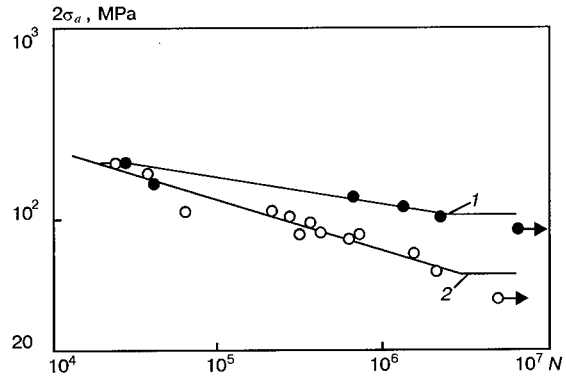

Figure 3. Fatigue curves plotted for tubular connections at asymmetrical loading cycle: *1* — connections treated by ultrasonic peening; *2* — untreated connections (σ_a — load amplitude)

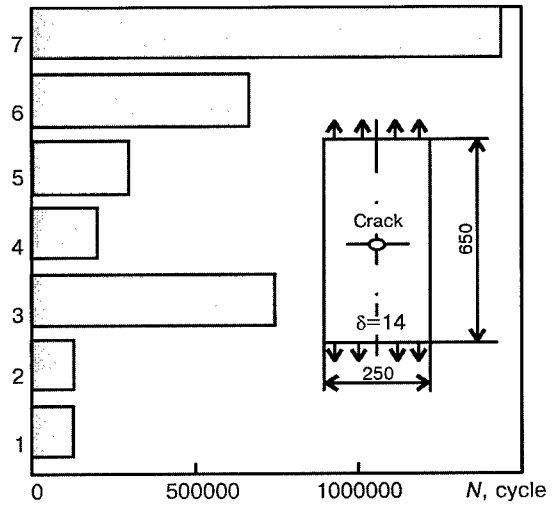

Figure 4. Cyclic fatigue life of samples at $R_\sigma = 0$ and $\sigma_{max} = 155$ MPa subjected to different methods of arresting of fatigue cracks: *1* — initial condition; *2* — drilling of holes at crack apex; *3* — same plus installing high-strength bolts in them; *4* — static overloading to 240 MPa; *5* — local explosion treatment; *6* — local heating; *7* — repair welding of cracks

the life of welded bridges, railway rolling stock, hoisting machines and apparatuses, off-shore stationary platforms, tower-type antenna structures, agricultural machines and many other structures. This makes it necessary to give a serious consideration to development of methods for increasing fatigue resistance of welded joints. An efficient means in this respect is the use of strengthening operational treatment of welds, especially ultrasonic peening. This method was elaborated from technologies of surface plastic deformation of welds. In addition, this treatment leads to relaxation of residual stresses in the weld and induces favourable tensile stresses in the surface layers of the metal.

Figure 3 illustrates the efficiency of ultrasonic peening of welded joints in terms of increasing fatigue resistance of tubular connections. It resulted in doubling the fatigue limit and increasing the fatigue life by an order of magnitude.

Premature formation of fatigue cracks was detected in welded joints of solid-wall superstructures of railway bridges, frames of cars and bodies of some types of railway locomotives and wagons, cranes and other structures at an early stage of their operation. Most often it is the case of those structural members in which formation of such cracks was not expected and which were not designed for the effect of alternating loads. Formation of cracks is attributable to ignoring the effect of local stresses and vibrations caused by a groundless choice of calculation diagrams used in design, as well as other factors. This gives rise to the requirement of development of efficient measures for deceleration and arresting of cracks in members of the existing structures.

Figure 4 shows results of comparison of the efficiency of different methods used to arrest fatigue cracks. The most common and practicable method for arresting fatigue cracks is welding on preliminarily made grooves in regions of structural members damaged by a crack. In the cases where repair of structural members by welding causes difficulties, the method recommended for crack arresting is drilling of holes at the crack tips and installing into them high-strength bolts, or it may be some other comparatively easy-to-use method based on inducing favourable residual compressive stresses ahead of the crack tip by applying static overloading, local explosion treatment or local heating.

The fundamental reserve for increasing reliability and fatigue life of welded structures and, at the same time, decreasing metal consumption lies in improvement of approaches to regulation of design loads and permissible stresses. Very topical are investigations of actual loads applied to welded connections. Basic causes of formation of extra stresses consist in differences between operational loading and actual service conditions of a structure and those used in design calculation diagrams. These differences are associated first of all with peculiarities of transfer of loads in structures, specific redistribution of forces in structural connections, mutual effects of members, use of tolerances for deviations of geometrical dimensions and vibration of individual structural components.

For example, in beam superstructures of railway bridges fatigue cracks are formed in webs of main beams near breaks of transverse stiffeners (Figure 5). Such a damage is caused by extra stresses formed as a result of interaction of members of the superstructure, as well as superposition of vibrations in sections of the beam webs. To increase fatigue life of such connections, it is recommended that stiffeners are welded to the beam chord and web with through penetration and the welds are subjected to ultrasonic peening. Results of testing the experimental ring at VNIIZhT (Russia) at an operating time equivalent to 20 years of service in

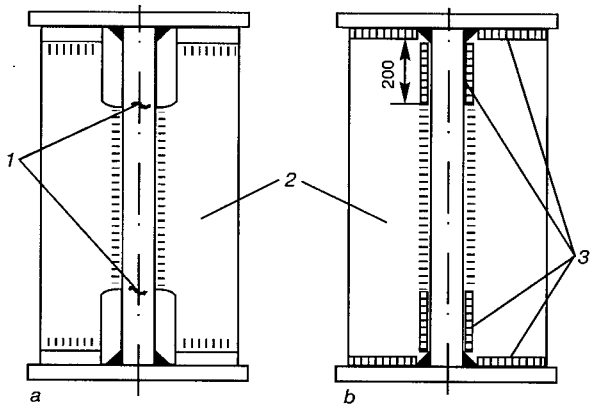

Figure 5. Attachment of stiffeners to increase fatigue life of beam superstructures of railway bridges: *a* — typical structure; *b* — special design ensuring fatigue resistance; *1* — fatigue cracks, *2* — transverse stiffeners; *3* — fillet weld with through penetration

a railway network proved efficiency of this approach to upgrading of a structure.

Another pressing problem is development of scientifically grounded approaches to extension of assigned life time of critical load-carrying structures and ensuring their safe operation. Extension of life of such structures leads to a fundamental saving, although it requires revision of specifications in force. Residual life can be increased through a more complete utilization of safety factors used in design and allowance for differences in calculated and actual operating time. The reserve for extension of service life can be found on the basis of analysis of actual service conditions of a structure, generalization of operational experience, upgrading, repair and reconditioning of the weakest connections, improvement of the design methods and use of new more substantiated criteria for evaluation of limiting states. Such an approach to providing the guaranteed residual life, aimed at extension of the total service life of structures, was tried out on superstructures of bridges, tanks for transportation of liquid carbon dioxide, travelling cranes and excavating machines. It is used currently for extension of life of load-carrying structures of traction rolling stock in railways of Ukraine.

Rational utilization of high-strength martensitic-bainitic steels with a yield strength of 600 – 1000 MPa plays an important role in solving the problems associated with decreasing specific metal consumption and increasing operational reliability and life of machines, mechanisms and engineering structures (Table 2). The desirable combination of their properties is achieved at a carbon content of 0.10 – 0.17 % by alloying them with manganese, chromium, nickel, molybdenum and other elements (total content of alloying elements — up to 4 – 6 %) and applying heat treatment.

Main difficulties in welding high-strength martensitic-bainitic steels are usually associated with the necessity to eliminate cold cracking of the weld and HAZ metal and formation of structures that decrease brittle fracture resistance of welded joints. Special filler metals were developed for the basic arc welding processes to produce welded joints in such steels with strength equal to that of base metal and prevent their cold cracking (Table 3). The absence of stress raisers and low level of residual stresses in high-strength steel welded joints contribute to a satisfactory resistance to initiation and propagation of fatigue and brittle fractures. Experience of manufacture and many-year successful operation of a number of critical welded structures made from high-strength steels (high-capacity mining and oil facilities, super-high tonnage truck beds, building and hoisting machinery, engineering structures, etc.) are a conclusive proof of reliability and efficiency of the developed welding materials and processes.

Increase in reliability and extension of life of welded structures depend upon improvement of the diagnostics methods. The method of acoustic emission (AE) shows high potential in this respect. Available are specialized procedures and devices based on the effect of AE formed in materials during their deformation and fracture.

Portable equipment provides a reliable monitoring of technical state of pressure vessels, main pipelines and other structures. Comparing AE sig-

Table 2. Chemical composition and strength properties of high-strength steels

Steel grade	*Content of elements, wt.%*						$\sigma_{0.2}$, *MPa*	σ_t, *MPa*	δ, %	*Impact toughness, J/cm²*		
										T_{test}, °C	*KCU*	*KCV*
	C	*Si*	*Mn*	*Cr*	*Ni*	*Mo*	*not less than*					
12GN2MFAYu	0.09 – 0.14	0.2 – 0.5	0.90 – 1.40	0.2 – 0.5	1.4 – 1.7	0.15 – 0.25	590	690	14	–70	29	–
12GN2MFAYu-U	0.09 – 0.14	0.2 – 0.5	0.90 – 1.40	0.2 – 0.5	1.4 – 1.7	0.15 – 0.25	590	690	14	–70	–	69
13KhGMRB	0.10 – 0.14	0.2 – 0.4	0.90 – 1.20	0.9 – 1.3	–	0.30 – 0.40	590	690	14	–70	29	–
14KhG2SAFD	0.12 – 0.18	0.4 – 0.7	1.40 – 1.90	0.5 – 0.8	–	–	590	690	14	–40	39	–
12GN3MFAYuDR	0.10 – 0.15	0.2 – 0.4	1.20 – 1.50	–	2.8 – 3.0	0.30 – 0.40	685	780	16	–40	–	78
14KhGN2MDAFB	0.12 – 0.17	0.2 – 0.4	1.10 – 1.40	0.9 – 1.3	1.7 – 2.2	0.20 – 0.30	685	780	16	–40	–	39
17Kh2MB	0.14 – 0.21	0.2 – 0.4	0.45 – 0.85	1.4 – 2.0	–	0.20 – 0.40	690	765	14	–50	39	–
12KhGN2MFBDAYu	0.09 – 0.15	0.2 – 0.5	0.60 – 1.10	0.6 – 0.9	1.4 – 1.7	0.40 – 0.60	785	885	15	–70	29	–
12KhGN3MAFD	0.10 – 0.15	0.2 – 0.5	1.00 – 1.30	0.6 – 1.0	2.5 – 3.0	0.40 – 0.60	980	1080	14	–70	59	–

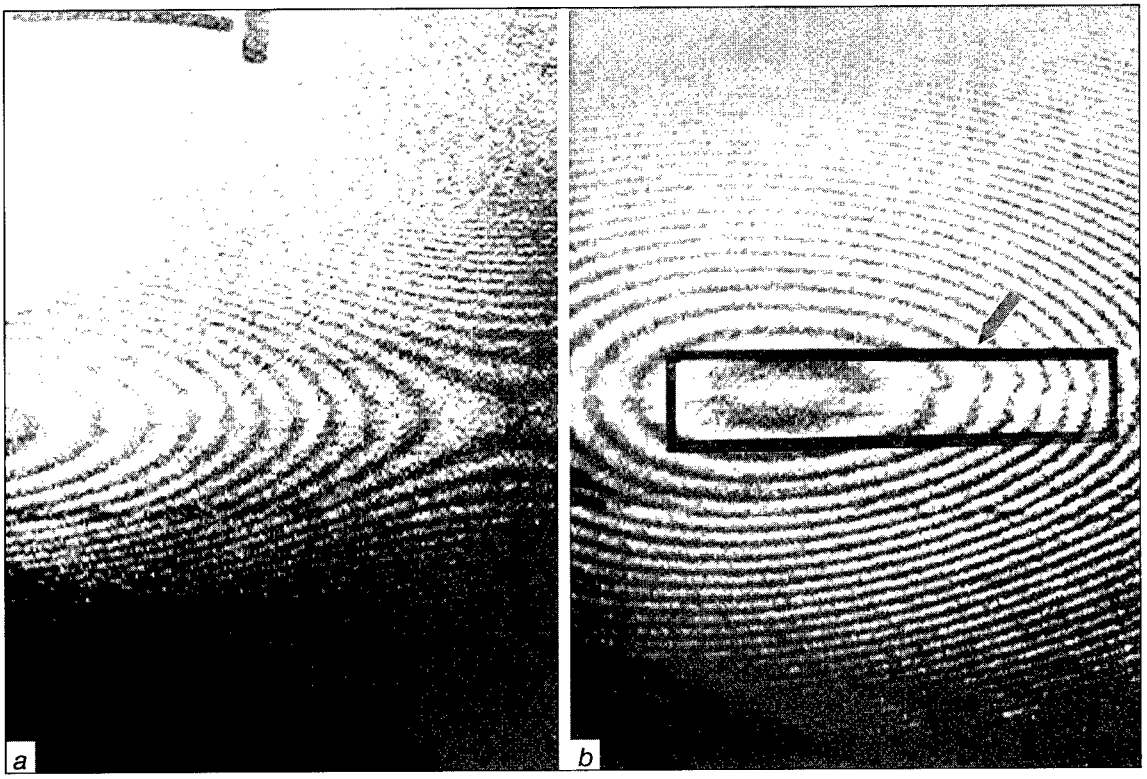

Figure 6. Interference fringes characterizing quality of a friction stir welded joint (material — aluminium alloy 6 mm thick): *a* — defect-free region; *b* — region containing defect

nals with actual defects proves the high level of confidence of the information obtained. The method is helpful in location of weakened zones at early stages of failure. The end task is to estimate the residual life. The AE method is used currently for diagnostics of various industrial objects.

The AE-based systems for continuous monitoring of performance of structures meeting increased requirements for safe operation can be created in the future. Such systems are capable of solving the problems of evaluation of a technical state not only of ground objects but also, for example, of space stations by transmitting the information to the Earth. The use of movable diagnostic laboratories equipped with the basic AE devices is also very efficient.

Methods of optical holography have high potential for diagnostics of welded structures. The PWI developed procedures based on holographic interferometry for quality control and evaluation of stressed-strained state of welded joints and structures. Available are compact holographic devices which are placed directly on an object investigated and require no special vibration isolation. Offered are the automated systems for computer processing of holographic interference patterns. Holography is especially helpful for revealing hard-to-control defects in structural members and assemblies of metallic and non-metallic materials. Figure 6 shows results of inspection of a welded joint produced by a new advanced welding method, i.e. friction stir welding. This method is now used to advantage for welding critical structures of aluminium alloys.

Table 3. Properties of welded joints in high-strength steels ($\sigma_{0.2}$ = 600 – 800 MPa)

Welding method	*Welding consumables*	*Brittle transition temperature, T, °C*	*Fracture toughness, δ_i, mm*	*Fatigue resistance, σ_{-1}, MPa*
Automatic submerged-arc welding	Welding wires Sv-08KhN2GMYu, Sv-10KhN2GSMFTYu, flux AN-17M	–60 – –70	0.22 – 0.23	70 – 90
Mechanized gas-shielded welding	Welding wires Sv-07KhN3GMFTYu, Sv-10KhN2GSMFTYu, shielding atmosphere Ar + CO_2	–70 – –80	0.20 – 0.24	50 – 70
Manual electric arc welding using covered electrodes	Electrodes of ANP-8, ANP-9, ANP-10 and ANP-11 grades (E70 and E85 types)	–40 – –60	0.18 – 0.20	50 – 80

However, the issue of ensuring reliable and efficient control of quality of welded joints is still open, as with this welding method the probability exists of formation of defects of the «sticking» type, which are difficult to detect by X-ray and ultrasonic methods. Holographic interferometry allows such defects to be revealed.

They are detected by changes in the interference fringes compared with those registered in a defect-free region of a welded joint.

In conclusion it is appropriate to note that finding solutions to important problems of increasing strength, reliability and life of welded structures requires active interaction of specialists from the world-leading welding centres.

NEW APPROACH TO THE TECHNOLOGY OF ULTRASONIC TESTING OF COARSE-GRAINED MATERIALS

N.P. ALYOSHIN and **S.P. GORNAYA**
N.E. Bauman MSTU, Moscow, Russia

ABSTRACT

The paper describes the solution of the problem of construction of an acousto-solidification model of coarse-grained materials, allowing for the features of structure formation, geometrical and energy factors of ultrasonic waves attenuation. Analytical dependencies were derived, a program was prepared and some results of calculation of the passage and scattering of all types of US waves are given. A conclusion is made on the need to take into account the actual geometry and energy of the US beam for a correct interpretation of the results of UT of the objects from materials of the above type.

Key words: *ultrasonic testing, weld, coarse-grained materials, crystalline structure.*

The main problems arising in performance of ultrasonic testing (UT) of coarse-grained materials (grain size is commensurate with the US wave length) are considerable attenuation and high level of structural noise caused by scattering of US waves in the polycrystalline material. At UT of coarse-grained materials with an oriented structure characteristic of austenitic welds, as well as the welds made by the process of electroslag welding, casting, etc., these problems are aggravated by deviation and distortion of the US beam, thus leading to incorrect interpretation of the control results, and very often also to the impossibility of its performance. The existing procedures of UT of coarse-grained materials provide a partial solution of this problem, as the majority of them do not take into account the actual crystalline structure of the materials. Therefore, a procedure suitable for control of certain types of coarse-grained materials, may be unfit for others.

N.E. Bauman MSTU performed the work allowing a new approach to the technology of UT of coarse-grained materials to be presented. Proceeding from analysis of the process of metal solidification, the weld or casting macrostructure is calculated and the solidification model is plotted. Then, the US wave passage through a non-uniform anisotropic polycrystalline medium is studied and an acoustic model is constructed which permits the main factors of damping to be taken into account, namely: attenuation, refraction on the fusion boundary and its transparency; deviation of the beam propagation from the wave normal and distortion of the sound beam.

The thus constructed acousto-solidification model enables determination by calculation of the optimal parameters and interpretation of the results of UT of coarse-grained materials with different polycrystalline structure.

Material structure. Three kinds of structures can be distinguished, namely coarse-grained with equiaxial crystals (HAZ of welded joints, central part of ingots, forgings), coarse-crystalline with columnar crystals (austenitic welds, welds made by electroslag welding, ingots) and fine-crystalline (base metal of the welded joints, outer crust of ingots).

Control of materials or zones of welded joints with a coarse-crystalline or coarse-grained structure where energy losses are found due to US wave scattering on the grain boundaries, deviation and distortion of US beams, is of special interest.

Description of the solidification model. An electroslag welded joint can serve as a typical ex-

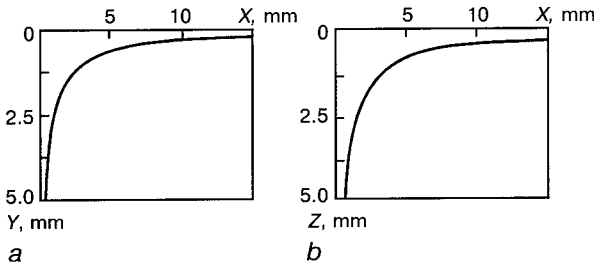

Figure 1. Projections of a crystallite axis on the coordinate planes $X0Y$ (a), $X0Z$ (b) (l = 30 mm, p = 10 mm, h = 15 mm, χ = 5)

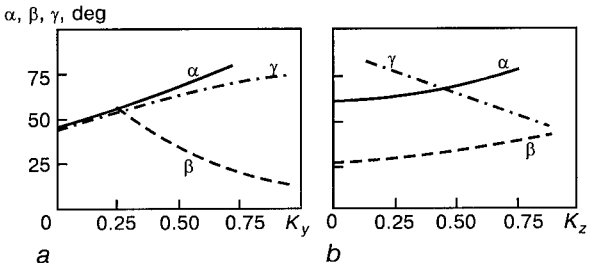

Figure 2. Change of the angles of inclination of the crystallite axis to the coordinate axes depending on $K_y = Y/P$ (a) and $K_z = Z/H$ (b) at Z/H = 0.5, X/L = 0.5, Y/P = 0.5

ample of production of the coarse-grained structure. When the welding model is constructed, the solidification front, shape of the crystallite axes and change of the crystallite width with its growth, are calculated.

Solidification front. The broadest class of weld pools found in practice, are described by the equation of an ellipsoid with semiaxes l, p and h

$$\frac{x^2}{l^2} + \frac{y^2}{p^2} + \frac{z^2}{h^2} = 1,$$

where x, y, z are the current coordinates; l, p, and h are the length, half-width and depth of the solidification front, respectively. Introducing a fictitious ellipsoid [1], we obtain the design section of the weld pool of an ellipsoidal shape.

Shape of the crystallite axes. Calculation of the spatial position of the crystallites axes is theoretically possible. Study [1] gives the basic solutions for calculation of the projections of the crystallite axes on the coordinate planes. For weld pools of an ellipsoidal shape, using expressions

$$x = \frac{p^2}{L}\int \sqrt{\frac{1}{y}\left(1 - \frac{y^2}{p^2} - \frac{\chi^2}{H^2}\, y^{2(P/H)^2}\right)}\, dy,$$

$$x = \frac{H^2}{L}\int \sqrt{\frac{1}{2}\left(1 - \frac{z^2}{H^2} - \frac{1}{P^2}\left(\frac{z}{\chi}\right)^{2(P/H)^2}\right)}\, dz,$$

where H, P, L are the semiaxes of the fictitious ellipsoid; $\chi = zy^{-(P/H)^2}$, we obtain the projections of the crystallite axes on planes $X0Y$ and $X0Z$ (Figure 1), as well as angles α, β and γ, made by the tangent to the crystallite axis with the coordinate axes (Figure 2).

Change of the crystallite width. Reduction of the crystallite cross-section with their growth lends itself to analytical assessment and depends on the solidification schematic. Calculation dependencies are given in [1].

Description of the acoustic model. In order to construct the acoustic model let us conditionally represent the coarse-grained structure in the form of a totality of grains disoriented relative to each other (Figure 3). In this case, we assume that the grains are cubes with side a, and crystallites are regular hexahedral prisms of length b and transverse dimension a, which are in close contact with each other. The acoustic properties of such media are characterised by moduli of elasticity produced by averaging the moduli of elasticity of the single-crystal by its possible orientations. Let us consider the passage of plane US waves through such inhomogeneous media.

Attenuation. In the general case, the coefficient of attenuation is made up by the coefficients of absorption and scattering. In the metal with a polycrystalline structure, the determinant factor is scattering, therefore let us only take into account the scattering of ultrasound in calculation of attenuation.

Let us consider an individual grain (scatterer) which is located in a system of disoriented grains (environment). Let us represent the moduli of elasticity of such an inhomogeneous medium in the form of

$$C_{ijkl} = C^0_{ijkl} + \delta C_{ijkl} \quad \text{at} \quad r \in V,$$

$$C_{ijkl} = C^0_{ijkl} + \delta C_{ijkl} \quad \text{at} \quad r \notin V,$$

where $\delta C_{ijkl} = C_{ijkl} - C^0_{ijkl}$ is the difference in moduli of elasticity in both media; V is the grain volume; r is the radius-vector of the point of observation.

It is known that the crystals of the ferritic-pearlitic and austenitic steels are characterised by

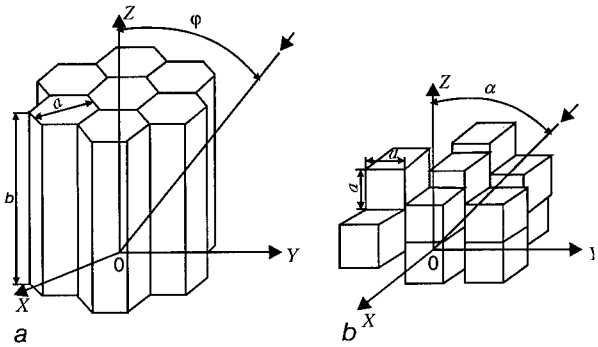

Figure 3. Models for design of the coarse-crystalline (a) and coarse-grained (b) structures

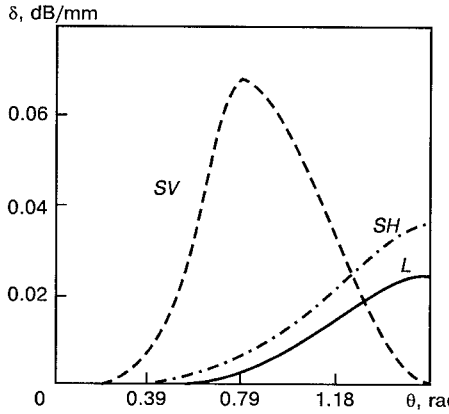

Figure 4. Change of the coefficient of scattering of US waves, depending on the angle of incidence on the crystallites (f = = 2.5 MHz, a = 100 μm, b = 4 mm); *SV*, *SH* — wave types

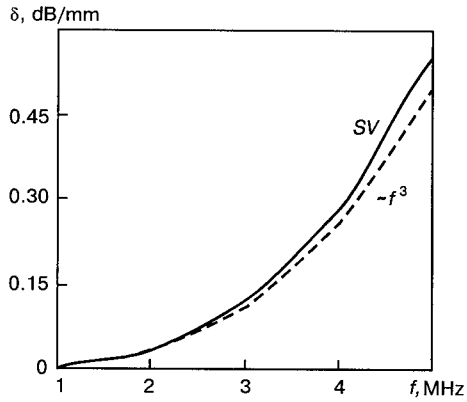

Figure 5. Dependence of the coefficient of scattering of an *SV* type transverse wave on frequency (a = 100 μm, b = 4 mm, θ = = 45°)

moduli of elasticity of the cubic system. The moduli of elasticity of the environment are derived by averaging the moduli of elasticity of the single-crystal by the possible crystallographic orientations

for the crystallites system (Figure 3, *a*)

$$C^0_{ijkl} = 1/(2\pi) \int_0^{2\pi} C_{ijkl}(\varphi)\, d\varphi,$$

for the grain system (Figure 3, *b*)

$$C^0_{ijkl} = 1/(2\pi^2) \int_0^{\pi} \int_0^{2\pi} C_{ijkl}(\alpha, \gamma)\, d\alpha d\gamma,$$

where φ is the angle of rotation of the crystallite relative to its axis; α and γ are the angles of the grain rotation.

In order to determine the scattered fields, let us use the volume integral equation of Lipman-Schwinger type. Let us calculate the scattered fields U^s_j in Born's approximation (first approximation of Lipman-Schwinger equation) using Green's function $G_{ij}(r', r'')$:

$$U^s_j(r'', U^0_i) = \int_V G_{ij}(r' - r'')\, f_i(r'', U^0_i)\, dr'',$$

where $f_i(r'', U^0_i)$ is the function dependent on the incident wave amplitude and describing the influence of inhomogeneities; r'' is the radius-vector of the source; s index denotes the scattered field.

Solving the problem [2] yielded analytical expressions for the coefficients of scattering for the coarse-crystalline structure which is the transversely-isotropic medium at the frequencies used in UT, as well as for the coarse-grained strucrure which is the isotropic medium. The coefficients of scattering in the HAZ have an especially simple form characteristic of Raleigh scattering ($\delta \sim a^3 f^4$). The weld metal unlike the metal of the HAZ, is not an equiaxial medium. The scatterer length exceeds the US wave length. Scattering in this region does not obey the laws characteristic of the equiaxial polycrystalline media. Calculation has shown that in the range of frequencies for which the ratio of wave length to the transverse size of the crystallite exceeds π, the coefficient of scattering in the weld metal approximately follows the $\delta \sim a^2 f^3$ law (Figure 4) and depends on the direction of the wave incidence and its polarisation (Figure 5). For all types of the waves, the coefficients of scattering become zero in the cases, when the direction of wave propagation or (and) its polarisation are parallel to the crystallite longer axis. For the longitudinal and the horizontally-polarised transverse wave, the coefficients of scattering are maximal, if the wave propagates normal to the crystallite long axis. The maximum of scattering of vertically-polarised transverse wave was registered at the angle of incidence on the crystallites θ = 45°.

Transparency of the fusion boundary. In UT of welded joints the problem of passage through the fusion boundary is of considerable importance as the establishment of the directions and determination of the intensities of the waves transformed at the boundary are necessary for a correct interpretation of the testing results. Considering that the boundary media differ not only in the wave velocities, but also in their crystalline structure, we have calculated the coefficients of transparency of the boundary of an isotropic (HAZ) and transversely-isotropic (weld metal) media (Figure 6). For the coefficient of transparency $D_H(\beta_{inc})$ of *SH* type wave, the following analytical expression was derived

$$D_H(\beta_{inc}) = 2v_0 \cos\beta_{inc}/[1 + v(\alpha_{ref}) \cos\alpha],$$

where v_0 is the transverse wave velocity in the HAZ; $v(\alpha_{ref})$ is the velocity of the horizontally-polarised wave in the weld metal; β_{inc} is the angle

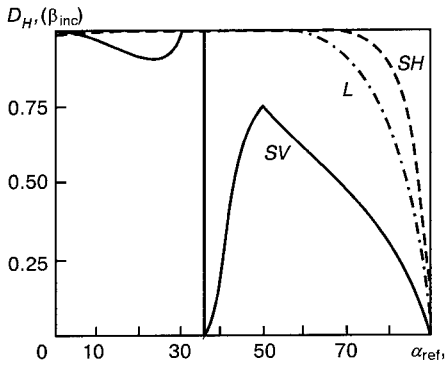

Figure 6. Coefficients of transparency by the energy of an austenitic weld fusion boundary

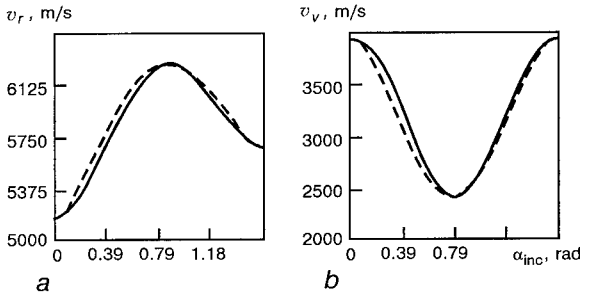

Figure 7. Dependencies of the velocities of the longitudinal *SH* (*a*) and transverse *SV* (*b*) waves on the angle of incidence on the crystallites (hexagonal system): solid, dashed curve — values calculated by equations (1), (2), respectively

of wave incidence on the boundary; α_{ref} is the angle of refraction into the weld. The coefficients of transparency of the fusion boundary were numerically calculated at the passage of longitudinal and vertically-polarised waves.

When the coefficients of transparency of the fusion boundary were calculated, the dependencies of the change of the elastic wave velocities on the direction of their propagation were investigated. The weld material presented in the form of a totality of disoriented crystallites, is characterised by the elastic constants of the hexagonal system. Solving the Christoffel's formula for the waves propagating in the plane which passes through the sixth order axis of crystals of the hexagonal system, yields the values of velocities of three waves [3]. However, the equations for calculation of the velocities of the quasi-longitudinal and quasi-transverse waves for engineering applications, are rather complex. Use of a coordinate system referenced to the wave vector, permitted derivation of simple enough expressions for determination of the velocities of the longitudinal v_r (α_{inc}) and vertically-polarised transverse v_v (α_{inc}) waves in the transversely-isotropic medium

$$v_r(\alpha_{inc}) = \sqrt{C_{11} - 0.25A[\sin^4\alpha + 2\sin^2(2\alpha)]} - \frac{1}{\sqrt{\rho}}, \quad (1)$$

$$v_v(\alpha_{inc}) = \sqrt{C_{44} - 0.44A\sin^2(2\alpha)}\,\frac{1}{\sqrt{\rho}}, \quad (2)$$

where α_{inc} is the angle of incidence on the crystallites; C_{11}, C_{12}, C_{44} are the elastic constants of the cubic system crystal; $A = C_{11} + C_{12} - 2C_{44}$; ρ is the density.

The velocities of the waves calculated by equations (1), (2) are given in Figure 7. Graphs (solid curves) calculated when solving Christoffel's formula are given for comparison.

Deviation of the direction of the beam propagation from the wave normal and beam distortion. In anisotropic materials the direction of energy propagation does not coincide with the direction of the US wave. This leads to deviation of the US beam from the wave normal. The maximal amplitudes of particle displacement in the wave which are the ones detected by the transducers, are observed in the direction of the Umov vector.

Proceeding from analysis of the directions of the wave energy transfer [3], we derived the relationships which correlate the beam deviation with the elastic constants of the single-crystal and the direction of the wave vector:

$$\Delta_r(\theta) = \left\{\frac{\text{arctg}\,[A\sin 2\theta(\cos^2\theta - 0.75\sin^2\theta)]}{2C_{11} - A(\cos^4\theta + 2\sin^2\theta)/2}\right\},$$

$$\Delta_v(\theta) = \left\{\frac{\text{arctg}\,[A\sin 2\theta(\sin^2\theta - 0.75\cos^2\theta)]}{(2C_{44} + 7A\sin^2 2\theta)/8}\right\},$$

$$\Delta_h(\theta) = \text{arctg}\left\{A\sin 2\theta/(8C_{44} + 2A\sin^2\theta)\right\},$$

where θ is the angle between the wave vector and the crystallite axis; *r*, *v*, and *h* indices pertain to the longitudinal, vertically- and horizontally-polarised transverse waves, respectively.

Calculation of angles Δ_c is given in Figure 8. We see that the greatest deviation of the wave vector from the direction of energy transfer (up to 33°) is found in the vertically-polarised transverse wave at the angles of incidence on the crystallites of 30 and 60°. The maximal deviation of the lon-

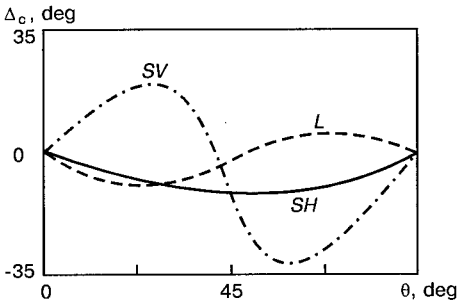

Figure 8. Deviation Δ_c of the acoustic axis from the wave normal in the metal of an austenitic weld, depending on the direction of incidence on the crystallite

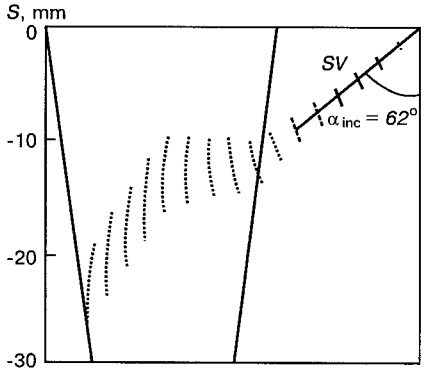

Figure 9. Model of deviation and distortion of a US beam of the transverse wave in the weld; S is the metal thickness

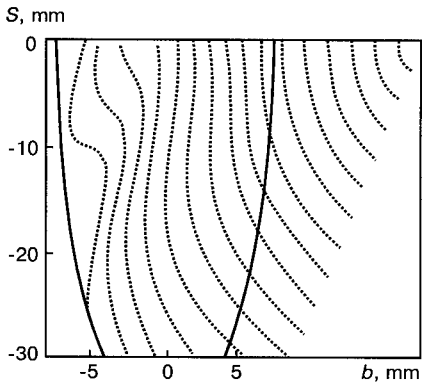

Figure 10. Model of distortion of the front of a transverse US wave in an electrosalg welded joint

gitudinal wave is 10°, that of the horizontally-polarised wave 12°.

Beam deviation from the wave normal leads to the sound beam distortion. As a result, focusing and defocusing of the sound beam can be observed when passing through the weld. This is the most pronounced in passage of a transverse wave with vertical polarisation (Figure 9).

Noise generation. Scattering of US waves in an austenitic welded joint, in addition to attenuation of the intensity of the valid signal, leads to generation of structural noise, which hinders the UT performance. At the ratio of valid signal and noise intensities below 1.5 to 2.0, defect detection is extremely difficult. This results in lowering of the control validity. From the equations of scattered fields, we obtain the dependence of the intensity of structural noise I_n on polar angle γ between the direction of US wave emission and the direction of observation

$$I_n(\gamma)/I_n^{max} = \cos^2\gamma. \quad (3)$$

The dependence was derived for the problems of UT of welds when the emitting and the receiving transducers are located from the same side of the item in one point (combined schematic) or are in points close to each other (transmitter-receiver schematic). The angles of introduction of the emitter and the receiver are the same. The expression is valid for any type of plane elastic waves. Analysis of equation (3) shows that the intensity of structural noise is maximal at $\gamma = 0$ (back scattering) and at $\gamma = 180°$. At the angles of observation of 70 to 110° with the emission direction, the minimum of structural noise intensity was registered ($I_n(\gamma)/I_n^{max}$ value does not exceed 0.1).

The above dependencies were used in preparation of a program of computation of an acousto-solidification model. The grain size, inclination of the fusion boundary, size and inclination of the crystallites are determined with the US beam passage, and the coefficients of transparency of the fusion boundary, coefficients of scattering, deviation and distortion of the US beam are calculated. The developed model can be used for calculation of the change in the front of US waves in their passage through coarse-grained structures (Figure 10), this permitting selection of the optimal UT parameters and correct interpretation of the results.

REFERENCES

1. Prokhorov, N.N. (1968) *Physical processes in metals in welding*. Moscow: Metallurgia.
2. Gornaja, S.P., Aljoschin, N.P. (1997) Attenuation of ultrasonic waves in austenitic steel welds. *Nondestr. Test. Eval.*, **13**, 149 – 168.
3. Djelesan, E., Ruaje, D. (1982) *Elastic waves in solids. Application for signal processing*. Moscow: Nauka.

ASSESSMENT OF THE STRENGTH AND RESIDUAL LIFE OF PIPELINES WITH EROSION-CORROSION DAMAGE

E.F. GARF and **M.A. NETREBSKY**
The E.O. Paton Electric Welding Institute, NASU, Kyiv, Ukraine

ABSTRACT

The urgency of the considered problem for nuclear and thermal power generation industry, is noted. It is shown that the codes now in force permit the pipeline wall thinning by 15 % of the design thickness, which, in a number of cases leads to a significant lowering of the structure reliability and can cause fracture. Introduction of a restriction not only on the wall thinning values, but also on the main dimensions of the thinning zone, is substantiated.

Key words: *nuclear and thermal power stations, pipelines, erosion-corrosion damage, strength, residual life, residual wall thickness, length of thinning zone, thinning depth.*

One of the main causes for premature wear under the conditions of high values of pressure, temperature and speed, is the joint action of mechanical (erosion) and electrochemical (corrosion) processes [1, 2]. Especially urgent is the problem of erosion-corrosion wear (ECW) of pipelines of the thermal and nuclear power stations.

As a rule, damage due to ECW is of a local nature. It reduces the pipeline reliability, and this leads to the need to perform expensive repair-restoration work in individual sections. The currently existent in CIS codes and provisions which specify the conditions for regarding the pipeline sections affected by ECW as unfit for service, do not provide an objective estimate of their performance. In particular, the anti-accident [3] and operational [4] provisions, specify the only criterion of admissibility of further service, namely the pipeline wall thickness in ECW zone, determined during the regular inspection, which is limited by 0.85 t_{min} value (t_{min} is the calculated pipeline wall thickness). Without denying the importance of this parameter influence on the pipeline strength, we believe it is absolutely unjustified to ignore the other parameters and, primarily, the extent of the ECW zone in the axial and circular directions. Taking into account just the wall thickness does not eliminate the fact that in some cases the section of pipeline with ECW will not have the necessary strength margin (which is confirmed by the damage occurring during service), and in other cases this strength margin will be sufficient for extension of the operational period between repairs.

If the extent of the defect is considerable, its influence on the pipeline strength cannot be regarded as a local influence. In this case, the strength of the section of pipeline with ECW is determined by the minimal value of the wall thickness and with the current requirements, it will be equal to 0.85 of the design value.

Not the least of the factors influencing the operational reliability of the pipeline, is the fact that the current standard procedure does not take into account the prehistory of formation of the defect caused by ECW. Probably, the situations when the wall thickness has reached a limit value during one operational period between inspections, and those when reaching the limit value was preceded by a long period of service, should not be treated as identical. As the safety of pipelines with ECW should be guaranteed till the next scheduled inspection, it is easy to see that in the most unfavourable case the thickness of the wall with ECW will be reduced to 0.7 t_{min}, and taking into account the non-linear dependence of the pipe wall thinning on time and the probable initial pipe wall thickness $t > t_{min}$, it can reach even smaller values.

Therefore, there is no doubt that with an unfavourable concurrence of circumstances, occurrence of an emergency situation is inevitable, and this is related to the need for reactor shut-down before time and great financial losses. Note, that in this case the current safety requirements will not be formally violated.

This paper gives the results of investigations which allow assessment of the influence of the individual factors on the strength and residual life of pipelines with ECW, and describes the procedure of design evaluation of the strength and residual life of such pipelines based on information about their operation and results of subsequent inspections.

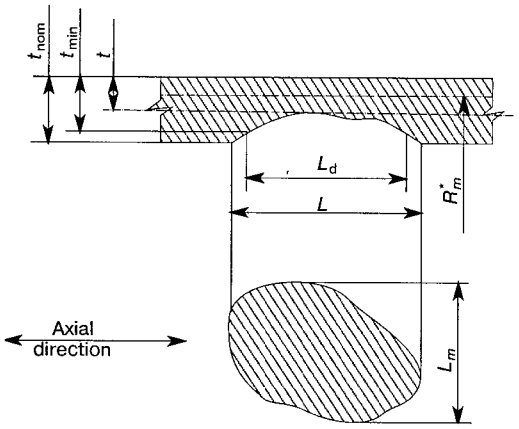

Figure 1. Diagram of ECW of a pipeline section: t_{nom} — nominal wall thickness; t — current wall thickness; L — current length of ECW; L_d — ECW length relative to design thickness of the pipe wall; L_m — ECW width; R_m^* — average radius relative to calculated wall thickness

The following approaches were incorporated into the developed procedure of evaluation of the strength and residual life of pipelines with ECW:

strength of the pipeline with ECW over the entire period of its service up to taking the decision on repair, should not be below the design strength;

strength of pipeline with ECW should not only be estimated at the moment of a regular inspection, but should be also forecast for the period up to the subsequent scheduled inspection;

prehistory of development of each concrete damage caused by ECW should be taken into account in design, i.e. duration of service of the section of pipeline with ECW and kinetics of defect development;

possible simplifications used in development of the procedure, should yield a conservative result.

The above approaches are implemented using a hypothesis according to which the influence of a defect caused by ECW on pipeline strength, will be similar to the influence of an individual through-thickness circular hole, at least, in the area of its diameter, not exceeding a critical value of d_0. The influence of an individual through-thickness hole is well studied, confirmed by numerous experimental studies, and, what is especially important, is incorporated into the codes [5 – 7]. The critical dimensions of the defects correspond to the diameter of the through-thickness hole not lowering the load-carrying capacity of the cylindrical shell and are defined by the following expression:

$$d_0 = 0.25\sqrt{2R_m t_{min}}, \qquad (1)$$

where R_m is the average radius of the shell.

Reduction of the defect caused by ECW to an individual through-thickness hole is rational to be performed through its area determined in the section along the pipeline axis, as the pipeline load-carrying capacity is determined by circumferential stresses.

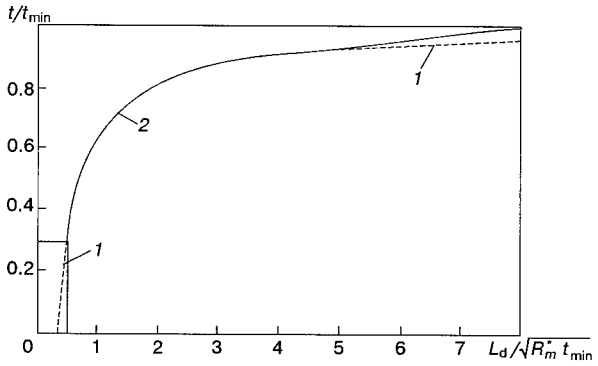

Figure 2. Limit admissible dimensions of ECW in the pipeline, not lowering its load-carrying capacity: *1* — theoretical; *2* — practical

Analysis of erosion-corrosion damage in pipelines in service shows that its shape and dimensions can be the most diverse, however, no defects caused by ECW which can be regarded as crack-like are found.

The area of weakening due to ECW is determined by the results of a regular inspection of the technical condition of the pipeline elements. For simplification of the inspection procedure, with preference for deliberately conservative results, it is rational to take this area to be the area of a rectangle (Figure 1):

$$F_u = L_i\,(t_{min} - t_i), \qquad (2)$$

where L_i is the total length of ECW in the direction of the pipeline axis; t_i is the minimal thickness of the pipe wall in the ECW zone determined during a regular inspection by the results of thickness measurement. On the other hand, it is also possible to more accurately determine the defect area and use the derived values in calculation.

Proceeding from the above, while allowing for the assumptions made, the admissible dimensions of ECW which do not lower the load-carrying capacity of the pipeline, are given by the following dependencies (1) and (2):

$$L_i\,(t_{min} - t_i) \le 0.25\,t_{min}\sqrt{2R_m t_{min}}. \qquad (3)$$

Figure 2 gives dependence (3) in dimensionless co-ordinates, according to which in the case of a through-thickness defect ($t_i = 0$) its length is determined by diameter d_0, while at $t_i \to t_{min}$, the defect length tends to infinity. In practical work the presence of a through-thickness defect is not allowed, and with the increase of its length the mechanism of pipeline fracture changes. Therefore, certain limitations should be introduced. It is rational to eliminate the possibility of appearance of a through-thickness defect caused by ECW by limiting the minimal admissible thickness of the pipe wall in the ECW zone by 0.3 t_{min} value, this being in compliance with the US codes [8].

With a rather long defect, the pipe strength will be determined by the remaining material thick-

Results of testing fragments of pipe with defects simulating erosion-corrosion wear

Sample No.	Average radius, R_m, mm	Design wall thickness, t_{min}, mm	ECW depth, Δt, mm	ECW length, L, mm	ECW width, L_m, mm	σ_t, MPa	Experimental breaking pressure, P_e, MPa
1	157.24	4.650	1.000	58.5	90.0	500.70	14.6
2	156.44	5.470	1.970	58.5	42.0	509.10	15.3
3	157.82	7.200	1.625	67.5	70.0	503.60	22.5
4	158.04	6.850	1.450	66.7	72.0	506.70	21.0
5	77.91	3.180	0.205	74.3	50.0	582.50	25.7
6	69.50	6.875	1.245	60.0	39.0	481.46	46.0
7	69.50	6.9000	0.497	110.0	26.0	481.46	47.8
8	69.49	6.820	0.565	127.5	27.6	481.46	47.4
9	69.49	6.895	0.435	150.0	24.5	481.46	47.4
10	158.41	8.180	1.420	100.6	60.0	490.70	25.2
11	158.40	8.200	0.690	160.0	60.0	490.70	25.5
12	158.40	8.200	1.100	214.0	60.0	490.70	24.4

(cont.)

Sample No.	$\frac{L}{\sqrt{R_m t_{min}}}$	$\frac{L_m}{\sqrt{R_m t_{min}}}$	$\frac{t_{min}-\Delta t}{t_{min}}$	$d_c=\frac{L\Delta t}{t_{min}}$, mm	d_c, mm	Coefficient of weakening	P_d, MPa	P_e/P_d
1	2.160	3.330	0.785	12.58	9.560	0.962	14.15	1.030
2	2.000	1.436	0.640	21.06	10.340	0.885	15.75	0.971
3	2.000	2.076	0.774	15.24	11.920	0.966	22.19	1.014
4	2.027	2.190	0.788	14.12	11.630	0.974	21.39	0.982
5	4.720	3.180	0.936	4.79	5.560	1.000	25.39	1.012
6	2.745	1.800	0.819	10.86	7.728	0.952	45.37	1.014
7	5.020	1.190	0.928	7.93	7.742	0.997	47.66	1.003
8	5.860	1.270	0.917	10.56	7.697	0.995	45.12	1.050
9	6.850	1.120	0.937	9.46	7.739	0.973	46.48	1.020
10	2.790	1.670	0.826	17.46	12.730	0.956	24.22	1.040
11	4.440	1.660	0.916	13.46	12.740	0.993	25.22	1.010
12	5.940	1.660	0.866	28.71	12.740	0.865	21.97	1.110

ness in the thinning zone. The limit admissible length of ECW at which it can be regarded as a local defect and no lowering of the load-carrying capacity of the pipeline will be registered, should be substantiated by experimental studies. According to [8], the length of the thinning zone should not exceed $8\sqrt{R_m t_{min}}$. Then, the area located above the dependence represented by a solid line in Figure 2, determines the ratio of dimensions (length and depth) of the damage due to ECW at which safe service of the pipeline is guaranteed.

According to this dependence, at the length of ECW zone $0 < L_i \le 0.5\sqrt{R_m t_{min}}$ $t_i = 0.3\ t_{min}$ and $0.5\sqrt{R_m t_{min}} < L_i \le 4\sqrt{R_m t_{min}}$, the minimal wall thickness in the damage zone is given by expression (3), while at $4\sqrt{R_m t_{min}} < L_i \le 8\sqrt{R_m t_{min}}$, the minimal wall thickness in ECW zone changes by a linear law from $0.91 t_{min}$ to t_{min}.

In order to ensure reliable operation of pipeline systems with ECW zones, it is necessary to take a decision on the pipeline operability by the results of the last inspection (at least, for the period till the next planned shut down of the technological system when the next inspection can be conducted). Therefore, it is necessary to guarantee that the limit condition of the pipeline elements with ECW will not set in before the next planned shut down of the system. This requires making a forecast of the condition of the ECW zone by the results of previous inspections. It can be performed by extrapolation. The task is made somewhat more difficult by a lack of information on the kinetics of development of ECW-related damage in time. It is known that the corrosion processes are slowed down with time because of formation of oxide films which impede oxygen penetration to the metal surface [9]. Erosion-corrosion processes have a somewhat different mechanism connected primarily with the continuous breaking up of oxide films. Therefore, one should not expect slowing down of the process of defect propagation. Apparently, the process of ECW development proceeds more or less uniformly in time.

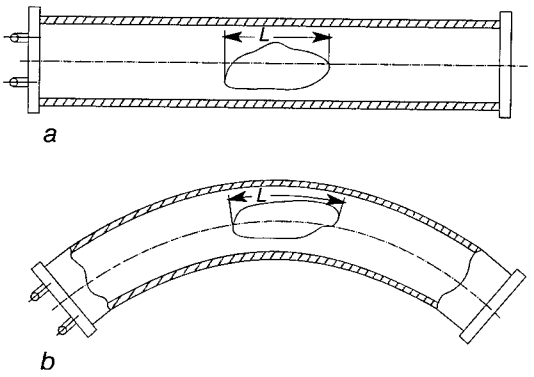

Figure 3. Samples of pipes with ECW for testing by internal pressure: *a* — rectilinear pipes; *b* — pipeline bend

The regularities of the process of damage development can only be derived as the inspection results are accumulated on each specific defect and a data bank is formed. At this stage (considering a lack of information on the kinetics of development of damage related to ECW), it is, probably, justified to introduce a certain correction factor K which would compensate the possible error. It is rational to assume a differentiated K value dependent on the number of inspections of each concrete defect over the period of pipeline service according to the following expression:

$$K = (i + 1.4)/(i + 1),$$

where i is the number of inspections of this defect due to ECW over the period of pipeline service.

Practical use of the above approach to evaluation of the strength of critical pipeline systems with ECW requires comprehensive experimental verification of its individual statements and the correctness of the accepted hypothesis. The series of experimental studies performed at the E.O. Paton Electric Welding Institute had the following goals:

verification of the hypothesis of adequacy of the influence on pipeline strength of the defect caused by ECW and of the through-thickness circular hole;

determination of the influence of the width of the defect caused by ECW on strength;

determination of limit length of ECW at which it can be regarded as local damage.

The laboratory of testing of welded joints certified by Gosstandard of Ukraine in the Ukr-SEPRO system, performed pressure testing of pipe samples, the results of which are given in the Table.

Sample No. 5 is a section of a pipeline bend cut out of the pipeline after 20 years of service. The other samples were made of rectilinear pipes with defects simulating ECW made in the middle part of the sample on the internal surface (Figure 3). The diameter of a circular hole d_c, equal over the area of the section along the pipe axis, was determined proceeding from the defect dimensions. The limit diameter of a circular hole not lowering the

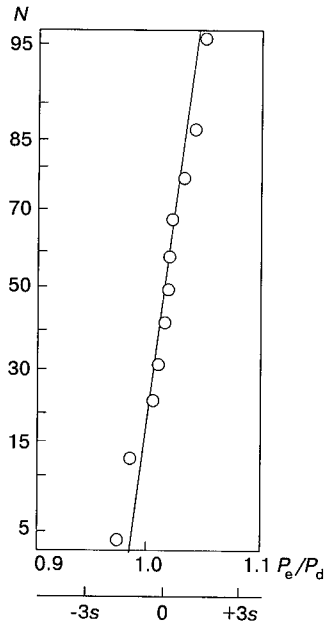

Figure 4. Distribution of the values of the ratio of experimental and design breaking pressure in the pipes with ECW (N — probability; s — standard deviation)

sample strength, is given for each sample for comparison purposes. The design strength of the samples was determined from expressions known from [6, 7]:

$$P_d = \varphi \frac{\sigma_t t_{min}}{R_m},$$

where $\varphi = 2/(d_c\sqrt{2R_m t_{min}} + 1.75)$.

The last column of the Table gives the ratio of breaking pressure at testing and breaking pressure derived from calculations. The ratios of these values are close to the normal law of distribution with the sample mean equal to 1.013 and standard deviation of 0.023 (Figure 4).

The results of experimental investigations provide convincing evidence of the validity of the proposed hypothesis not only in the region of $d_c < d_0$ values, but also in the case when the diameter of an adequate circular hole leads to decrease of the pipe strength.

The samples for experimental investigations, as can be seen from the Table, had different width of ECW zone. $L_m/\sqrt{R_m t_{min}}$ ratio changed in the range of 1.12 to 3.33. The dependence given in Figure 5 shows that the width of ECW zone does not influence the ratios of experimental and design breaking pressures. Considering that the width of ECW zone was ignored at the design breaking pressure, if it had an influence on strength, it would have been visible in the Figure.

The presented results give grounds to state that in evaluation of the strength of pipelines with ECW in the case of pressure loading, the width of the damage zone can be ignored. Note, however, that the US codes take into account the influence of the

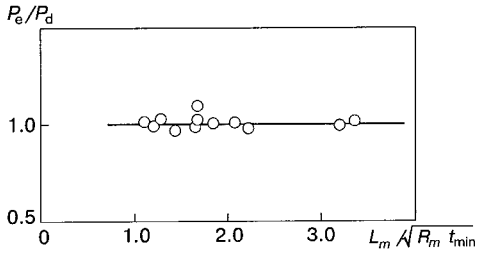

Figure 5. Influence of ECW zone width on pipe strength

width of ECW zone [8]. If it is smaller than $\sqrt{R_m t_{min}}$, curve *1* is recommended (Figure 6). With defect width > $2.65\sqrt{R_m t_{min}}$, admissible values of t/t_{min} are given by curve *2*. The dependence assumed in this study which determines the dimensions of ECW at which the design strength of the pipeline is ensured (Figure 2), is close to curve *2* (Figure 6). However, lowering of limit values of ECW length and depth with its width reduction from $2.65\sqrt{R_m t_{min}}$ to $\sqrt{R_m t_{min}}$, is, probably, unjustified.

The data of experimental investigations permit assessment of the degree of their correlation with the assumed dependence of limit admissible dimensions of ECW not leading to a decrease of the pipeline strength. With this purpose, only those of the results presented in the Table are considered, in which the influence of the coefficient is minor or equal to 1. From the comparison given in Figure 7 one can see that the testing results quite satisfactorily correlate with the proposed dependence of limit admissible dimensions of ECW, whereas the assumption of the limit length at which the defect can be considered as a local one, equal to $8\sqrt{R_m t_{min}}$, is quite justified.

Proceeding from the above, the procedure of taking a decision on the possibility of further operation of the pipeline with ECW, consists of the following steps.

The initial parameters of the considered pipeline section are determined. Among them are the pipe outer diameter D, nominal wall thickness t_{nom}, working pressure P in the pipeline, grade of steel of which the pipeline is made, and admissible stresses for it [σ], data of the start of pipeline operation, design thickness of the wall t_{min}. The latter can be determined from calculations.

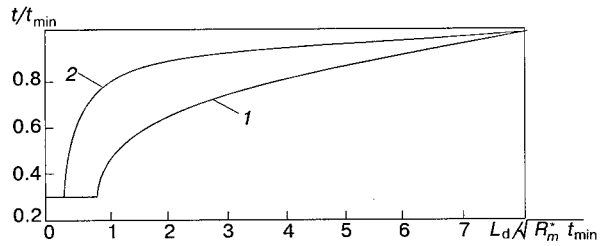

Figure 6. Dependencies for determination of limit admissible dimensions of ECW according to [8]: *1* — $L_m < \sqrt{R_m t_{min}}$; *2* — $L_m > 2.65\sqrt{R_m t_{min}}$

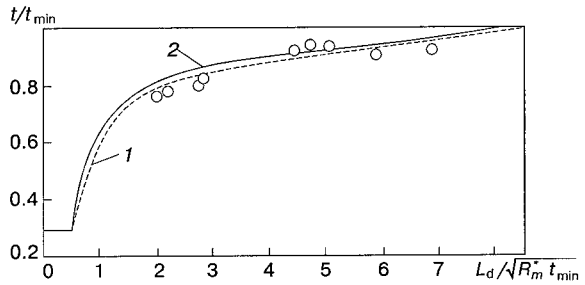

Figure 7. Comparison of limit dimensions of ECW zone by the results of testing pipes in which no loss of strength was found: *1* — experiment; *2* — design

The length of ECW zone in the direction of the axis of pipeline L_i, minimal thickness of pipe wall t_i in ECW zone, duration of the pipeline operation T_i, are determined proceeding from the results of the regular scheduled inspection of the pipeline section with ECW.

The period of pipeline operation till the next scheduled inspection T_{i+1} is determined.

The forecast thickness of the pipe wall in ECW zone at the moment of the scheduled examination is determined from the following expression:

$$T_{i+1} = \left[1 - \frac{t_{nom} - t_i}{t_{nom}} \frac{T_{i+1}}{T}\right] \frac{t_{nom}}{K}.$$

Length L_d of ECW zone on which the wall thickness is below t_{min} for the period of scheduled inspection, is calculated from the following expression:

$$L_d = KL_i \frac{T_{min} - t_{i+1}}{t_{nom} - t_i}.$$

Ratios t_{i+1}/t_{min} and $L_d/\sqrt{R_m^* t_{min}}$ are determined, where $R_m^* = (D - t_{min})/2$. The point with co-ordinates t_{i+1}/t_{min} and $L_d/\sqrt{R_m^* t_{min}}$ is marked in Figure 2. If this point falls on the dependence which determines the limit admissible ratios of the dimensions of ECW zone, or is above it, further operation of the pipeline section with ECW till the next scheduled examination, is possible. Now, if it is lower than the mentioned dependence, pipeline repair is required.

The safe residual life of the pipeline section with ECW dimensions established during a regular

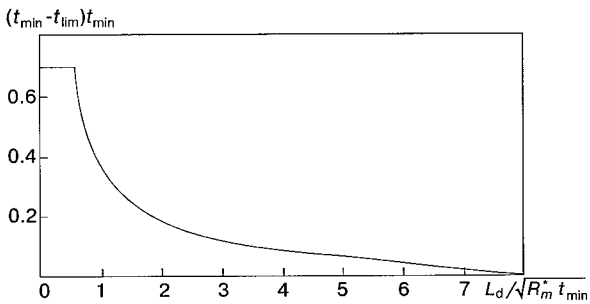

Figure 8. Dependence of limit admissible dimensions of ECW, used for assessment of the residual life of the pipeline

inspection, is determined by the following procedure.

The dependence shown in Figure 8 which is a mirror reflection of the dependence given in Figure 2, as well as the data of the last inspection of ECW zone, are used to determine the limit admissible values of length L_{lim} and depth $t_{min} - t_{lim}$ of the damage. With this aim, the point with co-ordinates $(t_{nom} - t_i)/t_{nom}$ and $L_i/\sqrt{R_m t_{nom}}$ is marked in Figure 8. A straight line is drawn through the origin of coordinates and this point up to the point of intersection with the curve of limit admissible dimensions of ECW and $(t_{min} - t_{lim})/t_{lim}$ and $L_{lim}/\sqrt{R_m^* t_{nom}}$ parameters are determined by the point of intersection.

Dimensions t_i and L_i of ECW zone derived in the last inspection and the limit admissible dimensions t_{lim} and L_{lim} of ECW zone derived from Figure 8, as well as the period T_i of operation of this pipeline section before the last inspection, are used to determine the safe life of the pipeline with ECW according to the following expression:

$$T = \frac{t_{nom} - t_{lim}}{t_{nom} - t_i} \frac{T_i}{K}.$$

The safe residual life ΔT of the pipeline section with ECW is determined from the following expression:

$$\Delta T = T - T_i.$$

The values of residual service life of the section of pipeline with ECW can be used for assigning the schedule of subsequent inspections and planning the repair operations.

CONCLUSIONS

1. The currently accepted in power generation industry procedure of processing from one side the pipeline sections with ECW, does not provide the required level of safety in their service, and on the other hand, in a number of cases does not permit full use of the actual residual life of the pipeline.

2. A procedure of evaluation of fitness for service and residual life of the pipelines with ECW zones in individual sections, has been developed, which is based on the principle of provision of the design strength during the entire period of the system service.

3. Limit admissible combinations of the depth and length of ECW zone in the direction of the pipeline axis have been established, which do not lower its load-carrying capacity.

4. The main postulates of the procedure have been experimentally confirmed. It is shown that the width of ECW zone does not influence the strength and residual life of pipelines with ECW.

REFERENCES

1. Torronen, K., Aaltonen, P., Hanninen, H. (1994) Water chemistry and materials degradation in LWRs. In: *Proc. of Specialists Meeting on Working Material Erosion and Corrosion of NPP organised by the IAEA,* Kyiv, Sept. 19 – 22, 1994. Viena.
2. Korhonen, R., Hietanen, O. (1994) Erosion-corrosion of parallel feed water discharge lines in Loviisa WWR 440. *Ibid*.
3. (1989) *Anti-accident provisions Ts-02–89*. Approv. on 01.01.89.
4. (1986) *Operational provisions Ts-01–86*. Approv. on 17.02.86.
5. Kats, Sh.N. (1964) Strength of pipes and drums with isolated reinforced hole. *Teploenergetika*, **10**, 51 – 56.
6. (1989) *PNAE G-7-002–86. Regulations and codes in nuclear power generation industry. Codes for strength analysis of equipment and pipelines in NPS*. Approv. on 01.07.87 with changes. Moscow: Energoizdat.
7. (1987) *OST 108.031.08–85. Stationary boilers and steam and hot water piping. Strength analysis codes*. Approv. on 01.07.87.
8. (1990) *Classes of ASME boiler and pressure vessel code*. Approv. on 10.05.90.
9. (1981) *Corrosion*. Refer. Book. Ed. L.L. Shrajyer. Moscow: Nauka.

ELIMINATION OF CRACKS IN STEEL STRUCTURES USING DESIGN-TECHNOLOGICAL MEASURES

H. HEROLD and **N. WOYWODE**
Magdeburg University, Germany

ABSTRACT

Numerous open and closed cracks were detected in thick-walled welded elements of span structures of a metallurgical workshop made from increased-strength steel plates 11 – 45 mm thick. Cracks were registered also in welds between shafts and drum bases of a belt conveyer. Explanations of formation of this type of defects are given. Design-technological measures are suggested for elimination of such cracks.

Key words: *welded structures, increased-strength steels, hot galvanizing, quenching structures, thermal stresses, preheating, groove preparation.*

Cracks in steel structures subjected to hot galvanazing. Frame span structures of workshops with a span 40 m wide (Figure 1) fabricated from welded double-T profiles are subjected to hot galvanazing followed by painting to ensure their long-time corrosion protection.

As it is specified in the hot galvanazing instructions, when welded steel parts are immersed into a hot zinc galvanizing bath with a temperature of at least 450 °C, this first induces temperature stresses in them and then, after they are heated through, causes a decrease in strength of the material. At the same time, this is accompanied by relaxation of welding stresses. However, prior to relaxation, these stresses may superimpose temperature stresses, which will lead to crack formation. Therefore, a welded structure subjected to hot galvanazing should have minimum residual welding stresses and, at the same time, such a configuration which itself would create minimum obstacles to strains [1]. Immersion of the structure and especially large-section elements into the zinc bath should be done slowly to decrease thermal stresses.

All large double-T beams (posts and collar beams) in the form of welded elements were prefabricated under factory conditions and then subjected to hot galvanazing. Webs and flanges of the double-T profiles were joined to each other by longitudinal fillet welds. Assembly of the span structures was done using bolted joints, for which cross-pieces were welded to ends of the double-T beams.

Webs and flanges of the double-T beams were 11 – 35 mm thick, the webs being 1700 mm high and flanges – up to 400 mm wide. The cross-pieces were 30 – 45 mm thick. Joining of the flange plates to the webs and double-T profiles to cross-pieces was done by fillet welds with a cross section of up to 4 – 15 mm. Normalized-rolling steels FE 510B and FE 510D1 according to standard BS EN 10025 (corresponding to steel S355JR or S355J2G3 according to DIN EN 10025), and steel Nr 1.0570 were used in the majority of applications.

The webs, flanges and cross-pieces were cut out from steel plates by gas or plasma cutting. The zinc drain openings at corners between the beam web

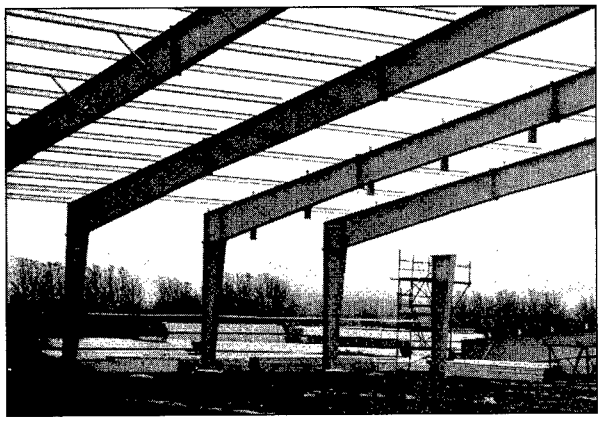

Figure 1. Assembly of the workshop structure

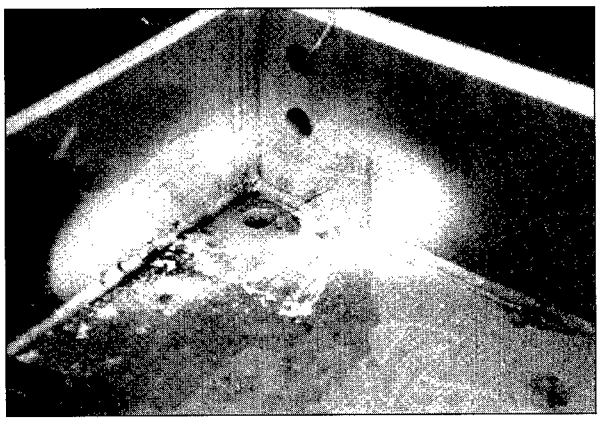

Figure 2. Zinc drain opening and crack propagating from the web plate to the cross-piece through the fillet weld

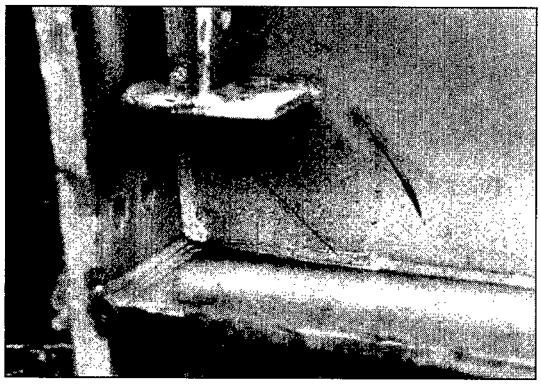

Figure 3. Crack in the web plate 18 mm thick between the cross-piece and flange

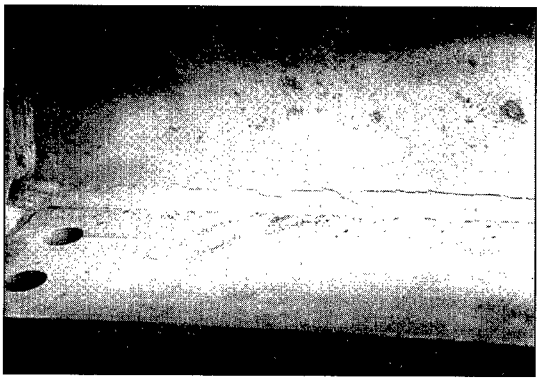

Figure 4. Open crack several meters long in the fillet weld to web plate transition zone between the cross-piece and web plate

and the cross-piece were partially drilled and partially cut out by gas cutting (Figure 2). Welding was done by both submerged-arc and metal-electrode gas-shielded (MAG) methods. Provisions were made to assess quality of all welds in compliance with group C of DIN EN 25 817.

After welding performed by the specified technology the parts were subjected to etching, degreasing, washing and drying, as well as hot galvanazing by immersing them into liquid zinc at a temperature of 440 – 460 °C.

Sand blasting of the galvanized surfaces for painting done in the erection site and NDT conducted after welding repair of defects (Figure 2) revealed cracks of different sizes in the beams treated by the hot galvanazing method. Cracks at corners between the beam flange and cross-piece, i.e. within the high-rigidity zone, can be seen in Figures 2 and 3. Very long cracks (over 1 m long) were registered in the connecting welds between the cross-pieces and web plates. Investigations show that such cracks propagate approximately parallel with the HAZ of the fillet weld and then penetrate into the flange (Figures 4 and 5). The opposite fillet weld on the other side of the cross-piece had already a tear at its root. A gray dense deposit was detected on the fracture surface. This deposit found also on the surfaces of cracks in the web plates (Figures 2 and 3) was identified by scanning electron microscopy (SEM) as zinc (Figure 6). This is probable only in the case if cracks are present in a material before it is immersed into the liquid zinc bath or are formed at the moment of immersion.

In the erection site the cracks in the web plates (Figures 2 and 3) were machined, repaired by welding and checked by the ultrasonic inspection method. Ultrasonic inspection showed that the cross-pieces contained other defects as well, which were also identified as cracks. Visual examination failed to detect these cracks, as they were filled with zinc to the entire depth (Figure 7). As a rule,

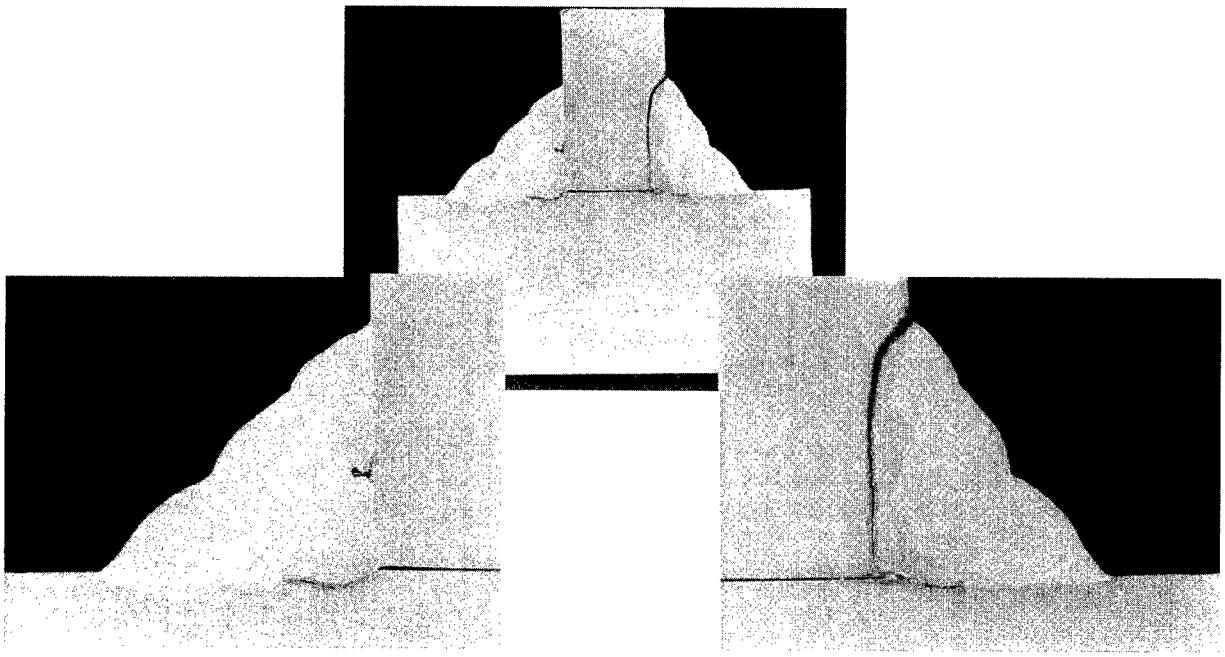

Figure 5. Cross section of the fillet weld (Figure 4) with a crack; the weld structure and the crack can be seen in the macrosection

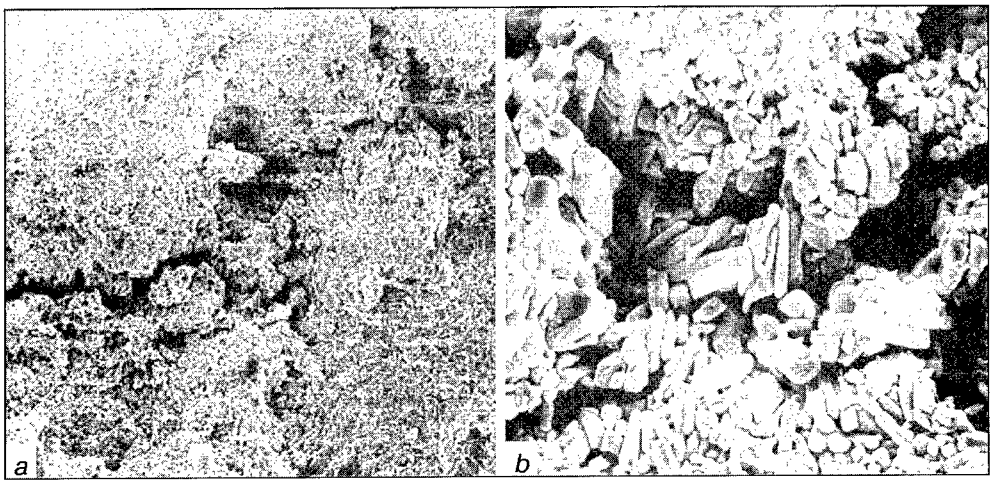

Figure 6. SEM patterns of the zinc crystals present on the fracture surface of an open crack

the cracks started from an undercut of the fillet weld, propagated in the HAZ metal on the flange side and then entered into the cross-piece.

All the cracks were intercrystalline, they initiated and propagated without any visible plastic deformations. Fracture of the material was of a brittle character. The embrittlement mechanism was similar to that taking place in the case of stress corrosion cracking.

Determination of causes of cracking. According to the data of a company which fabricates metal structures, parts had no cracks after welding. To establish causes of their formation in the galvanized parts, investigations [2] were conducted to study materials, design peculiarities of welded components, welding technology and specific features of the galvanizing process.

It was found that the above defects could be formed because the parts had non-optimized design for hot galvanizing, because of high thermal stresses induced in them and embrittlement of metal caused by zinc penetrating into steel. This article presents only the most important results of those investigations.

According to drawings, almost all of the longitudinal fillet welds should have height a equal to 0.5δ. Making fillet welds of such sizes leads to increased stresses and strains, as compared with fillet welds of minimum sizes. In addition, actual sizes of the welds on parts were always in excess of those indicated in the drawings.

Critical joints between the double-T profiles and cross-pieces were made in the form of fillet welds with height a equal to 15 – 18 mm (Figure 8). Welds with a K-groove in the double-T beam web provide a substantially decreased heat input, they are characterized by a shorter distance to the weld axis ($e_1 > e_2$) in the direction of which

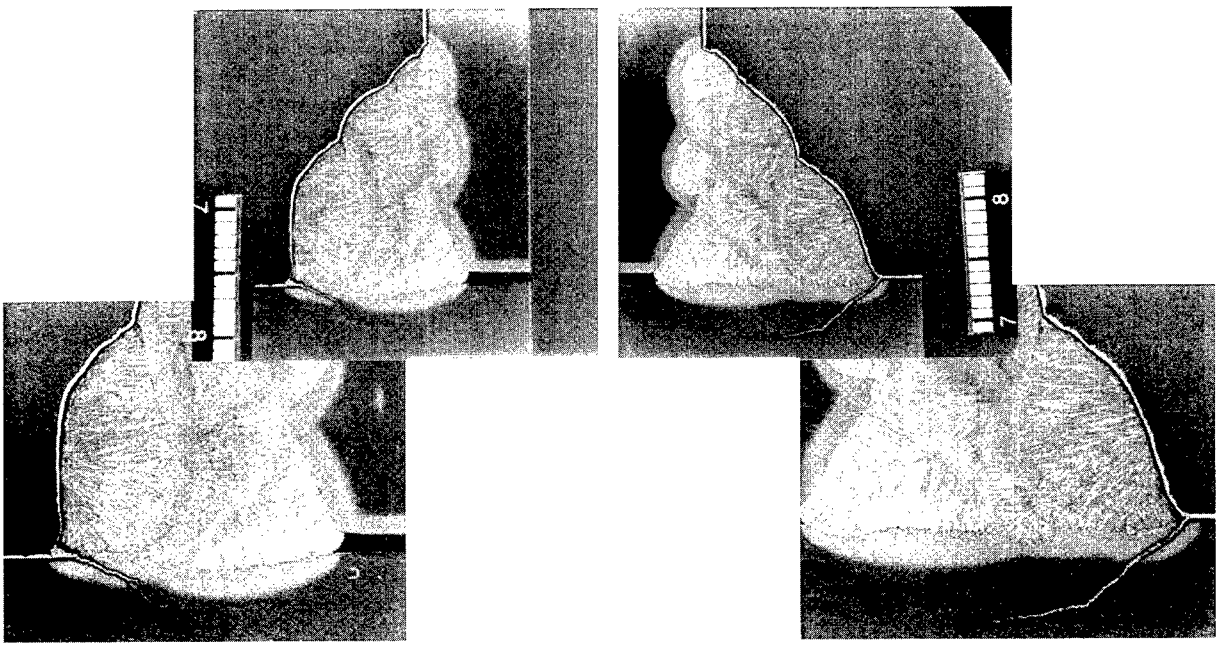

Figure 7. Closed zinc-filled crack between the cross-piece and web plate

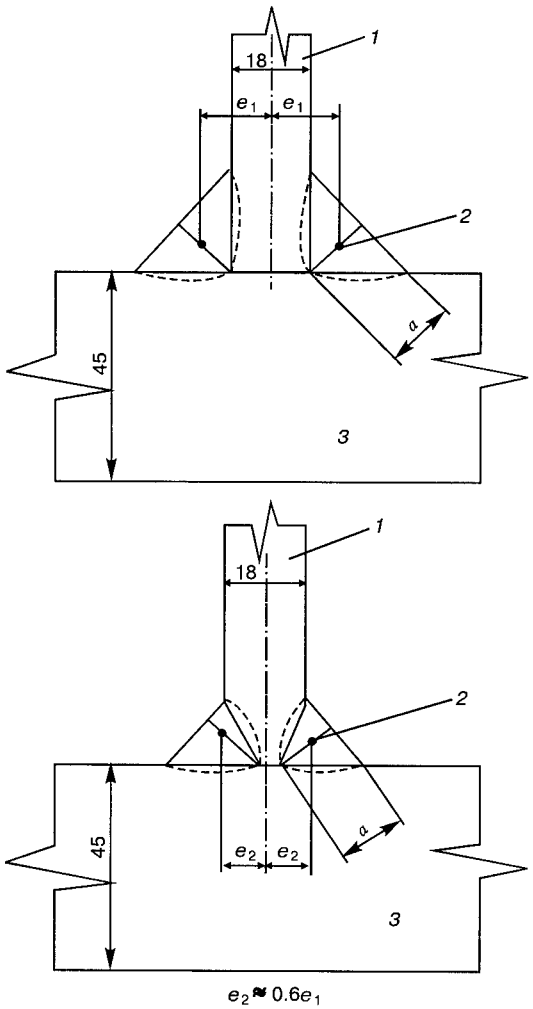

Figure 8. Variants of arrangement of the welds near the cross-piece: *1* — web plate; *2* — centre of gravity of the deposited metal and point of the effect exerted by shrinkage forces; *3* — cross-piece; *a* — height of the fillet weld; l_1 and l_2 — distances from the axis of the double-T beam web to the centre of gravity of the weld

the longitudinal shrinkage forces act. But even in this case, at a cross-piece thickness of 45 mm, the shrinkage in the transverse direction is hampered, this leading to extremely high values of residual welding stresses.

Cross-pieces were welded to double-T beams without slots at the corners. It is at these points, which are the points of crossing of the welds converging in three different directions, that the multiaxed stressed state is formed due to a high rigidity of the structure, which increases the risk of brittle fracture.

It should be noted that despite the requirement of ensuring a good quality of gas cutting and of the welds in compliance with assessment group C (DIN EN 25 817), the quality left much to be desired.

In immersing cold thick-walled steel parts into liquid zinc (Figure 9), the non-stationary temperature fields lead to formation in them of high thermal stresses. Superposition of these stresses on residual welding stresses may create conditions for liquid zinc to penetrate into steel. Liquid zinc, while penetrating into steel along the grain boundaries, makes these boundaries weaker, which leads to brittle fracture. The following three factors are required for this effect to show up:

- it is necessary that liquid and solid metals have low mutual solubility, which is the case of the zinc–iron pair;
- no intermetallic phases should be formed in the liquid-solid metal pair, which is also the case of the zinc–iron pair;
- solid metal in contact with liquid metal has no possibility of being plastically deformed, which was fixed in the region of welding cross-pieces to double-T beams.

Sensitivity of metal to embrittlement as a result of penetration of the liquid metal into the solid one depends upon effective tensile stresses and degree of alloying of steel. Thus, the effect exerted by liquid zinc on steel containing 0.22 % silicon is higher than on steel containing no silicon [13].

The presence of numerous defective welds made repair of welded span structures inexpedient. All the span structures in the workshop had to be replaced by the new ones.

Measures for elimination of cracks in hot galvanazing. With a wall thickness of the steel structures equal to more than 30 mm, even slow immersion into hot liquid zinc leads to high thermal stresses which cannot be compensated for by strength of the material. In this case the presence of obstacles to strain of the metal and high residual welding stresses complicate elimination of cracks. Preheating may decrease the risk of their formation, but it is hardly suitable for economical reasons. Therefore, while considering the problem of corrosion protection of steel structures by hot galvanizing, one should take into account the following aspects:

- need to develop a part with a design optimal for galvanizing;
- rational selection of materials to minimize the risk of penetration of liquid zinc along the grain boundaries;
- keeping to the welding technology;
- coordinating fabrication of welded structures with companies performing galvanazing.

The following requirements should be satisfied in hot galvanizing of steel parts:

- difference in thickness of the parts welded, t_{max}/t_{min}, should be not in excess of 2.5;
- it is necessary to limit thickness of cross sections of the plates and profiles ($t_{max} \leq 20 - 30$ mm), as well as round sections in combined structures ($d_{max} \leq 30$ mm);
- flanged edges of the parts should have a large radius;

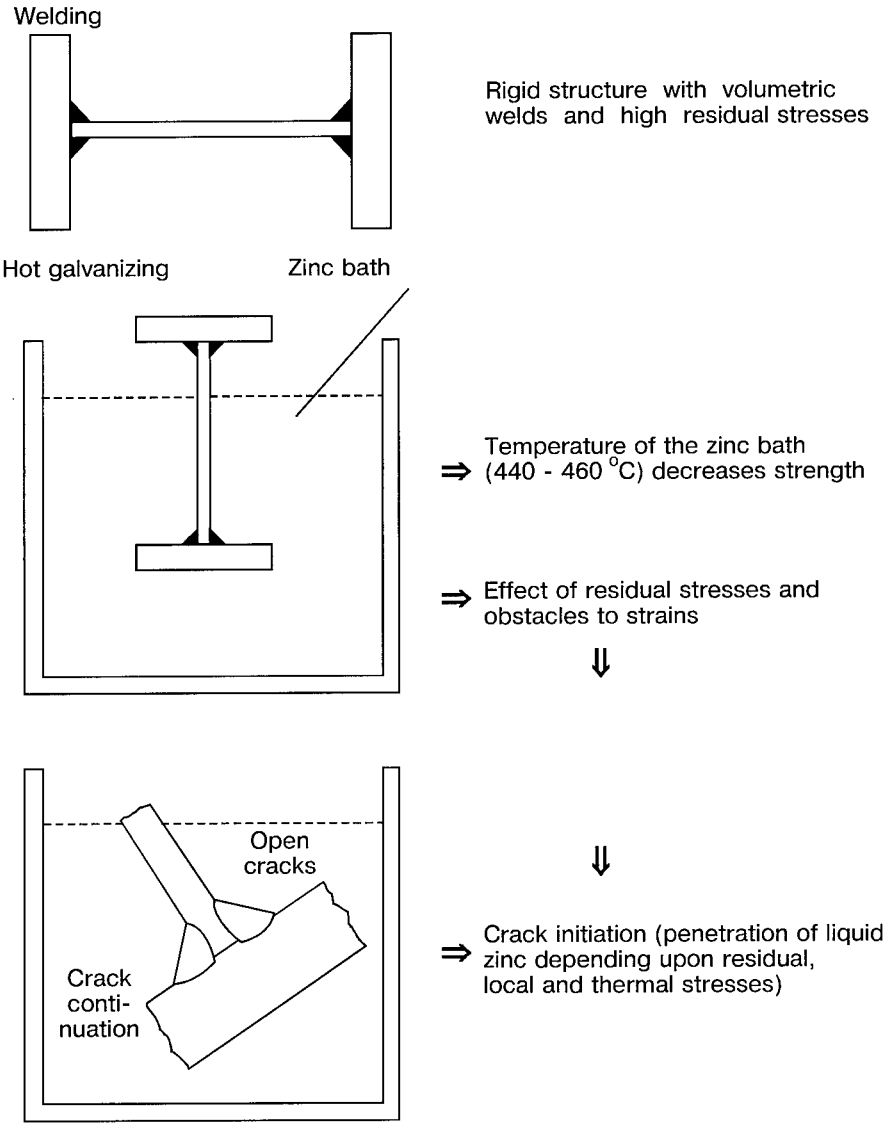

Figure 9. Flow diagram of the process of galvanizing and crack formation

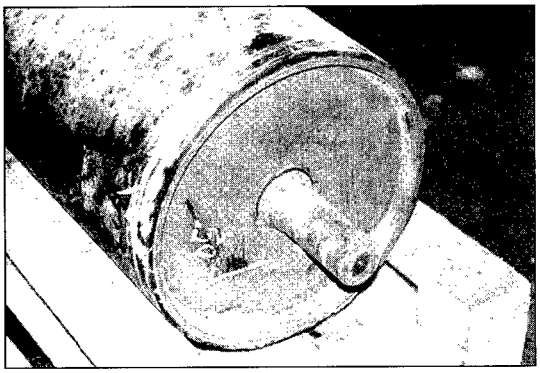

Figure 10. Drum with cracks

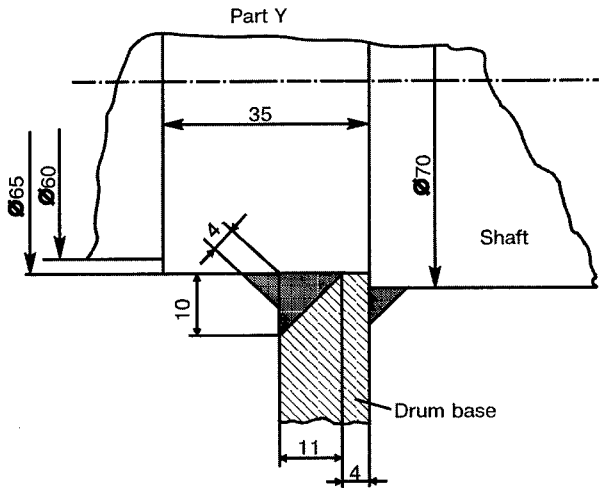

Figure 11. Circumferential connecting welds between the shaft and the drum base

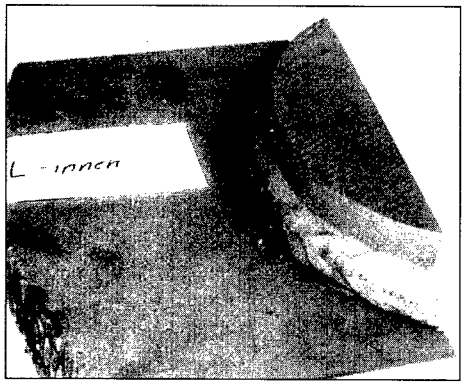

Figure 12. Connecting weld with cracks

- hollows should have openings to let zinc flow in and out;
- it is necessary to make slots in parts at the points where cross-pieces join a double-T beam;
- where possible, it is necessary to avoid fillet welds of large sizes and replace them by butt welds;
- it is necessary to avoid intermittent welds in design of the parts;
- patches with openings to remove air should be welded entirely on their perimeter;
- it is necessary to ensure the low level of residual welding stresses by optimal arrangement of the welds and keeping to the required sequence of their making;
- it is necessary to remove all welding slags prior to hot galvanizing;
- the speed of immersion in galvanizing should be 1 – 8 m/min, depending upon the thickness of a cross section;
- galvanizing of complicated parts should be done after preliminary experiments;
- it is necessary to follow the transportation and storage regulations specified for parts in the hot state (suspension, supports along the entire length, etc.).

Shrinkage cracks on drums of belt conveyers. It was thought initially that cracks in circumferential connecting welds (Figures 10 and 11) between the steel S355J2G3 (St.53-3) shaft 65 or 70 mm in diameter and steel S235JR (St.37) base 15 mm thick were caused by fatigue fracture which took place within only a few months of operation of the drums (Figures 12 and 13). However, as found during further investigations, it is probable that cracks were formed immediately after manufacture of the drums. The said cracks propagated in the material of the base in parallel with the HAZ of the welds (Figure 14). Structural elements did not fracture only because the welds had the V-groove preparation. As the welds were not subjected to NDT, the cracks were not detected during the manufacture. It is likely that manufacturers did not consider welding to be a critical process.

Figure 13. Circumferential shrinkage crack after fracture of the joint

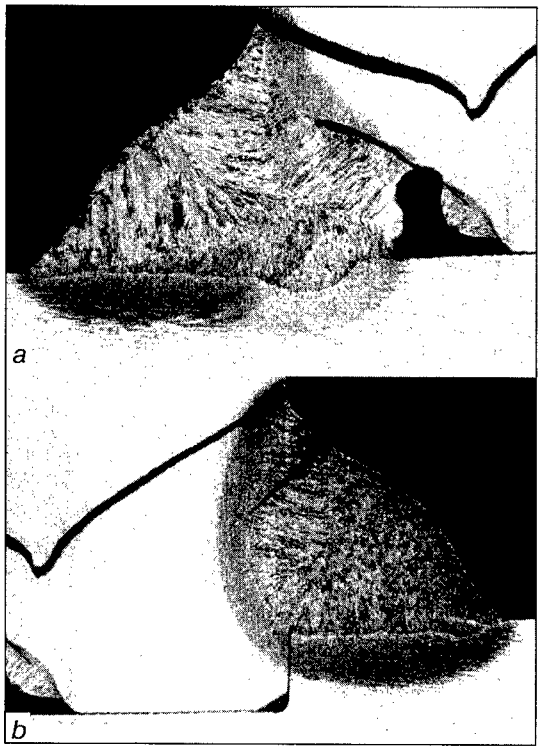

Figure 14. Transverse section of the joint containing cracks between the shaft (*a*) and the base (*b*)

In our opinion cracking was caused by formation of quenching structures in the HAZ of the fillet welds, which is proved by an extremely high microhardness of this zone. CO_2 welding was conducted without preheating. High tensile stresses favoured cracking and led to complete separation of the weld from the base. The situation was aggravated by the fact that groove preparation was done with a small angle, which caused defects in the weld root (Figure 14, *a*). In addition, parts were machined for welding and after assembly there was no gap between them, which prevented strains during welding and increased the level of residual welding stresses.

This assumption was confirmed by analysis of distribution of residual stresses in a welded joint between the shaft and the drum base during cooling (Figure 15). Distribution of residual stresses was investigated in cooling from 500 °C to room temperature. The presence of the zones with increased residual stresses was noted in the HAZ of the welds. Cracks were initiated particularly in these zones.

Cracks between the shaft and the drum base could have been avoided in the case of ensuring the

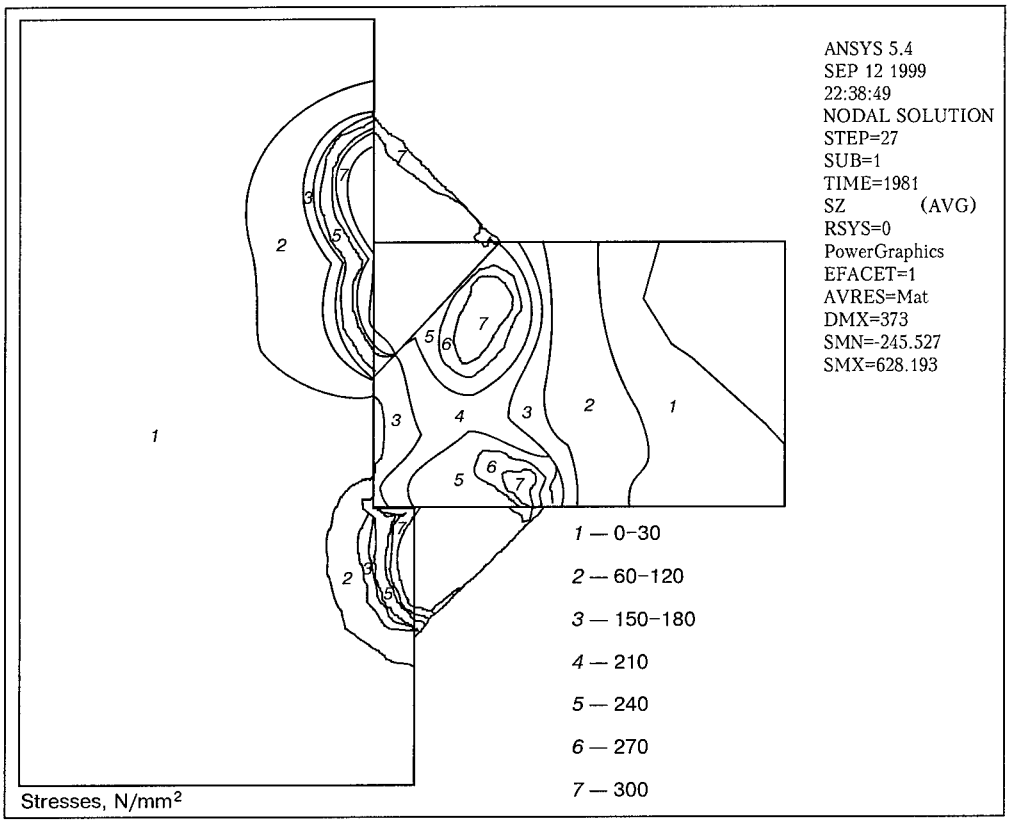

Figure 15. Residual stresses formed in the welded joint during cooling

satisfactory quality of the welds by meeting the following conditions:

- prior to welding it is necessary to preheat the parts and thus prevent formation of quenching structures;
- minimum groove angle for welding should be 55°;
- it is necessary to ensure a free shrinkage of metal during welding by fitting the shaft and the drum base with a gap between them;
- manual arc welding using electrodes which provide a high-ductility weld metal should be used instead of MAG welding.

CONCLUSIONS

Causes of formation of cracks in welds in thick-walled structures made from increased-strength steel plates 11 – 45 mm thick after hot galvanizing were determined. With a wall thickness of welded steel structures equal to more than 30 mm, even their slow immersion into hot liquid zinc leads to formation in them of high thermal stresses. It is difficult to prevent cracking in the case of the presence of obstacles to strain of the metal and high residual welding stresses. Cracking is favoured by the effect of penetration of liquid zinc into steel during the hot galvanizing process. Recommendations were developed for a rational design and technology for the fabrication of welded structures in order to prevent cracking of weldments during hot galvanizing.

Causes of cracking of the welds between the shaft and the drum base of the belt conveyers were investigated. It was established that cracks were caused by the formation of quenching structures in the HAZ of the welds. To eliminate cracks, it is necessary to change the groove shape and use preheating of parts prior to welding.

REFERENCES

1. Schmidt, J. (1996) Das chemische Element Zink. Bedeutung als Korrosionsschutzstoff. *Der Praktiker*, **11**, 508 – 513.
2. Herold, H. (1997) *Schadensfall-Hallenkonstruktion Institut für Füge- und Strahltechnik der Otto-von-Guericke-Universität*. Magdeburg.
3. Radeker, W. (1953) Die Erzeugung von Spannungsrissen in Stahl durch flussiges Zink. *Stahl und Eisen*, **10**, 654 – 658.

DESIGN-TECHNOLOGICAL STRENGTH OF WELDED JOINTS OF OFF-SHORE STRUCTURES

I.V. GORYNIN, A.V. ILJIN, V.P. LEONOV and **V.A. MALYSHEVSKY**
Central Research Institute of Structural Materials «Prometey», St.-Petersburg, Russia

ABSTRACT

Problems of assurance of reliability of off-shore engineering structures, which cover a wide range of spheres, are considered. Optimum results are obtained at a constant allowance for a real technology during the process of the structure fabrication. Approaches are described for the selection of materials, a system of safety factors, design of connections and recommendations for additional technological procedures, justification of requirements to the quality of welded joints, improvement of methods of assessment of a brittle strength and a cyclic life.

Key words: *stationary ice-resistant drilling rigs, deep-water apparatuses, welded joints, fatigue life, cyclic strength, crack resistance, requirements to the quality of welded joints.*

Reliability of the off-shore engineering structures and deep-water machinery during service is ensured by an obligatory monitoring of their state at all the stages of a life cycle, starting from designing and development of the material and finishing by inspection of the working conditions of the object. Here, the main attention should be paid to the welded joints as the most damage-subjected link in the composition of these structures. To provide the design-technological strength of welded connections it is necessary to solve a many-factor problem of allowance for an effect of a real technology of fabrication on the future serviceability of the structure. The technological aspects are complicated with a growth in strength of the materials used for the structures.

The design-technological strength is attained as a result of fulfilment of main tasks envisaged at each stage of the structure creation, namely at the stage of a preliminary (conceptual) designing (optimizing of material selection and system of safety factors); at the stage of a detail designing (selection of design of connections and welded joints, optimizing the sequence of assembly-welding operations, layout of welds), and also the additional technological procedures. During construction it is necessary to control the level of defects, technological changes and scope of repair, while at the service stage it is necessary to use a flaw detection and diagnostics of structure, expertise of fractures and optimization of the technology of repair.

This complex of problems was solved as a result of the development of the following trends of investigations:

- study of a real stress-strain state of the welded connections;
- development of physical and chemical models of fracture and methods of calculation of fatigue life at cyclic loading;
- development of methods of improving a cyclic strength of welded joints;
- justification of criteria and standards of quality of the welded joints;
- development of methods and criteria of evaluation of a brittle strength, methods of certification of materials, justification of requirements to the toughness and crack resistance of parent and welding materials;
- certification tests of materials and welded joints at different kinds of loading.

Study of stress-strain state of welded joints. The results of investigations in this trend are the basis for understanding the degree of overstressing in «critical» zones of the welded joints and for using the models which describe quantitatively the expected process of fracture. Factors, which influence the process of a cyclic fracture of the welded joints, are illustrated in Figure 1. Method of finite elements (FEM) in two- and three-dimensional statements in realization of physically non-linear models of the material deforming is the main tool of examination of the stress-strain state of the welded joints.

First of all, the stress concentration was analyzed in the HAZ metal of the welded joints (concentrators of a weld shape) which is a main point of initiation of cyclic and corrosion-mechanical damages in hull structures (Figure 1, *a*, *b*). After generalization of data obtained a number of new approximating formulae were suggested for typical joints of ship hull structures and structures of a deep-water equipment [1, 2]. As a whole, such relations have a form $K_t = 1 + A\sqrt{\rho}$, where K_t is the coefficient of stress concentration; ρ is the radius of weld mating with the parent metal: this parameter depends on the technology of welding

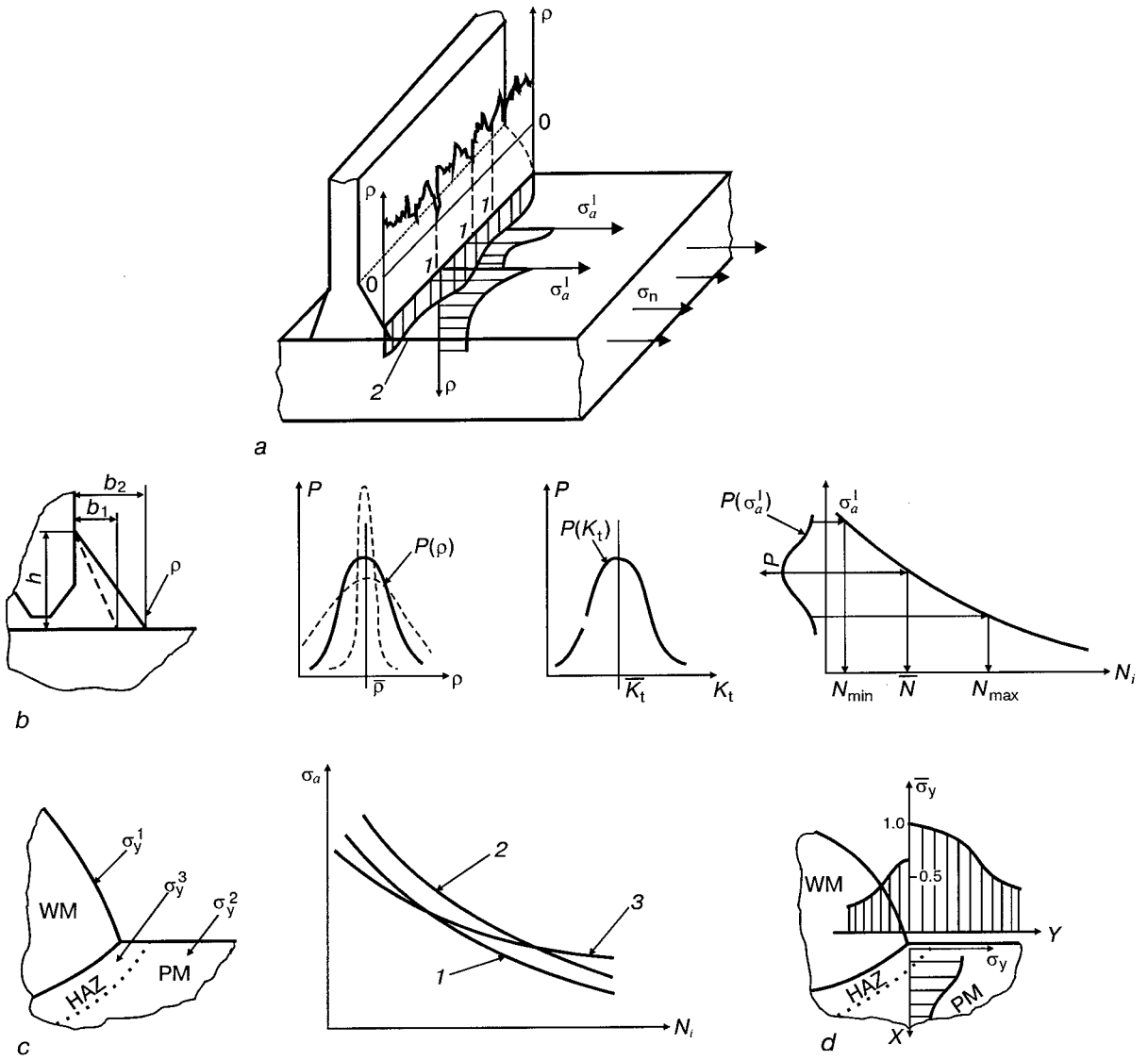

Figure 1. Typical factors that influence the process of fracture of welded joints: *a* — formation of damage (ρ is the radius of fransition from weld to the parent metal; σ_n, σ_a^l are the nominal and local amplitude values of stresses, respectivedy); *b* — variation of concentration of stresses in changing of local values ρ (h, h_1, h_2 are the legs of weld, P is the density of probability ρ and corresponding values of values of coefficient of stress concentration K_t; N_{min}, N_{max}, N are the minimum, maximum and mathematically expected estimates of fatigue life); *c* — mechanical heferogeneity of metal (σ_y, σ_y^2, σ_y^3 are the yield strength of weld metal, HAZ and parent metal, respectively; *1 – 3* are the corresponding curves of a cyclic damage); *d* — residual welding stresses ($\bar{\sigma}_y - \sigma_y/\sigma_t$ is the component normal to weld)

and has usually a nature of a random value with a high dispersity (Figure 1, *b*); A is the parameter of a macrogeometry of the joint, which is determined by preset sizes and kind of loading during designing.

Value A determines the long-range fields of stresses in the vicinity of a stress raiser and for the definite technology, characterized by a certain range of values, it can serve a measure of concentration of stresses in the welded joint. The data were obtained, which can estimate it for the welded joints of an intricate spatial geometry of a type of crossing of elements of ship framing, breaks of links, etc., which are the sources of premature cyclic fractures in ship hull structures.

Welded joints of high-strength steel are often characterized by a high mechanical heterogeneity of material in the zone of a concentration disturbance which influences the level of local deformations at an elastoplastic loading. In this connection the peculiarities of an elastoplastic deforming of the material in similar conditions were investigated. The results of investigations were generalized in the form of relations for calculation of coefficients of concentration of deformation K_ε at static and cyclic loadings [1]: $K_\varepsilon = f(K_t, \gamma, \sigma/\sigma_{0.2}^{PM})$, where $\sigma_{0.2}^{PM}$ is the comparative level of nominal stresses; γ is the relation between the strength characteristics of weld metal (WM) and the parent metal (PM). These relations make it

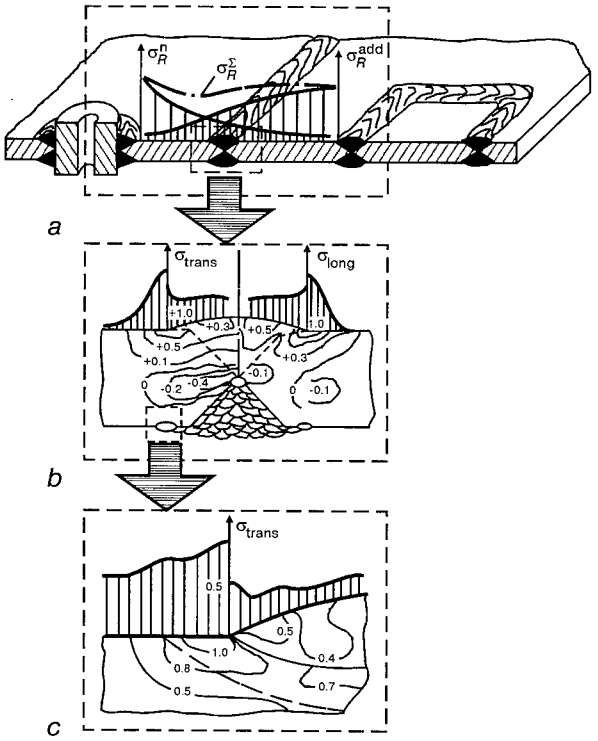

Figure 2. Schematic representation of residual welding stresses: $a - c$ — reactive, natural and local RWS, respectively; σ_R^n and σ_R^{add} are the reactive stresses from welded-in elements; σ_R^{Σ} are the total reactive stresses; σ_{trans} and σ_{long} are the transverse and longitudinal RWS, respectively

possible to describe the effects of localizing the deformations in a less stronger structural constituent of the welded joint and a partial unloading of its surrounding zones.

Welded nonheat-treatable structures are characterized by the presence of residual welding stresses (RWS) which can influence the formation of a cycle of deforming and fracture in the zones of stress concentration at the boundary of the weld reinforcement and at the contour of internal and external defects (Figure 2).

Due to impossibility of using analytical methods of evaluating RWS in multipass welded joints the basic information about the nature of their distribution was obtained with the help of numerical methods of solution of thermodeformational problems. Problems of FEM were solved in a plane and axisymmetric statement using the theory of nonisothermal plastic yielding and yield conditions of Mises for a perfect elastoplastic body [3, 4]. The calculated analysis made it possible to obtain the following results:

- the relation between the level of natural RWS and thickness of the joint, type of a groove and number of passes during its filling was established. For multipass joints (more than six passes) a rather typical distribution of the natural RWS, reaching the limiting tensile level in the zone of the weld reinforcement (0.6 – 0.8 of the yield strength in a transverse component and 1.0 of the yield strength in a longitudinal component with respect to the weld axis) at the compression in the weld root was established;
- local RWS reach maximum level at the joint thicknesses of more than 6 – 8 sizes of HAZ and for metals with high (> 400 °C) temperatures of $\gamma \rightarrow \alpha$ transition they reach the yield strength at high gradients of the RWS field and the presence of three-axial stressed state; a drastic decrease in temperature A_{r1} can lead to the occurrence of the compression zones;
- the relations between the residual shrinkage deformations and thickness, type of groove and used technology of weld making were determined. The application of an experimentally confirmed assumption about the independence of these deformations of adaptability of elements being welded makes it possible to calculate the distribution of reactive RWS for the joints, whose welds cut the shell of a hull structure and form a closed contour in the sheet plane. Such stresses are usually long-ranged, uniformly distributed in the thickness of the parent metal and they decrease monotonously with an increase in distance from the joint, i.e. their source. The procedure of calculation of reactive stresses is reduced to the solution of problems of the theory of elasticity with preset initial deformations, which are equal to the deformations of the weld shrinkage. They are solved using the analytical method (for axisymmetric joints) or numerically with the help of FEM in a plane statement (for the joints of a type of sealing holes of a rectangular or irregular shape in the sheet plane) [5]. In accordance with the developed procedure of calculation the level of reactive welding stresses in structure element considered is determined by a sum of natural reactive stresses for the given element and additional σ_R^{add}, caused by the presence of near-located sources ($\sigma_R^{add} = \eta\sigma_R^n$, where η is the coefficient of stress decreasing, which is a function of distance between the welds). The procedure can also take into account the effect of assembly operations when the initial displacements caused by assembly-erection tolerances are added to the volumes of a longitudinal shortening.

The developed calculated approaches to the defined analysis of local service and residual technological stresses could establish their effect on the formation and propagation of damages in welded nonheat-treated joints.

Assurance of cyclic strength. One of the most important problems of assurance of reliability of welded structures and selection of their optimum designing is the development of methods of calculation of service life at cyclic loading. For a low-cycle region of loading typical of elements of deep-water equipment there were no similar methodical

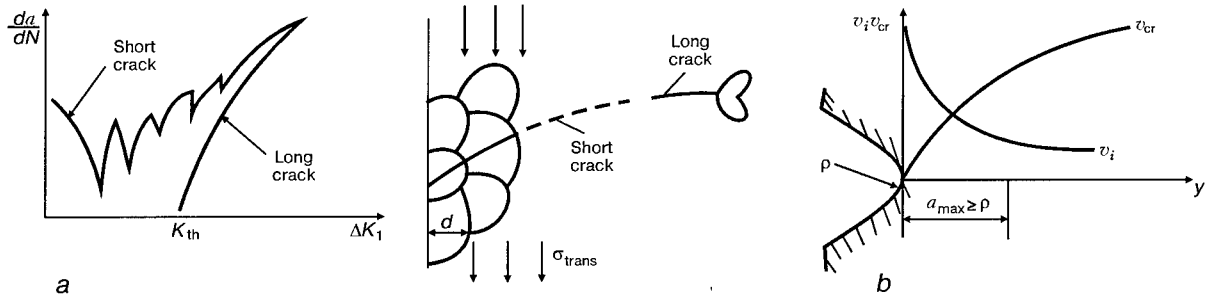

Figure 3. Modelling of initial stage of cyclic damages: *a* — peculiarities of propagation of a short crack; *b* — deformational-kinetic model

developments. For hull structures typical of ships and drilling platforms used at multicyclic loading under the action of a wind-water and ice loading the standardized methodologies of foreign classification societies are known. They are based mainly on the purely experimental proof of curves of allowable cyclic stresses. Within the scope of this approach it is difficult to take into account many design and technological factors which stipulate the cyclic strength. In addition, the transition from results of testing of specimens to the prediction of fracture of a full-scale structure element at different sizes and schemes of their loading leads always to the loss in accuracy if it is not accompanied by additional amount of analyses of these differences.

Scientific and methodological developments in the field of creation of methods of a calculated determination of a cyclic strength are based on the results of numerical investigations of stress-strain state (SSS) of the welded joints, experimental investigations of kinetics of fracture of ship hull steels and welded joints and also data obtained in the course of a physical modelling of fatigue fracture processes. Feasibility of using single dependences of the fatigue life before the crack initiation on the amplitude of a complete deformation and rate of the growth of the fatigue crack and on the range of the stress intensity factor (SIF) has been established. The data about the effect of such factors, as asymmetry of a loading cycle, action of corrosion environment, superposition of vibrating constituent of loading on these relations, are obtained. To predict the conditions of fracture in stress raisers of small radii (welded joints without an additional treatment refer to them), a deformational-kinetic model of formation of an avalanche crack based on summing of two rates of damage (Figure 3), i.e. rate of crack growth, determined from a diagram of cyclic crack resistance and which is a function of current SIF value in its tip, and an additional rate damage which is determined by an amplitude of local deformations in the same point, has been developed [6]. The determining equations for the rate of growth of the fatigue crack at different stages of its propagation have the following form:

in grain volume

$$\frac{da}{dN} = A(d - a)\Delta\varepsilon^{\alpha},$$

for short cracks

$$\frac{da}{dN} = B\Delta\varepsilon^{\beta}a,$$

for long cracks

$$\frac{da}{dN} = C(\Delta K)^{m}.$$

The calculated fatigue life is determined by the relation

$$N_{\Sigma} = \int_{0}^{a_{max}} \frac{da}{(v_i + v_{cr})},$$

where $v_i = v_i\,(\Delta\varepsilon^{*})$; $v_{cr} = da/dN = C\,(\Delta K)^{m}$; a_{max} is the recording depth of the crack.

Realization of the given model in the form of a computer program makes it possible to calculate the curves of the allowable cyclic stresses by using the following system of parameters:

- technological (parameters ρ of distribution of a radius of weld mating with the parent metal which depend on the method of welding, RWS level, degree of heterogeneity in combination of parent metal–weld);
- design (parameter A of macrogeometry of the welded joint, existing level of reactive stresses, which is determined by a mutual weld location).

The results of calculations coincide satisfactory with experimental data and standard curves of allowable stresses. This allows the developed methodology to be used for the solution of the formulated problems. For its effective use in designing two versions of the methodology of calculation of service life of welded units have been developed: relative to the structures of a deep-water machinery (a low-cycle area) and to the structures of ice-resistant drilling rigs (IRDR) (multicycle area). Main their procedures are reduced to the following operations:

- calculated determination of a coefficient of decreasing the cyclic strength of the welded joint K_f, which is the value, associated with parameters A and ρ;

• selection of a curve of allowable cyclic stresses for the preset level of RWS, sign of a loading cycle and determined value K_f;

• determination of a safety factor by the number of cycles in accordance with a procedure, summarizing the results of analysis of kinetics of the fatigue crack as a function of a level of tensile service and reactive stresses;

• application of a principle of a linear summing of a damage for a case of the non-stationary loading.

The application of the procedure for the prediction of the service life of welded joints of the deep-water equipment makes it possible to allow for main technological factors occurring in welding and to make grounded calculated evaluation of the service life by a criterion of formation of a visually recording crack. In this version the methodology has no analogues.

For the procedure of determination of a cyclic strength of welded joints of the stationary drilling rigs the most important corrections and clarifications for the existing standardized documents were due to the differentiation of limiting states at cyclic loading for the structure members of different extent of responsibility and also due to introduction of a formalized procedure of determination of a class of the welded joint by a cyclic strength. The latter promotes the allowance for the calculation of the larger amount of design and technological factors which affect the cyclic life of structure.

The developed approaches promoted the creation of calculated methods giving an opportunity to influence the design-technological designing of the off-shore structures. As a result of the investigations the requirements to a designed arrangement of elements and weld layout in hull structures of the deep-water machinery were formulated and formalized. General principles of optimizing the design-technological presentation of welded structure elements were determined and geometry of welded joints for the stationary drilling rigs were optimized.

The increase in a cyclic strength of the welded joints of ship hull structures can be attained by using special technological methods. They can be divided into the following groups: those which decrease stress concentration and RWS and those which create compressive residual stresses. The most effective methods of increasing the cyclic strength are those which provide the simultaneous decrease in stress concentration and creation of compressive stresses [7]. By the degree of effectiveness the examined methods can be arranged in the following row:

• surface plastic treatment with a formation of a preset radius;

• surface plastic treatment by a shot peening or by a bunched peening tool;

• argon-arc fusion;

• grinding of butt welded joint or machining of T-joint for a preset radius of mating.

For industrial conditions a technological process of a surface plastic treatment with a formation of a preset geometry of a concentrator on the basis of using an updated pneumatic hammer «Resurs-1» with a special head – striker, which provides the required parameters of treatment for 1 – 2 passes, has been developed. When using this technological process the fatigue life of welded structures in air and sea water is increased by an order within the wide variation of stresses.

Methodology of defectness standardizing. One of the most important trends of works for assurance of reliability of welded structures is justification and development of industrial criteria of an allowable technological defectness of the welds. The developed methodology of a calculated assessment of the fatigue life of welded joints with defects, whose block-diagram is presented in Figure 4, serves a basis for the prediction of a hazard of defects and creation of scientifically-grounded requirements to the quality of welded joints for structures of different classes and responsibility.

The main principles of assessment of a number of cycles before the appearance of a fatigue crack at the boundaries of the defect correspond to the method of calculation of a cyclic service life of the joints whose main statements were considered above. The largest difficulty is encountered in determination of SIF K_1 at the defect contour under the conditions of high-gradient fields of residual welding and service stresses and changing geometry of the propagating crack. Mathematical model for the solution of this problem was developed on the basis of a method of weight function for flat cracks of an elliptic shape [8]. Within the scope of this approach the internal defects are considered as a three-dimensional ellipsoid which creates the stress concentration in the weld metal, corresponding to a real defect. After the crack formation at its contour, further an elliptic crack is considered with parameters of an initial defect. The number of cycles at the stage of the crack propagation is determined by a step-by-step integrating of an experimental relation between the rate of crack propagation in weld metal and K_1.

The determination of the allowance of internal defects in welds is made coming from the following conditions: $N_{i.d}(\sigma) \mid_{a=a_{cr}} \geq [N_{pr}]$ or $N_{i.d}(\sigma) \mid_{a=a_{cr}} \geq N_{sh.d}(\sigma) \mid_{a=a_{cr}}$, where $N_{i.d}$ is the fatigue life determined in fracture caused by inner defect of weld; $N_{sh.d}$ is the fatigue life determined at fracture along the external contour, i.e. weld «shape defect»; $[N_{pr}]$ is the required (preset) cyclic life of the joint; a and a_{cr} are the current and critical sizes of the internal defect.

Such approach can correlate the requirements to the limiting allowable sizes of defects a_{cr}, that

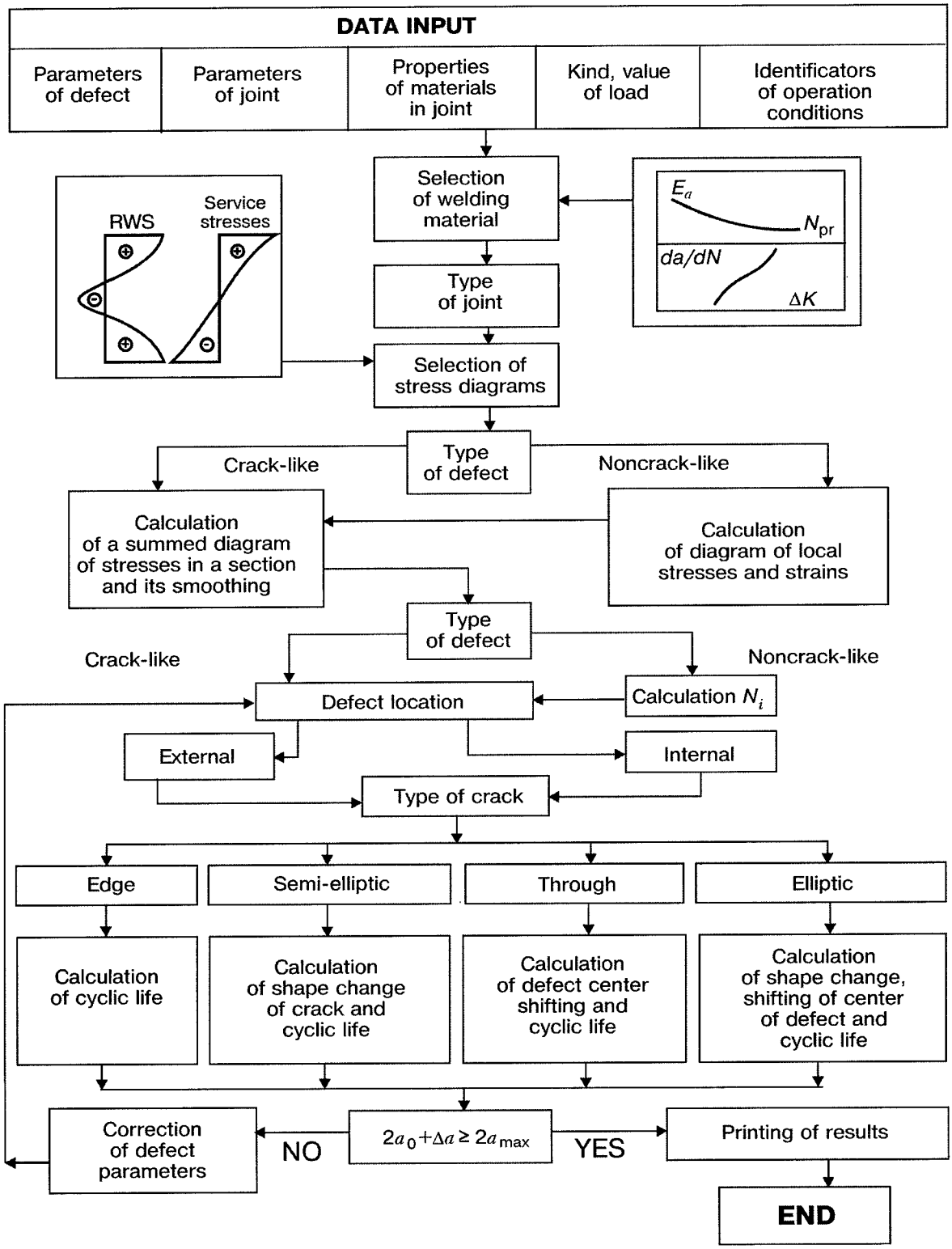

Figure 4. Block-diagram of calculation of a cyclic life of welded joint with a technological defect

provide the safe service of welded joints of the hull structures with the requirements to a resolution capability a_0 of NDT methods and catagory of the welded joint itself:

$$a_0 + \Delta a \le a_{cr}.$$

This gives a feasibility to determine an allowable growth of crack Δa for a number of cycles $[N_{pr}]$, which corresponds to different limiting states for welded joints which differ by a degree of responsibility (special, basic and auxiliary). In the first case the allowable value Δa is assumed equal to $0.1a_0$. For basic and auxiliary joints the feasibility of defect growth to 0.25 of thickness and more is allowed, excluding the hazard of a brittle fracture.

The problem of a comparative hazard of internal defects and repair regions requires a special discussion. It is shown experimentally, that the technological operations for removal of the weld defective metal and subsequent repair welding of this area leads to the appearance of additional reactive stresses whose level is decreased with the increase in the length of the area repaired and with the decrease in the removal depth. It was established analytically and experimentally that most root defects in multipass welds do not practically propagate due to compressive residual stresses in these zones. Therefore, the optimizing of design and technological solutions from the point of view of reduction in repair works becomes feasible in principle.

The numerous theoretical and experimental investigations on assessment of a degree of hazard and allowance of different kinds of defects, necessity and expediency in their repair, and also expertise of defects, occurring during service of the offshore structures, contributed to the feasibility of development of the required standardized documentation and keeping the design and technological strength at the level which guarantees the safe service of the structures.

Requirements to the toughness and cold resistance. Problems of assurance of a brittle strength of welded joints, first of all, of IRDR and ice breakers differ essentially from similar problems which are solved by the methods of fracture mechanics in the nuclear power engineering, when designing structures of pressure vessels type, etc. From the one hand, thicknesses here are relatively small and there are possibilities to make allowances for the reserves of the materials toughness which are associated with a difference in the stressed state at the front of the crack caused by the limiting rigid conditions of a plane deformation. From the other hand, the feasibility of existing defects of large sizes, which exceed significantly the thickness of the structure elements, dynamic conditions of loading, high level of RWS are the factors leading to the necessity in evaluating conditions which will prevent the brittle fractures and in formulating the strict enough requirements to the toughness and cold resistance of the materials used. From the positions of the fracture mechanics, the problem is specific in the necessity to take into account a mixed nature of the SSS at the crack front, a presence of its stable growth using characteristics of non-linear mechanics of fracture (CTOD, critical values of J-integral) in the course of the experimental determination of the crack resistance of the materials.

The calculated modelling of possible mechanisms of brittle fracture of elements of welded non-heat-treatable structures demonstrates the necessity in using different limiting states during assessment of a brittle strength and appropriate criteria:

- criterion of prevention of a crack initiation (brake-out). It is rational to use it, for example, for elements of structures of deep-water equipment and in other cases when the expected sizes of the calculated defect do not exceed the structure element thickness;
- criterion of prevention of transition to an instable fracture. It should be used in cases when the size of the calculated defect in the form of a through crack is assumed to exceed significantly the thickness of the structure element. Such limiting state should be considered, for example, for the IRDR elements with a high level of design stress concentration and a high cyclic loading. In these cases it is rational to take into account the feasibility of a multiple increase in loading at a stable crack growth, and the use of the criteria of a crack initiation (brake-out) is seemed to be rather conservative;
- criterion of a brittle crack arresting. It is formulated not with respect to any size of the calculated defect as a basic temperature criterion of tough-brittle transition for the material of the structure elements subjected to a dynamic loading (for example, ice belt of the IRDR).

Criterion of prevention of the crack initiation (brake-out) is formulated with respect to the conditions of a plane deformation in the form of requirements to the level of a relative crack resistance β:

$$\beta = \frac{1}{t}\left(\frac{K_{1c}}{\sigma_{0.2}}\right) = \frac{1}{t}\frac{J_{1c}E}{\sigma^2_{0.2}} \ge [\beta],$$

where t is the thickness; $\sigma_{0.2}$ is the yield strength of the material; K_{1c} is the critical value of SIF; J_{1c} is the critical value of J-integral; $[\beta]$ is the regulated level of β. From the results of modelling the conditions of a static fracture of the structure elements with crack-like defects, the conditions of adaptability of the material were determined. The value $[\beta]$ is set within the range from 0.4 to 1.2 depending on structure purpose, kind of loading, expected level of RWS. Correlation between the

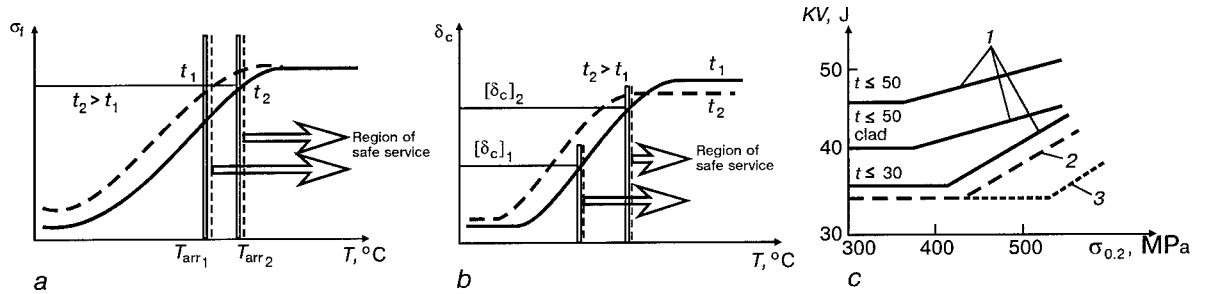

Figure 5. Assurance of service life and reliability of IRDR structures: *a* — ensuring of conditions of crack arresting; *b* — prevention of conditions of crack initiation (brake-out); *c* — quality control of metal using standard Charpy specimens; *1* — parent metal; *2* — manual welding; *3* — automatic welding; *t* — thickness of prefabrication used, mm

level of energy of impact KV and value K_{1c} for steels with yield strength in the range of $\sigma_{0.2}$ = = 400 – 1600 MPa was investigated; the mathematically-expected estimates correspond to the formula $K_{1c}[\text{MPa}\sqrt{\text{m}}] = 21\sqrt{KV[\text{J}]}$. The given approach makes it possible to regulate the level KV for the structure elements as a function of thickness, material strength, peculiarities of the technology, purpose and degree of their responsibility (Figure 5) [9].

Criterion of prevention of the instable fracture at a preset size of the calculated defect is formulated in the form of requirements to the CTOD parameter determined in accordance with the standards. There is no direct correlation of this parameter with KV level: within the region of temperatures of a tough-brittle transition, CTOD drastically depends on the thickness of a prefabrication, that causes the need in testing metal in a full-scale thickness during its certification. Proposals on differentiating requirements to CTOD for the parent metal and material of the welded joints depending on thickness, strength and category of responsibility of the structure element have been developed on the basis of the results of investigations of the processes of a stable growth of the cracks and instable fracture, which is accompanied by changing its micromechanism. The relation of temperatures corresponding to the CTOD level with a temperature of the crack arresting was analyzed.

A series of theoretical and experimental investigations of the resistance of the ship hull steels to the brittle fracture, establishment of interrelation of limiting states with category (or degree of responsibility) of the structure elements, comparative investigation of standardized approaches of different classification societies contributed to the development and suggestion of scientifically-grounded requirements to the materials used in construction of IRDR.

Experimental assurance. Assurance of strength and fatigue life of welded elements of a deep-water machinery and off-shore constructions cannot be based only on the theoretical developments but requires also the obligatory experimental confirmation. The comprehensive investigations carried out within the scope of the above-mentioned direction, accumulation of data on actual characteristics of fracture resistance of ship hull materials and welded joints were performed at unique-equipped experimental laboratory of «Promtest KM» of TsNII KM «Prometey». The laboratory was created in the 1980s on the base of versatile test machines of company «Shenk» (26 units of equipment) with a wide range of generated forces (from 10 to 8000 t) and a computer system of control of the test process and recording of information which can reproduce the complex service spectra of loading. The laboratory is accredited for technical competence and independence in Gosstandart of Russian Federation and Russian Navy Register of navigation. Over many years this laboratory carries out the research and expertise works for shipbuilding and different branches of engineering, as well as certification tests. To provide the attestation of materials by the parameters of crack resistance in accordance with a world level, the works were made on the creation of branch methodologies and series of tests were made for the domestic and foreign customers (including tests under the supervision of representatives of foreign classification societies). The methods of determination of temperatures of tough-brittle transition and crack arresting for the metal of large thicknesses (> 20 mm) were mastered. For this purpose, in particular, a unique vertical impact testing machine of 18 kJ capacity has been created.

Combination of new theoretical and calculation-analytic approaches with wide experimental capabilities will contribute to the solution of complex problems of design-technological strength of the deep-water machinery and structures of the off-shore constructions at the level of existing world requirements.

CONCLUSIONS

The described problems of assurance of design-technological strength of structures of the off-shore constructions and deep-water machinery demonstrate the complex interrelation of technology of their manufacture with a real reliability realized in practice. Solution of the above-given problems

made it possible to develop and to use successfully in service many samples of the off-shore machinery, starting from the nuclear ice breakers «Lenin» and «Rossiya», different modifications of deep-water apparatuses, and also different types of floating, semi-immersed and stationary drilling platforms for production of oil and gas, and finishing by such ships, as «Admiral Kuznetsov». Practical implementation of the developed methodologies and approaches of design-technological designing of hull structures of the off-shore machinery could increase their reliability at the stages of designing, construction and service. The further development of works of this direction is associated with the widening and adaptation of fulfilled research developments for new classes of structures, new materials and new spectra of effects.

REFERENCES

1. Gorynin, I.V., Iljin, A.V., Leonov, V.P. *et al.* (1990) Calculated determination of fatigue life of welded joints with allowance for effect of technological factors. In: *Shipbuilding industry. Series Materials Science. Welding*. Issue 10, 3 – 14.
2. Iljin, A.V., Karzov, G.P., Leonov, V.P. *et al.* (1983) Peculiarities of using the deformation criterion of fracture in assessment of fatigue life of welded joints. In: *Problems of shipbuilding. Series Welding*. Issue 36, 40 – 46.
3. Gatovsky, K.M., Leonov, V.P., Stakanov, V.I. *et al.* (1985) Examination of stressed state of metal after welding and repair of butt joints with multilayer welds. *Avtomaticheskaya Svarka*, **6**, 37 – 40.
4. Karzov, G.P., Leonov, V.P., Margolin, B.Z. (1992) Calculated determination of fields of residual welding stresses in structures of a shell type. *Ibid.*, **3**, 3 – 8.
5. Karzov, G.P., Leonov, V.P., Margolin, B.Z. (1992) Calculated determination of fields of residual welding stresses in structures of a shell type. *Ibid.*, **4**, 7 – 13.
6. Iljin, A.V., Leonov, V.P. (1992) Model of initial stage of damage for calculated estimation of fatigue life in zones of stress concentration. In. *Proc. of XI Int. Colloq. on Mechanical Fatigue of Metals*. Kyiv.
7. Danilov, G.I., Leonov, V.P., Zolotov, V.F. *et al.* (1996) Effectiveness of technological methods of increasing a cyclic life of welded units of ice-resistant stationary drilling rigs. *Voprosy Materialovedeniya*, **2**, 15 – 22.
8. Novozhilov, V.V., Rybakina, O.G. (1985) Examination of propagation of surface cracks at cyclic loads. In: *Proc. of XI Int. Colloq. on Mechanical Fatigue of Metals*. Kyiv.
9. Danilov, G.I., Leonov, V.P., Malyshevsky, V.A. *et al.* (1996) Justification of standardized requirements of cold resistance to steel for ice-resistant drilling rigs, used at the Arctic shelf. *Voprosy Materialovedeniya*, **2**, 5 – 14.

EVALUATION OF RESIDUAL LIFE OF LOAD-CARRYING WELDED STRUCTURES AND EXTENSION OF THEIR SERVICE LIFE

V.I. DVORETSKY
The E.O. Paton Electric Welding Institute, NASU, Kyiv, Ukraine

ABSTRACT

It is shown that service life of welded structures can be extended using safety factors allowed for in design of these structures and based on differences in their actual operating time and assigned life time. The method is suggested to reveal the above safety factors in order to estimate residual life of the structures on the basis of main design parameters affecting it.

Key words: *structure, residual life, service life, operating time, extension, accumulation of fatigue damage, fatigue resistance, durability, calculation.*

There are cases where load-carrying structures (LCS) have exhausted their assigned life time, but they have to remain in operation for some reasons of technical-economic or cultural-historical character. Examples are span structures of bridges, frames of industrial buildings, railway rolling stock, hoisting equipment etc.

At the same time, as shown by practice, premature damage (during the assigned life time) may occur in this type of the LCS. Estimation of residual life and change in the assigned life time of these structures require that the well-grounded package of scientific, technical, organizational and legal measures be taken to assure their safe operation during the newly specified service life. General statements and requirements for the systematic approach to assuring safe operation of the LCS should be based on scientific and technical solutions associated with modification (upgrading) of previous approaches to calculation and design, allowance for duty cycle and operating time of structural members, methods for technical diagnostics and evaluation of materials properties.

The assigned life time T_{as} versus actual operating time T_a is shown in Figure 1. Curve *1* characterizes the calculation data for conditions assumed

in design of the LCS, while the field between curves *2* and *2'* shows the possible operating time of an actual LCS at a probability of damage designated as p_d. There is a relationship between T_{as} and T_a. So, it is justifiable to consider distribution of T_{as} depending upon individual objects. In fact, the T_{as} parameter is determined as the lower limit of variance by prediction of a general set of the LCSs of the type under consideration. Comparing T_a and T_{as} indicates that for the majority of individual objects the safety factors are allowed for as early as at the stage of their design.

To estimate residual life and extend service life, each time we consider a specific LCS, which has already exhausted its assigned life time. In this connection, properties of this structure, including durability, can be specified on the basis of technical examination, as well as analysis of existing damage and its causes. Therefore, service life of the LCS can be extended without any decrease in the degree of its safe operation on the basis of results of estimation of the residual life, allowing for its actual technical condition.

In addition, the possibility of extending the service life of the LCS is determined on the basis of its operation conditions. Curve *1* (Figure 1) was plotted with allowance for the calculated (specified in technical assignment for design of the LCS) operating time of an object. The actual operating time of an individual object may differ substantially from the calculated life time. This also includes the safety factors for residual life of the LCS. Revealing the above safety factors for residual life and extension of the service life of the LCS can be done on the basis of improvement of the calculation methods.

Residual life of many LCSs is determined by their fatigue resistance. Methods for its estimation in design are based on two factors which are of a fundamental importance. The first includes a set of variable operational effects which the LCS withstands, and the second is a capability of the LCS of resisting, without fracture, stresses formed in its members. Both factors are characterized by a substantial spread of values. Therefore, in design made with allowance for these two factors the calculated load and fatigue resistance values are usually based on the safety factors. The rational utilization of the safety factors in design of structures can be an important reason for changing their assigned life time.

Verification of correspondence of fatigue properties of an object to variable loads used in the calculation methods is done in design in a traditional form

$$\sigma_{op} = \sigma_R , \qquad (1)$$

where σ_{op} is the effective variable stress and σ_R is the fatigue resistance. The value of σ_{op} is assumed

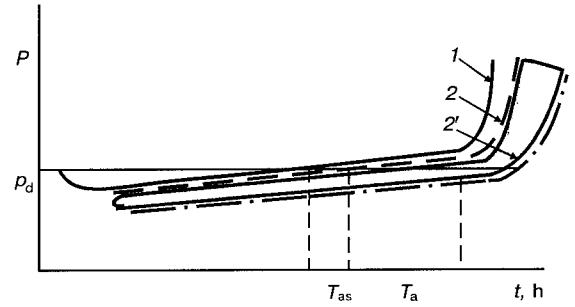

Figure 1. Assigned life T_{as} versus actual operating time T_a of LCS at damage probability p_d: *1* – calculated data; *2*, *2'* – possible operating time to failure for actual structures

to be equal to the stress which is equivalent in its damaging impact to the operational loading conditions of an object, the maximum one of the variable effects or that calculated on the basis of the rated loads [1 – 4]. The possibility of calculating residual life of the LCS depends to a considerable degree upon the method of estimation of σ_{op}.

The probability approach to fatigue analysis of the LCSs [5] enables residual life and reliability indicators to be estimated using the following type of the traditional form of equation (1) as a reference point:

$$D_a \le D_{cr}, \qquad (2)$$

where D_a is the actual stored fatigue damage and D_{cr} is the critical value of the stored fatigue damage. The D_a value is determined as a function of the loading conditions for a member under consideration and time T of operation of a given LCS.

An important peculiarity of the T dependence of D_a is that D_a increases monotonously with an increase in T. Therefore, condition (2) is considered with reference to the calculated time T_c. In this case the safety factor for fatigue resistance during T_c can be treated as the safety factor for stored fatigue damage or as the residual life:

$$\delta = D_{cr} - D_a. \qquad (3)$$

This form of description of the strength condition for machine parts and structural members is often used in calculations described in [6 – 8]. At the same time, a unified representation of conditions of the types of (1) to (3) does not exclude the possibility of applying different approaches to strength analysis. Therefore, to estimate residual life of the LCS and change its assigned life time, it is important to study how these approaches affect the safety factor for δ by accumulation of fatigue damage, as well as the estimation of durability of the LCS.

In fatigue analysis done by the method of permissible stresses [4, 9 – 11] the spread of values of the calculated loads and fatigue characteristics is taken into account conditionally, using safety factor n which is assumed to be the ratio of fatigue limit σ_R to effective stresses σ_e [11 – 13]. The de-

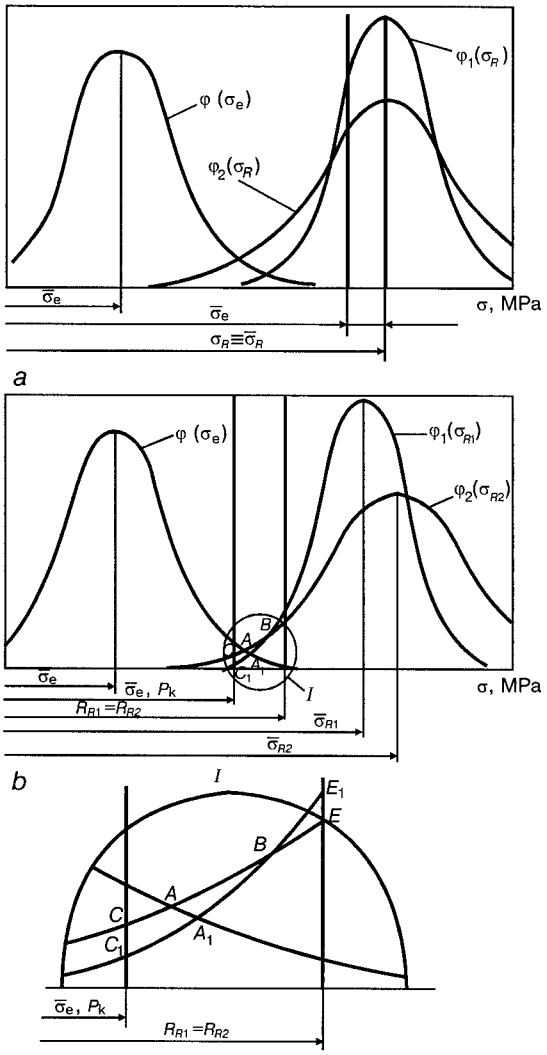

Figure 2. Assignment of σ_R and σ_e in fatigue analysis on the basis of acceptable values of stresses (*a*) and limiting states (*b*)

terminant values of the calculated characteristics σ_R and effective stresses σ_e are used in this case. Fatigue limit σ_R is assumed to be the mean quantity of this value found accurate up to ± 10 MPa. It is thought that factor n similarly converts effective loading cycles σ_e into calculated stresses $n\sigma_e$, i.e. it increases not only the maximum values but also the rest of the cycle components (amplitude, mean value).

The coefficient of asymmetry of calculated stresses, $n\sigma_e$, has the same value as effective σ_e. In addition, the value of σ_e is multiplied by safety factor n, and its amplitude component is increased fy a factor of k, which accounts for the effect of all of the basic factors on the fatigue resistance [10, 12].

In the considered approach to fatigue analysis the objective existing distribution of the fatigue limits is set only by one parameter, i.e. σ_R, and distribution of the effective stresses is replaced by a certain determinant value of $n\sigma_e$. The relationship between actual and assumed values of σ_e and σ_R used in the fatigue analysis are schematically shown in Figure 2. In such calculations the relationship between the safety factor and reliability is rather weak. As a result, the assumed safety factors $[n]$, similar in their values, often yield different reliability of the LCS.

As an example, Figure 2, *a* shows two distributions of the fatigue limits for the similar-type welded members, $\varphi_1(\sigma_R)$ and $\varphi_2(\sigma_R)$, which differ only in the value of standard deviation. Therefore, as to the safety factor, the use of these or those members is of equal worth. Although in practice the members characterized by a distribution of $\varphi_1(\sigma_R)$ with a lower standard deviation are more preferable. The unjustifiably wide limits of variations in the permissible value of the safety factor, $[n] = 1.2 - 2.5$, are attributable primarily to this fact [12].

Comparison of the actual values of σ_e and σ_R with those used in the fatigue analysis, based on the safety factor, allows a conclusion that the method of calculation by the permissible stresses takes an insufficient account for a random character of these values. In fact, fatigue tests of the LCS by the method of permissible stresses provide for a substantial durability margin. This, however, makes almost impossible to minimize its depen-dence upon the individual properties of the LCS.

In the fatigue analysis done by the method of the limiting states, condition (1) is considered in the form of $\sigma_e(\rho_s) \le R_R$. In this case the R_R characteristic is calculated with allowance for statistical fatigue limits of structural members and estimated as a value corresponding to the probability of non-fracture equal to 0.95 at a confidence level of 0.90 [14]. For the probability of fracture of a structure, ρ_s, stresses $\sigma_e(\rho_s)$ are calculated in a similar way. They are estimated from the fatigue curve plotted for the above probabilities and correspond to them [15, 16]. This approach to finding the calculated values of $\sigma_e(\rho_s)$ and R_R takes a certain account for the variance of the σ_e and R_R values.

Comparison between the function of distribution of effective stresses, $\varphi(\sigma_e)$, and the function of distribution of fatigue limits, $\varphi_2(\sigma_R)$, of the member tested, as well as between the calculated values of $\sigma_e(\rho_s)$ and R_R in estimation of fatigue by the method of the limiting states is shown in Figure 2, *b*. In this case the calculations used some determinant values of $\sigma_e(\rho_s)$ and R_R instead of random values of σ_e and R_R, although this imposes considerable restrictions on estimation of fatigue and residual lives of the LCS. This is attributable primarily to the fact that the relationship between values of calculated fatigue resistance R_R and reliability indices depends upon the standard deviation and the type of distribution.

For example, let two similar-type distributions of fatigue limits, φ_1 (σ_{R1}) and φ_2 (σ_{R2}) have the coinciding lower boundaries of variance for the accepted probabilities and, therefore, values of calculated fatigue resistances, R_{R1} and R_{R2}, equal to each other. Then the fatigue analysis by the method of the limiting states using both distributions will lead to the same result.

However, the preference is given to members characterized by distribution φ_1 (σ_{R1}) with a lower standard deviation. This conclusion follows from comparison of probabilities of failure of the members based on description of their properties using distributions φ_1 (σ_{R1}) and φ_2 (σ_{R2}). These probabilities (Figure 2, *b*) correspond to the area below curves $C_1A_1BE_1$ for distribution φ_1 (σ_{R1}) and the area of curvilinear triangle *CABE* for distribution φ_2 (σ_{R2}).

Transition to the fatigue analysis of the LCS using formula (3) and considering the safety factor for durability, δ, to be a random value allow a more substantiated approach to be used to estimation of residual life of the LCSs, based on their operational loading.

To calculate residual life and durability of the LCS, the real processes of variations in operational stresses are simplified and represented by a number of characteristics. The most important of them are the type of the process (periodical, random, etc.), the law $f(\sigma)$ of distribution of operational stresses (normal, exponential, etc.) and values of parameters of the distribution law (mean value $\overline{\sigma}$, standard deviation S_σ, etc.). These characteristics are determined more or less approximately by the results of the experimental investigation of the actual degree of loading of the LCS. Therefore, in estimation of residual life of the LCS, in order to change its assigned life time, it is very important to know how these characteristics affect accumulation of fatigue damage in structural members and their calculated durability.

Equation (2) in a differential form at $D_{cr} = 1$ makes it possible to determine the rate of accumulation of the fatigue damage, dD_a, by the number of cycles and effective stresses σ_i

$$dD_a = \frac{1}{N(\sigma_i)}\, dn(\sigma_i). \qquad (4)$$

Here variable (σ_i) is the characteristic of the calculated effect and expressed in terms of the distribution law $f(\sigma)$. It relates time T of operation of the structure to the level of the accumulated fatigue damage D_a. For this it is necessary to know the total number of cycles, $n_0(t)$, for a certain time t of operation of the structure. Variable $N(\sigma_i)$ is the calculated characteristic of the fatigue resistance of a structural member tested. In practical calculations its values are determined from equations of the fatigue curve. Based on the exponential equation of the fatigue curve with the number of cycles given in the exponent [5, 15, 16], it holds:

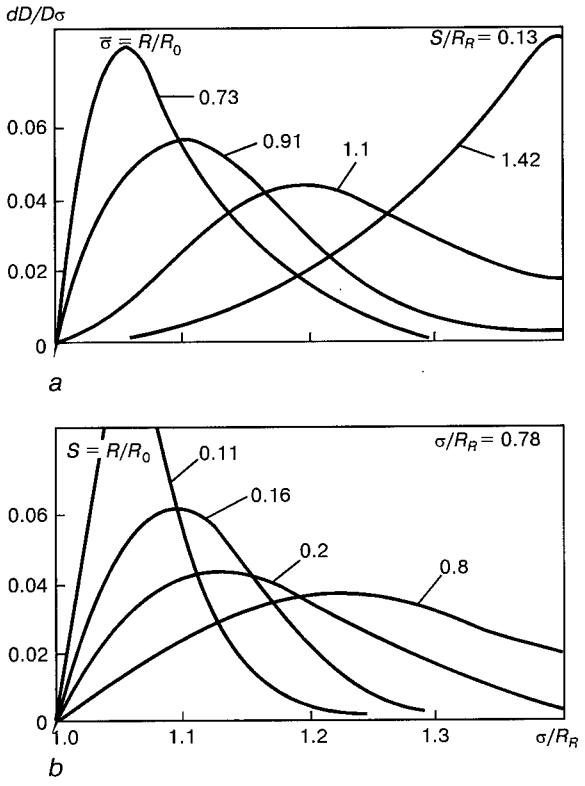

Figure 3. Dependence of the intensity of accumulation of fatigue damage upon σ and S at σ/R_R

$$dD_a = n_0(T)\left[f(\sigma) \Big/ \left(\frac{A}{\ln\sigma - \ln\sigma_R} - B\right)\right] d\sigma, \qquad (5)$$

$$n_0(T) = 1 \Big/ \int_{R_R}^{\max\sigma} \left[f(\sigma) \Big/ \left(\frac{A}{\ln\sigma - \ln\sigma_R} - B\right)\right] d\sigma,$$

where A, B and σ_R are the parameters of the fatigue curve equation.

Formulae (5) enable the calculation analysis of the effect of the type of the law of distribution of operational stresses, as well as characteristics of the fatigue resistance and durability of a structural member, providing that residual life of the LCS is sufficiently grounded.

Analysis performed by V.E. Filatov was done in relative units to facilitate generalization of the results. For this all variables in the loading cycles were measured with respect to parameter B, while cha-racteristics having the dimensions of stresses were measured in fractions of the calculated fatigue resistance R_R. As applied to the normal law of distribution of operational stresses, formulae (5) were represented as follows:

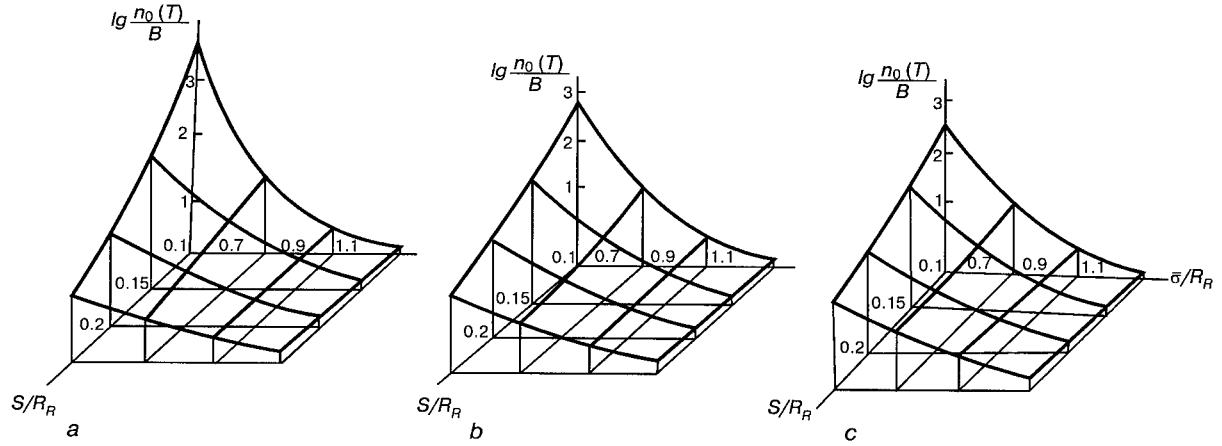

Figure 4. Dependence of durability upon parameters of distribution of stresses: *a* — normal; *b* — logarithmic-normal; *c* — exponential law

$$dD = \left[\frac{n_0(T)\,R_R}{\sqrt{2\pi}\,S_\sigma F_R} \Big/ \left(\frac{A}{\ln\sigma_i - \ln\sigma_R} - B\right)\exp\frac{(\sigma_i - \bar{\sigma})^2}{2S_\sigma^2}\right] d\left(\frac{\sigma}{R_R}\right),$$

$$n_0(T) = 1 \Big/ \int_{R_R}^{\max\sigma}\left[\frac{1}{\sqrt{2\pi}S_\sigma F_R} \Big/ \left(\frac{A}{\ln\sigma_i - \ln\sigma_R} - B\right)\exp\frac{(\sigma_i - \bar{\sigma})^2}{2S_\sigma^2}\right] d\sigma,$$

where F_R is the degree of truncation of the distribution law by stresses. Similarly, formulae (5) can be transformed also for other distributions of operational stresses.

Dependence of the intensity of accumulation of fatigue damage upon the mean value of $\bar{\sigma}/R_R$ of amplitudes of stresses (at a constant standard deviation S_σ/R_R) at the normal distribution law is shown in Figure 3, *a*. Curve *1* was plotted by the results of investigation of the operational loads applied to crane girders at a stripping shop of the metallurgical plant. The curve shows that the major part of fatigue damage is caused by stresses close to the calculated fatigue resistance R_R of a tested member. At the same time, stresses which exceed R_R by 20 % and more have no marked effect on durability of the crane girders. To compare, the Figure shows for the same girders the curves plotted by the hypothetical loads with the $\bar{\sigma}/R$ values equal to 0.91, 1.10 and 1.42. They are of interest because they characterize loading conditions by the intensity of accumulation of fatigue damage.

Dependence of the intensity of accumulation of fatigue damage upon the variance of operational stresses is shown in Figure 3, *b*. An increase in standard deviation S_σ (at constant $\bar{\sigma}/R_R$) is accompanied by a shift of the major part of the stored fatigue damage $dD/d\sigma$ to the region of increased stresses σ_i. The higher the values of static parameters of distribution of $\bar{\sigma}$ and S_σ, the higher the contribution of increased stresses close to the maximum possible ones into accumulation of fatigue damage. This relationship persists also for other laws of distribution of operational stresses, e.g. for the logarithmic normal and exponential distribution of operational stresses. At the same time, each of the distributions has its own peculiarities. In particular, in distribution of stresses following the exponential law the intensity of $dD/d\sigma$ is almost independent of the mean value of $\bar{\sigma}$, if $\bar{\sigma} \le R_R$.

In estimation of residual life of the LCS, the curves of the intensity of accumulation of fatigue damage make it possible to substantiate the calculated loading conditions and investigate the effect of their parameters on durability of the structures. Figure 4 shows the generalized dependence of durability $n_0(T)/B$ upon the mean value of $\bar{\sigma}$ and standard deviation S_σ for the normal, logarithmic-normal and exponential distributions. It follows from this Figure that the accuracy of estimation of S_σ has a pronounced effect on the calculated durability only at comparatively low mean values of $\bar{\sigma}$. At $\bar{\sigma} > R_R$ the variance of operational stresses has a very slight effect on durability of structural members. An important peculiarity of the above regularities (Figures 3 and 4) is that they allow quantitative estimation of the dependence of durability of the LCS upon the materials used (R, $[\sigma]$), design-technology solutions (R_R, σ_R) and operational loads ($\bar{\sigma}$, S_σ).

The procedure suggested for analysis of accumulation of fatigue damage in estimation of residual life of the LCS enables the comprehensive investigation of the dependence of durability upon all basic factors which determine fatigue resistance of the LCS. This procedure makes it possible to reveal general principles of the effect of characteristics of operational loading and fatigue resistance of structural members on reliability and durability of the LCS, as well as to realize the differential approach to accuracy of rating of each of the calculated values in order to substantiate residual life of the LCS.

REFERENCES

1. Meisner, B.A., Belousov, V.N. (1986) Methods for calculation of fatigue resistance of welded structures of the railway rolling stock. In: *Statistical problems of strength and dynamics of machines*. Riga: RPI.

2. (1972) *Specifications for strength analysis and design of the 1520 mm railway track cars (non-self-propelled) for the Ministry of Transport*. Moscow: VNIIZhT.
3. Evgrafov, G.K., Lyalin, N.B. (1962) *Design of bridges based on limiting states*. Moscow: Transzheldorizdat.
4. (1967) *Specifications for design and fabrication of welded structures of locomotive bogies*. Moscow: TsNII MPS.
5. (1990) *Strength of welded joints under alternating loads*. Ed. by V.I. Trufyakov. Kyiv: Naukova Dumka.
6. Bolotin, V.V. (1971) *Application of methods of the theories of probability and reliability in strength design of building structures*. Moscow: Strojizdat.
7. Gladky, V.F. (1982) *Probability methods for design of flying vehicle structures*. Moscow: Nauka.
8. Ratsiu, M., Shults, T. (1977) Analysis of reliability of welded joints under random loading. In: *COMECON Information Letters*. Kyiv: Naukova Dumka.
9. Gokhberg, M.M. (1976) *Metal structures of hoisting vehicles*. Leningrad: Mashinostroyeniye.
10. (1971) *Welded structures of locomotive bogies (basic principles of design and fabrication)*. Ed. by K.P. Korolev. Moscow: Transport.
11. Serensen, S.V., Kogaev, V.P., Shneiderovich, R.M. (1963) *Load-carrying capacity and strength design of machine parts*. Moscow: Mashgiz.
12. Kogaev, V.P., Markhutov, N.A., Gusenkov, A.P. (1985) *Strength and fatigue life design of machine parts and structures*. Handbook. Moscow: Mashinostroyeniye.
13. (1961) *Strength under non-stationary conditions*. Ed. by S.V. Serensen. Kyiv: AN USSR.
14. Dvoretsky, V.I. (1984) Calculation of residual life of welded metal structures under random loading. *Nadyozhnost i Dolgovechnost Mashin i Sooruzhenij*, **5**, 40 – 47.
15. Dvoretsky, V.I., Burenko, A.G. (1982) Estimation of service life of welded joints affected by variable compression. *Avtomaticheskaya Svarka*, **5**, 11 – 15.
16. Dvoretsky, V.I., Mikheev, P.P., Shonin, V.A. (1984) *A procedure of fatigue analysis of aluminium structures welded joints*. Kyiv: AN USSR.

APPLICATION OF LEAK-BEFORE-BREAK CONCEPT FOR PROVISION OF THE SAFETY OF WWER-1000 TYPE REACTORS

A.S. ZUBCHENKO[1], **G.S. VASILCHENKO**[1] and **Yu.G. DRAGUNOV**[2]
[1]SRC TsNIITMASh, Moscow, Russia
[2]«Gidropress» EDTB, Podolsk, Russia

ABSTRACT

A program of R&D on substantiation of applicability of leak-before-break concept to nuclear reactor piping has been outlined and fulfilled. J–R curves measured on full-scale samples cut out of a welded pipe with the working cross-section of 70 by 250 mm with through-thickness and semi-elliptical cracks in the circumferential weld metal were compared with similar curves derived on ST-1T compact samples. It is found that the parameters of plastic fracture toughness measured on ST-1T samples are characterised by a higher level of reliability compared to those of full-scale samples.

Key words: *reactor, strength, weld, crack, cyclic crack resistance, piping safety.*

The concept of «leak-before-break» (LBB) has been more and more often used over the last years instead of the guillotine fracture concept, in the local and foreign practice of designing nuclear power reactors and upgrading the equipment of the operating NPP, thus permitting a considerable cost reduction in construction of the new NPP and improvement of the safety of the currently operating ones.

The LBB concept is based on the known fact that propagation during operation of a non-through-thickness defect present in the piping and its development into a through-thickness defect, will not result in complete fracture, if the length of the through-thickness defect does not exceed a critical value. In this case it is important to detect the leak in time and shut-down the reactor to perform repair or replacement of part of the piping.

As the start of 1990 «Gidropress» EDTB, TsNIITMASh, NIKIET and TsKTI organisations put together a program of research and development work aimed at demonstrating the applicability of LBB concept to the bimetal piping of the main circulation circuit (MCC) of WWER-1000 type reactor of 10GN2MFA steel with 850 mm inner diameter and 70 mm wall thickness.

MCC piping was selected because of the greatest cross-section and working medium which is the primary circuit water in it. More over, its fracture would have had the most adverse impact on the surrounding equipment and building structures.

The research program consisted of the following main sections:

analysis by calculation of the limit condition of D_n 850 piping with the surface and postulated through-thickness cracks, based on the accepted

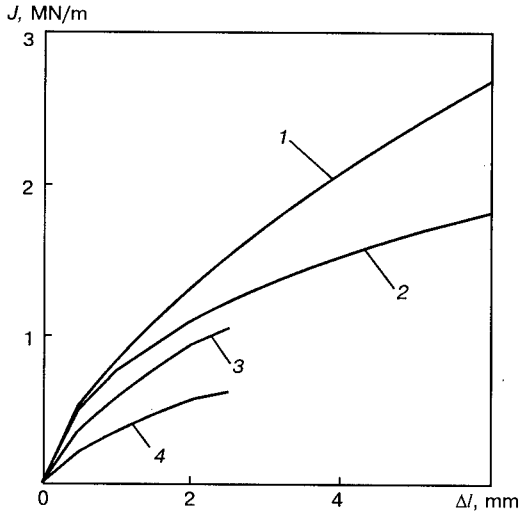

Figure 1. Comparison of J–R curves measured in testing samples of various types: *1* — full-scale with a through-thickness central crack, T = 20 °C; *2* — full-scale with a surface central crack, T = 20 °C; *3, 4* — compact ST-1T at T = 20, 320 °C, respectively; Δl — crack growth

standard characteristics of the materials for determination of the conditions of stability and critical size of the crack;

determination of the standard mechanical properties, as well as characteristics of static and cyclic crack resistance of the actual circumferential welded joints of D_n 850 piping;

statistical analysis of distribution of the mechanical properties of the piping material of foreign-made 10GN2MFA steel used in fabrication of WWER-1000 type reactors;

analysis of the fabrication technology, as well as defect level of MCC piping of WWER-1000 type reactor;

TsNIITMASh testing full-scale samples of the actual thickness with through-thickness and surface cracks, cut out of pipes with circumferential welds made by the standard technology in PO «Atommash» and PO «Izhorsk Zavod» in order to generate data on the static and cyclic crack resistance;

TsKTI determining the conditions of loss of tightness and instability of the actual pipe with a through-thickness crack of a postulated size in a circumferential weld, subjected to bending and inner pressure.

The results of unique testing of the full-scale samples and the actual pipe were used for substantiation of the applicability of LBB concept to D_n 850 piping and the required margins on the dimensions of the postulated crack relative to the critical value. They also served as the basis for the elaborated as a result of the program fulfilment, M-TPR-01–93 standard on design of NPP piping in Ukraine in terms of LBB concept.

Let us consider in greater detail some elements of the above program and the results of the subsequent experimental investigations.

Testing full-scale samples. Testing of 70 × × 250 × 2000 mm full-scale samples produced in PO «Atommash» by the standard technology, which were cut out of a straight pipe with through-thickness and surface cracks in a circumferential weld, was performed in TsNIITMASh testing machine MCC 10.OS of Schenk company [1] at 20 °C under the following conditions:

cyclic testing of each sample in tension for inducing fatigue cracks initiating from a through-thickness or surface notch in a circumferential weld;

tensile loading of samples with cracks for static growing of the fatigue crack;

periodical unloading of the sample and cyclic loading to create a mark indicating the extent of static growing of the crack after each stage of static loading;

sample failure in tension after a considerable static growing of the crack.

Comparison of the results of testing the full-scale and compact samples. ST-1T samples with cracks in the weld metal located in the weld axis plane were cut out of the remaining part of the D_n 850 circumferential welds after the full-scale samples have been cut out, and were tested at 20 and 320 °C. Analytical processing of the results of testing the compact and full-scale samples with the aim of plotting J–R curves was performed by the methods set forth in [2 – 8].

J–R curves derived in testing the full-scale samples with through-thickness and surface cracks at 20 °C, as well as compact samples at 20 and 320 °C, are given in Figure 1. Comparison of J–R curves plotted from the results of testing these types of samples at 20 °C, revealed the following features.

At the same extent of the crack growing the smallest values of J were recorded for the compact samples, the greatest for the full-scale samples with through-thickness cracks, and the intermediate ones for the full-scale samples with surface cracks. Therefore, for a reliable substantiation of the strength of welded joints of D_n 850 piping, use of the most conservative J–R curves derived in testing compact ST-1T samples can be recommended.

It should be noted that testing of the second series of full-scale samples cut out of the test model made in PO «Izhorsk Zavod» of a foreign-made bimetal pipe with through-thickness and surface cracks not only in the circumferential weld, but also in the base metal and the HAZ metal, confirmed the earlier formulated conclusion as J–R curves of the welds produced in PO «Atommash» and PO «Izhorsk Zavod» were similar, and J–R curves of the base metal and the HAZ metal had higher parameters.

Investigation of cyclic crack resistance. Study of the rate of crack growth in the metal of the weld of D_n 850 piping under cyclic loading was per-

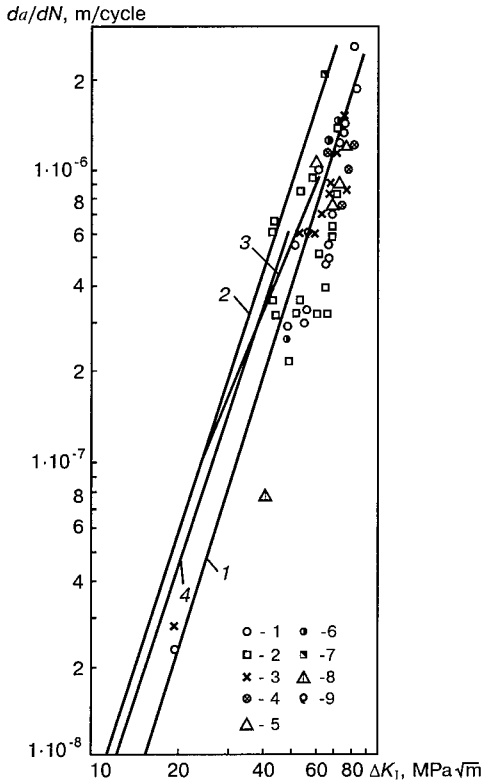

Figure 2. Rate of crack growth in the metal of the weld of D_n 850 piping of 10GN2MFA steel: *1* – *4* — samples with surface cracks; *5* – *9* — samples with through-thickness cracks (18 × × 12 × 160 mm bend testing samples) (*1* — f = 15 Hz; *2* — f = = 1 Hz; *3* — ST-1T at f = 10 Hz; *4* — 10 × 60 mm at f = = 20 Hz)

formed in air at 20 °C on small-sized samples tested by tension and bending, as well as full-scale samples with the through-thickness and surface cracks. It was found that the parameters of cyclic crack resistance measured on full-scale and small standard samples, were identical. The summarised data from all the testing are given in Figure 2. Averaged data on the crack growth rate, should be described by the following expression:

$$da/dN = 2.1 \cdot 10^{12} (\Delta K_I)^{3.1},$$

where a is the crack size by the depth; N is the cycle number; K_I is the coefficient of stress intensity.

For a reliable evaluation allowing for the scatter data, it is recommended to use the following expression:

$$da/dN = 4.75 \cdot 10^{12} (\Delta K_I)^{3.1},$$

where a is measured in meters, ΔK_I in MPa·m$^{0.5}$.

Calculation-based substantiation of applicability of LBB concept to MCC piping of WWER-1000 type reactor. Calculation was performed in keeping with the principles of the procedure of [9] and published in paper [10]. The size of the postulated crack $2l_0$ (130 mm) for a specified flow rate of 3.8 l/min of the heat-transfer medium

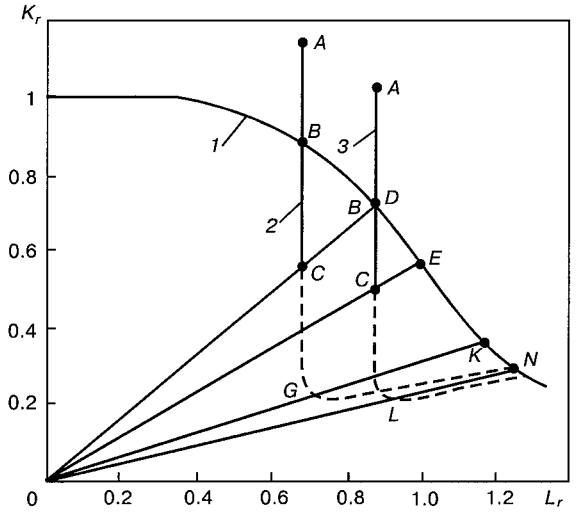

Figure 3. Analysis of the stability of a through-thickness crack in D_n 850 piping by the procedure of R6 method [12]: *1* — fracture evaluation curve; *2* — load (NOC + MCE); *3* — loads *1*, *4* (NOC + MCE)

through a through-thickness crack with introduction of a tenfold margin, was determined for the case of the crack location along the axis of a circumferential weld of D_n 850 piping. It was necessary to prove that a crack of a length two times greater than the postulated value ($2l$ = 260 mm) maintains its stability under loads of the first calculated case, i.e. for the normal operational conditions (NOC) and the maximal calculated earthquake (MCE), as well as that the crack of $2l_0$ size is stable under loads of the second calculated case, which are by 1.4 times higher than the loads in NOC + MCE.

From the calculation it was determined that in the NOC + MCE mode the axial membrane stresses are σ_m = 64 MPa, while bending stresses are σ_t = = 184 MPa [11]. Calculation was performed in keeping with the first method of R6 procedure [12]. The following values of guaranteed mechanical properties at 350 °C temperature were accepted for it: $R_{p0.2}$ = 294 MPa, and R_m = 490 MPa.

J–R curve for 320 °C temperature derived in testing compact samples (Figure 2) was used as the most conservative one described by the following expression:

$$J = 0.311 \cdot \Delta l^{0.705}.$$

The calculation results demonstrate (Figure 3) that the stability of the postulated in the D_n 850 piping weld through-thickness cracks $2l$ = 260 mm for the first calculated case and $2l_0$ = 130 mm for the second case, has been proved.

Evaluation of the critical length of the crack when a plastic hinge in the section of the cracked pipe is achieved as the limit state, yields $2l_c$ = = 828 mm for the first calculated case and $2l_c$ = = 532 mm for the second calculated case. One can see that the ratios of the critical dimensions of the

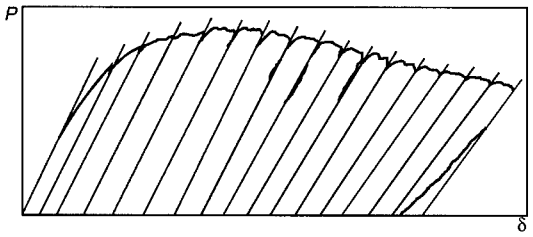

Figure 4. An example of recording the load-displacement diagram in testing ST-1T samples (P — load, δ — displacement)

cracks to the dimensions of those postulated in both calculated cases, greatly exceed the criterial coefficient of 2 accepted in the local [9] and foreign [13] codes.

The performed analysis indicated that the criteria of LBB concept are satisfied for MCC piping of WWER-1000 type reactor.

Mastering the method of experimental determination of plastic fracture toughness parameters. The conclusion on the suitability of J–R curves derived in testing the compact ST-1T samples for a reliable substantiation of applicability of LBB concept to thick piping joints, formulated above, necessitated mastering the method of experimental determination of the plastic fracture toughness parameters. This requirement arose from the need to derive guaranteed J–R curves for certain zones of welded joints of piping of various typesizes, for which the applicability of LBB should be substantiated. When J–R curves of individual zones of the welded joint were derived, their significant scatter was recorded. Therefore, 8 to 12 samples are to be tested for a reliable calculation of the lower envelopes of J–R curves of the studied zone at a certain temperature. The lower envelope of the derived field of the values scattering should be regarded as guaranteed, and it should be used to determine the parameters of plastic fracture toughness by the crack starting J_c and growth $J_{0.2}$ by 0.2 mm.

The main difficulty in plotting the J–R curves is determination of the current length of the crack. Analysis of the existing methods of its determination showed the method of partial unloading to be the most productive and efficient (Figure 4). It, essentially, consists in that the compact sample loaded by a growing force is periodically subjected to partial unloading in the plastic region, while the change in the compliance at unloading is used for calculation of the current crack length. Knowing the force achieved at each loading, and the calculated size of the crack in testing one sample with an induced fatigue crack, 15 to 20 points are derived to plot the sought J–R curve.

A standard compact sample was selected for performance of such testing. After inducing the initial fatigue crack, lateral notches were made in it of the total depth of 20 % for stabilisation of the movement plane at static growth of the crack. Then the sample was subjected to cyclic loading for recording the final dimension of the static growth of the crack and broken completely.

Calculation of J–R curves was performed in a computer by a specially developed program based on the procedure of [14] which allows for the change in the samples compliance at unloading. Moreover, the program envisaged calculation of J-integral by the local method [2] using the crack length determined by the compliance method. Comparison of J–R curves calculated by the methods given in [2] and [14] showed that at the initial stage within the validity square, J–R curves practically coincide, and then diverge. As the results derived by the procedure of [14], are more conservative, J–R curves calculated by this procedure are given **and compared further on.**

Determination of the parameters of plastic fracture toughness of the welded joint of the main D_n 630 steam piping. The procedure of determination of plastic fracture toughness parameters was mastered on a welded joint of a pipe of 16GS pearlitic steel of 630 mm diameter and 27 mm wall thickness applied in fabrication of the main D_n 630 steam piping of WWER-1000 type reactor. A nonsymmetrical circumferential weld was welded on the pipe by the standard technology with UONI 13/55 electrodes. Tensile testing of samples at 20 and 300 °C permitted establishing practically the same properties in the circumferential and axial directions of the base metal. The deposited metal, however, turned out to be much (by almost 1.5 times) stronger than the base metal.

Analysis of the serial impact toughness curves permitted determination of the critical brittleness temperatures $T_{c.b}$ of all the zones of the welded joint. Base metal $T_{c.b}$ values were equal to −50 °C, and those of the weld and HAZ metal to −20 °C.

Compact ST-1T samples were cut out of the welded joint so that the notch passed in the circumferential direction through the base metal, weld metal and HAZ metal and were tested at 20 and 300 °C. The derived J–R curves demonstrate a considerable scatter of the values. In this case, despite a relatively lower strength of the weld metal, the base metal has the highest values of J–R curves compared to those of the weld metal.

The values of J–R curves of the HAZ metal take an intermediate position. With such a scatter of values of J–R curves, it is recommended to use in practical calculations, the lower envelope of this scatter, expressed by the following equation:

$$J = A\,\Delta a^{B} \exp\,(C/\Delta a^{0.5}). \qquad (1)$$

A, B, C parameters for the studied zones of the welded joint of 16GS steel at 20 and 300 °C are given in Table 1.

Crossing of the curves of equation (1) with the lines which are at 0.2 mm distance from the defect to blunting lines, determined $J_{0.2}$ values corre-

Table 1. Main parameters of J–R curves of the welded joint of D_n 630 steam piping of 16GS steel of WWER-1000 type reactor

Welded joint zone	*Testing temperature, °C*	$J_{0.2}$, *kJ/m²*	*Approximation parameters from equation (1)*		
			A	*B*	*C*
Base metal	20	553	2221.0	0.0896	−1.3060
	300	200	481.2	0.2000	−0.4840
HAZ	20	228	688.8	0.2350	−0.6661
	300	150	242.5	0.2591	−0.1506
Weld metal	20	222	598.5	0.3249	−0.4553
	300	130	252.3	0.2207	−0.2352

sponding to the crack growing by 0.2 mm in the studied zones of the welded joint of 16GS steel.

Determination of the parameters of plastic fracture toughness of an austenitic welded joint of D_n 300 and D_n 350 piping. A feature of fabrication of D_n 300 piping of the system of automatic cooling and protection (SACP) and of D_n 350 piping of the cooling circuit (CC) of WWER-1000 type reactor, of 10GN2MFA pearlitic steel, consisted in the impossibility of applying the technology of welding with pearlitic welding consumables developed for D_n 850 piping of MCC of WWER-1000 type reactor. In D_n 850 piping after the circumferential welds had been made, the anticorrosion austenitic clad layer was restored by manual wel-ding from the inside, as a welder could fit in there with the pipe diameter of 850 mm, unlike the piping of 300 to 350 mm diameter. Therefore, a technology of welding the circumferential welds of pearlitic pipes from the outside with austenitic consumables was developed and applied in fabrication of SACP and CC piping.

Experimental studies were performed on the material of a test pipe of CC D_n 350 of WWER-1000 type reactor, welded by the standard technology in the Podolsk Machine-building Plant from pieces of three bimetal pipes of foreign-made 10GN2MFA pearlitic steel. These pipes had (according to certificate data) the lowest, intermediate and highest values of strength properties (within the range of the specification requirements). Pipe sections were welded by two circumferential welds (symmetrical and asymmetrical) by the manual arc process with austenitic electrodes of EA-400/10T grade after special two-layer facing of the pipe section edges.

Samples for tensile testing at 20 and 350 °C, Charpy impact samples and compact ST-1T samples for testing at 20 and 350 °C were cut out of the base metal, weld metal and HAZ metal of the test pipe and tested.

The results of testing standard samples demonstrated the compliance of the base metal and the metal of austenitic welds of the test pipe to the specification requirements. Experimental diagrams of deformation of the samples in tensile testing of the base metal, turned out to be similar both in the axial and the circumferential direction. Therefore, all of them were processed by the least squares method and presented in the form of Ramberg-Osgud diagram. For the base metal they have the form $\bar{\varepsilon} = \bar{\sigma} + 1.65\sigma^{-10.04}$ at the temperature of 20 °C and $\bar{\varepsilon} = \bar{\sigma} + 1.03\sigma^{-10.72}$ at 350 °C; for the weld metal at 20 °C $\bar{\varepsilon} = \bar{\sigma} + 1.90\sigma^{-9.76}$ and at 350 °C $\bar{\varepsilon} = \bar{\sigma} + 2.48\sigma^{-7.82}$.

The results of testing the Charpy samples showed that the materials of the test pipe also meet the specification requirements. The measured values of impact toughness and plastic component in the fractures of the tested samples permit the statement to be made that the critical brittleness temperatures $T_{c.b}$ of all the three samples of pipes of 10GN2MFA steel are below 70 °C. Compact ST-1T samples (56 pcs.) after inducing fatigue cracks and making lateral notches were subjected to static loading accompanied by a 12- to 20-fold partial unloading and processing by the procedure described above.

The derived values of J–R curves demonstrated considerable scatter. They were systematised in six groups for each of which the lower envelope was plotted. The plastic fracture toughness parameters J_c, $J_{0.2}$ and the mathematical expressions describing the lower envelopes, are given in Table 2.

The plastic fracture toughness parameters derived from the lower envelopes, express guaranteed properties of the studied zones of the austenitic welded joint at 20 and 350 °C and are recommended for substantiation by calculation of the applicability of LBB concept to SACP D_n 300. and CC D_n 350 of WWER-1000 type reactor.

It should be noted that $J_{0.2}$ values given in Table 2, are determined with a much greater accuracy than J–R parameters, because of a greater slope of J–R curves in the points of their crossing the defect blunting line.

CONCLUSIONS

1. A program of work on experimental and design substantiation of the applicability of LBB concept to D_n 850 piping of WWER-1000 MCC has been

Table 2. Main parameters of J–R curves of a welded joint on D_n 350 pipe of 10GN2MFA steel in CC of WWER-1000 type reactor

Welded joint zone	*Testing temperature, °C*	J_c, *kJ/m²*	$J_{0.2}$, *kJ/m²*	*Approximation parameters from equation (1)*		
				A	*B*	*C*
Base metal	20	483	729	1281	0.306	−0.5000
	350	190	322	449	0.530	0.0043
HAZ	20	408	523	757	0.264	−0.2300
	350	232	410	740	0.045	−0.4480
Weld metal	20	176	274	412	0.321	0.0823
	350	59	111	169	0.524	0.0926

put together and fulfilled. Comparison of the results of testing full-scale samples with the through-thickness and surface cracks in a circumferential weld with J–R curves derived in testing ST-1T compact samples showed that the smallest values of J at the same values of the crack growth, were found for the compact samples, and the largest for full-scale samples with through-thickness cracks. The intermediate values are characteristic of full-scale samples with surface cracks. This experimental result permitted recommending the use of J–R curves derived in testing ST-1T samples for a reliable substantiation of the strength of welded joints of D_n 850 piping. The parameters of cyclic crack resistance measured in testing the full-scale samples and the small samples for tension or bending, turned out to be identical for the weld metal and it is recommended to describe their results by general dependencies.

2.The calculations performed by the developed procedure [9] using J–R curve measured on ST-1T samples tested at 320 °C proved the stability of cracks postulated for D_n 850 piping, while the critical dimensions of the cracks in the weld metal in relation to those postulated, essentially exceed the values specified by the codes. Thus, it is shown that the criteria of LBB concept for MCC piping of WWER-1000 type reactor are satisfied.

3. An experimental procedure has been mastered of plotting guaranteed J–R curves and parameters of fracture toughness of the studied zones of welded joints, based on allowing for the change in the compliance of a compact sample, measured at partial unloading during the static growing of the crack. The method was tried out in experimental investigation of the zones of circumferential welded joints of D_n 630 main steam piping of 16GS steel and of dissimilar welded joints of D_n 350 piping of volume compensators of WWER-1000 type reactor. Guaranteed J–R curves were derived of the above zones of welded joints at the room and working temperatures, recommended for design evaluation of the applicability of LBB concept to WWER-1000 piping.

REFERENCES

1. Vasilchenko, G.S., Artemiev, V.I., Merinov, G.N. *et al.* (1995) The nature of thickness pipe element testing to validate the application of LBB concept. In: *Transact. of LBB-25.1.* Lion.
2. (1985) *GOST 25-506–85. Calculations and strength testing. Methods of mechanical testing of metals. Determination of the characteristics of crack resistance (fracture toughness) at static loading.* Approv. on 01.01.85.
3. Kanaweera, M.P., Leckie, F.A. (1982) *J*-integrals for same crack and notch geometry. *Int. J. Fracture*, **18**, 3 – 18.
4. Kummar, V., German, M.D., Shin, C.F. (1981) *An engineering approach for elastic fracture analysis.* California.
5. Garwood, S.J. (1979) A method of estimating the value of J_R (the value of J for propagating crack) from a single specimen. *Int. J. Fracture*, **12**, 18 – 21.
6. Takahashi, Y. (1987) Ductile cracks growth test for surface cracked plates of carbon steel STS42. *Criepi Report*, **5**, 35.
7. Yagawa, G., Ueda, H., Takahashi, Y. (1986) Numerical and experimental study on ductile fracture of plate with surface crack. *ASME PVP*, **103**, 43 – 48.
8. Adams, N.H., Garwood, S.J., Robinson, J.N. (1985) Elasto-plastic fracture mechanics applied to the safety assessment of nuclear power station. In: *Transact. of 8th Int. Conf. on Structural Mechanics in Reactor Technology.*
9. (1993) *M-TPR–93. Procedure of calculation of NPP piping in terms of «leak-before-break» concept.* Moscow.
10. Vasilchenko, G.S., Vasnin, A.M., Getmanchuk, A.V. *et al.* (1994) Investigation of fracture resistance characteristics of the weld metal of 10GN2MFA steel. *Tyazh. Mashinostroyeniye*, **11 – 12**, 19 – 29.
11. Kiselyov, V.A., Rivkin, E.Ju., Smirnov, Y.I. *et al.* (1994) Application of leak-before-break concept to integrity and safety of PWR primary piping with WWER-1000. *Nucl. Eng. and Design*, **151**, 400 – 424.
12. Milne, I., Dinsworth, R.A., Dowling, A.K. *et al.* (1986) Assessment of the integrity of structures containing defects. In: *CEGB Report R/H/R6, Rev. 3. UK.*
13. (1984) Evaluation of potential for pipe break. In: *The Pipe Break Group, Report of the US Nuclear Regulatory Commission, Piping Review Committee, NUREG-1061.*
14. (1987) *ASTM E1152–87. Standard test method for determining J–R curves.*

CORROSION-MECHANICAL STRENGTH OF WELDED PIPING OF AUSTENITIC STEELS OF RBMK REACTORS

A.S. ZUBCHENKO, I.L. KHARINA, A.E. RUNOV and V.O. MAKHANEV
SRC TsNIITMASh, Moscow, Russia

ABSTRACT

Corrosion-mechanical strength of welded piping of nuclear reactors equipment of 08Kh18N10T austenitic steel is considered. Numerous circular and axial crack-like defects were detected, which initiate and propagate by the mechanism of intercrystalline stress corrosion cracking. It is found that the main factors which determine the incubation period and intensity of welded joint damage are the level and nature of distribution of residual welding and service stresses, presence of the zones of plastically deformed metal and composition of the medium which is in contact with the inner surface of the piping.

Key words: *piping, welded joint, crack, strength, stresses, corrosion.*

Over the recent years crack-like defects in welded joints of 08Kh18N10T steel, whose nature of propagation is intercrystalline, were recorded during NPP operation, alongside with the damage of the equipment components of austenitic stainless steels caused by transcrystalline corrosion cracking (TCC) as a result of the action of tensile stresses and high-parameter water on the metal (for instance, fracture of the upper rows of heat exchanger pipes of horizontal steam generators of WWER type reactors, etc.).

The total time to appearance of the found cracks, which consists of the incubation period and period of the initiated crack propagation, is equal to 7 to 10 years, on average. The minimal time to appearance of non-through-thickness cracks, recorded by X-ray inspection, is equal to approximately 4 years. Damage is found in welded joints made both in the piping manufacturing plants and under the conditions of erection work performance in NPP. No differences are traceable in the welded joints susceptibility to appearance of such defects, depending on the piping geometry and orientation of welded joints location in them (horizontal and vertical sections). No regularity of defects development in welded joints, depending on the sequence of their welding in the piping, was found, either. Proceeding from all these data, it can be stated that the considered crack-like defects develop in service.

In the US practice the BWR piping in the welded joints of which such defects were found for the first time in 1988, was made of unstabilised ASTM304 (08Kh18N10), ASTM316 (08Kh16N17M3) steels [1]. The piping of BWR type reactors in Germany, in the welded joints of which similar cracks were also detected, is made of stabilised austenitic chromium-nickel ASTM321 (DIN 1.4541, 08Kh18N10T), ASTM347 (DIN 1.4550, 08Kh18N10B) steels [2, 3]. These cracks were first revealed by the methods of NDT in 1991. A special program of monitoring the piping welded joints was developed, the implementation of which later on (1993 – 1994) resulted in detection of numerous cracks, including those formed during the four years after the start of piping operation.

When considering the conditions for crack formation, it should be taken into account that according to the published and experimental data, stabilised austenitic steels of 08Kh18N10T, 321, 347 grades do not demonstrate any susceptibility to intercrystalline corrosion (ICC) when tested in keeping with GOST 6032–75 or by the Strauss method, i.e. they are not sensitised at heating specified by these documents in the range of critical temperatures (650 – 550 °C), also in welding during the short time when the metal of the HAZ stays in this temperature range [3, 4].

It should be noted that prior to the start of the reactor operation, all the piping welded joints were subjected to X-ray inspection (according to OD-428-201, OST 108.004.110–80). Welded joints without cracks or other defects in the HAZ were approved for operation. Just shrinkage cavities were found in the root part of some welded joints.

The results of investigation of the damaged welded joints of D_n 300 piping in the reactors of the Kursk and Chernobyl NPP conducted with participation of TsNIITMASh experts, allowed the following to be stated:

cracks initiate on the welded joints inner surface near the fusion line and propagate for the distance of 0.7 to 1.0 mm from it into the cross-section and for 1/3 of the pipe circumference in the circular direction;

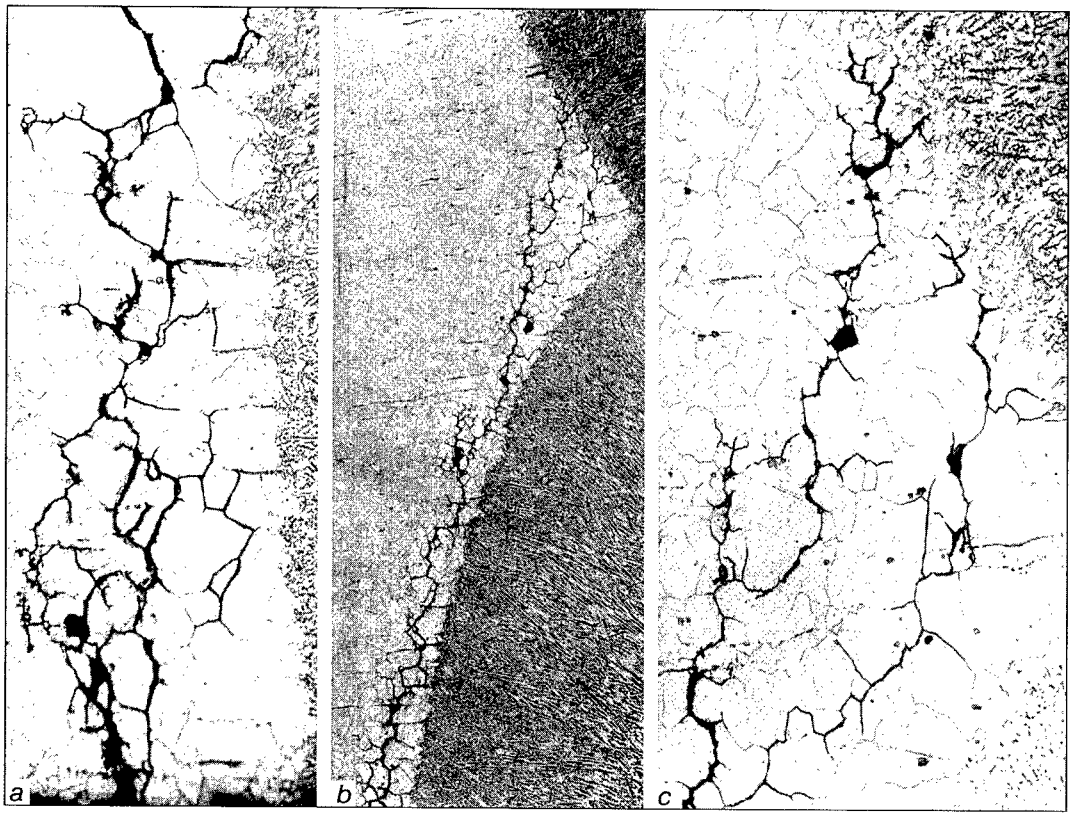

Figure 1. Microstructure of circular service cracks in the HAZ of D_n 300 welded joint: *a* — crack start (×100); *b, c* — crack end (×50 and ×20, respectively) (reduced by 0.75)

visual examination of the template with the area of a circular crack initiation site (15 × 30 mm template from a welded joint of D_n 300 water levelling piping (WLP) of the first reactor of the Chernobyl NPP) showed that the crack which initiates as though in one point (at 1.5 mm distance from the fusion line in the weld root), propagates , predominantly into the base metal and the weld metal (to a smaller degree).

Metallographic investigations made in TsNII-TMASh confirmed the intercrystalline nature of propagation of the circular cracks, found in analysis of the sections at NPP. Their typical appearance (illustrated by a template received from Chernobyl NPP), is shown in Figure 1. It gives an idea about the nature of crack propagation in different areas.

Along the entire length of crack propagation, the HAZ metal is characterised by coarse-grained structure formed under the impact of the high-temperature thermal cycle of welding (TCW) (grain size No.1), while the pipe metal at a distance from the damaged areas, has an austenitic structure with grain size No. 8 – 9. The intensity of intercrystalline cracks propagation along the fusion line in-depth of the pipe section and around welded joint perimeter and crack branching lead to damage of large volumes of the HAZ metal.

Fractographic studies of the fractures made in the crack middle zone, are indicative of the grain boundary nature of such fracture; grain boundaries are smooth with traces of a slight relief. A somewhat distorted grain shape can result from microplastic deformations which precede fracture.

Radiographic analysis of the oxides, also in the crack, showed them to contain chromium, zirconium, niobium, cobalt and manganese isotopes. Particles of a loose non-conducting phase containing zirconium, are also present in the oxides.

Alongside with the numerous revealed circular cracks, in one of the studied WLP welded joints (1987, Kursk NPP) a crack was found during template preparation for metallographic analysis, which propagated into the HAZ base metal from the fusion line normal to the weld (axial crack, oriented along the pipe generatrix). Further on, when special destructive testing of the continuity of the templates cut out of welded joints of D_n 300 piping was conducted (1988, Chernobyl NPP), similar cracks were detected, also propagating into the base metal from the boundary of its fusion with the weld root part.

A detailed metallographic investigation of the nature of axial cracks showed that they initiate in the fusion zone and developing to a limited extent in the metal of the weld root part, mostly propagate into the base metal of the pipe (Figure 2). Propagation of these cracks in the base metal has (similar to circular cracks) a branching, pronounced intercrystalline nature with further development of these cracks in the longitudinal and normal direc-

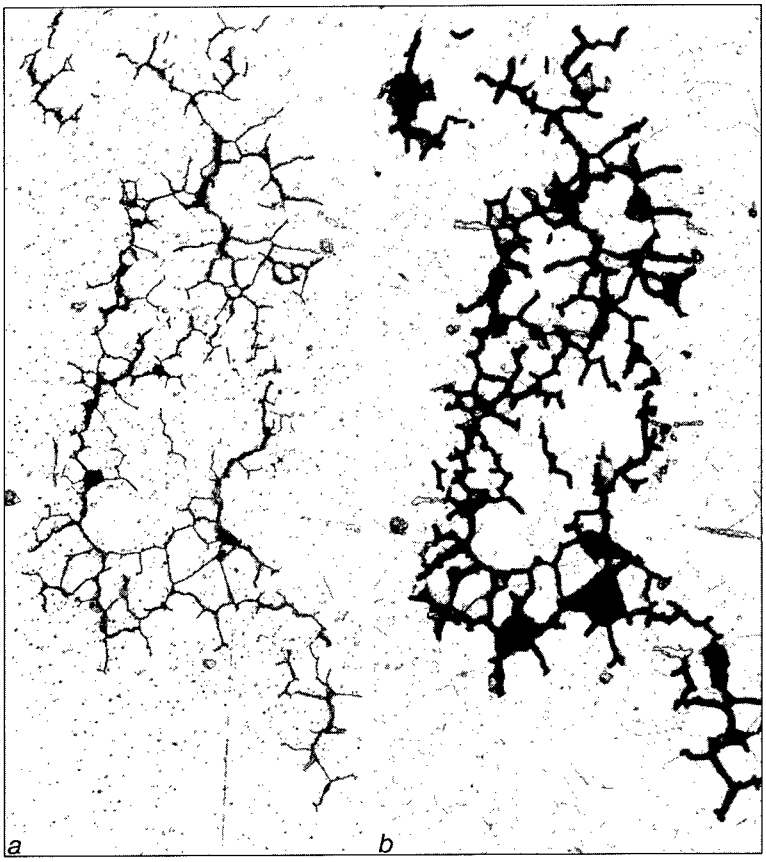

Figure 2. Microstructure of an axial service crack in the base metal near the HAZ of D_n 300 welded joint: *a* — (×320); *b* — (×500) (reduced by 0.50)

tions. As a result, a great extent and considerable volumes of intercrystalline damage of the metal were found.

Similar to cracks formed in WLP welded joints, circular cracks are detected in welded joints of bottoms with ducts of distributing group headers (DGH). These cracks also propagate along the grain boundaries and are branching, thus leading to considerable intensity of metal damage in the HAZ. One of such cracks in a welded joint of the bottom with DGH duct of third reactor of Kursk NPP was 460 mm long with up to 9 mm depth of penetration into the pipe metal (in the plane of the studied macrosections), propagating through the pipe thickness along the fusion boundary at a distance of 0.1 to 2.0 mm from it.

The intercrystalline nature of fracture of D_n 300 piping welded joints necessitated testing the defective welded joint metal for ICC susceptibility. Numerous tests by AM method to GOST 6032–75, as well as by PDRA method to GOST 9.914–91, performed in NPP, TsNIITMASh and other organisations, did not reveal any susceptibility of the metal to ICC.

By the data of KM TsNII «Prometey», isolated carbide precipitates and (in a very narrow zone) partial depletion of the intergranular boundaries in chromium, can be found on the grain boundaries in the HAZ of such welded joints in some cases. In our opinion, this should not be regarded as an indication of the metal sensitising (in the generally accepted meaning of this term), as, according to the data of the same authors, scanning of grain boundaries in different directions with simultaneous recording of X-ray radiation of chromium, did not reveal any intensity fluctuations attributable to lower chromium concentration on the boundary, despite the presence of etching pits in the assumed sites of chromium carbide precipitation. The ratio of the length of the grain boundaries with the channel structure and the total length of the boundaries in the zone with the coarse-grained structure in this case was 13 to 20 %.

The extensive nature of damage of welded joints of D_n 300 piping and other equipment components of various functional purposes, made of stabilised austenitic steel of 08Kh18N10T grade, in RBMK reactors, as well as BWR in Germany, where stabilised austenitic steels of grades 321 and 347 were used, similarity of such cracks initiation in contact with the primary circuit medium, presence of the incubation period, specific characteristics of propagation along the grain boundaries and other identical features of circular and axial cracks, are indicative of the fact that initiation and propagation of service cracks proceeds by one mechanism.

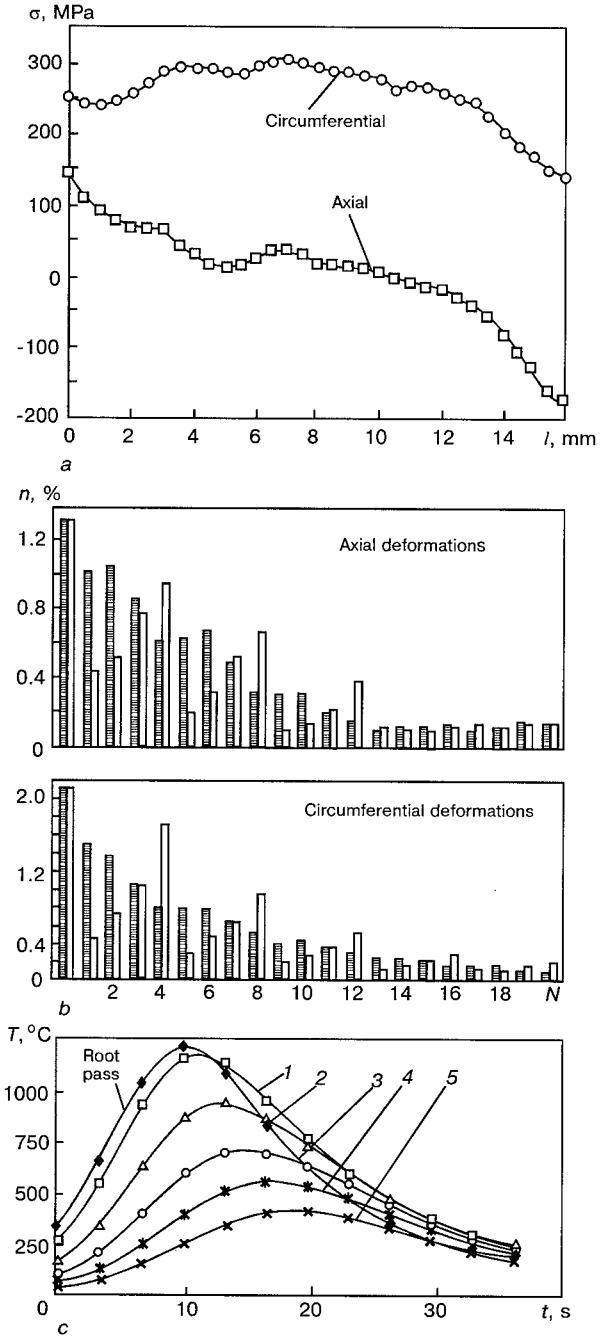

Figure 3. Initial condition of the metal of D_n 300 piping welded joints: *a* — residual stresses in piping welded joints; *b* — increment of plastic deformations on the inner surface; *c* — temperature cycles on the inner surface in the root pass and subsequent layers *1* – *5*; *l* — distance from inner surface; σ — stresses; *N* — bead number; *n* — deformation

Cycles of plasto-elastic deformation at the reactor start-up and shut-down are superposed on the stressed-strained state of welded joint metal induced during welding. In the operational mode the welded joint stresses and strains preserve all the characteristic features of distribution which were in place in as-welded condition; high tensile stresses in combination with the accumulated plastic deformation, are present on the piping inner surface in welded joint zone.

Numerical simulation by the FEM of thermomechanical processes in multipass welding of D_n 300 piping revealed the general pattern of the initial condition of welded joint metal, including the level and nature of the residual welding stresses, increment of plastic deformations, and temperature cycles (Figure 3).

The composition of heat-transfer medium circulating in the multiple forced circulation contour (MFCC) is limited by the norms of unadjustable water regime for single-loop systems of RBMK. This is high-purity water with low values of conductivity, containing practically no chlorides (≤ 70 mg/kg) at pH 6.5 (also the concentrations of iron of ≤ 50 and of copper of ≤ 20 mg/kg are rated in the medium).

Oxygen content in RBMK heat-transfer medium is not limited. In the periods of normal operation, oxygen concentration in the heat-transfer medium varies from 0.2 to 0.8 mg/kg. In the periods of scheduled preventive maintenance, however, saturation with oxygen can reach 8 mg/kg. As was noted above, long-lived radionuclides of corrosion origin were detected both in the cracks and in the heat-transfer medium, in particular in WLP of the separator drum.

Comparison of the above mentioned features of the circular and axial cracks developing in welded joints of D_n 300 piping and other welded elements of MFCC of 08Kh18N10T steel, of the topography of their initiation and development, intercrystalline nature of propagation, large scope of damage, conditions of the stressed-strained state of the HAZ metal, incubation period before crack initiation, contact on the inner surface with high-parameter water in operation, taking into account the operational conditions of the piping, allows the fracture to be unambiguously identified as the process of intercrystalline stress corrosion cracking (ICSCC).

It is known that stabilised austenitic stainless steels after heating in the critical temperature range (650 – 550 °C) do not manifest any ICC susceptibility when tested at the potentials of active-passive transition (by AM procedure to GOST 6032–75). As a rule, austenitic steels fail by TCC mechanism under the conditions of stress corrosion in high-parameter water containing chlorides and oxygen, or even one of these components [5].

After heating in the critical temperature range, i.e. in the sensitised condition, unstabilised steels demonstrate an ICC susceptibility (when tested by AM procedure to GOST 6032–75). Under the conditions of stress corrosion in high-parameter water, these steels fail along the grain boundaries, where they are depleted in chromium at the expense of

carbide precipitation and different rate of diffusion of chromium and carbon in austenite (ASTM304, ASTM316 steels, etc.) [6].

However, soaking of sensitised steels in high-temperature water even with their considerable ICC susceptibility, does not lead to a high rate of crack propagation in overstressed metal — ICC usually is not more than 50 μm after 20 to 30 years of equipment operation. By the data of laboratory studies and operation experience, soaking of sensitised steels in pure high-parameter water in the presence of tensile stresses, results in an increase of the intercrystalline crack growth rate up to 1 to 10 mm/year and this process is classified as ICSCC [5]. ICSCC usually intensively develops at stresses in the metal exceeding the yield point. ICSCC development in high-temperature water requires a higher level of tensile stresses in the metal compared to TCC. This fact, as well as the possibility of ICSCC developing in the absence of the specific medium activators (chlorine ions), are due to a great contribution of the mechanical factor. At corrosion cracking the mechanical stresses increase the level of defects in the passive layer of the metal and lead to a high current density (up to 1 mA/cm^2) at the crack tip.

The mechanism of ICSCC of unsensitised austenite has not been studied so far. Sufficient experimental data, theoretical prerequisites and postulates on the issue are absent. However, in this case the electrochemical nature of ICSCC is also obvious.

In steels not susceptible to ICSCC without load at the active-passive transition potentials, tensile stresses should by not less than an order of magnitude, increase the current density at the grain boundaries, which is little different from that of the matrix (intercrystalline) in the absence of the load.

It is known that the stresses somewhat increase the rate of stress corrosion cracking of stainless steels, until a noticeable plastic deformation of the metal has taken place. In some studies ICSCC of unsensitised Cr–Ni–Mo steel was produced by influencing the fine structure of austenite and inducing local deformation at the grain boundaries. The increase of the extent of deformation in these zones up to 8 to 10 % leads to regrouping of dislocations at the boundaries.

In the work-hardened state, the deformation-induced defects slow down the sliding inside the grain, its strength becomes close to that of the boundaries, shear stresses increase, microplastic deformation is localised in the near-boundary and boundary regions. This is further promoted by the role of grain boundaries as defect drains, especially at elevated temperatures. Element segregation in the defects, such as vacancies, boundary dislocations and pores is found at the grain boundaries. As a result, in the highly stressed deformed austenite metal the activation and anode dissolution are localised with a higher degree of probability in the region of the boundaries which also have a poorer chemical resistance because of impurities segregation and a higher activation energy. These factors changing the electronic structure of the boundaries, promote ICSCC initiation and development.

The necessary condition for ICSCC cracks initiation and development in stabilised austenitic stainless steels in high-parameter water, is a set of external and internal factors in the considered metal–medium system. The main of them are the high level of tensile stresses, macro- and microplastic deformation, microdefects of grain boundaries, medium (especially its oxidising properties) and metal service conditions.

The causes behind the process of ICSCC of welded joints of D_n 300 piping and DGH bottoms consist in the following:

high level of axial and circumferential residual welding stresses and of accumulated strain creating a specific stressed-strained state of the metal;

influence of the TCW on the structure of the metal in the HAZ (visible coarsening of grains, change of grain boundary activity, precipitation of individual carbides, not leading, according to experimental data, to grain boundaries depletion in chromium);

the impact on the metal of heat-transfer medium with unlimited oxygen concentration value when operating at full power and possibility of heat-transfer medium saturation with oxygen up to 8 mg/kg during start-up periods;

operational conditions contributing to the nature and level of the stressed-strained state of the metal;

possible deviations from the technologies of multipass welding (overheating, etc.), as well as presence of microdefects which can be the stress raisers; absence of the ferrite phase in the fusion zone metal can be another factor in the case of axial cracks.

Thus, ICSCC of welded joints of unstabilised steels of ASTM304, ASTM316 grades in BWR piping in the US NPP, is related to precipitation of $M_{23}C_6$ chromium carbides under the thermal impact of multipass welding and boundary depletion in chromium caused by this process; cracks in this case develop at a somewhat greater distance from the fusion zone [5, 6].

Corrosion-mechanical damage of welded joints of D_n 300 piping and DGH bottoms of 08Kh18N10T steel of RBMK reactors, as well as welded joints of stabilised steels of ASTM321, ASTM347 grades of BWR piping is mainly determined by the stressed-strained state due to the residual welding and service stresses, and plastic deformation accu-

Table 1. Results of testing U-shaped samples of a welded joint of pipes of 325 diameter and 16 mm wall thickness of 08Kh18N10T steel in deionized water (350 °C, 16.5 MPa, 3000 h)

Medium	*Cracks*
Bidistillate	ICSCC cracking
with addition of zirconium chips	»
with addition of hydrazine hydrate	No cracks

mulated in welding. The second aspect of ICSCC susceptibility is the condition of the boundaries of grains exposed to TCW [4, 7 – 11].

Special investigations were conducted in TsNII-TMASh in order to substantiate the ICSCC concept.

Tests for evaluation of the behaviour of 08Kh18N10T steel welded joints were conducted on samples cut out of an actual welded joint of a pipe of 325 mm diameter and 16 mm wall thickness. The weld root was welded by manual argon-arc process with a filler of Sv-04Kh19N11M3 welding wire. The groove was filled by manual-arc welding with EA 400/10T electrodes. The welded joint was not subjected to annealing. U-shaped samples were used, loaded by the method of constant deformation, which were bent so that the stresses in the most deformed part were in the welding zone. Tensile bending stresses were on the level of the yield point, while bending deformation was ~ 75 %. Testing was conducted in 8 l autoclaves at the temperature of 350 °C and equilibrium pressure under the static isothermal conditions. The corrosive medium was deeply desalinated water with pH^{20} 6.2 – 6.5. The initial concentration of oxygen dissolved in the water was 8.9 mg/kg. A series of tests were conducted under the same conditions in the reaction space of the autoclave in the presence of zirconium chips, as well as with addition of hydrazine hydrate to the bidistillate at the initial pH^{20} value of 8.2. Examination of the sample surface for cracks and change of the solution in the autoclave were performed every 250 h of testing.

Welded joints studied in deeply desalinated water (bidistillate) under the conditions of high stresses, deformations and rather high initial concentration of oxygen, manifest a corrosion cracking susceptibility. Sample fracture was registered after soaking for 3000 h. A high rate of crack propagation was found with a rather long duration of the incubation period. Samples failed through more than 2/3 of the thickness (Table 1).

Metallographic analysis showed that cracks propagate along the fusion line with transition into the base metal and are of a predominantly intercrystalline nature (Figure 4), i.e. they can be identified as stress corrosion cracks.

The formed cracks by their morphology and nature of propagation, are identical to the cracks found in welded joints of the actual D_n 300 piping of 08Kh18N10T steel, which is in contact with high-purity water at the temperature of 290 °C with chlorine ion concentration of ≤ 0.8 mg/kg. Addition of zirconium chips to the reaction medium intensifies the process; a considerable growth of the cracks of a more ramified pattern was found; they mostly developing into the base metal. Reduction of dissolved oxygen content at insignificant increase of pH value by addition of hydrazine hydrate has an inhibiting influence on the process. No cracks were detected in the samples during 3000 h of testing.

It was found that the studied welded joints did not manifest any susceptibility to ICC when tested by AM procedure to GOST 6032–75.

A series of experiments on evaluation of resistance to stress corrosion cracking in high-temperature water was conducted on the base metal of 08Kh18N10T-VD steel. In this case also the samples loaded by the method of constant deformation at $\sigma > \sigma_t$ load were used in autoclave testing. Testing was conducted in bidistillate and chloride containing solutions with a variable concentration of chlorine ions at the temperatures of 250, 280, 320 °C and equilibrium pressures. The initial concentration of oxygen dissolved in the liquid phase was 8 mg/kg, the periodicity of the samples examination and replacement of the corrosive medium in the autoclave was 250 h.

The steel was tested after heat-treatment at the temperature of 1050 – 800 °C in the condition not susceptible to ICC, also after the metal exposure to the thermal impact of temperatures in the range of 350 – 750 °C of 0.5 to 3000 h duration.

After ~ 3000 h of testing, corrosion cracking was only found in the tangential samples in the solutions with chlorine ion concentration of 0.5 and 5.0 mg/kg at the temperatures of 280, 320 °C and pH^{20} 6.5 – 6.8 (Table 2).

Table 2. Results of testing 08Kh18N10-VD steel for corrosion cracking resistance in high-temperature water at loading by constant deformation method

[Cl], mg/kg	*pH^{20}*	*Time to fracture (testing time), h, at the temperatures, °C*		
		250	*280*	*320*
–	6.5 – 6.8	3000, no fracture	3000, no fracture	3000, no fracture
0.5	6.5 – 6.8	3000, no fracture	2750, cracks	2750, cracks
0.5	4.0 – 4.5	–	–	3000, no fracture
5.0	6.5 – 6.8	2750, cracks	–	2750, cracks

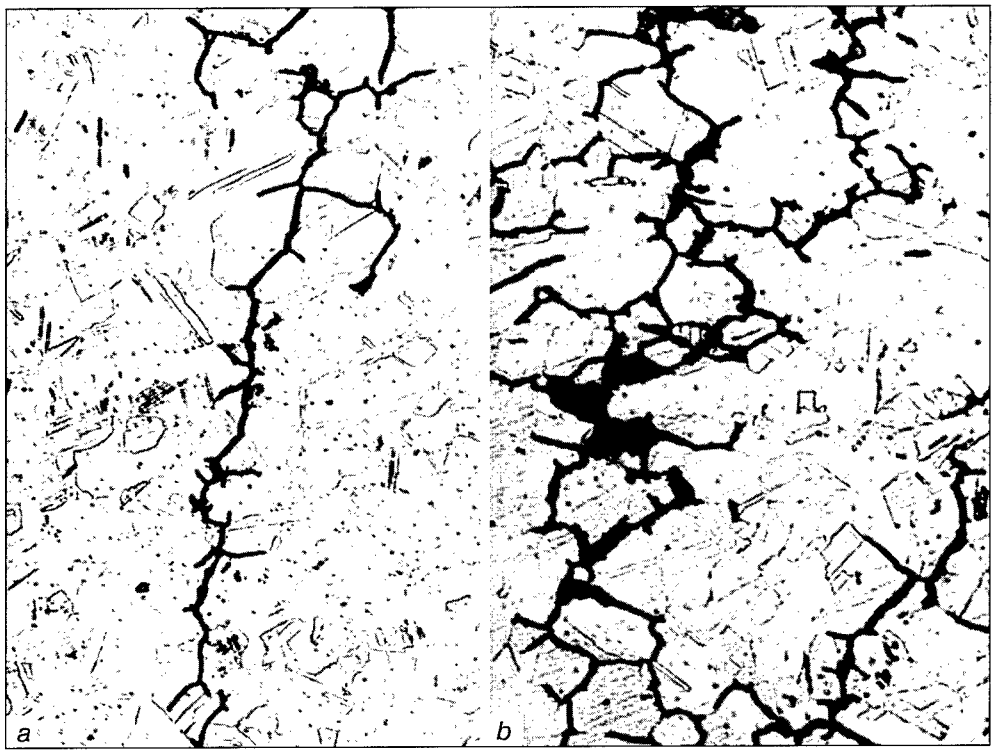

Figure 4. Microstructure of ICSCC cracks in the welding HAZ with propagation into the base metal in testing of U-shaped samples in bidistillate (*a*) and in bidistillate with zirconium chips in the autoclave space (*b*) at 350 °C temperature, 16.5 MPa pressure, testing duration of 3000 h (×550) (reduced by 0.60)

A feature of these fractures is the intercrystalline nature of crack propagation, an essentially greater localisation of fracture, smaller number of crack nucleation sites than it is usually found at TCC, high rate of crack propagation (Figure 5) and independence of the above factors on concentration of chlorine ions in the medium and the testing temperature.

Testing of 08Kh18N10T-VD steel demonstrated its susceptibility to delayed corrosion cracking at deformation in demineralized water at a certain combination of temperature and concentration of dissolved oxygen. An extremal dependence of brittle fracture on temperature (Figures 6, 7) was found in the temperature range of 250 to 340 °C. For water with the initial concentration of oxygen of 7.5 to 8.0 mg/kg, the fracture is of a brittle deformation-free nature and is accompanied by formation on the surface of secondary circular corrosion cracks at the temperatures of 250 to 290 °C. Corrosion cracking resistance abruptly increases at 300 °C. In the range of 320 to 340 °C the temperature change does no influence the value of relative reduction in area, however, in this case also it is lower than in testing in air.

In the solution with 0.5 mg/kg chlorine ions at oxygen concentration of 7.5 to 8.0 mg/kg, the dependence of relative reduction in area on temperature is preserved in the temperature range of intensive lowering of ductility. However, at 320 °C

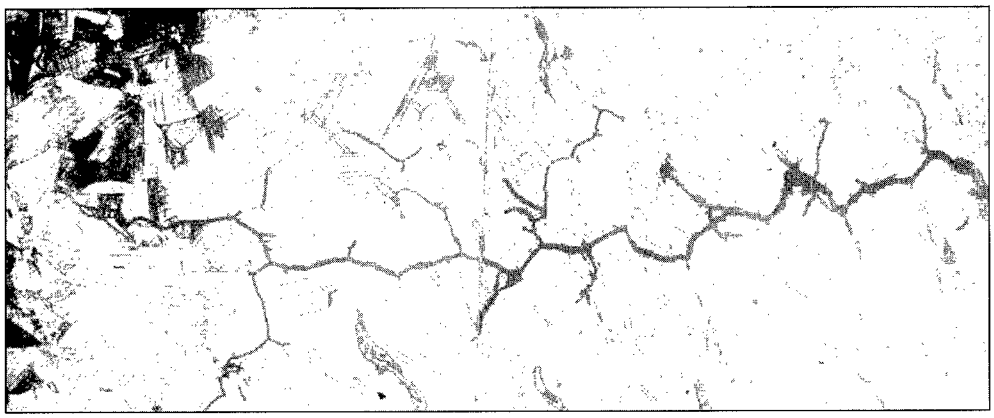

Figure 5. Microstructure of corrosion cracking in U-shaped sample of 08Kh18N10T-VD steel (heat-treatment from (1050 + + 800) °C temperature) when tested in a water solution with 0.5 mg/kg [Cl] and initial concentration of O_2 = 7.5 – 8.0 mg/kg at 320 °C, 11.3 MPa, for 2750 h (×550) (reduced by 0.50)

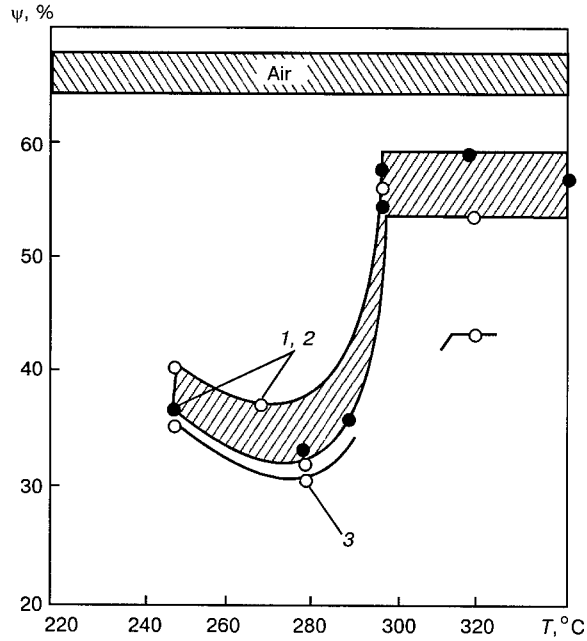

Figure 6. Influence of temperature on stress corrosion cracking susceptibility in tensile testing with a low straining rate ($\varepsilon = 1.4 \cdot 10^{-7}$ s^{-1}) of 08Kh18N10T-VD steel at the initial concentration of O_2 = 7.5 – 8.0 mg/kg: *1, 2* — heat treatment at 950 and (1050 + 800) °C, bidistillate; *3* — heat treatment at 950 °C, 0.5 mg/kg [Cl] solution

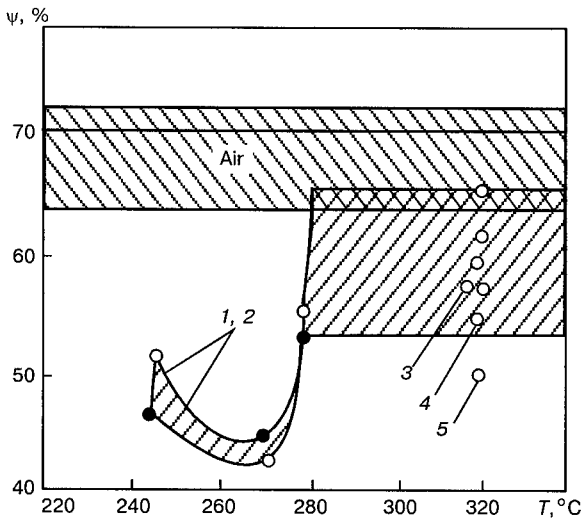

Figure 7. Influence of temperature on the susceptibility to delayed corrosion cracking at deformation of 08Kh18N10T-VD, 08Kh18N10T steels and welded joints in demineralized water with the initial concentration of oxygen of 3.5 – 4.0 mg/kg: *1, 2* — 08Kh18N10T-VD, heat treatment (1050 + 800) and 950 °C; *3* – *5* — 08Kh18N10T (pipe metal) after different tempering modes (650 °C, 1 h; 550 °C, 1000 h; 350 °C, 3000 h)

the presence of chlorine ions has a negative influence on the resistance to delayed corrosion cracking.

In the water with the initial concentration of oxygen of 3.5 to 4.0 mg/kg, the general nature of the extremal dependence of ductility on temperature is preserved with its maximal lowering at 270 °C. The interval of temperatures of brittle fracture susceptibility is narrowed and shifted towards lower values. The degree of the medium influence on ductility drop is also essentially lower (Figure 7).

Metallographic analysis showed that at tension with a low straining rate, crack propagation in 08Kh18N10T steel in unsensitised state can be of

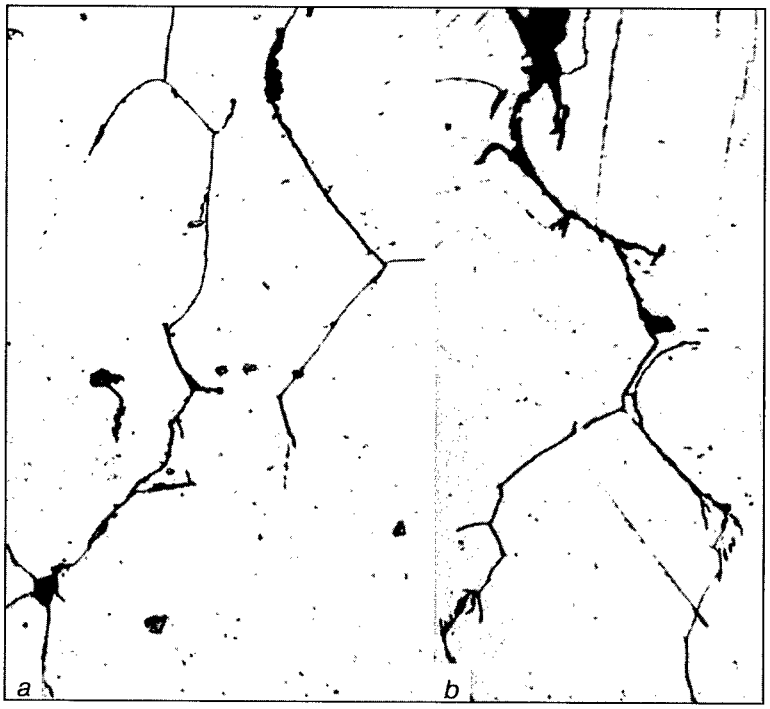

Figure 8. Microstructure of a crack in corrosion cracking of 08Kh18N10T-VD steel in the HAZ when tested for delayed corrosion cracking at deformation ($\varepsilon = 1.4 \cdot 10^{-7}$ s^{-1}) in demineralized water (320 °C, 11.3 MPa): *a* — initial stage; *b* — crack development in-depth of the sample (×500) (reduced by 0.60)

intercrystalline or mixed nature, depending on the metal condition, medium composition and parameters (Figure 8).

The fracture topography indicates that for the conditions giving rise to proneness to delayed corrosion cracking, the fracture surface contains a sufficient proportion of brittle fracture and crack initiation sites over the entire perimeter of the cross-section. Fracture in the crack is of a step-wise nature, flaked fracture, secondary cracks and a multitude of pores are found.

Thus, it has been experimentally established that steels of 08Kh18N10T grade in unsensitised state, can also manifest ICSCC susceptibility in high-parameter demineralised water.

CONCLUSIONS

1. Numerous circular and axial crack-like defects have been found in welded joints of the piping of all the operating RBMK reactors (WLP and water discharge piping, pipe to bottom joints) of stabilised 08Kh18N10T austenitic steel. Analysis of the morphology, propagation mode and origin of such cracks showed that the process of their initiation and propagation proceeds by the ICSCC mechanism.

2. The main factors which determine the incubation period and the intensity of welded joint damage, are the level and nature of distribution of the residual welding and service stresses, presence of the zones of plastically deformed metal in the welded joints, features of the water-chemical composition of the medium contacting the piping inner surface. Greater ICSCC susceptibility of welded joints of 08Kh18N10T steel is promoted by structural changes in the metal caused by the temperature impact of the process of multipass welding (grain coarsening, microlocal sensitisation at the expense of the possible phase precipitations and impurities segregation on the intergranular boundaries).

3. Laboratory investigations performed for substantiation of ICSCC mechanism concept, showed that stabilised stainless steels of 08Kh18N10T grades can demonstrate a susceptibility to ICSCC in high-parameter demineralized water even without the impact of TCW, namely at a high level of stresses and plastic deformation and in the presence of oxygen in the metal. Welded joint metal is more susceptible to ICSCC.

REFERENCES

1. (1998) TC Project RER/9/052 RBMK-SC-060. In: *Report of a Regional Workshop on Environmentally Assisted Cracking of NPP Austenitic Piping,* Slavutich, Ukraine, June 22 – 26, 1998. Slavutich.
2. Erve, M., Wesseling, U., Kilian, R. *et al.* (1997) Cracking in stabilized austenitic stainless steel piping of German BWR – characteristic features and root causes. *Nuclear Engineering and Design*, **171**, 113 – 123.
3. Wachter, O. (1996) Experience with austenitic steels type 321 and type 347 in German BWR. *VGB Kraftwerkstechnik*, **10**, 777 – 785.
4. Kharina, I.L. (1998) Some features of stress corrosion cracking of austenitic stainless steels in high-parameter water. In: *Transact. of 5th Int. Conf. on Material Science Problems in Design, Fabrication and Operation of NPP Equipment*. St. Petersburg.
5. Bogoyavlensky, V.L. (1984) *Steel corrosion in NPP with a water heat-transfer agent*. Moscow: Energoatomizdat.
6. Bruemmer, S., Chariot, L., Atteridge, D. (1988) Sensitization development in austenitic stainless steel – measurement and prediction of thermomechanical history effects. *Corrosion Science*, **44**, 427 – 434.
7. Aladinsky, V.V., Makhanev, V.O., Bugaenko, S.E. *et al.* (1998) Investigation of residual welding stresses in welded joints of D_n 300 piping. In: *Report of a Regional Workshop on Environmentally Assisted Cracking of NPP Austenitic Piping,* Slavutich, Ukraine, June 22 – 26, 1998. Slavutich.
8. Speidel, M., Magdowski, R. (1995) Environmental degradation assessment and life prediction of nuclear piping made of stabilized austenitic stainless steels. In: *Proc. of Int. Symp. on Plant Ageing and Life Predictions of Corrodible Structures,* Supporo, Japan, May 15 – 18, 1995. Supporo.
9. Ulg, U. (1995) Renewal of austenitic stainless steel piping in German BWR. In: *Proc. of PLEX'95 Conf.,* Nice, France. Nice.
10. Azbukin, V.G., Krylova, R.P., Mikhaleva, E.I., *et al.* (1998) Methods of improvement of corrosion cracking resistance of RBMK piping. In: *Transact. of 5th Int. Conf. on Material Science Problems in Design, Fabrication and Operation of NPP Equipment*. St. Petersburg.
11. Karzov, G.P., Margolin, B.Z., Markov, V.G. *et al.* (1998) Nature of damage of discharge piping of MFCC of RBMK reactors in operation and ways of its elimination. *Ibid*.

ASSESSMENT OF RESIDUAL LIFE OF WELDS IN PIPINGS OF THE FIRST LOOP OF NUCLEAR POWER STATIONS DAMAGED BY INTERCRYSTALLINE CORROSION

A.Ya. KRASOVSKY and **I.V. ORYNYAK**
Institute for Strength Problems, NASU, Kyiv, Ukraine

ABSTRACT

Considered are the methodological principles of comprehensive estimation of strength and residual life of spatial piping systems containing cracks. The method suggested consists of such components as global stressed-strained state of a piping allowing for all affecting force factors, allowance for residual welding stresses, calculation of stress intensity factors, prediction of stable forms of development of fatigue cracks and intercrystalline corrosion, estimation of actual residual life of a piping containing defects and prediction of conditions causing leak to fracture.

Key words: *piping, crack, stress, residual life, leak to fracture.*

Reliable operation of power generating equipment greatly depends upon failure-free functioning of the piping systems. In nuclear power engineering the special requirements are imposed on ensuring reliability of these systems. Primarily, this involves regular diagnostics of metal quality, strength analysis and prediction of residual life. As to the last two aspects, they include several problems without the efficient solution of which it is impossible to obtain the reliable information on the actual state of a structure.

The most labour-consuming and least-elaborated problem is that of assessment of the stressed-strained state (SSS) of repeatedly statically indeterminate spatial piping systems subjected to complex loading. The existing design methods based on traditional approaches involving force or finite element methods are not always efficient enough, because of a highly labour-extensive procedure used commonly for strength analysis of a long piping with complex spatial configuration and a large number of intermediate supports. Friction experienced in the supports leads to a non-linear statement of the problem, which makes calculations much more complicated [1]. The second important problem consists in determining more precisely the stressed state within the zone of assembly welds, which always contain residual stresses. Finally, there is one more problem which is directly related to integrity of the structure, i.e. stress corrosion cracking of austenitic steels and growth of stress corrosion defects in boiling and light-water nuclear reactors.

In the CIS countries, the problem of intercrystalline corrosion of the welds in austenitic steels has come to light only recently. Such a late attention to this problem by leading organizations in the field evidences their lacking knowledge of the international experience gained by date. Thus, intercrystalline corrosion cracks (more than 1000 cracks) were detected for the first time in the second unit of the «Dresden» NPS (USA) in September 1974 [2]. In the USA about 25 % of welded joints had indications of cracks [3]. Studies of intercrystalline corrosion in Japan have been performed under the national program of reliability of the piping systems since 1975 [4]. Search for the improvement methods for elimination of cracking generated considerable scientific and technical interest in this problem and substantial investments.

It was found that primary causes of corrosion cracking were as follows: unstable steel with the sensitized HAZ, exposure to the corrosive environment and effect of a high level of stresses (both effective and residual).

The following improvement methods were suggested as being most substantiated and affordable: induction heating to relieve residual stresses, deposition of an external coating by welding and estimation of residual life of defective regions. In addition, replacement of the piping systems by the new ones made of steels resistant to sensitization and corrosion was offered by KWU SIEMENS as a long-term solution to the problem. One of the most important initiatives under the US program was development of a special supplement to the ASME Codes concerning procedures for estimation of a risk of defects in pipes of austenitic steels [5].

The essential aspect which determines accuracy of calculations and reliability of predictions is the

quality performance of the work on technical diagnostics of pipings. However, diagnostics of high-ductility austenitic steels by the NDT methods do not always allows the depth of a defect to be evaluated with a sufficient accuracy. This is evidenced by numerous experimental data on mechanical opening displacement of actual cracks. In such cases the only method that can be used to evaluate the shape of a crack is prediction of variations in its size by the stable crack propagation shape. With a limited scope of information available on sizes of defects, the stable shape method offers promise for prediction of the depth of a defect, providing its length is known or vice versa.

Apparently, the problem of corrosion cracking of welded joints in pipings is so serious that it generated efforts on updating the existing approaches to evaluation of structural strength, imposing increased requirements on the entire «chain» of the strength design, starting from the quality of diagnostics, estimation of the global SSS of a structure and finishing with prediction of the development of a specific defect with time.

This work is an example of the integrated solution to the problem of strength design of specific structures, such as downcoming and pressure pipes in the 3rd power unit of the Chornobyl NPS, as well as of certification of the state and prediction of the fatigue life of each defective element. As the existing codes on calculations of the nuclear power station pipings do not include strength design with allowance for the effect of crack-like defects, the primary purpose of this work consisted in the development of methodology for integrated investigation of spatial piping systems containing cracks.

Methods of calculations. *General sequence of calculations.* With only few exceptions, all calculations in this work associated with strength design were made in accordance with the sequence accepted in the Codes [5]. All procedures, methods and experimental characteristics used were selected so that they provided conservative results of the calculations made in the following sequence:

calculation of the global SSS of a piping. Analysis of uncertainties associated with possible displacement of points at which a piping is joined to pressure vessels or fittings, as well as uncertainties which could be caused by errors in estimation of compliance of the supports;

more precise determination of an actual distribution of stresses induced by effective loads within the weld zone on the basis of allowance for residual stresses;

calculation of stress intensity factors for semi-elliptical cracks with a circular orientation. Prediction of the shape of propagation of fatigue and corrosion cracks;

calculation of actual fatigue life of a welded joint with a corrosion defect. Assessment of a limiting state and maximum permissible lengths of defects. Prediction of condition of a leak to fracture.

Evaluation of global SSS of the structure. As noted above, evaluation of the global SSS of spatial piping systems by traditional methods does not always yield a sufficient accuracy. In this connection, in 1996 the specialists of the Institute for Strength Problems of the NAS of Ukraine developed a new efficient method for the calculation [6]. It is based on a method of initial elasticity parameters and intended for the calculation of statically indeterminate three-dimensional frame systems. The method is based on a set of equations for displacement of the points of a rod for the internal forces over the region of a known length. These equations enable evaluation of SSS of a complex piping system and, at the same time, account for all effective factors, such as dead weight, internal pressure, temperature gradient, actual rigidity of intermediate supports and spatial displacements of structural members, and for all changes in the pipe axis, both drastic and gradual caused by bends.

Evaluation of the local stressed state of the structure. Welding is a commonly accepted method for assembly and extension of a piping system, this determining a large number of circumferential welds in the structure. In turn, the weld is a potential source of fracture, at least for three reasons: properties of a material in the HAZ are different; because of design peculiarities, the weld zone acts as a stress raiser; and welding results in substantial axial residual stresses.

These reasons should by all means be allowed for in strength design. For quantitative estimation of the concentration of stresses, it is necessary to calculate elasticity of a welded joint by the finite element method (FEM) by applying uniform unit stresses at infinity.

Butt welding of pipes results in the formation of residual stresses caused by shrinkage of the weld, temperature gradient formed during metal deposition and restraint of the welded joint. The value and distribution of these stresses exert a fundamental effect on the rate of development of defects. Sinse the effective and residual stresses in the weld exceed the material yield strength, a non-linear boundary problem of distribution of stresses in the weld zone should be solved using equations of the theory of thermal plasticity. In this work they are solved by the method of elastic solutions based on a mixed diagram of the FEM. The length of a pipe is set so that the edge effect has no impact on the stressed state of the weld, and it is conservatively assumed for modelling of residual stresses that the weld is «put» on the base metal at a temperature of 600 °C, which corresponds to single-pass welding.

The data obtained from analysis of the FEM results complement well the global SSS calculation owing to allowance for distribution of stresses through the wall thickness in the weld zone and, thus, make it possible to go over to analysis of strength of the local defect-containing zones.

Structural strength of welded joints. As noted above, the main factors causing displacement of a crack in welds in the piping systems are stress intercrystalline corrosion (SICC) and vibration. It is thought that at the beginning the crack is initiated and propagated by the SICC mechanism, and then, as it increases in length, fatigue damage (due to vibration) becomes dominant, leading to its rapid growth. Therefore, the calculations should be made with regard for the two fracture mechanisms.

Based on [7, 8], assume the following law of the rate of growth of a corrosion defect expressed in meters per second:

$$\frac{da}{dt} = C_k K_I^n, \qquad (1)$$

where K_I is the value of the stress intensity factor, MPa$\sqrt{\text{m}}$; C_k and n are the material constants.

For analysis of the fatigue mechanism of propagation of defects, we will use the similar law of the rate of their growth expressed in meters per cycle [9]:

$$\frac{da}{dN} = \frac{C_y \Delta K_I^m}{\sqrt{(1-R)^m}}, \qquad (2)$$

where $\Delta K_I = K_I^{\max} - K_I^{\min}$ is the spread of the stress intensity factor in a cycle, R is the cycle asymmetry coefficient, C_y and m are the material constants.

Values of the effective stress intensity factors are determined by calculations by the method of weighting functions, which was developed by the authors [10, 11]. Its main point is that if a solution for K_I under homogeneous loading on the crack lips, $\sigma(x) = \mu_0$, (this loading is called basic) is known

$$K_I = \mu_0 \sqrt{\pi a}\, Y_0(a; w),$$

where a is the set of parameters characterizing the shape, size and coordinate of the crack front point under consideration and w is the set of geometrical parameters and elastic parameters of a crack-containing body, the value of K_I under heterogeneous loading can be calculated from the following formula:

$$K_I = \sqrt{\pi a}\left\{Y_0(a; w)\,\mu_0 + \left(I_1 + \frac{Y_0 - I_0}{J_1}\right)\mu_1 \frac{a}{H}\right\} +$$

$$+\left\{\left(I_2 + \frac{Y_0 - I_0}{J_2}\right)\mu_2 \left(\frac{a}{H}\right)^2\right\} +$$

$$+\left\{\left(I_3 + \frac{Y_0 - I_0}{J_3}\right)\mu_3 \left(\frac{a}{H}\right)^3\right\},$$

where coefficients μ_i ($i = 0, 1, 2, 3$) and regulating parameter H follow the exponential law of distribution of stresses across the crack section

$$\sigma(x) = \mu_0 + \mu_1 \frac{x}{H} + \mu_2 \left(\frac{x}{H}\right)^2 + \mu_3 \left(\frac{x}{H}\right)^3$$

and values of functions $I_i(a; w)$ and $J_i(a; w)$ are determined beforehand by the method of point weighting functions [12]. The basic solutions are selected in accordance with [13, 14].

Prediction of the defect development shape. In prediction of propagation of a crack, of special importance is the problem of prediction of the crack shape. The conventional assumption proved experimentally and in practice for both fatigue and corrosion is that a stable crack takes the shape of an ellipse. Then, to predict propagation of a surface crack, it is enough to consider only two points, i.e. the deepest point and the point located on the surface. Let the depth of the crack be a and its half-length be L. Then, according to (1), the following expression will hold for a corrosion crack:

$$\frac{da}{dL} = \left(\frac{K_I(a)}{K_I(L)}\right)^n, \qquad (3)$$

where da is the increment in depth of the crack and dL is the increment in length of the crack. Equations (1) and (3) considered in combination allow the calculation of both fatigue life and kinetics of variation in the crack shape.

For a fatigue crack, the shape of its development within a set field of stresses can be calculated using equation (2):

$$\frac{da}{dL} = \left(\frac{(K_I^{\max}(a) - K_I^{\min}(a))\, K_I^{\max}(a)}{(K_I^{\max}(L) - K_I^{\min}(L))\, K_I^{\max}(L)}\right)^{m/2}. \qquad (4)$$

If the dynamic component of stresses (vibrational) is assumed to be much lower than the static one (the sum of effective and residual stresses), equations (4) and (2) can be simplified as follows:

$$\frac{da}{dL} = \left(\frac{K_I^{dyn}(a)\, K_I^{st}(a)}{K_I^{dyn}(L)\, K_I^{st}(L)} \right)^{m/2}, \qquad (5)$$

$$\frac{da}{dN} = C_y \left(2K_I^{dyn}(a)\, K_I^{st}(a)\right)^{m/2},$$

where K_I^{dyn} and K_I^{st} are the dynamic and static components of K_I, respectively. The defect development shape calculated from equations (3) and (5) and determined by the a/L length ratio hardly depends upon the preset initially small values a_0 and L_0, which is proved by numerous experimental and calculation works [15]. Within the frames of the model under consideration, the defect development shape does not depend upon the level of effective stresses, although it is sensitive to the character of their distribution.

It should be noted that shapes of actual defects can differ fundamentally from the stable shapes, providing that the crack is formed as a result of coalescence of two or more initial cracks. As the defect coalescence does not cause an increase in the total depth, and the length is equal to the sum of lengths of individual defects, the depth of the actual crack cannot exceed that of the crack of a stable shape, having the same length. Therefore, in the case where only the length of a defect is known, the approach that uses the notion of the stable shapes leads to concervative estimates.

Calculation of the limiting state. Calculation of the limiting state and selection of the safety factors are an important complement to the suggested strength design. As no procedure is available in Ukraine for the calculation of the limiting state of pipings with circumferential cracks, which are subjected during operation to mechanical and thermal loading, the calculation was made using a model suggested in [16, 17]. The problem of the calculation of the limiting state of a pipe with a circumferential through or surface crack is statically determinate and its solutions can be found in many references. The advantage of the suggested model is that it allows for a decrease in compressive limiting axial stresses in the presence of positive circumferential stresses due to internal pressure, which makes the model more conservative. Thus, it holds

$$\begin{cases} \left(2 - \dfrac{pR}{[\sigma]H}\right)\cos\varphi_1 - \dfrac{a}{H}\left(1 + \dfrac{p}{[\sigma]}\right)\sin\varphi_0 + 2k, \\ \dfrac{pR}{[\sigma]H} \le 1, \end{cases}$$

where

$$\varphi_1 = \frac{q\,\pi - \dfrac{pR}{2[\sigma]}\pi + \varphi_0 \dfrac{a}{H}\left(1 + \dfrac{p}{[\sigma]}\right)}{2 - \dfrac{pR}{[\sigma]H}},$$

if $\varphi \le \pi$, where $[\sigma]$ is the permissible stress, p is the internal pressure, while the dimensionless parameters k and q are determined from the values of bending moment M and axial force N, respectively,

$$k = \frac{M}{4R^2 H\,[\sigma]}, \quad q = \frac{N}{2\,\pi RH\,[\sigma]}. \qquad (6)$$

Formulae of the type of (6) were validated on a large amount of full-scale and experimental data, which revealed certain decrease in the load-carrying capacity of the welded joint, as compared with the base metal. Expressions for coefficient z were derived from the underrated boundary values of these results to concervatively correct external loads and take into account plastic increment in length of the crack for analysis of the limiting state and determination of permissible sizes of defects [4]:

$$z = 1.3\left[1 + 0.01\left(\frac{D}{25.4} - 4\right)\right],$$

where D is the outside diameter of the pipe.

In these calculations permissible stresses were determined by dividing aqual to the value of ultimate strength by safety factor 2.5 [1].

Estimation of the limiting state makes it possible to employ the procedure of prediction of the fatigue life for the case of propagation of through cracks to critical sizes and confirm whether the time reserve is sufficient from the moment of appearance of a leak to a catastrophic fracture.

Estimation of the fatigue life of the structure. Practical calculations of the fatigue life for the case of surface corrosion cracks are based on integration of equations (1) with respect to the depth of a defect, starting from its initial value corresponding to the actual length of the defect and obtained by prediction based on the stable crack development shapes, and up to the depth equal to the wall thickness.

The estimate of the residual life for through-type defects can be obtained in a similar way. For this, it is necessary to integrate the same equation of the crack growth rate with respect to half-length of the defect from its lower value corresponding to an increment in length of the defect in the through crack up to the upper value, i.e. the critical half-length of the through crack determined from analysis of the limiting state of the structure. In the case of the through defect, it is referenced to a maximum level of stresses in a given section of the pipe, while residual stresses can be neglected as they are self-balancing.

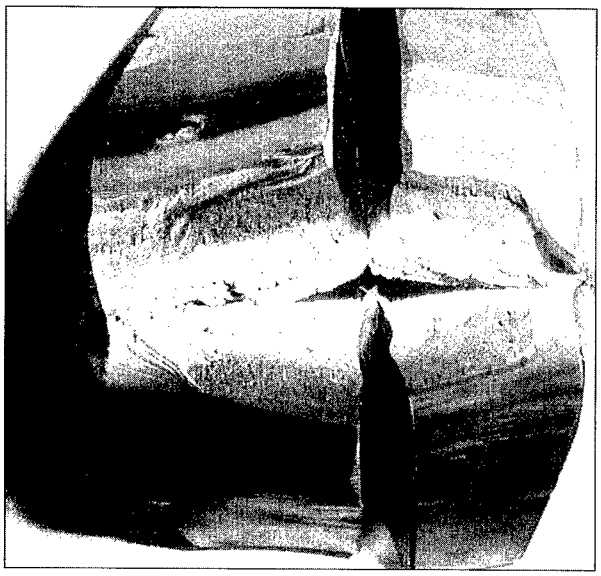

Figure 1. Appearance of fracture surface of the circumferential weld in D_n 300 piping

Character of damages in welds and properties of materials. *Peculiarities of propagation of intercrystalline corrosion cracks.* As shown by the investigations conducted by staff members of the Chornobyl NPS on circumferential welds cut out from pipings of the 3rd unit (the 1st loop pipings with an outside diameter of 325 mm and wall thickness of 16 mm), the intercrystalline corrosion cracks initiate near the root weld on the internal wall of the pipe and propagate as a rule within the HAZ along the fusion line. The crack initiation centres are the local stress raisers caused either by shrinkage of metal in cooling of the root weld or by coarse machining marks left from groove preparation on the internal surface of the pipe for welding. Abundance of such stress raisers present on the internal surface of the weld and HAZ leads to initiation of several cracks. These cracks are located in different parallel sections of the pipe, and during propagation they often coalesce into one crack with several embryos. As the moments of initiation of these cracks do not coincide in time, some cracks get ahead of the others. As a result, they coalesce into one common avalanche crack having a sinuous front.

Figure 1 shows appearance of such a crack and two neighbouring templates cut out from the welded joint with a damage. Each opposite half of the template comprises a mating surface of the same corrosion crack (dark, looking outward) and surface of the crack of final fracture (light, looking inward), resulting from mechanical final fracture of the template in bending. The corrosion crack surfaces are covered with a thick layer of corrosion deposits, dark-brown in colour and very radioactive.

Fractography and metallography of the crack surface cleaned from the corrosion deposits showed that the primary mechanism was intergranular fracture with a branched crack characteristic of corrosion. Certain indications of fatigue fracture, i.e. fatigue grooves with a groove spacing of about 1 μm, can also be seen in some locations on the fracture surface.

Mechanical properties of materials. Steel 08Kh18N9T used for the manufacture of pipes is an analogue of Western austenitic titanium-stabilized stainless steel AISI 321. Chemical analysis of material of the pipes shows that it meets requirements of the regulatory documents, i.e. all relevant standards and delivery specifications.

Metallography of the base, weld and HAZ metal confirms that in size of grains and in character of non-metallic inclusions (oxides and silicates, sulphides, nitrides and carbonitrides) this material also meets requirements of the regulatory documents. The HAZ contains coarsened grains that correspond to point 3 – 4, according to the ASTM gradation. Standard tensile and impact toughness tests on specimens cut out from the pipe and weld were conducted at room temperature and at 350 °C. These tests also showed an agreement between actual mechanical properties of the base and weld metal and those specified by the regulatory documents.

The critical values of J-integral at the moment of the crack start and the kinetic diagrams of growth of the fatigue cracks were derived to evaluate cracking resistance of the material under static and cyclic loading at the above two temperatures on the compact off-centre tension specimens 12.5 mm thick. Afterwards, these data were used to evaluate the rate of growth of the crack, its critical size and residual life of the welded joint.

Fractography and X-ray microanalysis of fracture surfaces of specimens under cyclic loading revealed clearly defined fatigue grooves located at a constant spacing corresponding to each stage of cyclic loading. This constant character of the groove spacing is attributable to the test conditions, i.e. constant amplitude of the load at each loading stage. In this case, the measured groove spacing related to the central region of the kinetic diagram of fatigue fracture. Besides, over the entire range of the loads where the fatigue grooves were observed, their spacing corresponded to an average rate of the crack measured directly on a specimen during the experiment. This correspondence between the micro-rate of the crack measured by the groove spacing and its macro-rate was observed at the crack rates in excess of $1 \cdot 10^{-7}$ m/cycle, while the measured groove spacing ranged from 0.3 μm to 2.0 μm.

The spacing of the less regular grooves seen on the surface of the intercrystalline corrosion cracks in welds in the pipes ranged from 0.4 to 1.0 μm, this falling within the range of the groove spacing

measured on the specimens. This correspondence might be regarded as a proof that the cyclic component of stresses in the pipe has an effect on growth of the corrosion crack, i.e. here we are dealing with superposition of the processes of stress corrosion cracking and fatigue crack growth or, in other words, corrosion fatigue.

Examination of the defective welds. It was noted in investigation of peculiarities of growth of corrosion cracks that the path chosen by a crack greatly depended upon its initiation location, which in turn depended upon the efficiency (i.e. sharpness) of a local stress raiser. Therefore, the damaged welded joints cut out from the pipes contained both cracks propagating in the HAZ along the fusion line and cracks (less common) growing into the weld metal. To take into account these peculiarities, it was necessary, firstly, to evaluate strength of the weld metal and, secondly, estimate the ultimate fracture load acting on part of the weld that remained intact.

The first part of this problem was solved by cutting out cylindrical tensile specimens from the weld, so that the specimen axis coincided with a circumferential direction of the weld in the pipe, whereas the second part of the problem was solved by final fracture bend testing of the templates cut out from the pipe so that they contained in their centre the weld damaged by crack. Both tests were conducted at two temperatures, i.e. room temperature and 350 °C.

The tensile tests showed that the weld metal at both temperatures had a higher yield strength than the base metal and a bit higher tensile strength. Thus, the weld metal turned out to be stronger and slightly less ductile than the base metal.

The bend tests of the templates at the said temperatures showed that fracture of the part of the template section not affected by the crack was of a very tough character. This is indicative of the fact that prior to fracture the intact part of the template secton is transformed into a fully ductile state. The load P_{max} was registered after testing each template, and after final fracture the contours of the intercrystalline corrosion cracks were measured on the fracture surfaces of the templates.

Maximum stress effective at the moment of fracture was calculated from maximum load that corresponded to the formation of a ductile hinge in a central section of the template weakened by the crack. This stress corresponded to the level of ultimate strength of the material.

The results obtained show that the material in the crack-free part of the central section of the template preserves its initial properties and the ability to resist fracture caused by the loads acting on the pipe.

Associates of the Chornobyl NPS obtained very important results by measuring geometrical characteristics of the intercrystalline corrosion cracks directly on the exposed fracture surfaces, which were opened as a result of final fracture of the templates (Figure 2).

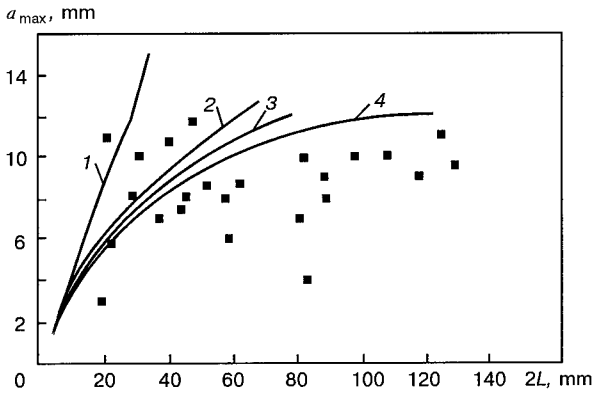

Figure 2. Dependence of maximum depth of a crack upon its length on the internal surface of the circumferential weld plotted by the results of measurements directly on the fracture surfaces of 39 welded joints (squares) damaged by intercrystalline corrosion. Solid lines show the calculated dependencies corresponding to a stable shape of the intercrystalline corrosion crack, assuming one crack embryo, for different levels of applied stresses: *1* — 90; *2* — 60; *3* — 38 and *4* — 0 MPa

As was already noted, the crack front is very sinuous, which is associated first of all with a multinuclei character of crack initiation, and probably with heterogeneity of the material in the weld zone. The Figure shows dependence of the maximum depth of the crack upon its entire length on the internal surface of the weld. Here each experimental point corresponds to a separate crack. As it can be seen from the Figure, the maximum depth of the cracks investigated is not in excess of 12 mm, which makes 3/4 of the nominal wall thickness of the pipe. It can also be seen that the shape of the crack, which can be characterized as the ratio of maximum depth a_{max} to half-length L of the crack, i.e. a_{max}/L, varies over the wide ranges, i.e. $0.05 \leq a_{max}/L \leq 0.55$. This is associated with two circumstances: quantity of embryos in one crack (the larger the quantity of the embryos, the lower the value of a_{max}/L) and the level of applied stresses effective in the section damaged by crack (the higher the level, the higher the rate of propagation of the crack from the basic embryo, making all other embryos less efficient).

Calculation results and analysis. Based on the source data presented, the complex strength design calculations were conducted on 35 downcoming and 39 pressure pipings at the Chronobyl NPS, where discontinuities were detected in the welds caused by SICC. It was assumed for the calcultions that diameter of the piping was 325 mm, wall thickness was 16 mm and operating pressure was 8 MPa.

The calculation of global SSS of the pipings, which was conducted using the special software package, indicates that the level of the calculated axial stresses for the most stressed joint is relatively

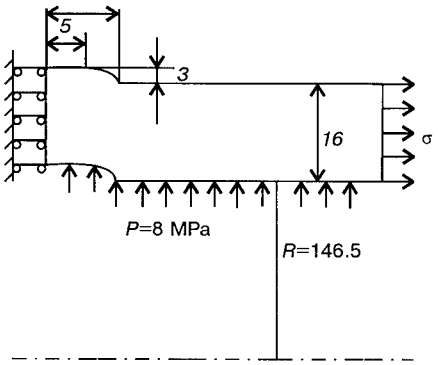

Figure 3. Calculation scheme for the circumferential weld zone in a piping

low, i.e. not higher than 130 MPa. First of all, this is associated with a sufficient compliance of the intermediate supports and displacements of the structural members, ensuring partial unloading of the pipings. Failure of the intermediate support has hardly any serious effect on the stressed state of the piping. The main contribution to the stressed state is made by the temperature gradient. The component of axial stresses induced by internal pressure is approximately constant and equals 35 MPa, while stresses induced by dead weight are not higher than 20 MPa.

The stressed state within the HAZ was estimated on the basis of a non-linear boundary problem of the theory of thermoplasticity solved by the FEM. The calculation scheme and initial geometrical sizes of the section of a shell are shown in Figure 3. Note that the geometry selected features the highest concentration of stresses and leads to conservative estimates in further calculations.

As a result of sampling, 2437 units and 3876 triangular members were obtained.

Results of the calculations of distribution of axial stresses through the wall thickness are shown in Figure 4. The reading is started from the internal side of the wall with thickness designated as H.

The calculations conducted made it possible to achieve the main purpose of the investigtions –

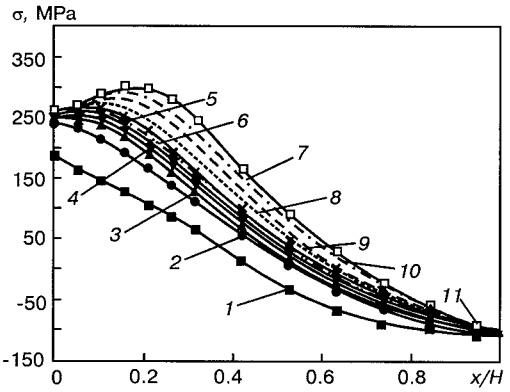

Figure 4. Distribution of stresses through the wall thickness of a pipe for different levels of effective stresses: *1* – residual stresses; *2* – 40; *3* – 50; *4* – 55; *5* – 60; *6* – 65; *7* – 70; *8* – 80; *9* – 90; *10* – 100; *11* – 110 MPa

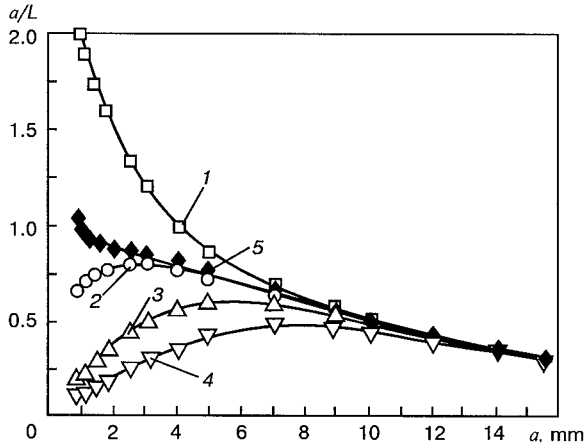

Figure 5. Example of the stable shape of propagation of the crack: *1* – a_0/L_0 = 2.0; *2* – 0.666; *3* – 0.2; *4* – 0.1; *5* – stable shape

dividing of defects into dangerous (requiring repair) and permissible. Methods used for estimation of structural strength and prediction of fatigue life, described in the previous Section, were algorithmically described and a number of technological problems were developed, using the method of weighing functions to determine the stress intensity factors and the stable development shapes in prediction of the residual life.

An example of the stable shapes of development of a defect is illustrated in Figure 5. Dependencies of variations in sizes a and L of the crack in corrosion cracking for their different initial values were plotted for a level of applied stresses equal to 40 MPa with an account made for residual stresses. As can be seen from the Figure, independently of its initial shape, the crack takes a stable shape after it propagates to a depth of 8 – 9 mm.

Similar calculations were also made for other levels of the applied stresses (residual welding stresses were assumed to be identical for all the joints, as the welding technology was the same). Therefrom, the stable shapes of the crack, a/L, predicted in an assumption of one embryo, were superimposed on the experimental data of Figure 2. Comparison of the levels of applied stresses with a measured shape of the crack for each damaged joint showed that in all cases the experimental points of Figure 2 were to the right from the predicted stable shape of the crack (for one embryo) corresponding to this joint. This is attributable to the fact that the majority of the cracks had more than one embryo. And this means that prediction of the shape of growth of a fatigue crack based on an assumption of one embryo is a conservative approximation to the estimate of the residual life of the welded joint.

Results of the calculations of the fatigue life measured in years, depending upon the length of a defect and level of stresses, can most conveniently be presented in the form of isolines of the same

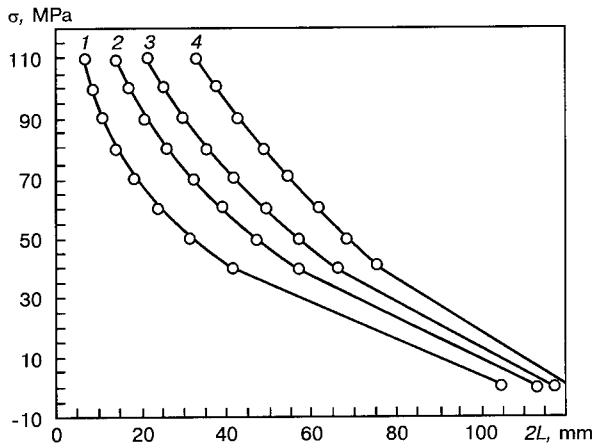

Figure 6. Diagrams for prediction of service life depending upon the level of effective stresses and initial length of a defect: *1* — Y = 1.5; *2* — 1.0; *3* — 0.75; *4* — 0.5 year

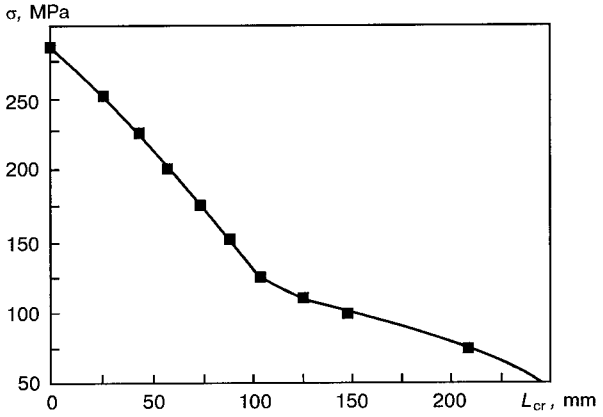

Figure 7. Calculation of a critical half-length of the through crack depending upon the level of effective stresses

fatigue life (Figure 6). Note that the value of 0.96 H is assumed to be a critical permissible depth of the surface crack.

Prediction of propagation of the through cracks was made to determine the margin of time to catastrophic fracture of the pipe since the moment of initiation of the through crack. Preliminarily, the limiting state of the structure was evaluated and the maximum permissible half-lengths of the through cracks, depending upon the level of the effective stresses, were calculated. Results of these calculations, with no allowiance for erosion wear, are shown in Figure 7. The plot in Figure 7 illustrates very clearly how large the lengths of the permissible through defects could be.

It should be noted that actual fatigue life Y for a given defect and a preset level of stresses is determined by the following expression:

$$Y\,(L_{cr}\,L_{in}) = Y\,(L_{cr}) - Y\,(L_{in}),$$

where L_{cr} is the critical half-length of the through crack determined from Figure 7, and L_{in} is the initial half-length of the through defects corresponding to a maximum length of the surface defect and depth of 0.96 H. The equations of the rate of growth of corrosion defects used to consider the through defects are identical to those used for the surface defects.

CONCLUSIONS

1. The efficient methodology has been developed for prediction of integrity of pipings, making it possible to solve a wide range of problems arising in strength design of complex piping systems with corrosion and fatigue defects, including those located near the welds, to ensure their failure-free operation. This methodology is based on the latest developments in the field of design of the SSS of frame structures, theory of shells and FEM, and on the mathematical models of fracture mechanics and the limiting state analysis.

2. The basic components of the above methodology have a high applied importance and can be used independently.

3. Practical application of this methodology enabled the residual life of members of 80 piping systems to be estimated. On this basis it can be concluded whether their residual service life could be extended or they require a repair.

REFERENCES

1. (1989) *PNAE G-7-002–86. Codes for strength design of equipment and pipings used in nuclear power plants.* Moscow: Energoatomizdat.
2. Erve, M., Tenckhoff, E. (1993) Residual life assessment, technical improvements and backfittng of components and systems from the materials standpoint. *Nuclear Engineering and Design*, **144**, 139 – 148.
3. (1975) *NUREG–75/061. US NRC Pipe Crack Study Group. Investigation and Evaluation of Cracking in Austenitic Stainless Steel Piping of BWR Plants.* Washington.
4. Ando, Y., Ikedami, R., Minematsu, A. (1980) TEPCO's experience of BWR cracking and current practice. In: *Proc. of IAEA Specialists Meeting on Environmental Factors Causing Pipe Cracks and Degradation in Primary System Component.* Vienna.
5. (1986) Pressure vessel and piping codes. Evaluation of flaws in austenitic steel piping. *Transact. of ASME J. of Press. Vess. Techn.*, **3**, 357.
6. Orynyak, I.V., Torop, V.M., Romashchenko, V.A. *et al.* (1998) Calculation of spatial branched piping system using the software package for assessment of strength of the NPP equipment. *Problemy Prochnosti*, **3**, 87 – 100.
7. Bergman, M., Brickstad, B. (1995) A procedure for analysis of leak before break in pipes subjected to fatigue or IGSCC accounting for complex crack shapes. *Fatigue and Fract. of Eng. Mat. and Struct.*, **18**, 1173 – 1188.
8. Bergmann, M., Brickstad, B., Dahlberg, L. *et al.* (1991) A procedure for safety assessment of components with cracks. Handbook. In: *Far. SA/Fou Report 91/01.* Stockholm.
9. (1987) *The time-based procedure for calculation of permissble defects in metal of equipment and pipings during operation of NPP.* Moscow.
10. Orynyak, I.V., Borodij, M.V. (1992) Engineering method for plotting weight function for the normal-tear plane cracks in three-dimensional bodies. *Problemy Prochnosti*, **10**, 14 – 22.
11. Orynyak, I.V., Borodij, M.V. (1994) The combined weight function method application for a hole emanated crack. *Eng. Fract. Mech.*, **6**, 891 – 894.

12. Orynyak, I.V., Borodij, M.V., Krasovsky, A.Ya. (1994) The problem of plotting of weight function for the normal-tear cracks having the shape of part of ellipse. *Problemy Prochnosti*, **4**, 58 – 63.
13. Savruk, M.P. (1988) *Stress intensity factors in bodies containing cracks. Fracture mechanics and strength of materials*. Kyiv: Naukova Dumka.
14. Kumar, V., German, M.D., Wilkening, W.W. *et al.* (1984) Advances in elastic-plastic fracture analysis. *EPRI Report NP-3607*, **8**, 1 – 236.
15. Varfolomeev, I.V., Vainshtok, V.A., Krasovsky, A.Ya. (1990) Criteria and stable shapes of growth of non-through cracks under cyclic loading. *Problemy Prochnosti*, **8**, 3 – 10.
16. Orynyak, I.V., Torop, V.M., Borodij, M.V. (1996) Ductile fracture of a pipe with a part-through slot. *Int. J. Press. Vess. & Piping*, **2**, 171 – 180.
17. Orynyak, I.V., Torop, V.M., Borodij, M.V. (1995) Tough fracture of a pipe with a three-dimensional rectangular defect. *Problemy Prochnosti*, **8**, 34 – 44.

PROBLEMS REGARDING WELDED STRUCTURES OF THE «SHELTER» OBJECT AT THE CHORNOBYL NUCLEAR POWER STATION

P.I. KRIVOSHEEV
State Research Institute for Building Structures, Kyiv, Ukraine

ABSTRACT

Problems with structures in the «Shelter» object at the Chornobyl Nuclear Power Station (ChNPS) are outlined. The most important measures intended for implementation of the strategy of stabilization of the «Shelter» object are indicated. They are based on building of the new and reinforcement of existing metal structures by making an extensive use of welding. The experience gained will be applied for further work aimed at long-term stabilization of the «Shelter» object.

Key words: *Shelter, safety, stabilization measures, metal structures, welding operations, quality control.*

It is a well known fact that the Shelter was built in 1986 within a very short period of time to protect the environment from radioactive wastes of unit 4 of the ChNPS destroyed by the accident. This object is unique both in terms that it is extremely hazardous for the environment on the global scale and in terms of construction involving problems which are not peculiar to a conventional building. All of them are of an integrated character.

The protective skin of the Shelter (Figure 1) is designed so that it consists of a northern cascade and eastern walls, southern fragment with a concrete wall, western counterfort wall and roofing (of a complicated design made from metal structures). Beams B1 and B2 with a tubular counter floor placed on them are mounted on the air pits on the eastern side and on the wall along axis 50 on the western side of the Shelter. The northern hook shields are mounted on the counterforts of the northern cascade wall and beams B1 (Figure 2).

In the southern end the flat shields are mounted on Beam B1 and beam «Mammoth» (Figure 3) installed via supports on the concrete wall along axes C – D. The southern hook shields are placed on beams «Mammoth» and «Octopus» (Figure 4) mounted on the roofing and consisting of a heap

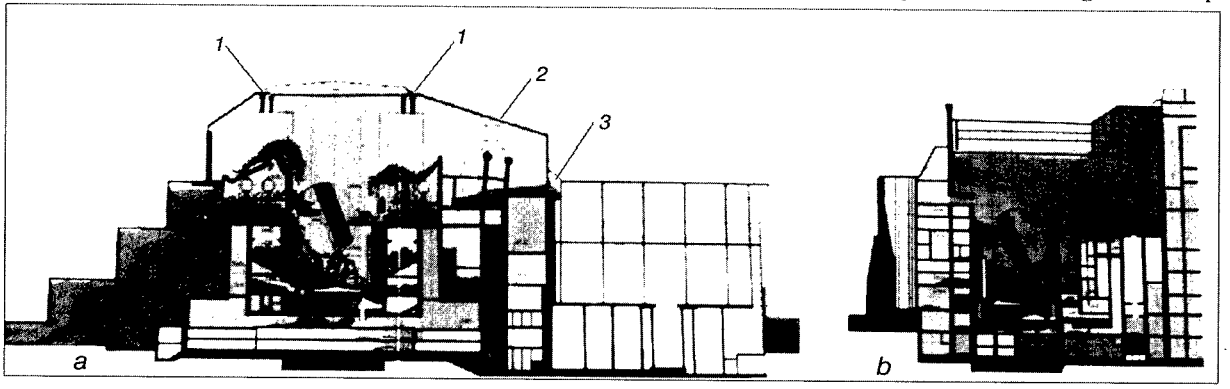

Figure 1. General view of the Shelter: *a* — sectional view along axis L; *b* — sectional view along axis 47; *1* — blocks of beams B1 and B2; *2* — «Mammoth» beam; *3* — «Octopus» beam

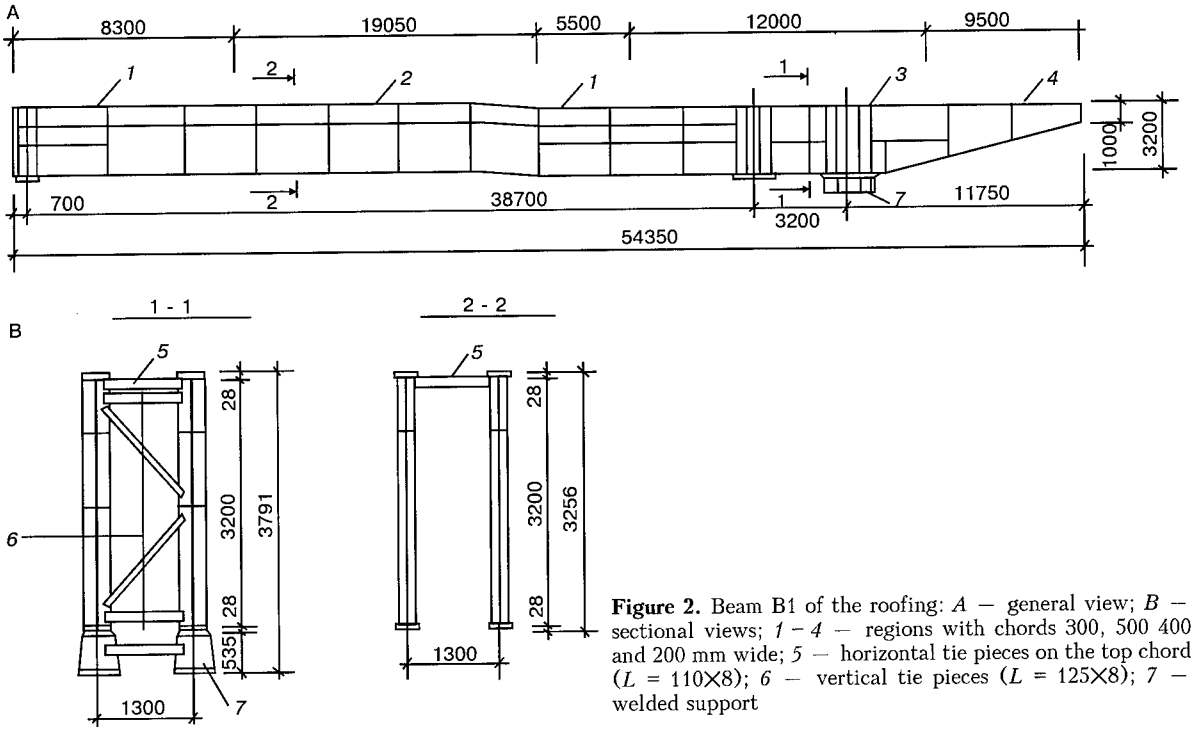

Figure 2. Beam B1 of the roofing: *A* — general view; *B* — sectional views; *1* – *4* — regions with chords 300, 500 400 and 200 mm wide; *5* — horizontal tie pieces on the top chord (L = 110×8); *6* — vertical tie pieces (L = 125×8); *7* — welded support

of ruined structures of the deaeration stack. On the western side there are western shields and hook shields mounted between the counterfort wall and the wall along axis 50.

It should be noted that there exists the problem of uncertainty or extreme scantiness of reliable data on the object. In the majority of the cases it is impossible to thoroughly examine the actual state of structures that remained, as during the process of elimination of consequences of the accident and building of the Shelter some structures were dropped from helicopters, some were buried in heaps and some were encased in concrete. Almost everywhere their examination is hindered by radiation which is dangerous for the health.

Building of new structures was done under extremely difficult radiation conditions, most often with no direct access of the personnel to the building site, by using the remote control. That is why the conventional control was hardly possible. Further examinations revealed very many deviations from the initial design. For the same reason the majority of structural members were joined by simply bringing them into contact, and their remaining

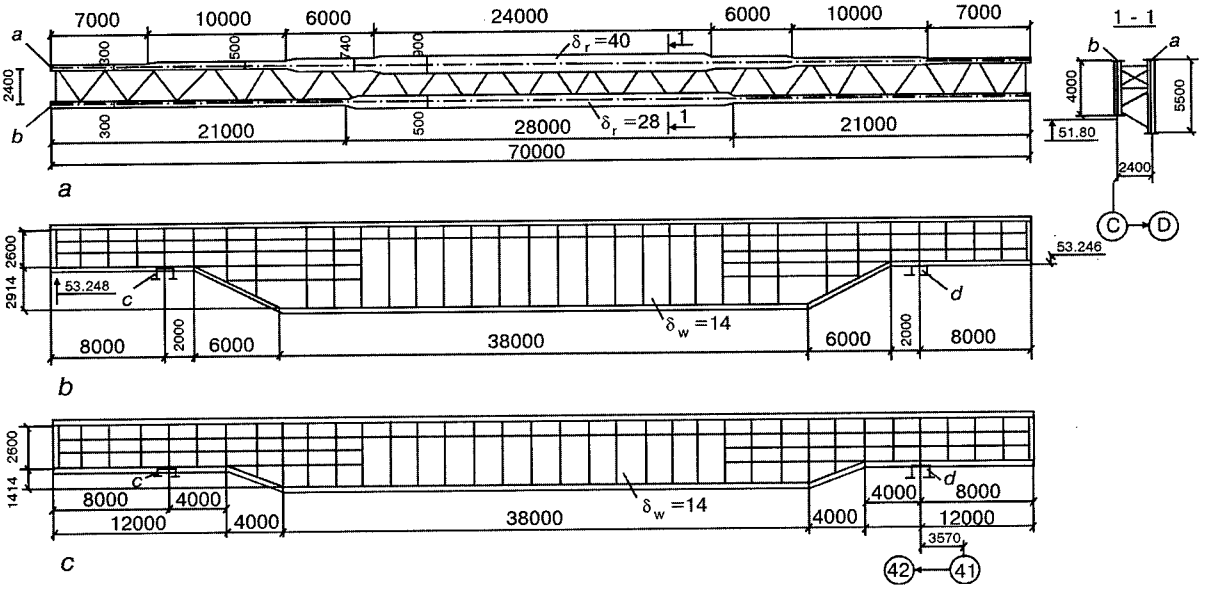

Figure 3. Diagram of the «Mammoth» beam: *a* — rear beam (large); *b* — front beam (small); *c* — support near axis 51; *d* — support near axis 41

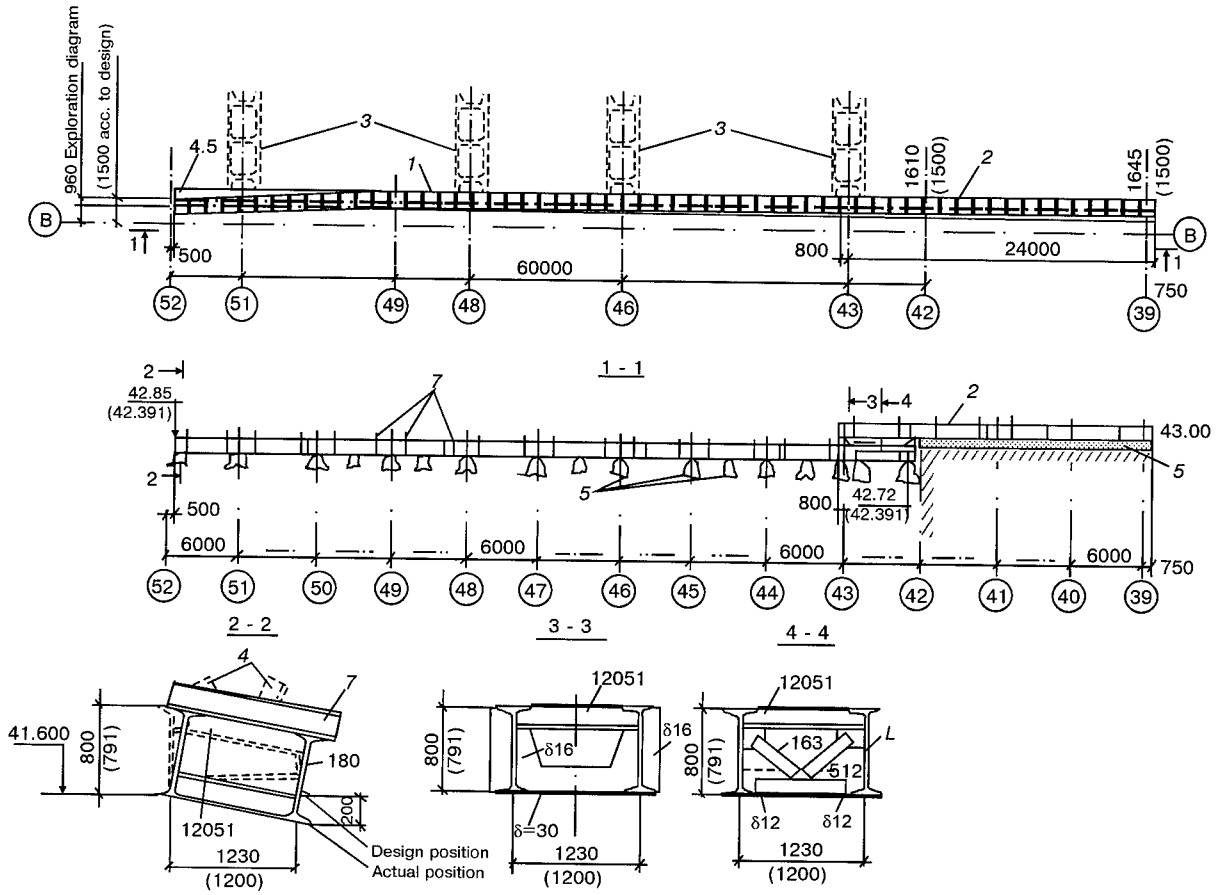

Figure 4. Diagram of the «Octopus» beam: *1* — the «Octopus» beam on axes 42 – 52; *2* — same on axes 43 – 30; *3* — armature; *4* — collector supports; *5* — concrete supports; *6* — concrete grout; *7* — transverse beams

in a permanent condition is maintained only by friction forces, which is hardly ever practiced under normal conditions.

The above peculiarities required investigation of the problem of revealing coarse defects. The point is that in the last years both domestic and foreign specialists have made sure that it is these defects, as well as errors in design, construction and operation, that most often cause accidents at building structures.

During the expert supervision of the construction, the Designer General, which was the All-Russian Research and Development Institute for Experimental Technologies in St.Petersburg, revealed and repaired in 1986 – 1991 a number of serious defect. In particular, they reconstructed roofing of the machine room and reinforced cross bars of the top ceiling of the deaeration stack. Since 1992 such a supervision has been performed by the State Research Institute for Building Structures.

Statistical analysis of the examination results led to a conclusion that the number of critical defects in structures of the Shelter, including defects missed in examination, was extremely large. Based on analysis of all available data and results of its examinations, the Research Institute for Building Structures compiled a list of 29 probable critical zones. The problem of stabilization (reconstruction) of the Shelter to ensure its failure-free operation for the calculated service life is multifactorial. It also includes the issue of maintaining the integrity of external enclosures without the requirement to preserve the current state of internal structures.

First of all, the service life itself cannot be infinite, primarily because of corrosion of metal under conditions of the humid (due to atmospheric precipitation) environment. According to the available data (still very scanty to date), the life time of the structure can be approximately 50 years. It is not clear either when the permanent construction (designed for a long-term operation) will be started and how long it will take.

Stabilization should be done first of all to those structural members the reliability of which causes doubts. Further on the necessity of realization of the preliminarily scheduled precautions could be revised. In this case it should be borne in mind that in the future radioactive materials will have to be removed from the object. The work associated with stabilization should hinder neither removal of radioactive materials nor construction of a capital shelter. It is not improbable that some of the existing structures will be included into it.

Preliminary study of the specific stabilization works showed the crucial importance of their rational technological implementation, which determine to a substantial degree the amount of extra costs, the reasons for this being as follows:

it will be necessary to allocate part of the total manpower to do the radiation-hazardous jobs, take into account their increase because of a psychological effect and the fact that the use of protection means will make the job more difficult to do;

it will be necessary to estimate an extra dose in doing auxiliary operations;

it will be necessary to take into account specifications for limitations on permissible doses per day, month and year;

in many cases the use of protective screens will be required.

All this should be taken into account both in plans and specifications for arrangement of works (they should be specified in detail in flow charts), and in a radiation safety report without the approval of which no work on the Shelter is permitted.

Solving the above problems, as well as some less critical one, requires involvement of a wide circle of highly skilled specialists.

In December 1996 the Cabinet of Ministers of Ukraine issued the Resolution «Measures for Conversion of the «Shelter» Object into the Environmentally Safe System», which formulated the main goal of the works – to remove within the maximum short terms the remaining nuclear fuel, isolate and bury it in compliance with the national and international standards in force. This Resolution was used as the basis for development of «The Strategy of Conversion of the «Shelter» Object», which clearly stated the position of Ukraine regarding conversion of the object into the environmentally safe system.

Works performed in the last years on selection of the optimal ways of ensuring safety of the Shelter showed their extreme complexity and the need to use a step-by-step approach. To solve these problems, it is necessary to join intellectual forces and economical resources of many countries.

In 1994 – 1995 the European Consortium «Alliance» developed under the TASIC program the feasibility study for stabilization of the existing Shelter and construction of Shelter-2. As indicated by results of this work, construction of the new Shelter-2 is a project which is too expensive for Ukraine.

The International Chornobyl Fund was established to provide financial support to the project. In December 1995 the European Commission and Ukraine signed the «Memorandum of Understanding ...» which was later agreed upon by the G7 countries. The international group of experts was formed in 1996. The group includes experts from the European Union, USA, Japan, Ukraine and Russia. Under the TASIC nuclear safety project «Chornobyl Unit 4. Short and Long Term Measures», this group accomplished analysis and optimization of technical solutions and worked out the «Recommended Course of Actions» to describe the basic concept of handling the problems regarding the short and long term stabilization.

Later on, based on the already accomplished works, on February 11, 1997, in Washington, DC, the G7 nuclear safety work group (G7-NSWG) in collaboration with representatives of Ukraine decided to develop a plan for realization of short and long term measures.

The stabilization strategy has become the subject of detailed discussions. In development of the plan of the immediate measures regarding the revealed 29 critical zones, the comprehensive analysis and computations based on the use of decreased loads (for an operation term of 15 years) resulted in reducing the above list to 15 zones:

control of beams B1/B2 along axes 50G and 50P;

reinforcement of the western fragment of the Shelter (counterfort wall and wall along axis 50);

stabilization of the frame of the deaeration stack;

reinforcement of the air pits;

reinforcement of the northern wall along axis R and its connection to the northern hooks;

joining of the southern shields to each other;

joining of the southern hook shields to each other;

joining of the southern hook shields to the southern shields;

joining of the northern hook shields to each other;

securing of the northern shields to beam B1 using cross pieces;

joining of the northern hook shields with the counterfort wall using fixation anchors;

setting the southern flat shields against the wall along axis 50;

joining the disks of the northern and southern hipped plates via the tubular counter floor member;

reinforcement of the western support of the «Mammoth» beam;

setting the southern hook shields against the machine room walls.

Fulfillment of the immediate measures should be done by construction of the new and reinforcement of existing metal structures by making an extensive use of welding operations (Figure 5).

Defects in supports B1 and B2 were repaired (safety supports on the western side were constructed and missing tie pieces in the cantilever of southern beams B1 were installed) and the ventilation duct was reinforced in the selected critical zones. Reinforcement of the supports of beams B1 and B2 is schematically shown in Figure 6.

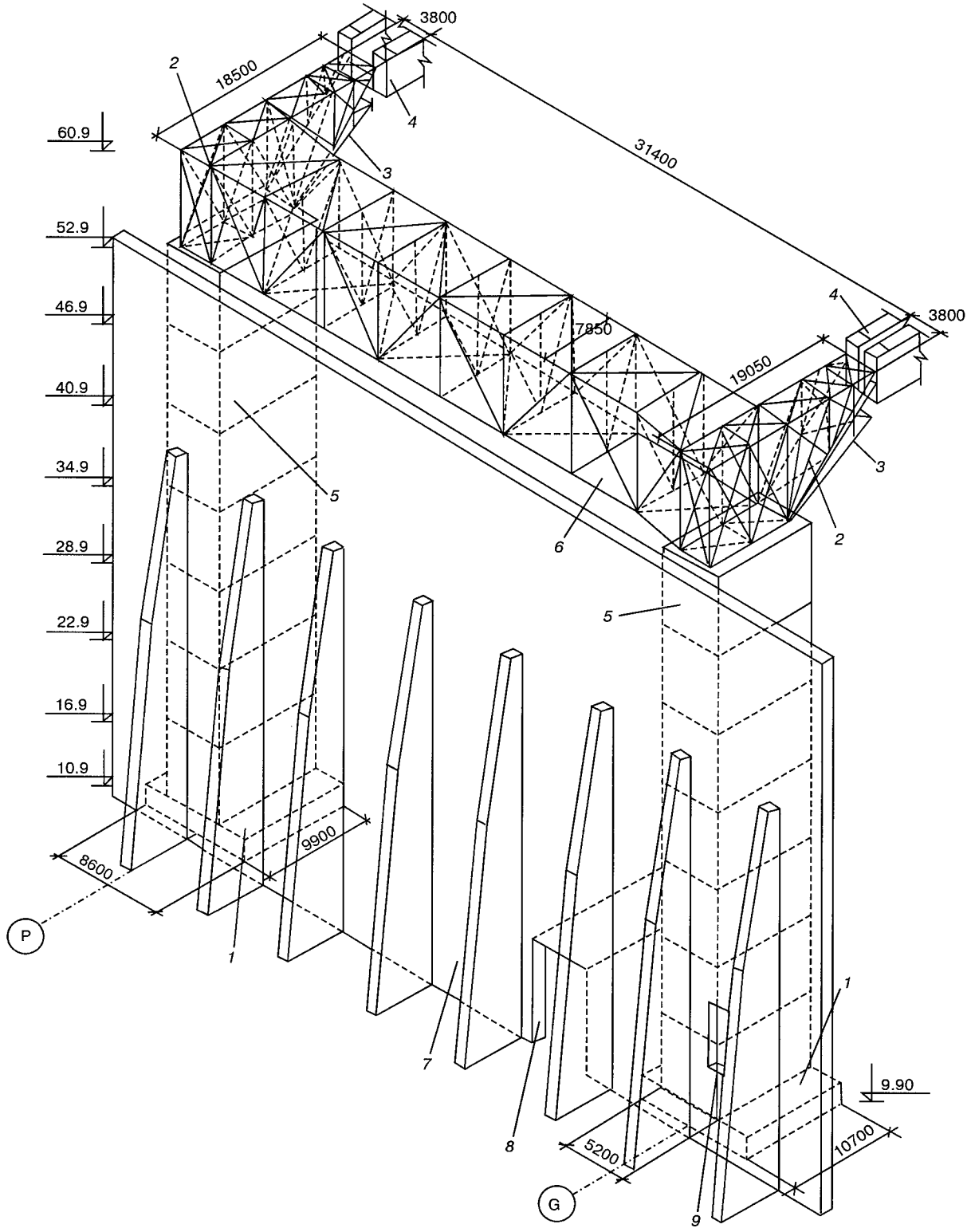

Figure 5. One of the variants of reinforcement of the western fragment of the Shelter (wall along axis 50): *1* — reinforced concrete bedplate; *2* — cantilever member; *3* — rest; *4* — block of beams B1 – B2; *5* — reinforced concrete column; *6* — spatial tie member; *7* — counterfort wall; *8* — transport corridor; *9* — opening

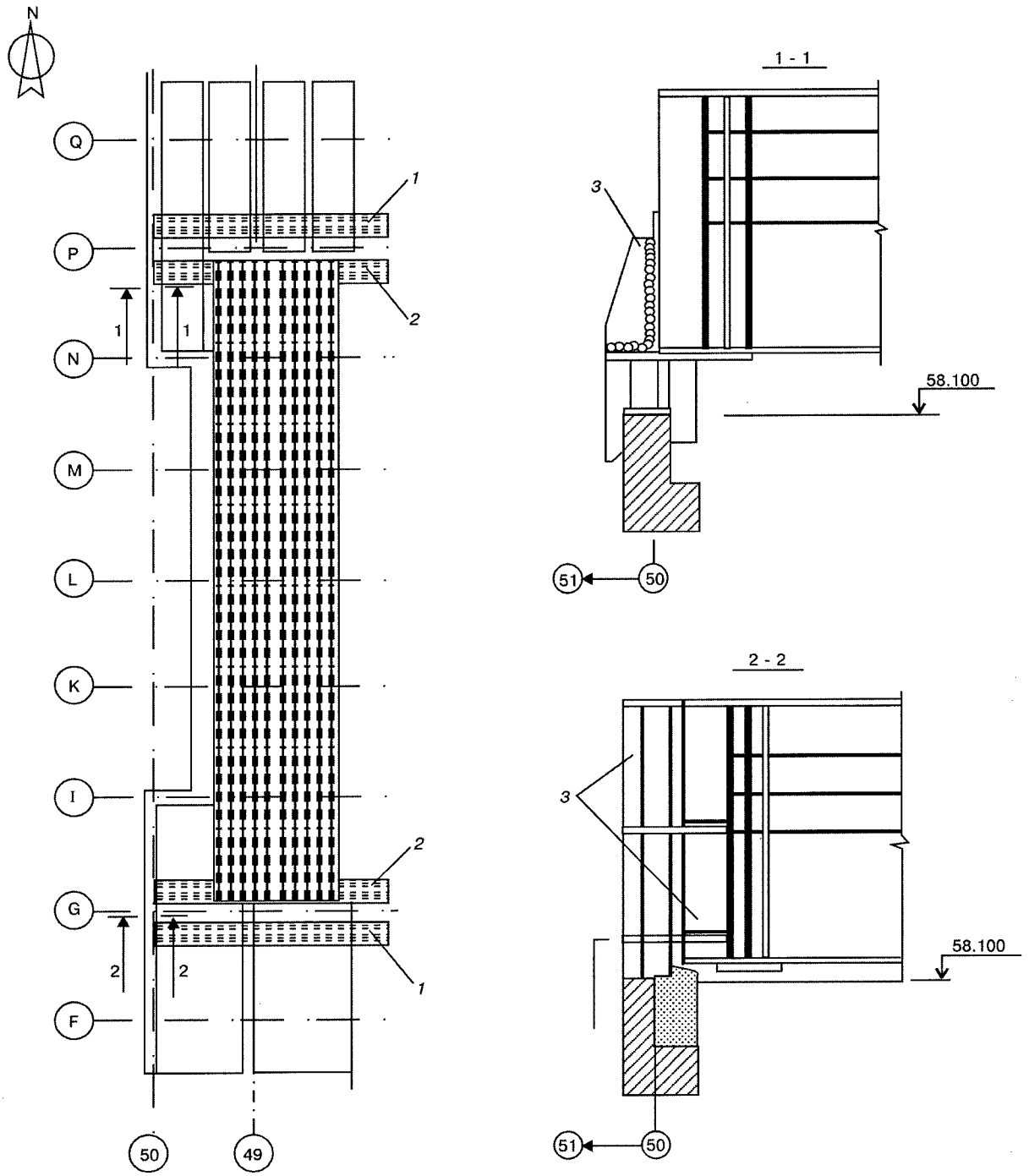

Figure 6. Reinforcement of supports of beams B1 and B2 along axes 50P and 50G: *1* — beam B1; *2* — beam B2; *3* — reinforcing member

Flow charts were developed for performing welding operations. The works indicated in the flow charts include:

preparation of welding consumables and equipment;

removal of dust from the welding operations sites;

performance of welding operations;

inspection of welded joints;

repair of defects in welds;

corrosion protection of the weld regions.

The general preparatory work includes:

training of welding operators and inspectors (flaw detection);

training of welding engineers, supervisors and work managers;

input control of base materials and welding consumables;

control of quality of structures to be welded;

inspection of condition of welding equipment;

use of control and measurement instruments, devices and equipment.

Training of personnel involved in doing welding operations and inspection of welded joints, as well as work managers was done in compliance with the approved training programs. The programs were worked out on the basis of the regulatory and technical documents and requirements specified in Section 5 of the Instruction «Radiation Safety Regulations in Performing the Works on the «Shelter» Object, 6E-OU».

Welders qualified for performing welding operations in accordance with DNAOP.0.00-1.16–96 «Welders' Qualification Regulations» were involved in performing welding and inspection of welded joints.

The input control of the quality of base materials and welding consumables was carried out according to requirements of the flow charts to determine their compliance with working drawings, certificates, standards and delivery specifications.

Based on comprehensive analysis and study of available welding processes using different types of automatic and semi-automatic devices, which were recognized as unsuitable for the purpose because of the too labour-extensive maintenance of the equipment under the high radiation conditions, the necessity of using manual methods to complete welding, and because of a highly complicated configuration of structural members, the method of choice was manual electric-arc welding using covered electrodes.

Large dimensions and heavy sections of the members welded imposed special requirements on the quality of welded joints.

The works were preceded by a period of training and optimization of all technological operations using a welding simulator which was built for the purpose in the «clean» zone of Chornobyl.

Welding operations were performed in the following sequence:

a team (welder and supervisor), being in a protected box, received an instruction from the work manager to make a weld according to the approved flow chart, as well as the information on the work done by a previous team;

the welder and supervisor put on respiratory organs protection means, switched on individual radio sets, checked performance of the latter and moved from the protected box to the erection site;

the welder went downstairs to the shields of the counter floor with biological protection and fixed himself at the work place using the safety belt. The supervisor switched on the welding equipment and the ventilation device on command given by the welder;

the welder was working in the field of view of the supervisor;

on a command given by the work manager from the protected box, the welder stopped the work and the supervisor switched off the equipment, then the welder cleaned the weld from slag;

the welder and supervisor left the work place, switched off the equipment and ventilation device, took off the respiratory organs protection means, put them into a plastic bag and went out to the protected box;

the welder reported to the work manager on the amount of the weld he made;

the inspector came downstairs to the shields of the counter floor with biological protection and fixed himself there using the safety belt, remaining in the field of view of the supervisor, then he visually examined the weld or its region;

on a command given by the work manager from the protected box the inspector, upon examination of the weld, stopped the work and left the work place together with the supervisor;

the supervisor reported to the work manager on the amount and results of the weld inspection.

In the case of detecting defects in the weld or its regions, the work manager gave an appropriate instruction to the special repair staff, which consisted of erectors or highly skilled welders.

Regions of the welds containing defects were cut out by grinding machines equipped with abrasive wheels. Then followed the works aimed at removal of defects in the welds.

Upon completion of welding, the welded joints were subjected to corrosion protection by painting using sprayers.

The level of radiation at the work places and duration of the works were controlled by the Shelter radiation control staff.

Sequence of welding operations, change of the teams of welders and supervisors were checked by the work manager. Communication between participants in the works performed on beams and the work manager was done via radio sets.

Industrial TV cameras installed at different angles displayed the entire course of the works on the work manager's monitor which was located in the «clean» zone room. The course of welding operations was watched from a separate monitor by the staff getting prepared to come out to the Shelter roofing.

The experience gained will be used for performing the works in all critical zones and for the long-term stabilization of the Shelter.

DETERMINATION OF CYCLIC LIFE OF STRUCTURE ELEMENTS IN ARRESTING FATIGUE CRACKS

V.V. KNYSH
The E.O. Paton Electric Welding Institute, NASU, Kyiv, Ukraine

ABSTRACT

Method of calculated determination of a cyclic life of structure elements with propagating fatigue cracks at their arresting by an artificially-induced field of residual compressive stresses ahead of tips of these cracks has been developed on the basis of approaches of fracture mechanics.

Key words: *fatigue crack, crack arresting, residual stresses, cyclic life, stress intensity factor, effective range.*

The well-founded application of methods of an artificial inducing of residual compressive stresses ahead of a fatigue crack tip to arrest it in a structure welded element requires a creation of methods of a calculated estimation of effectiveness of these methods. This estimate will make it possible to determine the most rational fields of application of different structures, and also to optimize their parameters depending on an initial length of a fatigue crack, characteristics of a cycle of an alternating load and material properties. In this aspect, the method of a calculated determination of a cyclic life of the structure elements with propagating fatigue cracks at artificially-induced residual compressive stresses ahead of the crack tip, is most rational.

Experimental investigations showed the significant increase in life of the specimens with fatigue cracks after using different kinds of treatment for inducing residual compressive stresses ahead of the crack tip. In addition, the growth of a fatigue crack is essentially decreased with next increase in its values, which in both cases correspond to a linear (Perisovsky) region of the fatigue fracture diagram. Such kinetics of the fatigue fracture of the structure elements considered allows the approaches of a linear mechanics of fracture to be used in the development of a method of a calculated determination of their cyclic life.

It is known, that ahead of the propagating fatigue crack the so-called reversible zone of plastic deformation is formed, whose size is much smaller than the length of the plastic deformation zone, which corresponds to a static loading. Size of the «reversible» zone undergone a plastic yielding which alternates due to load-unload half-cycles, can be presented for alternating tensile stresses in the form [1]

$$r_p = \frac{1}{2\pi}\left(\frac{\Delta K}{2\sigma_y}\right)^2,$$

where ΔK is the range of the stress intensity factor (SIF).

The residual compressive stresses σ^c_{ry}, which are artificially induced ahead of a tip of $2l_0$ long fatigue crack, promote a restricted developing of the plastic deformation ahead of a crack tip and, thus, influence the size of the «reversible» zone of the plastic deformation by its diminishing. In this case the size of the «reversible» zone is suggested to be calculated by a relation in the form

$$r_{p0} = \frac{1}{2\pi}\left[\frac{\Delta K_{\text{eff}}\,(l_0)}{2(\sigma_y + \sigma^c_{ry})}\right], \qquad (1)$$

where $\Delta K_{\text{eff}} = K_{\max} - K_{\text{op}}$ is the effective range of SIF of a cycle of alternating load for a preset crack of $2l_0$ length.

In earlier investigations [2] the expression for ΔK_{eff} was established in the form

$$\Delta K_{\text{eff}} = \exp\left[\frac{\lambda\,(R_\sigma - 0.5)}{m_{-1}}\right]\Delta K, \qquad (2)$$

where $\Delta K = K_{\max} - K_{\min}$ is the range of SIF of a cycle of alternating load with asymmetry R_σ; λ and m_{-1} are the material constants.

If the artificially-induced residual compressive stresses do not arrest the crack ahead the fatigue crack tip, but only minimize the rate of its growth, then at maximum value SIF of a cycle of alternating load $K_{\max}$ the crack is open. In addition, the size of the zone of the plastic deformation ahead of a tip of the arresting fatigue crack is determined by a relation (1) taking into account the formula (2).

To calculate the effective SIF range of a cycle ΔK^c_{eff} that corresponds to arresting the fatigue crack induced ahead of its tip by the field of compressive stresses σ^c_{ry}, let us consider a model of the crack growth given in Figure 1.

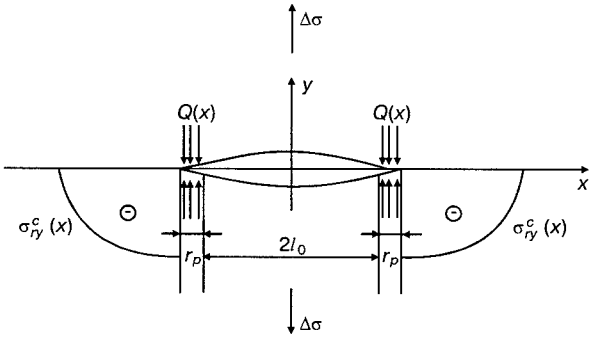

Figure 1. Model of fatigue crack growth in the field of residual compressive stresses, artificially-induced ahead of the crack tip

Let assume that the crack of an effective length $2(l_0 + r_p)$ (where l_0 — a half-length of arresting fatigue crack; r_p — «reversible» zone of plastic deformation) is located in a finite elastic plate and nonhomogeneous compressive stresses $\sigma^c_{ry}(x)$ are acting ahead of its tips. Here, the elastic plate is subjected to the action of alternating stresses (range $\Delta\sigma = \sigma_{max} - \sigma_{min}$ with a cycle asymmetry $R_\sigma = \sigma_{min}/\sigma_{max}$), which are directed normal to the crack plane, while towards the lips of cracks at the regions equal to r_p near its tips the forces $Q(x)$ are applied which are directed opposite the acting alternating stresses. Within the scope of mentioned model conceptions we can write the following relation for calculation of value of maximum SIF of cycle K_{max}, assuming $Q(x)$ equal to the material yield strength, σ_y, according to Leonov-Panasyuk approach [3]

$$K_{max} = \sigma_{max}\sqrt{\pi(l_0 + r_{p0})} - 2\sigma_y\sqrt{\frac{l_0 + r_{p0}}{\pi}}\arccos\frac{l_0}{l_0 + r_{p0}}.$$

The calculated value SIF of a cycle of alternating load of the preset asymmetry R_σ which corresponds to the moment of opening the fatigue crack K_{op} will be calculated on the basis of using the model of G.I. Barenblatt [4]. By assuming in the mentioned model that the cohesive forces at the crack tip $Q(x) = 2\sigma_y + \sigma^c_{ry}$ and by presetting the zone of their action $a = r_{p0}$, and after calculating the appropriate integral, we shall obtain

$$K_{op} = 2\sqrt{\frac{2r_{p0}}{\pi}}(2\sigma_y + \sigma^c_{ry}).$$

Thus, the model of effective crack considered (Figure 1) makes it possible to calculate the effective range of SIF of the cycle ΔK^c_{eff} for the fatigue crack of length $2l_0$ which takes into account the residual compressive stresses acting ahead of the crack tip. The appropriate calculating formula takes the form

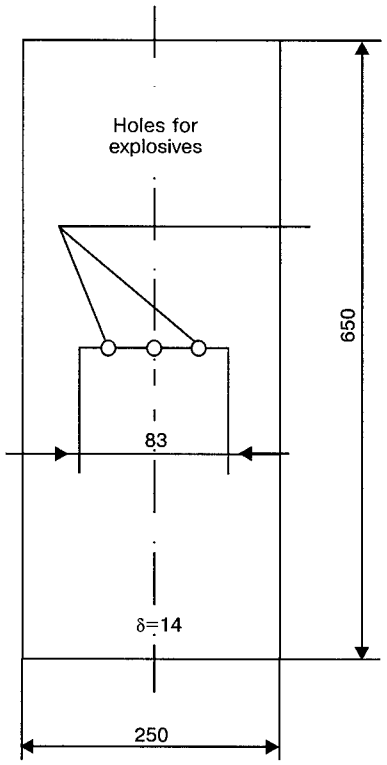

Figure 2. Sample for experimental estimation of effectiveness of a local explosion treatment in arresting the fatigue crack

$$\Delta K^c_{eff}(l_0) = \sigma_{max}\sqrt{\pi(l_0 + r_{p0})} - 2\sigma_y\sqrt{\frac{l_0 + r_{p0}}{\pi}}\arccos\frac{l_0}{l_0 + r_{p0}} - 2\sqrt{\frac{2r_{p0}}{\pi}}(2\sigma_y + \sigma^c_{ry}). \quad (3)$$

It is assumed that the effective range of SIF $\Delta K^c_{eff}(l_0)$, calculated from the expression (3), determines the kinetics of the fatigue fracture at growing the fatigue crack from $2l_0$ to $2(l_0 + r_{p0})$. Here, the calculation of a proper quantity of cycles of stress changes, required for the mentioned growing the fatigue crack is made on the basis of a kinetic fatigue fracture, suggested in [2]. Substituting the value of effective range of SIF, calculated from (3), in the used equation of a crack propagation, and fulfilling the necessary transformations, we shall obtain the calculated value of life N_0 in the form

$$N_0 = \frac{r_{p0}}{C_{-1}\, e^{1.5\lambda}\,[\Delta K^c_{eff}(l_0)]^{m_{-1}}}, \quad (4)$$

where C_{-1}, m_{-1} and λ are the material constants determined during tests on cyclic crack resistance of reference samples [5]. During growing the arresting crack from the beginning of its arrest ($2l_0$ crack length) until the complete intersection of the zone of distribution of residual compressive stresses

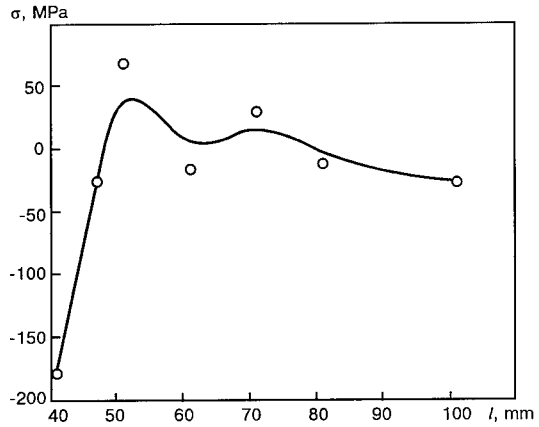

Figure 3. Diagram of distribution of residual compressive stresses induced ahead of the fatigue crack tip by a local explosion treatment

with a crack ($2l_k$), the appropriate calculated value of a cyclic life is determined by the formula

$$N = N_0 + \sum_{i=1}^{k} \frac{r_{pi}}{C_{-1}\, e^{1.5\lambda}\left[\Delta K_{\text{eff}}^{c}\left(l_0 + \sum_{j=0}^{i=1} r_{pj}\right)\right]^{m_{-1}}}.$$

Suggested method of a calculated estimation of a cyclic life was tested on the base of experimental data of a cyclic crack resistance of steel St.3 (killed) (σ_y = 296 MPa, σ_t = 476 MPa) after arresting the fatigue crack using the explosion treatment.

Flat samples were tested (Figure 2) with a fatigue crack of a half length l_0 = 41.5 mm at axial from-zero cyclic loading. Ahead of the crack tips the field of residual compressive stresses was induced using a local explosion treatment technology suggested at the E.O. Paton Electric Welding Institute.

The appropriate diagram of distribution of residual compressive stresses ahead of a crack tip is given in Figure 3. It is seen from the Figure that the maximum compressive stress reaches values close to 0.6 σ_y of material. After the local explosion treatment the sample was tested on a cyclic crack

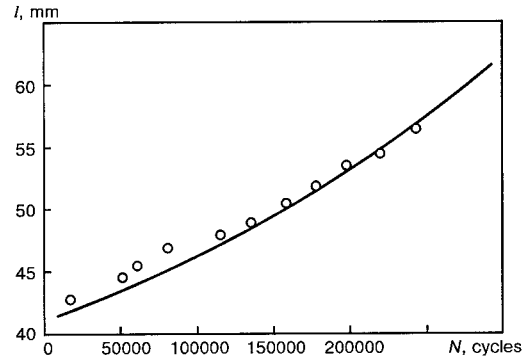

Figure 4. Dependence of a length of arresting fatigue crack on a number of cycles of alternating load

resistance at from-zero axial loading with maximum stresses of cycle in a net section, equal to 155 MPa.

Figure 4 presents the experimental data (circles) and calculated values (solid line) of dependence of the length of arresting fatigue crack on the number of cycles of the alternating load. The necessary characteristics of cyclic crack resistance of steel St.3 (killed) for a calculated determination of the life, were taken equal to $C_{-1} = 0.73 \cdot 10^{-13}$, m_{-1} = 3.96 and λ =1.1, according to data of [5]. Comparison of obtained calculated values of life with experimental data (Figure 4) shows their satisfactory correlation during the propagation of the fatigue crack from its half-length l_0 = 41.5 mm (beginning of crack arresting) and up to a half-length l_0 = 57 mm when the crack intersects completely the zone of distribution of residual compressive stresses which arrest its growth.

REFERENCES

1. Khertsberg, R.V. (1989) *Deformation and fracture mechanics of structural materials*. Moscow: Metallurgia.
2. Trufyakov, V.I., Knysh, V.V., Mikheev, P.P. *et al.* (1990) Method of calculated estimation of a cyclic crack resistance of welded joints with allowance for effect of residual stresses. *Avtomaticheskaya Svarka*, **1**, 1 – 4.
3. Panasyuk, V.V. (1968) *Limiting equilibrium of brittle bodies with cracks*. Kyiv: Naukova Dumka.
4. Kachanov, L.M. (1974) *Fundamentals of fracture mechanics*. Moscow: Nauka.
5. Trufyakov, V.I., Knysh, V.V., Mikheev, P.P. *et al.* (1987) Dependence of rate of fatigue crack propagation on cycle asymmetry. *Problemy Prochnosti*, **3**, 5 – 7.

DIAGNOSTICS OF STRUCTURES OF METALLIC AND COMPOSITE MATERIALS USING HOLOGRAPHY, ELECTRON SPECKLE-INTERFEROMETRY AND SHEAROGRAPHY

L.M. LOBANOV[1], **V.A. PIVTORAK**[1] and **N.G. KUVSHINSKY**[2]
[1]The E.O. Paton Electric Welding Institute, NASU, Kyiv, Ukraine
[2]T.G. Shevchenko National University, Kyiv, Ukraine

ABSTRACT

Results of application of methods of holographic interferometry, electron speckle-interferometry and shearography for nondestructive quality control and determination of residual stresses in elements and members of the welded and adhesion-bonded structures made of metallic and nonmetallic materials are presented. To make diagnostics of structures, the compact holographic schemes and devices have been designed and manufactured with the help of which the local fields of displacements and deformations in the zones of defects and relaxation of residual stresses are recorded. Examples of diagnostics of aircraft and machine-building structures using the holographic interferometry, electron speckle-interferometry and shearography are given.

Key words: *holographic interferometry, electron speckle-interferometry, shearography, nondestructive testing, residual stresses, computer processing.*

Assurance of the high quality of structures is one of the most important scientific-technical problems, whose importance is growing with making structures more complicated. This problem is many-sided and solved in several directions. Among them, the responsible role belongs to the development and spreading of the advanced methods and equipment for NDT, and also to the determination of residual stresses, whose effectiveness depends, first of all, on their adequacy and efficiency.

In industry the radiographic, ultrasonic, magnetic, eddy-current and other NDT methods are widely used. The advanced research centres develop and implement new methods of the quality control and determination of residual stresses of different products and materials. Integral methods of control which combine several methods are very challenging. New feasibility for diagnostics of structures consists in using methods of optical holography, electron speckle-interferometry and shearography.

The method of the holographic interferometry is used in different branches of industry. Its principle is based on the comparison of holographic images reproduced from a hologram on which the initial and changed states of the product are recorded. The changes can be caused by a mechanical loading, thermal deformation and some other factors occurring in the process of service of the product or during its strength testing [1].

The expensive large vibroinsulating stands and equipment are usually used for diagnostics of quality of different structures. When the structure elements are examined using this equipment the rather complicated schemes, containing a large amount of different optical elements are used in holographic interferometers. To use the above-mentioned holographic equipment is difficult in many cases as it is not always possible to arrange the objects on a holographic stand.

The E.O. Paton Electric Welding Institute has developed small-sized devices, instruments and optical schemes which can be arranged on the objects to be examined without any special vibroprotection. In collaboration with T.G. Shevchenko National University a small-sized thermoplastic camera has been developed, in which a new composition of the film of amorphous molecular semiconductors, deposited on a glass plate, is used for the hologram recording. One such plate with a coating can record at least 1000 holograms (record-erase cycle).

The highly-sensitive compact thermoplastic camera of an instantaneous recording of holograms in real time gives new opportunities for the development of portable holographic devices and instruments for diagnostics of structures under the site and service conditions (Figure 1).

The application of fibrous optics in optical schemes of interferometers could reduce to minimum the number of optical elements and to eliminate the use of a special vibroprotection of holographic devices. Thus, a compact device, which could perform diagnostics of pipes without a holographic stand, was designed and manufactured for

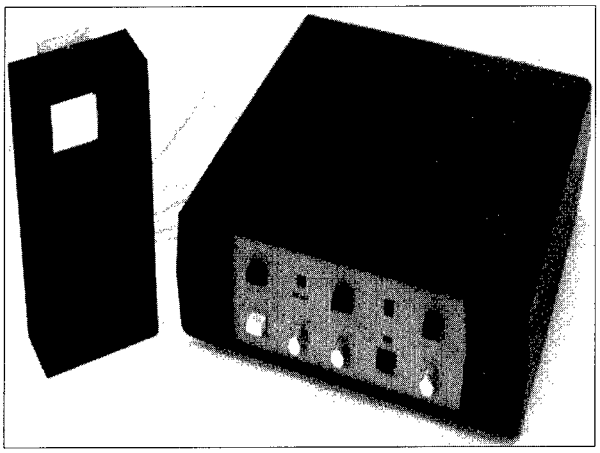

Figure 1. General view of a compact thermoplastic camera with an electron control unit for an instantaneous recording of holograms

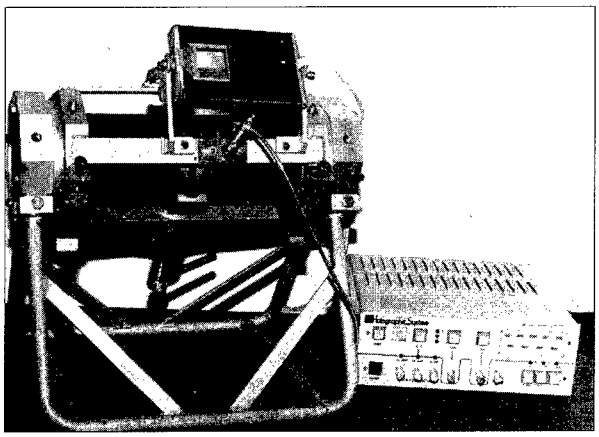

Figure 2. General view of a holographic unit for nondestructive quality control of elements of tubular structures

nondestructive holographic quality control of welded and adhesive-bonded thin-walled pipes from polymeric and composite materials, widely used in advanced branches of industry (Figure 2) [2].

The most important problem in holographic nondestructive quality control of the structure elements is the optimization of the method of loading the object being examined. Many researchers could not in a number of cases apply the holographic nondestructive examination, because they did not manage to select the optimum method of loading the object being examined. The conception of the optimum loading of the object is based on the selection of such a loading which will concentrate stresses in the zone of an expected defect. Moreover, the more massive object examined, the more difficult to select the most simple method of loading which will make it possible to create the stress concentration in the zone of expected defects.

The reliability of revealing defects on the basis of the qualitative analysis of the interferograms depends, first of all, on the right allowance for the following two factors. First, it depends on the selection of an optimum method of the object loading, i.e. the creation of such a stressed state which leads to the largest differences in distribution of displacements and deformations over the object surface in defective and defect-free regions for the given type of defects. Secondly, it depends on using interferometer during researches whose efficiency is increased with a growth of sensitivity to that component of a vector of displacement whose distribution is affected to a greatest extent in the presence of defect at the given type of loading.

The sensitivity of the holographic interferometry to a normal component of vector of displacement is often much higher than to the tangential component and reaches the level of $\lambda/2$. Therefore, in a general case when the holographic methods are used it is rational to select the optimum scheme which is sensitive mainly to the displacements out of a plane, and the object loading is realized in such a way that the anomalies in the field of displacement corresponded to this component namely.

Thus, the decisive factor for an effective application of the holographic interferometry in nondestructive examination of products and materials is a selection of an optimum type and mode of the object loading. It should be noted that the selection of the method of loading is not a trivial problem and it influences greatly on the final result.

In holographic flaw detection four basic methods of loading (direct mechanical, pressure, thermal and vibroexciting) are used which can be applied both separately and in combination [3, 4].

Let us consider the fields of application and peculiarities of using the most wide-spread methods of loading.

Mechanical loading. In this case the object examined is subjected to a simple tension, compression, torque, bending or a local loading. The mechanical loading is often used for detection of defects in the form of cracks. The crack visualization is based on the fact that under the action of loading the field of displacements of the object surface in the crack vicinity loses its continuity in a number of cases, thus leading to a break or bending of the interference fringes. Therefore, the condition of a direct detection of crack in the interferogram is an abrupt localization of displacements in the crack vicinity because of the continuity disturbance.

Coming from the general requirements, the selection of a mechanical loading depends on the object geometric sizes, physical and mechanical properties of the material, and also on the most probable location and sizes of the crack. In each definite case the applying of the mechanical loading is optimized experimentally. It should be noted that during diagnostics of structures, for example, in crack determination in accordance with the Saint-Venant principle, such defect disturbs the deformed state at the distance equal approximately

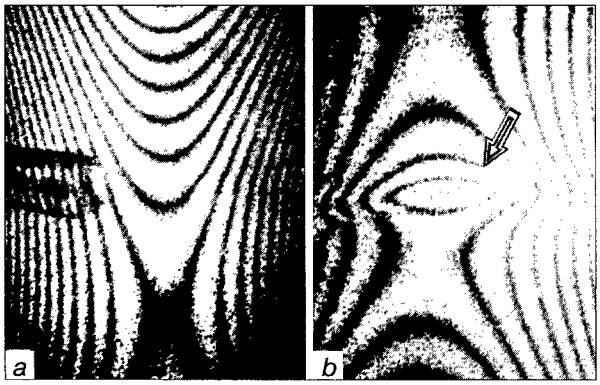

Figure 3. Interference fringe patterns which characterize the quality of welded polyethylene pipes: *a* — defect-free region of weld; *b* — 40 mm long defective region of weld

to its length, and to visualize crack it is necessary to have at least one fringe in the area of disturbance. Here, the minimum size of the defect detected depends on the frequency of the interference fringes. The increase in load can increase their frequency, however, it leads to a deterioration of their resolution. Therefore, it is rational to use special methods of holographic interferometry for detection of small defects (less than 1 mm).

Experiments on optimizing the method of loading the pipes were performed using a compact holographic device for the quality control of tubular elements (Figure 2). They showed that an elastic bending of the examined area is an optimum loading for the tubular specimens. In addition, there is no need in vibroprotection of the holographic unit, because in spite of including a device for an elastic bending, recording medium, thermoplastic camera and a light guide with an optical element, it is fixed rigidly on the element being examined. The optimized method of loading made it possible to perform the quality control of high-density polyethylene welded tubular elements of 110 mm diameter and 8 mm wall thickness, and elements of composite pipes of 100 mm diameter and 4 mm wall thickness.

In resistance welding of polyethylene pipes (Figure 3) the long defects of «sticking» type are occurred, which cannot be detected by other NDT methods.

Large difficulties in case of using the traditional methods of control are encountered when testing the composite adhesive-bonded pipes. Figure 4, *a* shows the scheme of a coupling joining of two tubular elements made from a glass fibre. The wall thickness of the coupling is 8 mm. Using the elastic bending at the area examined, it was possible to reveal the unquality adhesion of two pipes in the coupling. Figure 4, *b* shows a defect-free region of the coupling, while Figure 4, *c* shows the 35 mm long inner defect of a poor adhesion.

Pressure loading. In this method of loading an object or its part is subjected to deformation due to change in pressure (increase or decrease). This

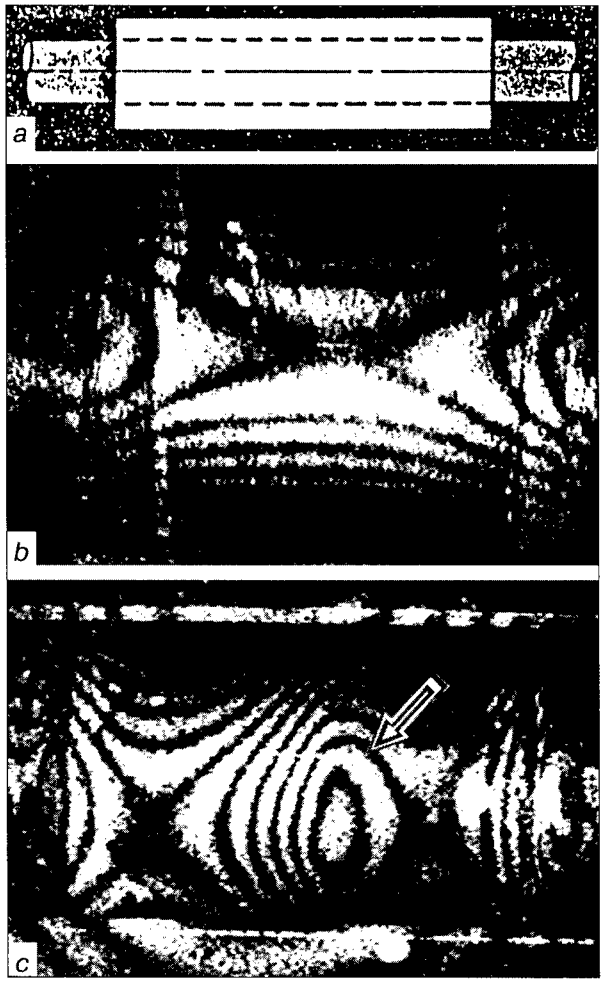

Figure 4. Scheme of a coupling joint of composite pipes (*a*) and interference fringe patterns which characterize its quality (*b* — defect-free region; *c* — 35 mm long defective region)

loading is often used in combination with a two-exposure holographic interferometry, when the pressure is varied between the exposures for the visualization of defects mainly in the form of wall thinning in hollow products, laminations in multilayer materials, etc. Its application in the holographic flaw detection is based on the following principle. When the pressure is changed the elastic displacement of the object surface occurs and the wall thickness influences the size of displacement. Thinning or lamination of the wall material leads to an anomalous pattern of the interference fringes in the defect area.

This method of loading (inner pressure) was used for the nondestructive quality control of the three-layer thin-walled cylindrical shell made from stainless steel using spot resistance and arc welding. The cylindrical shell, made of three layers, had an access to the inner cavity, thus allowing the inner pressure to be easily created with the help of an air (Figure 5). The interference fringe pattern demonstrated the areas of the shell with unquality spot welding.

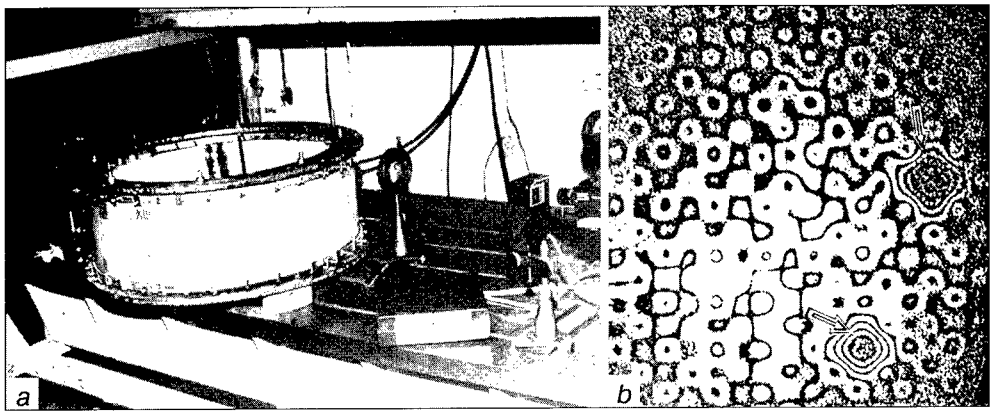

Figure 5. General view of three-layer cylindrical shell (*a*) and interference fringe pattern, which characterizes the defective regions (*b*)

The application of loading with an inner pressure is especially effective in the quality control of welded high-pressure cylinders used in the motor transport. Figure 6 gives a general view of the welded thin-walled cylinder, made from a high-strength steel, and also shows an interference fringe pattern obtained during changing the inner pressure in the cylinder. This interference fringe pattern characterizes the localization of displacements at the area of revealed inner defects (flaws). With increase in the inner pressure the fracture of a thin-walled cylinder in the zone of the revealed defects was observed.

Thermal loading. The application of this method in the holographic flaw detection is based on the formation of an anomalous deformation at the presence of difference in values of a heat expansion in the elements of volume. Depending on the conditions of control the object examined can be heated by a jet of a warm air or by a heat radiation both locally and over the whole surface. This loading is especially convenient in combination with a real time interferometry, as in this case it is possible to observe the dynamics of changing the interference pattern during heating.

The class of defects detected during thermal loading is rather wide and includes all types of defects which lead to the distortion of fields of surface displacements (lamination, local thinning of walls, etc.).

The temperature loading was used for the quality control of an adhesive-bonded honeycomb panel of 30×1000×1500 mm size with an aluminium filler. The external plates of 0.8 mm thickness made from a glass plastic was adhesive-bonded to the aluminium filler. The panel area examined was heated with a warm air (approximately 60 °C) from 100 mm distance for 30 s. The general view of the honeycomb panel and interference fringe patterns which characterize the quality of different regions of the honeycomb panel are given in Figure 7. At the preset temperatures of thermal loading it was possible to reveal a poor adhesion at the local areas of 4 – 35 mm length. The application of hot air was also effective in the quality control of the honeycomb aluminium panels which are used in the aerospace industry.

The application of thermal loading for the quality control of thin-walled lining of the aircraft fuselage having a single-sided access is challenging. The hazardous defect in a long service of the aircrafts is a corrosion of the material from the inner side of lining, especially in the places of contact of different rigid sections with a thin lining. Figure 8 shows the general view of an 3.5×1700×1700 mm element of the aircraft aluminium lining with rivets and the interference fringe patterns which characterize the defect-free zones and regions of the lining corrosion (wall thinning is above 45 %).

In fabrication of different welded structures the important problem is residual stresses which in many cases decrease the strength and serviceability of structures. In this connection the development of effective methods of obtaining comprehensive information about the peculiarities of formation

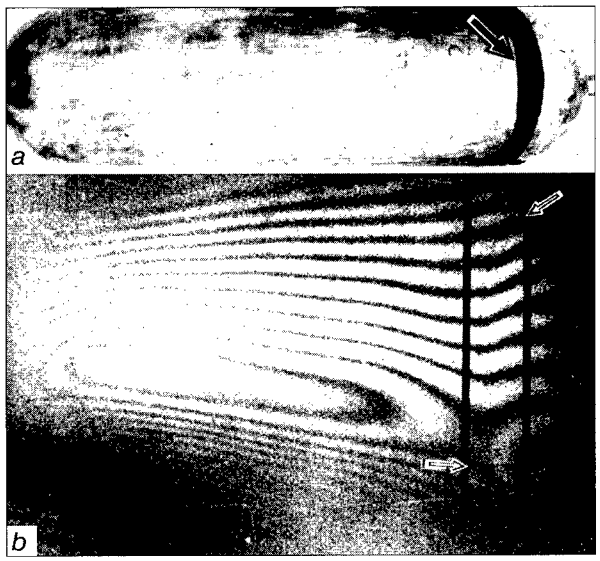

Figure 6. General view of welded thin-walled cylinder (*a*) and interference fringe pattern (*b*), which characterizes the defective region

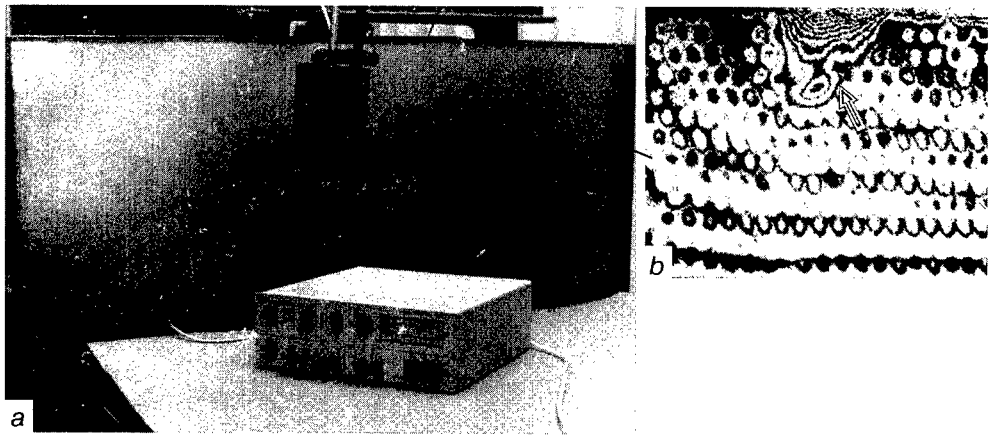

Figure 7. General view of honeycomb panel (*a*), interference fringe pattern (*b*), which characterizes the panel quality

and distribution of residual stresses over the whole field of examined objects made from metallic and non-metallic materials is actual.

Different methods of determination of residual stresses and also the problems of their measurement are known [5]. The method of holes found the widest spreading. To measure the fields of displacements caused by a relaxation of stresses in the zone of a drilled hole, the contactless methods of an optical holography are used.

To solve the problems of measurement of the residual stresses, we have designed and manufactured different compact holographic devices which can measure the fields of displacements in the zone of a stress relaxation [2]. The holograms are recorded both on high-resolution glass photographic plates using a wet chemical developing and also on thermoplastic materials without chemical developing, the latter can record the hologram during fractions of a second. Here, the technology of determination of residual stresses is as follows. A small-sized device is mounted on the area of the structure where the residual stresses are to be determined. The examining area is illuminated with a laser light and the reflected light is recorded with the help of a thermoplastc camera. Then, a local relaxation of the field of residual stresses is made (by drilling, heating, ball indentation, discharge, etc.) and a reflected light wave is again recorded on the same recording medium. This wave carries information about the displacements in a local zone of relaxation. With the help of a standard CCD-camera the interferogram is put to the computer memory and processed and the level of the residual stresses is determined.

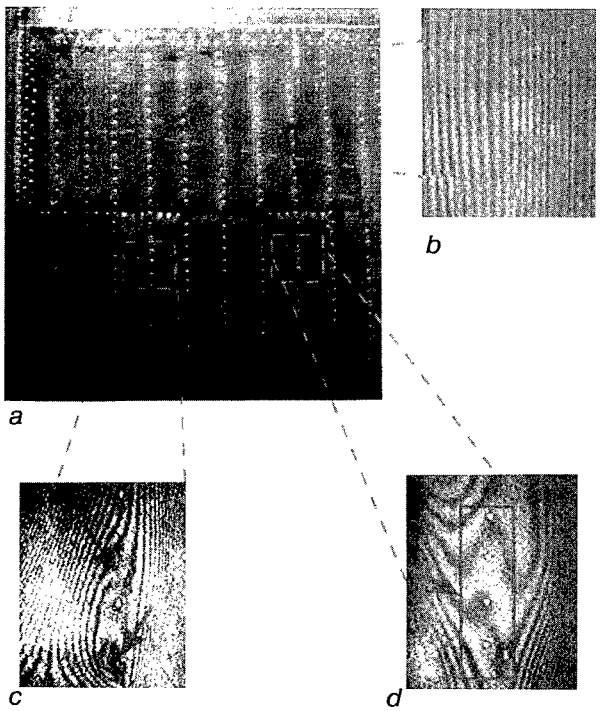

Figure 8. General view of aircraft lining element (*a*) and interference fringe patterns, which characterize the presence of lining corrosion (*b* — defect-free region; *c*, *d* — defective regions)

The calculated relations between the residual stresses and displacements caused by relaxation of stresses make it possible to determine the quantitative values of residual stresses.

Application of compact holographic devices for diagnostics of structures gives an opportunity to solve a number of important engineering problems concerning the determination of residual stresses in elements of full-scale welded structures. Thus, for example, with the help of the developed technology the residual stresses were determined in a framework of fastening the aircraft engine turbines, made from a magnesium alloy, after their repair welding. The experiments showed that after the repair welding the cracks are often occur due to a gradient of residual stresses. The general view of the framework, fringe pattern which characterizes the residual stresses and their level are given in Figure 9.

The further development of methods of optical holography promoted the creation of the new methods of nondestructive quality control and determination of residual stresses which are based on

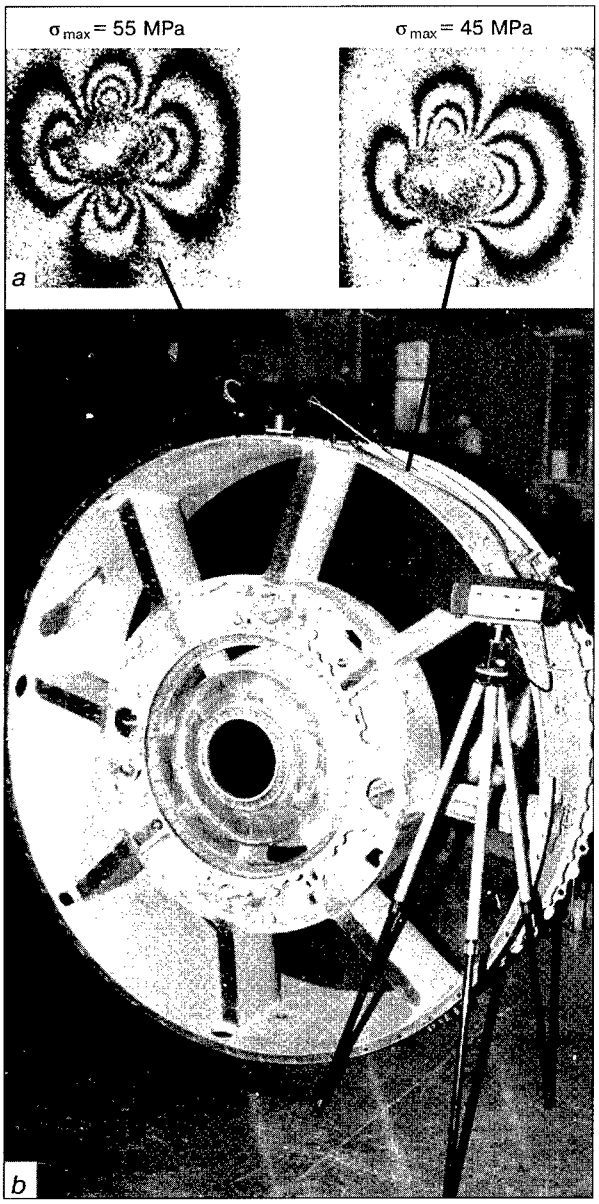

Figure 9. General view of framework for fastening turbines of aircraft engines (*a*) and interference fringe patterns (*b*), which characterize the level of residual stresses

electronic processing of the optical information, namely the methods of an electron speckle-interferometry and shearography [4, 6].

There are not theoretical differences between the ordinary and electron methods, but the latter are the computer processes which eliminate the wet chemical and electrostatic developing and subsequent reproduction of the interference patterns. This advantage makes electron methods more effective and applicable.

In our investigations the method of the electron speckle-interferometry was used for the determination of residual stresses in welded joints. For this purpose an optical scheme was assembled (Figure 10) which consisted of a coherent light helium-neon laser *1* with a wave length $\lambda = 0.63$ μm,

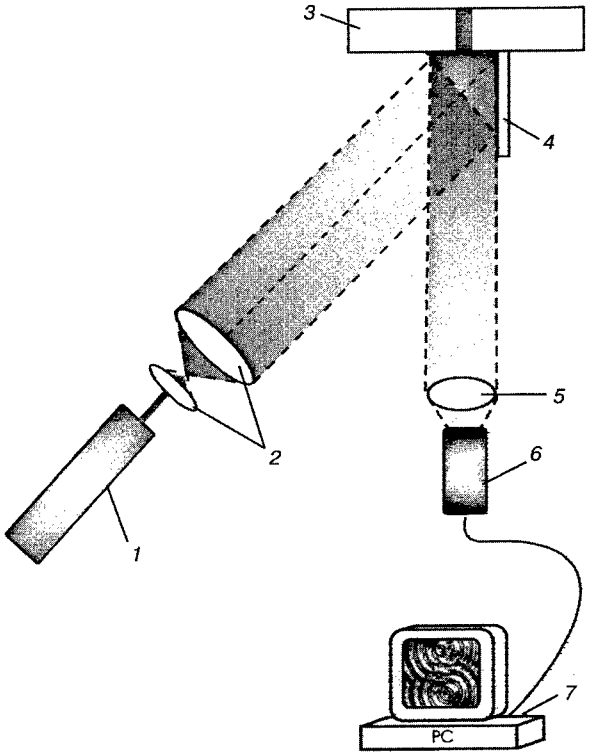

Figure 10. Optical scheme of method of electron speckle-interferometry (see designations *1* – *7* in text)

collimators *2*, object *3* to be examined, mirror *4*, objective *5*, CCD-camera *6*, connected to a computer unit *7*. The computer unit consists of PC on the Pentium 133 MHz base, a monitor, built-in into computer, an analog-digital converter (ADC), which is connected to the CCD-camera. Wave front, dissipated diffusively by the object, enters the high-sensitivity matrix of CCD-camera (752×582 points). The ADC will digitize the analog signal and display it on the screen. The displayed speckle-pattern is recorded on a hard disc in the form of a graphical file which can be used in any moment. Then, a small hole is drilled in the zone of examination for relaxation of stresses and the reflected wave is recorded again. With the help of a special program the recorded graphical files are processed. The obtained thus image (specklogram) is also recorded in the form of a graphical file. This specklogram represents a speckle-pattern with black and white regions or fringes and requires a special processing. The image processing includes some main operations (reduction of a speckle-noise level, increase in a pattern contrast, etc.). The welding residual stresses in a welded AMg6 alloy T-joint, made by the argon arc welding, were determined using the method of an electron speckle-interferometry. The general view of the element examined, a specklogram and a level of the residual stresses are shown in Figure 11.

The method of the electron shearography was used by us for the nondestructive quality control

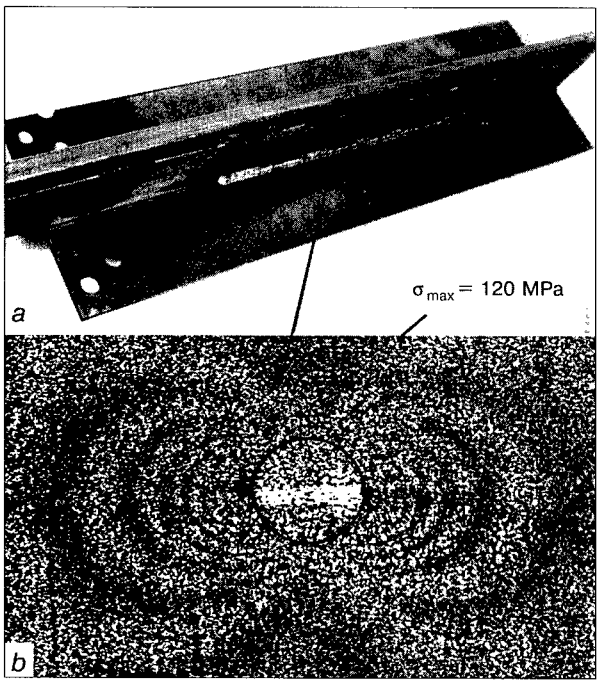

Figure 11. General view of element examined (*a*) and specklogram at the region examined (*b*)

of the structure elements. This method makes it possible to determine deformations without a numerical differentiation of data. In addition, its main advantage is a low sensitivity to vibrations. This method is suitable for application in industry for the following purposes:

measurement and analysis of deformations;

nondestructive quality control of structures of an intricate geometric shape.

The principle of the method of an electron shearography is as follows [6, 7]. The surface of the object examined is illuminated with a coherent laser radiation. The light, dissipated by a diffusive surface of the object and forming a speckle-structure, enters a shear element and is focused in the plane of the CCD-camera image. A glass wedge is used as a shear element and with its help a pair of transversely sheared images of the object are formed. These two images interfere with each other, thus forming a chaotic interference pattern which is entered to the CCD-camera connected to the computer unit where it is processed to obtain the shearogram.

Owing to using the above-mentioned method the nondestructive quality control of adhesive-bonded elements of the honeycomb structure was made. The aluminium honeycombs were used as an inner filler. The external sheets of 0.5 mm thickness, made from carbon- and glass plastic, were

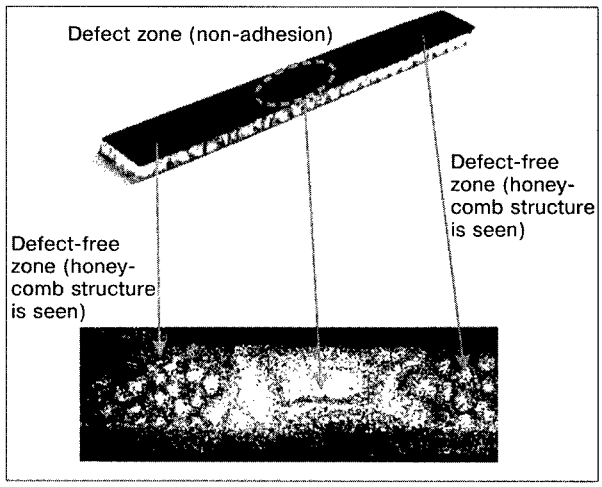

Figure 12. Shearogram, which characterizes the quality of the honeycomb panel element

bonded to the aluminium filler. The shearograms which characterize the quality of the honeycomb elements are shown in Figure 12.

The described optical methods, compact devices and instruments make it possible to perform the nondestructive quality control and to determine the stressed state of elements and members od structures made from metallic and composite materials using a contactless method. The application of the methods of an electron speckle-interferometry and shearography opens up the new opportunities for the nondestructive diagnostics of structures under the conditions of their manufacture and service.

REFERENCES

1. Ostrovsky, Yu.I., Shchepinov, V.P., Yakovlev, V.V. (1988) *Holographic interference methods of measurement of deformations*. Moscow: Nauka.
2. Lobanov, L.M., Pivtorak, V.A. (1998) Development of holographic interferometry for study of stress-strain states of quality control of structures. In: *Advanced materials science of the XXI century*. Kyiv: Naukova Dumka.
3. Kudrin, A.B., Bakhtin, V.G. (1988) *Applied holography (investigation of processes of metal deformation)*. Moscow: Metallurgia.
4. Jones, R., Whikes, K. (1986) *Holographic speckle-interferometry*. Moscow: Mir.
5. (1988) Technological residual stresses. In: *Proc. of III All-Union Symp*. Moscow.
6. Schuth, M. (1995) *Aufbau und Anwendung der shearographie als praxisgerechtes, optisches Pruef- und messverfahren zur Dehnungsanalyse, Qualitaetssicherung und Bauteiloptimierung*. Dissertation zur Erlangung des akademischen Grades eines Doktor-Ingenieurs. Kassel.
7. Lobanov, L.M., Pivtorak, V.A., Oleinik, E.M. (1998) State-of-the-art and prospects of application of method of electron shearography for diagnostics of elements and members of structures. *Avtomaticheskaya Svarka*, **11**, 26 – 31.

New Version!

CASPSP

Software Package for Computer Aided Simulation of Plasma Spraying Process
Version 3.1

Prof. Yu. Borisov, Dr. I. Krivtsun and A. Muzhichenko
E. O. Paton Electric Welding Institute, Kyiv, Ukraine

CASPSP is a package of computer programs for modeling both subsonic turbulent plasma jets used in plasma spraying and behavior of spray particles in such jets. It enables to perform quickly and easily the computer estimation of the temperature and velocity distributions for a plasma jet, as well as the trajectory, velocity and thermal state of particles being sprayed, depending on the plasma spraying process parameters. This software may be useful for experts in the field of plasma spraying and for students interested in this topic.

COMPONENTS

CASPSP is a recently improved software package and its new version consists of two connected modules:

• CASPSP – Simulation of Plasma Jet

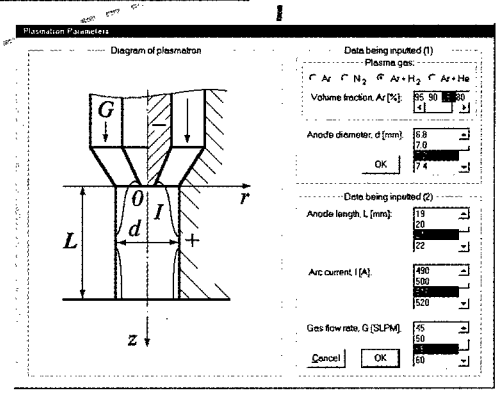

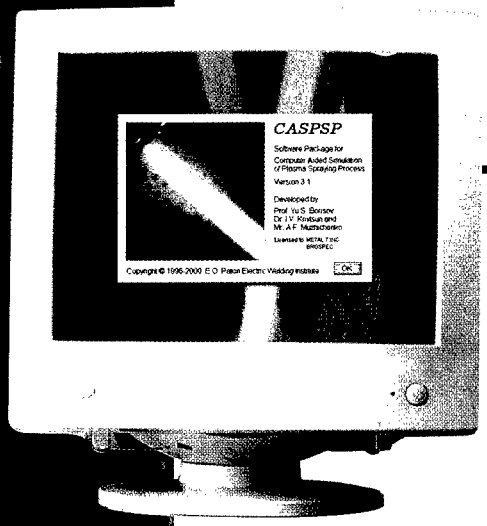

• CASPSP – Simulation of Spray Particles

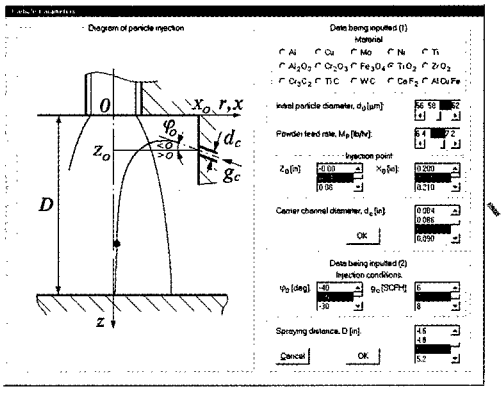

CASPSP has Windows 9x/NT/2000 friendly interface, which involves the following systems for each module:

- **Control Menu** • **Input-Output Data Editing System**
- **Graphical Result Displaying System** • **Help System**

FEATURES

The first module is intended for computer simulation of subsonic turbulent plasma jets, which are formed by plasmatrons with smooth channel of nozzle-anode and emitted into the open atmosphere (APS). The corresponding calculation programs are based on the mathematical model for gas dynamic and heat transfer processes in subsonic flow of arc plasma, which are described by the set of MGD equations within the turbulent boundary layer approximation. This module permits to calculate and display spatial distributions of the plasma temperature and velocity for free jets with taking into account the electric arc processes occurring inside plasmatron, in dependence on its nozzle-anode channel dimensions, arc current, composition and flow rate of plasma-forming gas.

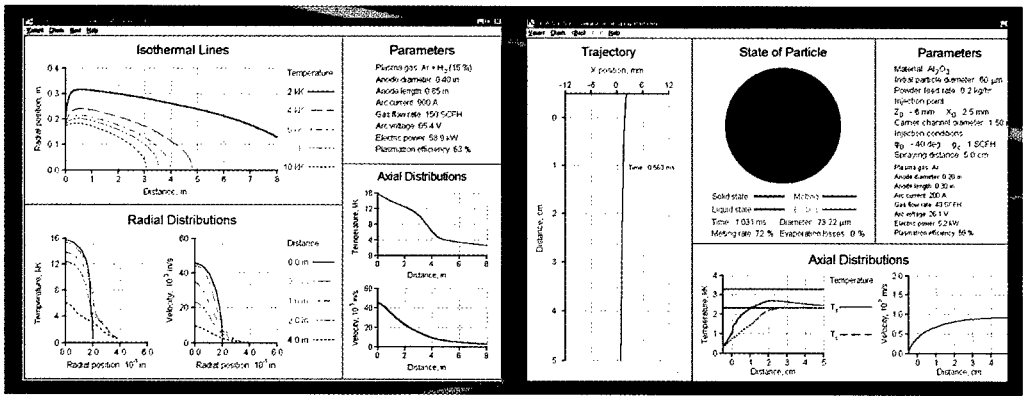

The second module is intended for computer simulation of behavior of spray particles in the plasma jet with pre-calculated distributions of the plasma temperature and velocity. The corresponding calculation program is based on the mathematical model for processes of particle heating and acceleration, which are described by the non-linear, non-stationary thermal conductivity equation and the equation of motion for a spherical particle in plasma flow with taking into account the reducing of temperature and velocity of the plasma jet due to spray powder loading. This module permits to calculate and display trajectory, velocity and temperature field for particles being sprayed, according to composition of material and initial diameter of the particles, their feed rate and conditions of their injection into the jet.

The new version of the software allows to choose preferable units for data being inputted and outputted:

- **Dimensions (cm\in)** • **Temperatures (K\F\C)**
- **Gas Flow Rates (SLPM\SCFH)** • **Powder Feed Rates (kg/hr\lb/hr)**

Modification of this software can be made, e.g., for simulation of various type non-transferred arc plasmatrons; for simulation of plasma jets emitted into limited space (SPS); for simulation of supersonic plasma jets and for simulation of many particles simultaneously.

DATABASES

Plasma-forming gases: • **Ar** • **N_2** • **Ar + H_2** • **Ar + He**

Particle materials: • **Al** • **Cu** • **Mo** • **Ni** • **Ti** • **Al_2O_3** • **Cr_2O_3** • **Fe_3O_4** • **TiO_2** • **ZrO_2** • **Cr_3C_2** • **TiC** • **WC** • **CaF_2** • **AlCuFe**

Changes to these databases are possible.

SYSTEM REQUIREMENTS

IBM PC and compatibles with installed Windows 9x/NT/2000. CPU: Pentium (faster clock rate is preferable); RAM: at least 32 MB; HDD free space: at least 5 MB; CD-ROM (software provided on CD); Monitor: SVGA, 1024×768 pixels, 16 bit color controller; Printer: optional (color printer is preferable).

Complete software package: Distribution CD and User's Manual (36 pp., A4) **$1.400,00**

Modifications of the software on the customer's requirements can be made at extra pay.

Demo version of the software is available free of charge: **http://www.kar.net/~plasma**

To order ***CASPSP*** package call:

Prof. Yu. S. Borisov, Head of Coating Department, E. O. Paton Electric Welding Institute National Academy of Sciences of Ukraine, 11, Bozhenko St., Kyiv 03680, Ukraine, Tel./Fax: 38-044/220-9215, E-mail: borisov@pwi.ru.kiev.ua

CASPSP

DEVELOPMENT OF CALCULATION PROCEDURES FOR ASSESSMENT OF ALLOWABLE DEFECTS IN WELDED JOINTS OF CRITICAL STRUCTURES

V.I. MAKHNENKO and **O.V. MAKHNENKO**
The E.O. Paton Electric Welding Institute, NASU, Kyiv, Ukraine

ABSTRACT

Algorithms of assessment of allowable defects in welded joints of the critical structures are considered on the basis of a well-known concept «fitness-for-purpose», developed by the International Institute of Welding and advanced approaches of fracture mechanics of bodies with cracks. A significant role of residual welding stresses, geometric peculiarities of welded joints, mechanical heterogeneity, caused by the effect of a welding thermal cycle and appropriate impurities in weld metal, is outlined.

Key words: *equivalent cracks, intercrystalline stress corrosion, radiation, fluence of fast neutrons, embrittlement, critical temperature of brittleness.*

Development of fracture mechanics of bodies with cracks, the improvement of mathematical models describing the main laws of such fracture under various loading conditions, as well as of the means of their realization contribute to the development of predictive algorithms for calculation of the behavior of structures with the preset cracks under the real service conditions. These form a basis for the majority of modern approaches to assessment of allowable revealed defects. With this respect, a fairly large amount of investigations carried out in many countries in this field should be mentioned [1 – 5, etc.].

In most these studies, the development of a calculation scheme is based on the replacement of various rather concentrated defects (cracks, pores, inclusions, incomplete penetrations, undercuts, etc.) by the corresponding equivalent cracks which are considered as the most dangerous defect types. At selection of the equivalent cracks the canonical crack shapes are commonly used which are well-studied, and for which the stress intensity factor (SIF) calculation is a rather routine procedure.

Accordingly, the rules of schematizing single- and group-defects with equivalent cracks are defined in various countries in corresponding documents, e.g. in British Standards Institution PD6493 in UK, in ASME Boiler and Pressure Vessel Code in the USA, in Methodical Recommendations MR 125-0–90 in the former Soviet Union, etc. This creates a definite legal base for the assessment of the allowable defects, including those in the welded joints [6].

Nevertheless, the effective practical use of these approaches encounters definite problems, since in many cases the justification of numerical results needs many additional data, including manufacture peculiarities, service loading history of the structure, analysis of causes of defects initiation and the kinetics of their in-service growth, degradation of material properties, distribution of residual stresses (strains) in the vicinity of defects, etc. The information concerning these parameters is far not always easy to obtain, i.e. significant efforts are required to receive it and in a number of cases they considerably exceed those associated with the strength calculations themselves.

Thus, the practical assessment of the allowable revealed defects transforms in practice into a rather cost- and time-consuming investigation. Certainly, this should be taken into account in formulating problems of this kind, especially when prompt solutions are needed. Undoubtedly, with the accumulation of experience, appropriate information data banks, etc., the prompt justification concerning the allowable defects revealed in critical welded structures will find a wide use in practice.

Below, the specific examples of possible numerical procedures for implementing the problem of the assessment of allowable revealed defects are illustrated.

Example 1. In late October 1997, during the scheduled repair of the power unit No.3 at the Chernobyl NPS, a 100 % inspection of all 1451 butt welded joints of the pipelines of the D_n 300 type of a loop of multiple forced circulation was performed. Among them, 208 butt welds had defects which were classified as the intercrystalline stress corrosion cracks (ICSCC). The pipings of 325×16 mm section were put into operation in April, 1981. The material is a pipe steel 08Kh18N10T. Butts were welded using a wire 04Kh19N11M3.

Table 1. Distribution of defected welds depending on the defect length ($L = 2c$, mm)

$L = 2c$	< 25	$25<L< 50$	$50<L<75$	$75<L<100$	$100<L<125$	$125<L<150$	$150<L<175$	$175<L<200$	< 200
Quantity of welds	40	82	36	22	9	6	4	5	4

Similar defects were revealed earlier in similar units of Leningrad (November, 1996) and Kursk (early 1994) NPS. Moreover, similar failures were observed in the power units BWR, USA, where, on average, 25 % of welded joints of the type AISI 304 steel exhibited such cracks [7]. The conventional repair of these butts on pipelines is cutting off the defective area of the pipe of a length of about 200 mm in both sides from the defect and welding-on of a corresponding pipe piece by two butt welds. Such repair under radiation contamination is highly labor-, cost- and time-consuming. The station had no mentioned funds, so the question was put forward as to the admissibility of some revealed defects of relatively small lengths (Table 1). The circumstance mentioned became the basis for numerical assessments of admissibility of a part of the revealed defective welds for service. The work has been started from determining the causes of occurrence and growth of the revealed defects.

The results of experimental examinations using macro- and microsections prepared from the defective welds, as well as generalization of experience available at the other power plants and literature data [7] made it possible to accept the already known hypothesis of three basic factors:

susceptibility of steel 08Kh18N10T to ICSCC formation in the HAZ of welds, i.e. sensitivity of the piping base metal;

critical level of stresses in definite parts of the weld;

service environment, which promotes the ICSCC formation.

The susceptibility of the base metal in the HAZ occurs by the heating during welding to 1200 – 1300 °C, by a partial dissolution of titanium carbides, the fixing of carbon in a solid solution and by a formation of chromium carbides during the post-weld cooling and repeated reheatings within the temperature range 500 – 650 °C.

The forming chromium carbides of the $Cr_{23}C_6$ type contribute to the Cr-depletion of areas near the grain boundaries. Since the corrosion resistance of such types of steels is specified by the chromium, the local Cr-depletion of the steel increases its sensitivity to ICSCC in a distilled water at temperatures about 280 – 300 °C [7]. Thus, the radical measure to prevent ICSCC formation was recognized a use of steels with a lowered carbon content (less than 0.02 %) and alloying with nitrogen, niobium, and other stabilizing elements. The weld metal with a lower carbon content and alloyed with molybdenum forming rather stable carbides Mo_2C (as compared to TiC) and inducing formation of fine-grained structure of primary ferrite, possesses rather high resistance against ICSCC. Thus, the ICSCC in the weld metals of the pipelines investigated were observed only very seldom. The low width of the sensitivity zone adjacent to the weld is the reason of the crack absence transverse the weld (along the pipeline axis). Only small branching of circumferential cracks were observed in axial (relative to the pipe axis) direction at the distance of not more than 2 – 3 mm.

Thus, the objects of assessment are the defects in a form of circumferential cracks, located in the HAZ at the inner surface of the pipe. At certain idealization they can be considered as surface (on the inner surface of a pipe) semi-elliptical cracks of a depth a and length $2c$ whose plane is perpendicular to the pipe axis (Figure 1). The propagation rates for ICSCC are usually presented in the form [8]

$$\frac{dl}{dt} = AK_I^n \quad \text{at} \quad K_I > K_*,$$

$$\frac{dl}{dt} \approx 0 \quad \text{at} \quad K_I < K_*,$$

where $l = a, c$; K_I is the SIF in a corresponding point of a crack contour (C, D) of Figure 1; A and n are the empirical coefficients, depending on the material sensitivity degree; K_* is the threshold value of K_I.

Unfortunately, the precise values K_*, A and n for steel 08Kh18N10T are unknown. So, the corresponding data for AISI 304 are commonly used as conservative estimates, as this steel is characterized by the higher susceptibility than the 08Kh18N10T steel. For the steel AISI 304 at high degree of sensitivity, according to [8], it can be assumed that $n = 3.33$, $A = 4.07 \cdot 10^{-7}$ mm/year at $[K_I]$, MPa·mm$^{1/2}$; for the average degree of sensitivity $n = 2.161$, $A = 3.74 \cdot 10^{-6}$ mm/year; at a negligible sensitivity degree $dl/dt \approx 1$ mm/year.

To receive information about K_I in HAZ of the butt weld, the data of stresses in this area should be known. These stresses are defined both by the service loads and the residual welding stresses. It is natural that the decisive here are the normal stresses σ_{zz}, acting along the pipe axis.

The service axial stresses σ_{zz}^S in the pipelines, designed according to standards [9], are specified

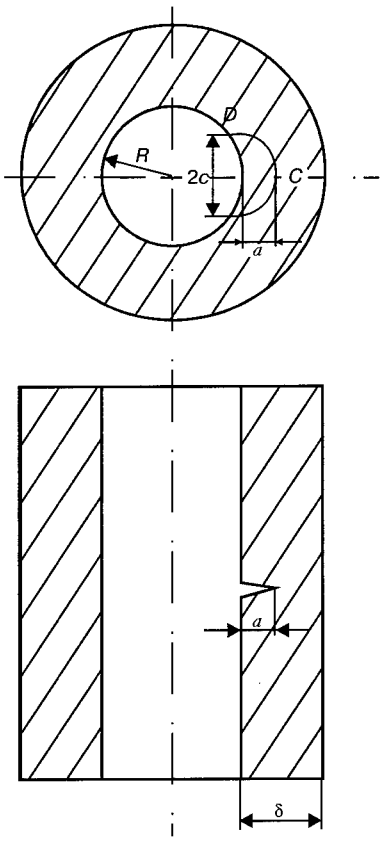

Figure 1. Scheme of semi-elliptical cracks at the inner surface of the cylinder (pipe)

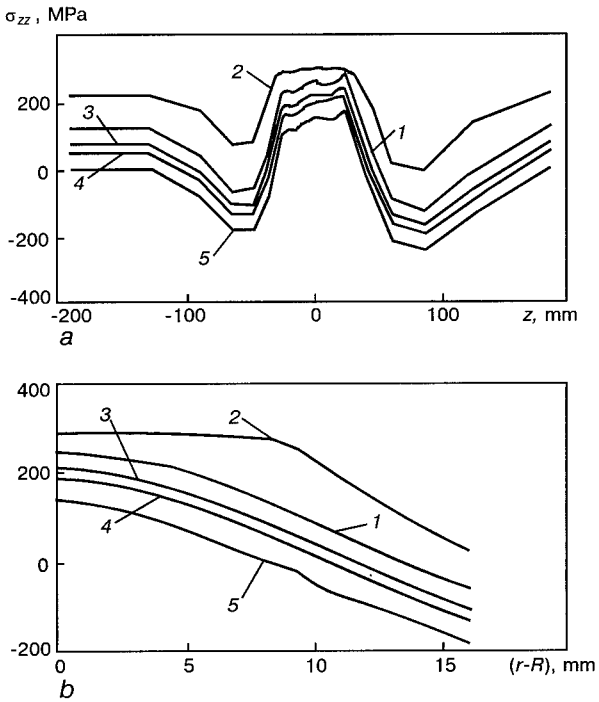

Figure 2. Distribution of total stresses σ_{zz} (residual σ_{zz}^{res} and service σ_{zz}^{s}) in the zone of a circumferential weld: *a* — at the inner surface along the axis *z*; *b* — in thickness of HAZ at different values σ_{zz}^{s} (*1* — 120; *2* — 220; *3* — 75; *4* — 50; *5* — 0 MPa); *R* — inner radius of pipe

by bending and axial distortions of the pipeline during service, i.e. by internal water pressure and by temperature. These stresses may vary within rather wide limits depending on the configuration of the pipeline, the effectiveness of the system of a temperature compensation, etc. According to the calculations made at the Institute for Strength Problems of NASU under the supervision of Prof. A.Ya. Krasovsky, the level of the tensile service stresses σ_{zz}^{s} may lie within the range of $50 < \sigma_{zz}^{s} < 220$ MPa depending on the type of the pipeline, its configuration, system of a temperature compensation, etc. At steady operation of the temperature compensation system these stresses amount to 50 – 75 MPa, while in opposite case they increase to 120 – 220 MPa.

To obtain required data about the welding residual stresses and their interaction with the service loads, special calculation and experimental studies have been performed [10]. Furthermore, the experiments were mainly carried out to verify the validity of calculations. The calculation procedure is based on the theory of non-isothermal thermo-plasticity. In more details, this study is presented in [10].

In parallel with loading of the weld with a pressure $p = 8.45$ MPa and temperature $T = 285$ °C, the loading with above-mentioned axial service loads σ_{zz}^{s} was considered.

Figure 2 gives results of the mentioned interaction for different σ_{zz}^{s} (from 0 to 220 MPa). It is clear, that at σ_{zz}^{s} in the most real ranges (50 – 120 MPa), the diagram of the total stresses in the butt zone, both in wall thickness and at the inner surface vary in relatively narrow limits (about 46 MPa), i.e. the role of service stresses σ_{zz}^{s} is levelled to a certain degree. This can explain the absence of clear correlation between the level of service stresses σ_{zz}^{s} and the level of intercrystalline stress corrosion cracking observed in welded joints.

The data in Figure 2, *b* make it possible to calculate the value K_I in corresponding points of the crack detected. It is obvious for small cracks ($L < 50$ mm) that the diagram of distribution of total stresses σ_{zz} with a crack growth is changed negligibly.

Figure 3 gives results of calculation of the kinetics of growth of the crack of 50 mm length and 3 mm depth (i.e. $a = 3$ mm, $c = 25$ mm) in time. The stresses and K_I are shown in characteristic points *C*, *D* (Figure 1), and also the sizes a (t) and c (t) at values A and n for the average degree of sensitivity of the AISI 304 grade steel and different values σ_{zz}^{s} in the ranges of $0 \le \sigma_{zz}^{s} \le 220$ MPa, i.e. for different curves of total stresses σ_{zz} (Figure 2, *b*).

In calculation of K_I the method of weight functions was used, i.e. the value $K_I(j)$ for $j = D$ (at

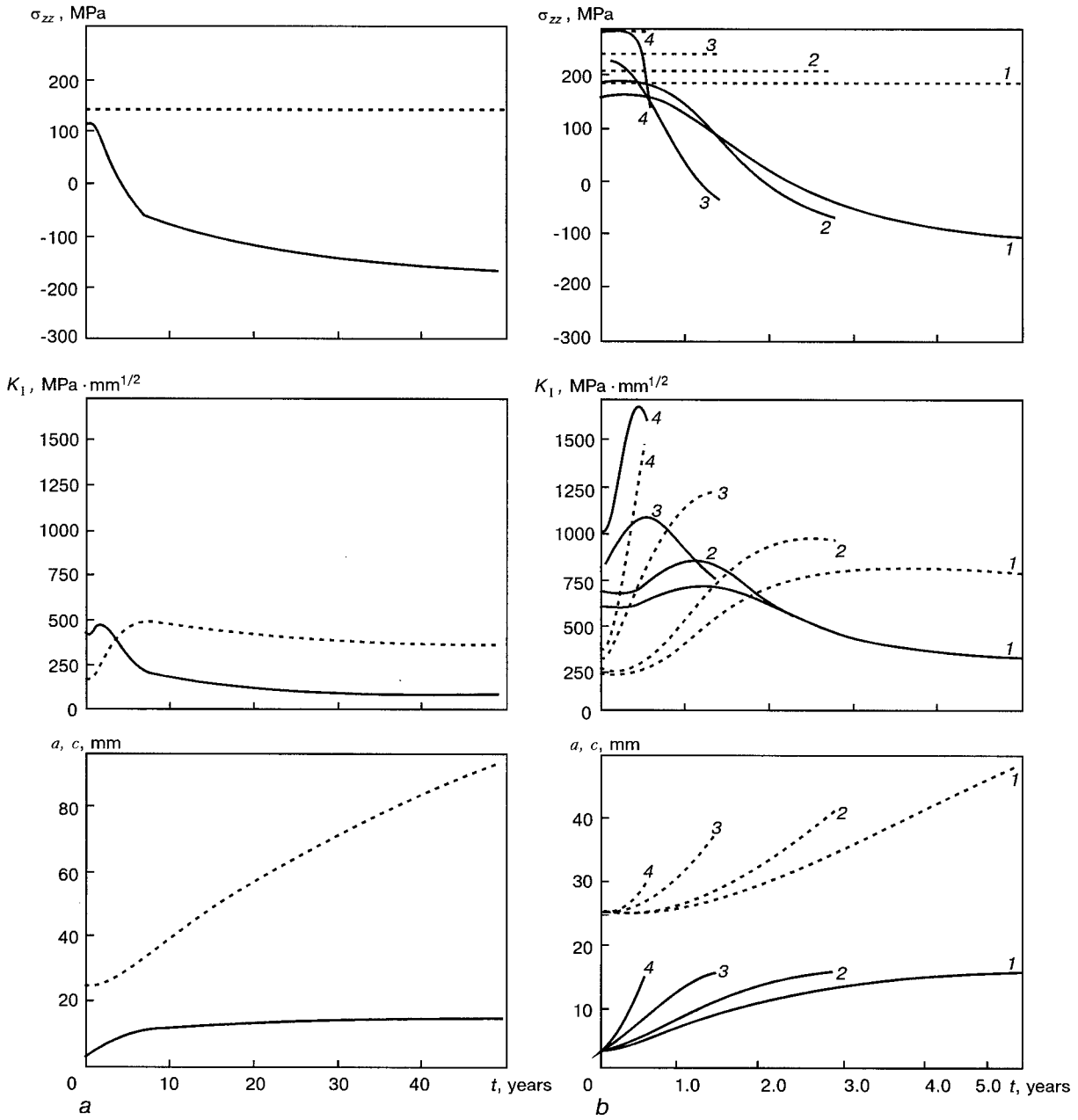

Figure 3. Variation of nominal total stresses σ_{zz}, coefficients of stress intensity K_I and sizes of cracks a (t), c (t) depending on service duration: a — $\sigma^s_{zz} = 0$; b — σ^s_{zz} =50 (*1*); 75 (*2*); 120 (*3*); 220 (*4*) MPa. Dashed lines are connected with a crack D tip, solid lines — with a crack C tip

the surface) and $j = C$ (in the crack depth) is presented in the form

$$K_I(j) = \frac{\sqrt{\pi} S_j \gamma_j}{\Pi\,(a/c,\ a/\delta)},$$

where

$$\Pi\,(a/c,\ a/\delta) = \left[1 - \left(0.89 - 0.57\sqrt{\frac{a}{c}}^{3}\left(\frac{a}{\delta}\right)^{1.5}\right]^{3.25} \times \left[1 + 1.464\,(a/c)^{1.65}\right]^{0.5},\ (j = C,\ D),$$

$$\gamma_c = 1.12 - 0.08\,\frac{a}{c}, \qquad (1)$$

$$\gamma_D = [1 + 0.32\,(a/\delta)]\,(1.23 - 0.09\,a/c)\,\sqrt{a/c},$$

$$S_j = a\int_0^1 \sigma_{zz}\,(\xi) f_j\,(\xi)\,d\xi.$$

Here, $f_j(\xi)$ is the weight function presented as follows:

$$f_C\,(\xi) = \tilde{C}\,(\xi) + \frac{a}{c}\,\tilde{D}\,(\xi) + \lambda E(\xi),\ f_D(\xi) = f(\xi),$$

$$\lambda = \frac{a}{\delta}\left[1 - 1.9\left(\frac{a}{c}\right)^{0.75} + 0.9\left(\frac{a}{c}\right)^{1.5}\right],$$

where $\tilde{C}\,(\xi)$, $\tilde{D}\,(\xi)$, $E(\xi)$ and $f(\xi)$ are the tabulated functions [5].

Analysis of Figure 3 showed that at rather conservative data on the susceptibility of HAZ of the pipe welded joints of steel 08Kh18N10T, the admission to service of such butts with cracks of sizes $2c = L \le 50$ mm and $a \le 3$ mm can lead to their gradual growth. However, this growth for about one-year service time (till the next scheduled repair) can not result in fairly serious consequences except for a low-probable variant $\sigma^s_{zz} = 220$ MPa at which, according to calculations, the formation of through-crack of a small size $L \approx 50$ mm is possible. Nevertheless, this should not also lead to a «guillotine»-type fracture [5].

Such calculations were the basis for admission to start the operation of the third power unit at the Chernobyl NPS in spring 1998 till the next scheduled repair in the second half of 1999, with a mandatory short-term break in December 1998 to perform control operations on 113 weld butts with the remained cracks of sizes $L = 2c \le 50$ mm (Table 1).

The results of this control after about seven months of operation indicated fairly insignificant changes in the crack sizes (not more than 1 mm/year).

Example 2. It referred to the evaluation of admissibility of a crack-like defect in a welded joint. However, it is a hypothetical defect which may be present in a welded joint at a very low probability.

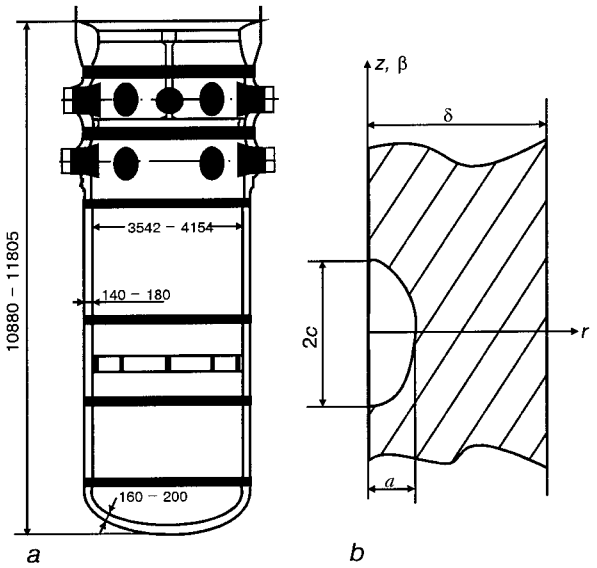

Figure 4. Scheme of location of welded joints in the WWER type reactor vessel (*a*) and a postulated crack (*b*): $a = 0.25\delta$; $2c = 3.0a$

Welded joints in the WWER type reactor vessels of NPS used in Ukraine are considered. 13 reactors of this type (11 reactors of a WWER-1000 type, and 2 of WWER-440 type) generate currently up to 45 % of total energy in Ukraine, so their reliable operation is of a great importance.

Meanwhile, the increased susceptibility of the weld metal of girth welds of reactor vessels (Figure 4) to radiation embrittlement is a problem that is of a large interest for pertinent institutions both in the countries where such reactors are in use, and in other countries such as the USA, Germany, etc. This problem is very comprehensively studied now at the E.O.Paton Electric Welding Institute of the National Academy of Sciences of Ukraine.

The residual life of the reactor vessel taking into account the degradation of properties of welded joints is specified by the probability of attaining the ultimate state at the accident in the course of service of the reactor in case of filling the vessel with a cold water (a thermal shock). It is assumed that in the zone of the welded joint, there is a spectrum of single surface (semi-elliptic) cracks of depth $a \approx 0.25\delta$ and length $2l$, where $l = (3/2)a$, δ is the wall thickness. For such welded joint, the ultimate state is calculated on the basis of advanced methods of fracture mechanics using a two-parameter criterion [1, 2]:

$$K_r \le f(L_r), \qquad (2)$$

where $K_r = K^{\max}_{\omega\theta}\ /K_{Ic}$; $K_{\omega\theta}$ is the SIF at the crack tip under consideration according to the theory of generalized normal break [11], i.e. the value $K_{\omega\theta}$ is the function of corresponding modes K_I, K_{II}, K_{III}, caused by service force and thermal loads under the accident conditions, and also modes

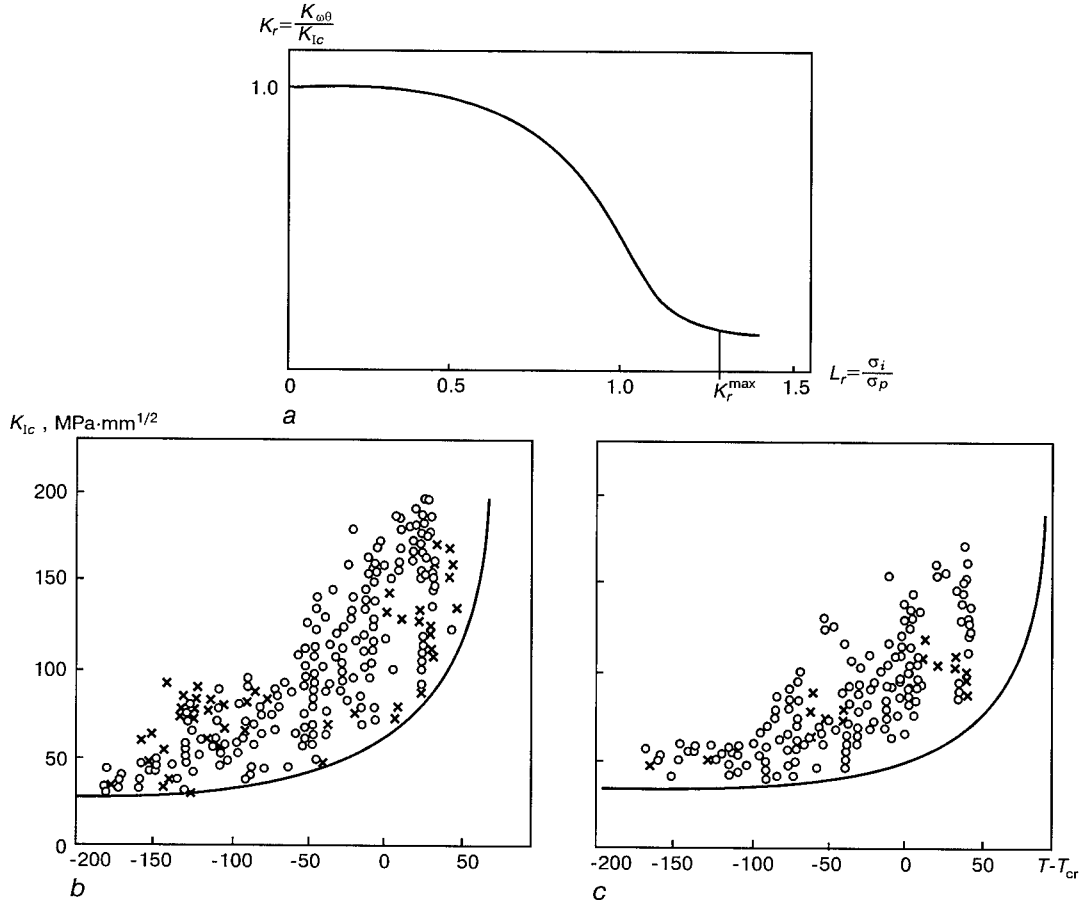

Figure 5. Diagram of tough-brittle fracture at the crack presence (*a*) and experimental data relative to K_{Ic} for steels of WWER type reactor vessels (*b* — for steel 15Kh2MFA (O) and steel 15Kh2MFAA (X), solid line acc. to (6) at A =27, B = 38, C= 0.02; *c* — for steel 15Kh2NMFA, solid line acc. to (6) at A = 38, B = 17, C = 0.028)

K_I^{res}, K_{II}^{res}, K_{III}^{res}, induced by non-relaxed residual stresses associated with the manufacture of the vessel (accounting for welding, heat treatment, cladding of the inner surface).

$$K_{\omega\theta} = \left[\left(K_I + K_I^{res}\right)\cos^3\frac{\omega}{2} - 3\left(K_{II} + K_{II}^{res}\right)\sin\frac{\omega}{2}\cos^2\frac{\omega}{2}\right] \times$$

$$\times \cos^2\theta + \left(K_{III} + K_{III}^{res}\right)\cos\frac{\omega}{2}\sin 2\theta, \quad (3)$$

where θ, ω are the corresponding angular coordinates at a definite point of the crack tip. The maximum value $K_{\omega\theta}$ in this point are defined from (3) at $\theta = \theta_*$ and $\omega = \omega_*$, that, in turn, are determined by a system of equations

$$\frac{\partial K_{\omega\theta}}{\partial\theta}\Big|_{\theta=\theta_*} = 0, \quad \frac{\partial K_{\omega\theta}}{\partial\omega}\Big|_{\omega=\omega_*} = 0.$$

In formula (2) $L_r = \sigma_i/\sigma_p$, where σ_i is the intensity of nominal stresses in corresponding points of the crack tip caused by thermal and force loadings at the given moment of time t of the accident condition; $\sigma_p = 1/2(\sigma_y + \sigma_t)$, where σ_y is the yield strength, σ_t is ultimate strength, K_{Ic} is the fracture toughness of the material at the temperature of accident condition with account for a degradation of properties during service. Commonly, the type of the function $f(L_r)$ for given material is defined experimentally. According to [1, 2] for many structural steels the relationship may be used shown in Figure 5, *a*

$$f(L_r) = (1 - 0.14\,L_r^2)\,[0.3 + 0.7\exp(-0.65\,l_r^6)]. \quad (4)$$

It follows from the above-mentioned that the most important problem is the determination of characteristics of a stress-strain state, induced by internal pressure and the thermal load at the thermal shock. According to the standards of Russia the conditions of the thermal shock should correspond to the accident situation «Break of a Steam Piping of a Steam Generator». One of the primary characteristics of the thermal shock is a temperature of a water flow near the wall T_w during the accidental filling the reactor vessel with the water at the temperature of filling water T_{water} = 55 °C (Figure 6). Based on these data, the changes of temperature T (r, z, β, t) and thermal stresses σ_{ij}^T (i, j = r, z, β) may be calculated in various parts of the reactor wall. If the intensity σ_i of the

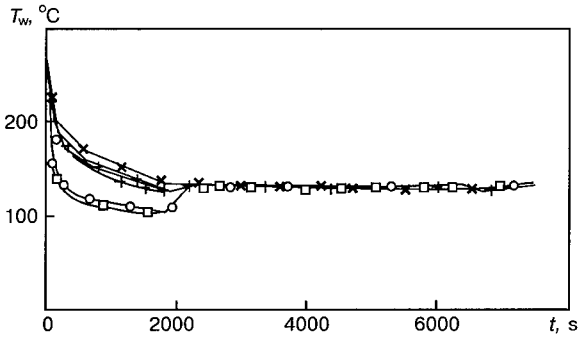

Figure 6. Intensity of water cooling at the reactor vessel wall during a thermal shock at different distances from the place of water filling along the reactor vessel wall: □ – 0; ○ – 0.64; + – 2.6; × – 3.4 m

tensor of total stresses (induced by internal pressure and temperature) $\sigma_{ij} = \sigma_{ij}^T + \sigma_{ij}^p$ is less than $0.5\sigma_p$, then according to the diagram in Figure 5 and formula (4) $f(L_r) \approx 1$, i.e. the carrying capacity is defined mainly by the brittle fracture of by the condition

$$K_{\omega\theta}^{\max} = K_{Ic}. \qquad (5)$$

This condition is laid into the ground of safety rules of operation of equipment at the NPS in Russia. Since for the weld metal and for adjacent base metal of the WWER type reactor vessel the value σ_p at temperatures 200 – 100 °C is the ranges of 650 – 1000 MPa [12], and intensity of total stresses σ_i can reach 350 MPa at the surface (Figure 7), that was obtained for WWER-440 vessel (weld No.4) at changing the temperature T_w in Figure 6 and pressure p = 11.7 MPa, then condition (5) may be non-equivalent to (2). This should be undoubtedly taken into account in calculations.

Figure 7 illustrates the calculated values $K_{\omega\theta}^{\max} = K_I$ for two characteristic points of a semi-elliptical crack a = 35 mm at $c = (3/2)a$. Relationships (1) have been applied. The resistance of a welded joint material to a tough-brittle fracture with allowance for characteristics of a stressed state (Figure 7) according to (2) is determined by values σ_p and K_{Ic}. Under the influence of neutron flows with energies higher than 0.5 MeV these values are changed in time due to accumulation of the fluence of neutrons F. Most noticeable is decrease in values K_{Ic}, i.e. material embrittlement as a result of a neutron radiation. Physics of this phenomenon is relatively complicated and, currently, there is no theory, which could describe it comprehensively. The experimental data show more drastic decrease in K_{Ic} for weld metals having higher content of impurities, in particular, phosphorus.

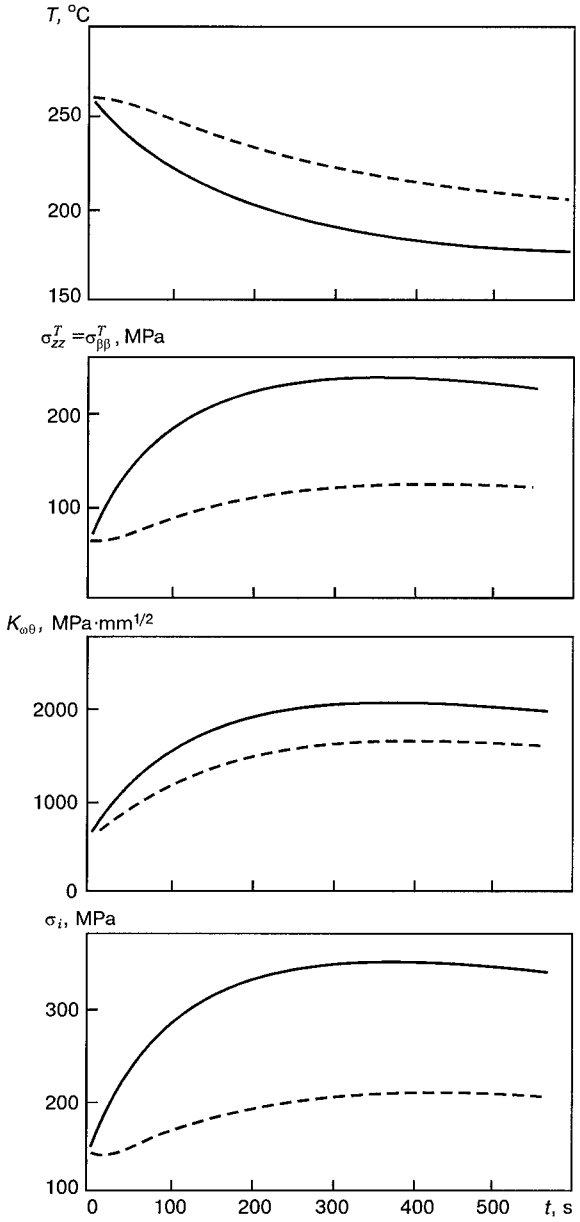

Figure 7. Results of calculation of temperatures T, temperature stresses σ_{zz}^T and $\sigma_{\beta\beta}^T$, coefficients of stress intensity $K_{\omega\theta}^{\max}$ and stress intensity σ_i at different moments of a thermal shock for tips D (solid lines) and C (dashed lines)

Table 2. Values ΔT_{cr} (°C) depending on type of weld metal and fluence

Weld metal	*Fluence $F \cdot 10^{22}$, N/m^2*						
	1	*8*	*27*	*64*	*125*	*216*	*343*
Sv-10KhMFT (P = 0.39 %, Cu = 0.17 %)	41	81	122	163	203	244	285
Sv-08KhGNMTA (P = 0.006 %, Ni = 1.287 %, Cu = 0.1 %)	8	8	11	47	88	100	102
Sv-08KhGNMTA (P = 0.010 %, Ni = 1.5 %, Cu = 0.1 %)	8	8	12	57	108	123	126

Table 3. Dependence of value T_{total} on time t of a thermal shock

Location of conditional crack	Value T_{total} (°C) depending on t (s) of a thermal shock					
	100	200	300	400	500	600
C	301	247	254	239	240	241
D	244	202	183	178	172	177

There is a great problem, concerning the determination of K_{Ic} depending on the fluence F, as the sufficiently reliable values K_{Ic} can be obtained only on large specimens, that greatly reduces direct measurement of K_{Ic} for the irradiated material. In practice, the large specimens are applied only for assessing the material properties in initial state.

Figure 5, *b, c* shows typical results of such tests for steels 15Kh2MFA (WWER-440) and 15Kh2NMFA (WWER-1000) of different heats [12] depending on the difference in temperatures $T - T_{cr}$, where T_{cr} is the critical temperature of material brittleness. According to the acting standards [5], the degradation of material properties in service is assessed by the shifting of ΔT_{cr} along the axis of temperatures according to the relation K_{Ic} (T). It is assumed (and this is adopted in Russian rules and in the world practice), that the dependence of impact strength of KCV material on temperature is similar to K_{Ic} (T), and their shifting ΔT_{cr} is the same.

Thus, if for the non-irradiated material

$$K_{Ic} = A + B \exp [C(T - T_{cr})], \quad (6)$$

where A, B, C are the constants obtained by processing the data presented in the Figure 5, *b*, then for the irradiated material

$$K^*_{Ic} = A + B \exp [C (T - T_{cr} - \Delta T_{cr})]. \quad (7)$$

The whole number of experimental relationships obtained on survey samples is available which associate ΔT_{cr} and F.

An example of such a relationship is given in [9]:

$$\Delta T_{cr} + A_F (F \cdot 10^{-22})^{1/3},$$

$$A_F = 800 \text{ (P + 0.07Cu)}, \quad (8)$$

where A_F is the coefficient of radiation embrittlement, depending on the impurity contents (phosphorus and copper), %; F is the fluence of neutrons with energy $F > 0.5$ MeV, $1 \cdot 10^{22} < F < 3 \cdot 10^{24}$ N/m^2.

Equation (8) gives rather close results for nickel-free steels used in the WWER-440 reactor vessels.

For the base metal and the weld metal of type WWER-1000 reactors that contain nickel, at TsNIITMASh the following relationship was suggested in [13]:

$$\Delta T_{cr} = [220 \text{ Ni}^{0.5} + \text{Cu} + 3400 \text{ P} + 39 \text{ Ni}] \times \frac{(F/D)^3}{1 + (F/D)^3} + 8, \quad (9)$$

where $D = 72 \cdot 10^{22}$ N/m^2.

Table 2 gives results of assessment calculation of ΔT_{cr} according to (8) for the weld metal Sv-10KhMFT (WWER-440) and according to (9) for Sv-08KhGNMTA (WWER-1000) depending on F.

Using the values of A, B and C from ultimate conservative conditions (envelope curve in Figure 5, *b*) for the relationship (7) we shall obtain for the case of WWER-440

$$K^*_{Ic} = 854 + 1201 \exp [0.02 (T - T_{cr} - \Delta T_{cr})], \text{ MPa·mm}^{1/2}. \quad (10)$$

Based on the calculation results of values $K^{max}_{\omega\theta}$ and corresponding temperatures T (Figure 7), it is possible to evaluate the critical values of total $T_{cr} + \Delta T_{cr}$ from the condition (5) for the crack under consideration

$$T_{total} = T_{cr} + \Delta T_{cr} = T - 50 \ln \frac{K^{max}_{\omega\theta} - 854}{1201}, \quad (11)$$

where T_{total} is the critical value $T_{cr} + \Delta T_{cr}$ from the strength conditions.

Table 3 gives the values T_{total} for points C and D of a conditional crack, calculated according to (11) depending on the time t of a thermal shock. Thus, during the time of a thermal shock $t = 500$ s the T_{total} reaches minimum value 172 °C. Accordingly, the allowable increments are determined as

$$[\Delta T_{cr}] = T_{total} - T_{cr0},$$

where T_{cr0} is the initial value of a critical temperature before radiation.

Knowing $[\Delta T_{cr}]$ it is possible to evaluate the critical fluence F for the given case and residual life of the reactor vessel from the Table 3.

REFERENCES

1. Harrison, R.P., Loosemore, K., Milne, I. *et al.* (1980) Assessment of the integrity of structures containing defects. In: *Report R/H/R6-Rev. 2 of CEGB*. Berkley.
2. Harrison, J.D. (1984) Fracture mechanics developments related to the weld defect acceptance methods given in British Standard PD 6493. In: *Proc. of 2nd Math. Conf. on Fract. and Fract. Mech.*, Johannesburgh, Nov. 26 – 27. Johannesburgh.
3. (1991) *Methodology of determination of admissible defect sizes in metal of equipment and pipelines during the Operation of NPS*. Moscow: NIKIET.
4. Zvezdin, Yu.I., Rivkin, Ye.Yu., Vasilchenko, G.S. *et al.* (1990) Application of results of NDT in strength calculations. *Tyazholoye Mashinostroyeniye*, **3**, 12 – 14.
5. (1990) *MR-125-01-90*. Calculation of stress intensity factors and section-weakening coefficients for defects in welded joints. Kyiv.
6. (1990) *IIW/IIS-SST-1157-90*. IIW Guidance on assessment of the fitness for purpose of welded structures.

7. Rumyantsev, V.V. (1993) Pipings at NPS: increasing their reliability and service life duration. *Atomnaya Tekhnika za Rubezhom*, **3**, 3 – 8.
8. Horn, R.M., Kass, J.N., Ranganath, K. (1984) Evaluation of the growth and stability of stress corrosion cracking in sensitized austenitic pipings. *J. of Pressure Vessel Technology*, **2**, 201 – 208.
9. (1989) *Norms of strength calculation for equipment and pipings of nuclear power units PNAE-G-7-002–86*. Moscow: Energoatomizdat.
10. Makhnenko, V.I., Kasatkin, O.G., Velikoivanenko, E.A. *et al.* (1998) Computational and experimental study of residual welding stresses within the zone of circumferential welded joints in D_n 300 KMPTs ChNPS-3 piping. In: *Proc. of the 5th Int. Conf. on Material-Induced Problems at Design, Manufacture and Operation of Equipment of NPS*. St.-Petersburgh.
11. Andreykiv, A.E. (1982) *Spatial problems of a crack theory*. Kyiv: Naukova Dumka.
12. Pokrovsky, V.V., Kaplunenko, V.G., Kovrizhkin, Yu.I. *et al.* (1998) Assessment of the resistance of reactor steels to brittle fracture after different conditions of thermal-mechanical pre-loading and sustainability of positive effect of thermal pressing. In: *Proc. of the 5th Int. Conf. on Material-Induced Problems at Design, Manufacture and Operation of Equipment of NPS*. St.-Petersburgh.
13. Zubchenko, A.S. (1997) Reliability and service life of welded structures of nuclear power equipment. *Avtomaticheskaya Svarka*, **6**, 3 – 10.

NEW APPROACHES TO ASSESSING THE WELDED JOINTS LIFE

V.V. PANASYUK and **O.Ye. ANDREYKIV**
G.V. Karpenko Physico-Mechanical Institute, NASU, Lviv, Ukraine

ABSTRACT

The calculation model for solving the problems of welded joint life has been formulated. In the proposed model a welded joint is considered as a heterogeneous (by the physical and mechanical properties) deformed solid with a defect like faulty fusion-crack that propagates under cyclic loading of a body. The equations for estimating the fatigue crack growth rate were obtained on the basis of the balance of heterogeneous joint material fatigue fracture energy and reversive elastoplastic deformation of the process zone in the vicinity of the defect tip. The fatigue crack propagation direction with respect to initial defect plane was established from the condition that this direction provides the maximum crack rate. The proposed model was applied for assessing residual life of the butt and T-joints and a good correlation between the calculational and experimental data was found.

Key words: *welded joints, fatigue life, fatigue, crack, residual stresses, material inhomogeneity, fracture, energy criterion.*

The problem of welded joints strength especially when subjected to the influence of variable loadings, is one of the most urgent. Such type of structures is widely used in engineering practice. A welded joint always contains metallurgical defects (faulty fusion, cracks, heterogeneous areas of material, etc.). In the welded joint vicinity, as known, high residual stresses develop and thermal cycles of welding cause the change in the physical and mechanical properties of the base metal around the weld [1]. Therefore in the welded joint vicinity the following areas are distinguished by the physical and mechanical properties of material [2 – 4]: *I* – a weld metal (WM), *II* – HAZ and *III* – a base metal (BM) (Figure 1). At present there are different approaches to evaluation of the residual life of welded joints, with account of the presence of defects [2 – 5]. The known approaches usually do not consider the material inhomogeneity around the weld and thus, a certain discrepancy between the calculated and the experimental data can be found. In this paper, using the results of [6 – 8], a new approach to assessing the welded joints life was formulated. It allows us to take into account the material physical and mechanical properties variation in the vicinity of the weld.

Calculation model. Consider an elastoplastic plate, weakened by a crack and introduce a rectan-

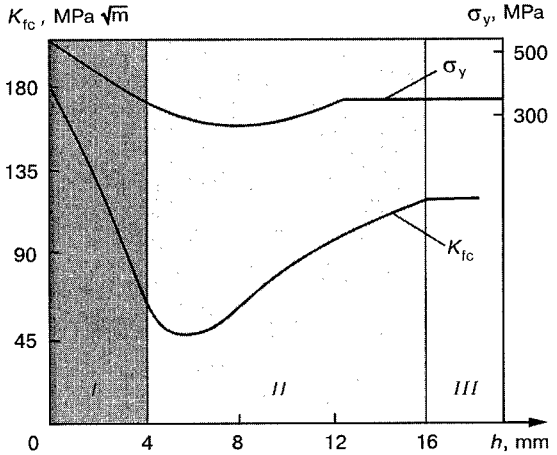

Figure 1. Distribution of physical and mechanical characteristics in the vicinity of the 10XSND steel welded joint: h is a distance from the weld middle part in the direction of the base metal

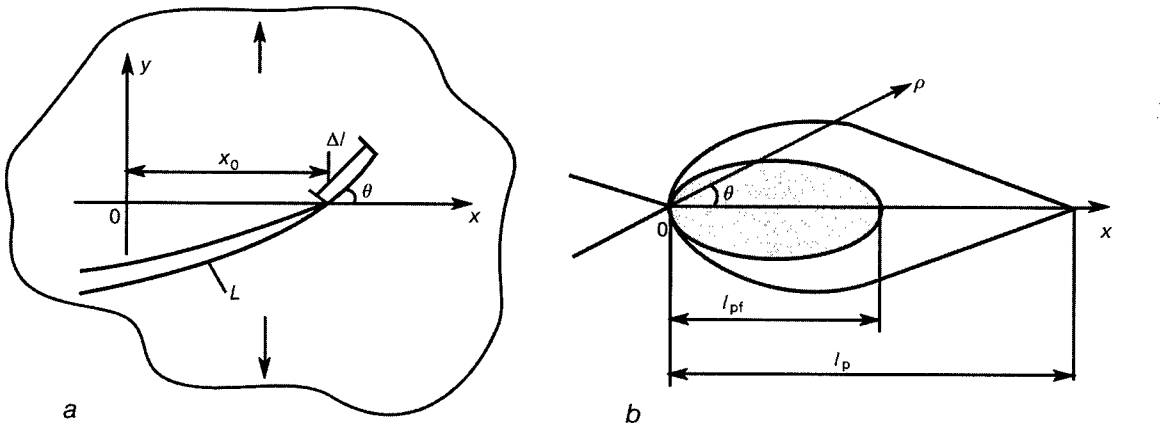

Figure 2. A plate with a crack (*a*) and a plastic zone at the crack tip (*b*) (schematically)

gular Cartesian coordinate system O_{xy} (Figure 2). Let this plate be subjected to cyclic tension. In this case a certain cyclic plastic zone of length l_{pf} is formed at the crack tip (Figure 2, *b*). As known [9], l_{pf} is less than the length of the static plastic zone l_p and depends on the stress ratio $R(R = K_{I\,min}/K_{I\,max})$, while the characteristic length $l_{pf} = 0.25(1 - R)^2 l_p$, where $K_{I\,max}/K_{I\,min}$ is maximum and minimum value of the stress intensity factor (SIF) in a cycle.

Consider now the kinetics of fatigue macrocrack growth rate. Let for ΔN number of loading cycles, the original crack increase by Δl in the direction that forms angle θ in the given coordinate system (Figure 2, *a*). To establish the equations of the crack growth kinetics, use the energetic fracture criterion [10 – 12]. This criterion presupposes the existence for each material of the critical value of energy W_f, necessary for the elementary event of material fracture, that is formation of a unit of the free surface (energy of material fracture). Thus, to get the fatigue crack length increment Δl for ΔN loading cycles, the dissipation of the deformation energy in the material at points (x, y) on the crack growth path $(W = W(x, y))$ should be equal to the value of material fracture energy $(W_f = W_f(x, y))$, i. e. crack growth proceeds under condition

$$W = W_f. \tag{1}$$

The character of elastoplastic deformations of the material in the crack tip vicinity, as shown in Figure 3, *a*, allows us to write equation (1) as

$$W_s + \Delta N W_c = W_f, \tag{2}$$

where $W_s = W_s(x, y)$ is the energy of elastoplastic deformations of the material in the first cycle of the body loading up to the averaged amplitude values (σ_a); $W_c = W_c(x, y)$ is dissipation of plastic deformations energy for one loading cycle (starting from the second cycle). Since during one fracture event at every point of section Δl the maximum crack opening displacement δ_{max} at the moving (forwards θ) crack tip occurs, the energy W_s can be evaluated from the equation

$$\begin{gathered} W_s = \delta_{max}(\rho, \theta)\,\sigma_0\,\Delta l, \\ x = x_0 + \rho\cos\theta, \\ y = \rho\sin\theta, \end{gathered} \tag{3}$$

where $\sigma_0 = \sigma_0(x, y)\tilde{\sigma}_0(\rho, \theta)$ is the averaged stress value in the process zone according to the δ_c-model (this characteristic of the material is a variable one in case of its heterogeneity); ρ, θ are polar coordinates (Figure 2, *b*) [13]. Cyclic tension diagram is modelled by the diagram for a perfect elastoplastic material (Figure 3, *b*). Assume that $\sigma_0 \approx 0.5(\sigma_y + \sigma_s)$, where $\sigma_y = \sigma_y(x, y)$ is yield strength and $\sigma_s = \sigma_s(x, y)$ is ultimate strength of the material. During macrocrack growth, the plastic zone at its tip also moves and the elementary material volume at this tip undergoes all stages of plastic deformation, typical of the plastic zone of length $l_{pf}(l_{pf} < \Delta l)$. Considering this fact and using results of [10] we obtain the correlation for evaluation of the energy of cyclic deformations W_c

$$W_c = \int_0^{l_{pf}} \sigma_0(s, \theta)\,\Delta\delta(s, \theta)\,ds, \tag{4}$$

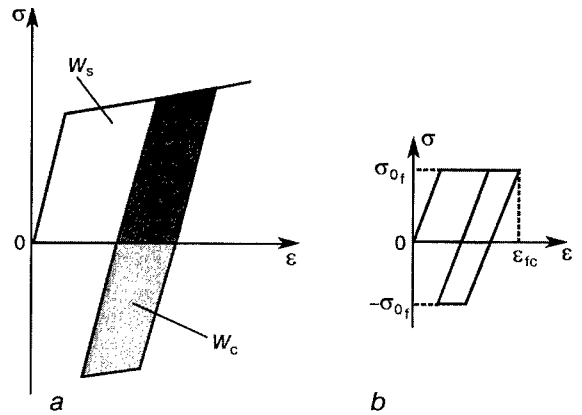

Figure 3. Tension-compression diagram of material in the process zone (*a*) and a diagram model (*b*)

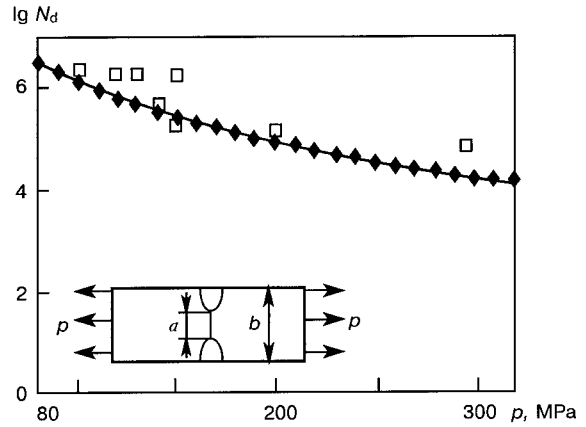

Figure 4. A welded joint with a faulty fusion and comparison of the calculational (◆) and experimental (□) [20] data of the residual life (N_d) (schematically)

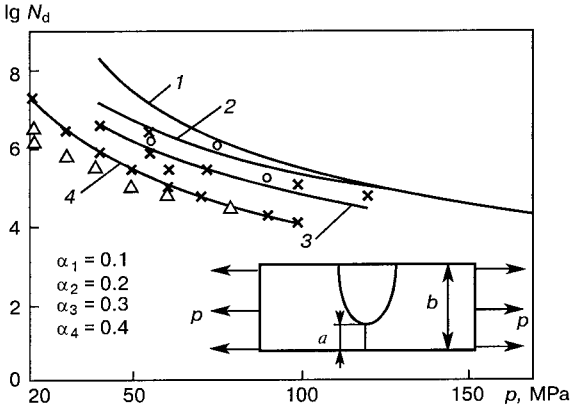

Figure 5. A welded joint with a faulty fusion at different values of α_i ($i = 1 - 4$) and comparison of the calculational (lines *1* – *4*, respectively) and experimental (points) [20] residual life data at $\alpha_1 = 0.17 - 0.20$; $\alpha_2 = 0.26 - 0.31$; $\alpha_3 = 0.44 - 0.49$

where $\Delta\delta(s, \theta) = \delta_{max}(\rho, \theta) - \delta_0(\rho, \theta)$ is the amplitude of the model crack opening according to δ_c-model [13] at point s of the plastic process zone ($0 \le s \le l_{pf}$);

$$\delta_0 = \max(\delta_{min}, \delta_{op}, \delta_{th}),$$
$$\delta_{min} = [1 - 0.5(1 - R)^2]\,\delta_{max}(\rho, \theta), \quad (5)$$

where δ_{max}, δ_{min} are maximum and minimum crack tip opening displacements in a cycle; δ_{op} is the residual crack opening displacement [9]; δ_{th} is the threshold crack tip opening displacement δ_0 (at $\delta_{max} \le \delta_{th}$ the crack does not propagate).

The energy of material fracture W_f, needed for creation of the crack area of length Δl, is defined as $W_f = \beta\gamma\Delta l$, where γ is specific energy of fracture of the given volume of the material, i. e. necessary for formation of a unit of the crack length; β is a Morrow's coefficient [14], that shows the difference between cyclic and static fracture energy, it is determined as $\beta = \left(\frac{\sigma_s}{\sigma_a}\right)^4$. Specific fracture energy is determined by the equation

$$\gamma = \sigma_0\delta_c,$$

where $\delta_c = \delta_c(x, y)$ is a value of critical fatigue crack opening displacement and $\sigma_0 = \sigma_0(x, y)$. In this case we get

$$W_f = \beta\,\sigma_0\,\delta_c\,\Delta l. \quad (6)$$

By substitution of (3), (4) and (6) into equation (2), get the following relationship:

$$\Delta l\,\sigma_0\,\delta_{max}(0, \theta) + \Delta N \int_0^{l_{pf}} \sigma_0(s, \theta)\,\Delta\delta(s, \theta)\,ds = \beta\,\Delta l\,\sigma_0\,\delta_c.$$

Thus, it is easy to find that

$$\frac{\Delta l}{\Delta N} = \frac{\int_0^{l_{pf}} \sigma_0(\theta)\,\Delta\delta(s, \theta)\,ds}{\beta\,\sigma_0(\theta)\,\delta_c - \sigma_0(\theta)\,\delta_{max}(0, \theta)}.$$

Putting $\Delta N \to 0$ in this equation, get the kinetic equation for assessing the crack growth rate ($v = v(\rho, \theta)$) under cyclic loading of a body

$$v(\rho, \theta) = \frac{\int_0^{l_{pf}} \sigma_0(\theta)\,\Delta\delta(s, \theta)\,ds}{\beta\sigma_0(\theta)\,\delta_c - \sigma_0(\theta)\,\delta_{max}(0, \theta)}. \quad (7)$$

Note that the rate v depends on the orientation angle θ of fatigue crack growth with respect to the chosen system of coordinates (Figure 2, *b*).

Let $\theta = \theta_*$ be the angle between the crack propagation direction about the abscissa of the chosen coordinate system (Figure 2). Since we further assume, that the crack propagates in the direction of

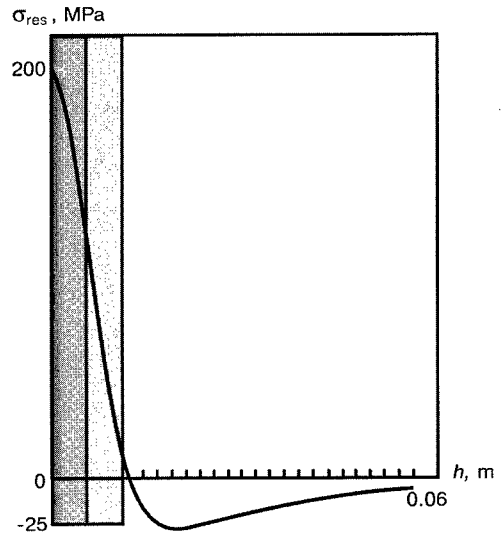

Figure 6. Distribution of residual stresses in St.3 steel welded plate

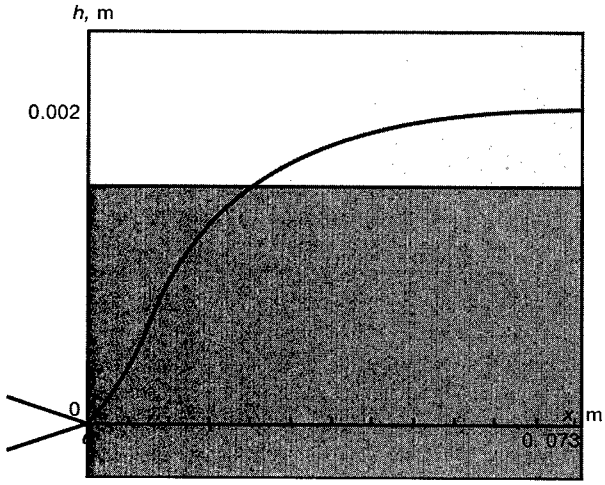

Figure 7. A path of crack propagation from a faulty fusion tip

the maximum rate, i. e. ($\partial v/\partial \theta = 0$ at $\theta = \theta_*$), then from equation (7) we get the second kinetic equation for evaluation of the crack propagation direction

$$\frac{\partial}{\partial \theta}\left(\frac{\int_0^{l_{pf}} \sigma_0(\theta)\Delta\delta(s, \theta)\, ds}{\beta\sigma_0(\theta)\,\delta_c - \sigma_0(\theta)\,\delta_{max}(0, \theta)}\right) = 0 \qquad (8)$$

$$\text{at } \theta = \theta_*.$$

To get equations (7) and (8) it is necessary to add the initial and terminal conditions, namely

$$N = 0 \text{ at } l = l_0, \quad N = N_d \text{ at } l = l_*, \qquad (9)$$

where l_* is the critical crack length, achieved for N_d loading cycles and is determined by the criterion of critical crack opening displacement [15]

$$\delta_{max}(l_*) = \delta_{fc}(x, y). \qquad (10)$$

So, kinetic equations (7), (8) and conditions (9), (10) determine the calculation model for investigation of the subcritical fatigue crack growth in heterogeneous plates. Below the results of the proposed model usage for calculations of residual life of the butt and T-joints are presented.

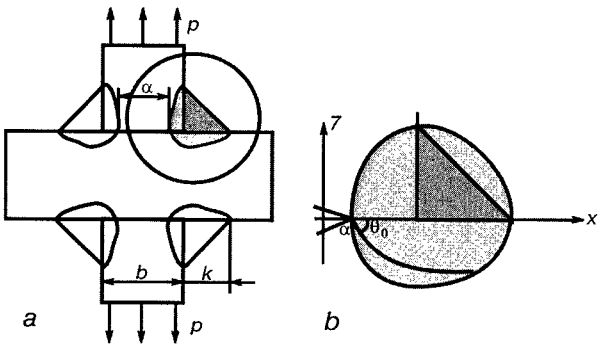

Figure 8. X-joint with a faulty fusion (*a*) and a path of fatigue crack growth from this faulty fusion (*b*)

Table 1. Physical and mechanical characteristics of the material of different areas of St.3 steel welded joint

Welded joint area	σ_y, *MPa*	σ_t, *MPa*	K_{fc}, *MPa*$\sqrt{m}$
WM	250	490	35
HAZ	167	388	23
BM	194	446	27

Butt welded joints. Consider an St.3 steel butt welded joint, produced by submerged-arc process with OSTs-45 flux and Sv-08A wire, with a faulty fusion of a length a (see chart in Figures 4 and 5). Distribution of the physical and mechanical characteristics of the welded joint material is presented in Table 1 [16]. A welded structure (plate) is subjected to cyclic tension by the maximum stresses of intensity p, and stress ratio of the external loading is $R = \dfrac{p_{min}}{p_{max}} = 0.1$. It is necessary to determine the kinetics of the fatigue crack path and evaluate the residual life of the welded joint at different values of stresses p, and also the ratio $\alpha = a/b$ (see Figures 4 and 5).

When solving this problem, first of all, the distribution of residual stresses in the welded joint zone was evaluated using the calculational test method [16] (Figure 6). For the given problem, equations (7) and (8) of the model are written as

$$v = \frac{0.01}{\sigma_0^2}\frac{\left(K_{I\max}^4\left(1 + \frac{c_1 d c_0}{\sigma_0^3}K_{I\max}^2 \sin\theta\right) - K_0^4\left(1 + \frac{c_1 d c_0}{\sigma_0^3}K_0^2 \sin\theta\right)\right)}{\beta K_c^2 - K_{I\max}^2}, \qquad (11)$$

$$\frac{\partial}{\partial\theta}\left(\frac{0.01}{\sigma_0^2}\frac{\left(K_{I\max}^4\left(1 + \frac{c_1 d c_0}{\sigma_0^3}K_{I\max}^2 \sin\theta\right) - K_0^4\left(1 + \frac{c_1 d c_0}{\sigma_0^3}K_0^2 \sin\theta\right)\right)}{\beta K_c^2 - K_{I\max}^2}\right) = 0,$$

where

$$c_1 = 0.663;\ c_0 = 0.6\,(1 - \mu^2)\left(\frac{2(1 + \mu)\,(1 + \eta)\,\sigma_0}{3\sqrt{\eta E}}\right)^{\eta};$$

μ is Poisson's coefficient; η is the coefficient of strain hardening of the material; $d = \dfrac{\partial \sigma_0(0, y)}{\partial y}$; according to equation (5) $K_0 = \max(K_{I\,min}, K_{op}, K_{th})$.

Using the method, proposed in [17, 18] for evaluation of the SIF at the curvilinear cracks, these equations were numerically solved by M.V.

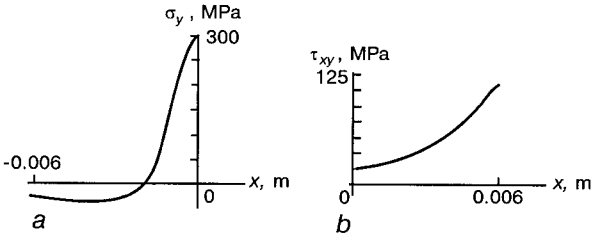

Figure 9. Distribution of residual normal (*a*) and tangential (*b*) stresses in the region of E355 steel T-joint

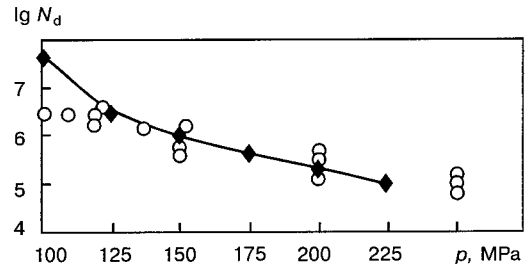

Figure 10. Comparison of the life (N_d) of X-joint, using calculation (solid line) and large-scale testing (points) [20] data for E355 steel

Lishchynska and the shape of the crack path for this problem has been obtained (Figure 7). The residual life (N_d) of the structure was estimated by the known [19] formula

$$N_d = \int_{l_0}^{l_*} v^{-1} dl, \qquad (12)$$

where the fatigue crack growth rate v is found from equation (11).

Calculational data obtained from (11) and (12) are compared with the results of large-scale testing of the same joints as presented in [20] (see Figures 4 and 5).

X-joints. Consider the X-joints with incomplete faulty fusion of length a in one of the elements (Figure 8). The joint is made of E355 steel, the physical and mechanical characteristics of the material of its different areas are given in Table 2 [16]. A structure with a corresponding joint is cyclically tensioned by the maximum intensive forces p, and the stress ratio of the external loading $R = 0.1$. It is necessary to find the fatigue crack path kinetics and to plot the curve of the residual life caused by stresses p.

For the given problem, the distribution of residual (normal σ_y and tangential τ_{xy}) stresses in the T-joint region is evaluated using the calculation test method [16] and is shown in Figure 9.

When solving equations (11), (12), the SIF value was approximately calculated [17, 18], taking into account the above-mentioned residual stresses. A path of fatigue crack, growing from the right tip of the faulty fusion, calculated by the proposed model, is presented in Figure 8, *b*. A period of subcritical fatigue crack growth was evaluated for different values of tensile stress p, using equations (11) and (12) and is shown in Figure 10 by a solid line. The same figure also illustrates the experimental results, designated by points [20]. The comparison of the theoretical and experimental results shows good correlation.

The analysis of the data in Figures 4, 5 and 10 allows us to draw a conclusion that the calculation values of the residual life agree well with experimental results. Thus, we can speak about the correctness of the usage of the proposed calculation model for solving of the problems about the life of structural elements made of heterogeneous (by their physical and mechanical properties) materials, like welded joints.

Table 2. Physical and mechanical properties of different areas of E355 steel welded joints

Weld zone	σ_y, *MPa*	σ_t, *MPa*	K_{Ic}, $MPa\sqrt{m}$
WM	579	680	62
HAZ	395	540	41
BM	449	620	48

REFERENCES

1. Lepikhin, A.M., Moskvichyov, V.V. (1991) Characteristics of crack growth resistance of welded joints – estimation, calculations and statistical analysis. *Zavod. Laboratoria*, **12**, 48 – 51.
2. (1993) *The bases of structures design*. Ed. by L.M. Lobanov. Kyiv: Naukova Dumka.
3. Karzov, G.P., Leonov, V.P., Timofeyev, B.T. (1982) *Welded high pressure vessels. Strength and life*. Leningrad: Mashinostroyeniye.
4. Trufyakov, V.I. (1990) *Strength of welded joints under alternating loading*. Kyiv: Naukova Dumka.
5. Makhnenko, V.I., Pochinok, V.Ye. (1982) Application of fracture mechanics criteria to the strength calculations of welded joints with the discontinuities like cracks. *Avtomaticheskaya Svarka*, **1**, 1 – 6.
6. Andreykiv, O.Ye., Lishchynska, M.V. (1999) An equation of fatigue crack growth in heterogeneous plates. *Fis.-khim. Mekhanika Materialov*, **3**, 53 – 58.
7. Andreykiv, O.Ye., Lishchynska, M.V. (1999) Determination of the fatigue crack growth kinetics in butt welded joints. *Mashinoznavstvo*, **2**, 11 – 16.
8. Andreykiv, O.Ye., Lishchynska, M.V. (1999) Kinetic of fatigue crack growth and residual life of the welded joints. In: *Fracture mechanics of materials and structural integrity*. Lviv: Kamenyar.
9. Panasyuk, V.V., Andreykiv, O.Ye., Darchuk, O.I. *et al.* (1994) Analysis of short and long fatigue cracks growth kinetics under non-regular loading. In: *Proc. of 10th Europ. Conf. on Fracture*.
10. Li, Y.C., Huang, N.C. (1991) Fatigue crack speed of materials with linear hardening. *Int. J. Solids and Struct.*, **7**, 865 – 883.
11. Panasyuk, V.V., Andreykiv, O.Ye., Darchuk, O.I. (1995) Calculation model of fatigue crack growth in elastic-plastic materials under mixed mode loading. In: *Abstr. of 7th Int. Conf. on Mechanical Behaviour of Materials*, Hague, Netherlands, May 28 – June 2, 1995. Hague.
12. Panasyuk, V.V., Andreykiv, O.Ye., Kovchyk, S.Ye. (1977) *Methods of estimating the structural material crack growth resistance*. Kyiv: Naukova Dumka.
13. Panasyuk, V.V. (1968) *Limit equilibrium of brittle bodies with cracks*. Kyiv: Naukova Dumka.
14. Morrow, J. (1950) Investigation of plastic strain energy as a criterion for finite fatigue life. In: *The Garret Corporation Report*. Phaeniz Ariz.
15. Panasyuk, V.V., Andreykiv, O.Ye., Parton, V.Z. (1988) Fracture mechanics and strength of materials. In: *Bases of fracture mechanics*. Kyiv: Naukova Dumka.
16. (1979) *Welding in mechanical engineering*. Refer. Book. Moscow: Mashinostroyeniye.
17. Lishchynska, M. V. (1998) Estimation of stress intensity factors in the plates near curvilinear cracks. *Fis.-khim. Mekhanika Materialov*, **1**, 113 – 114.
18. Lishchynska, M.V. (1998) Propagation kinetics of piecewise-broken cracks in thin-walled elements subjected to long-term static loading. In: *Fracture mechanics and physics of building materials and structures*. Lviv: Kamenyar.
19. Andreykiv, O.Ye., Darchuk, A.I. (1992) *Fatigue fracture and structural life*. Kyiv: Naukova Dumka.
20. Makhnenko, V.I., Pochinok, V.Ye. (1984) Resistance to cyclic loading of the welded joints containing welds with incomplete faulty fusion. *Avtomaticheskaya Svarka*, **10**, 33 – 40.

NEW APPROACH TO EVALUATION OF THE CONDITION OF WELDED STRUCTURES

B.E. PATON and **A.Ya. NEDOSEKA**
The E.O. Paton Electric Welding Institute, NASU, Kyiv, Ukraine

ABSTRACT

New approaches to evaluation of the condition of welded structures in service are considered. Shown is the need to apply the technology of structure diagnostic based on 100 % control of materials and structures which makes it necessary to implement a package of measures including use of special diagnostic systems and equipment, procedures of their application and standards which regulate this work.

Key words: *technical diagnostics, non-destructive testing, residual life, operability, load-carrying capacity, structure testing, monitoring.*

Evaluation of the condition of the structures in service should be based on information on the defects present in them, features of the kinetics of their propagation and development. The task is rather complicated, as its solution is related to the need of not only revealing the defects, but also to their efficient interpretation. This is further complicated by the fact that the destructive processes can proceed in such areas of the structure which are usually not subjected to selective control. Evaluation should also take into account the features of the structure material, conditions of its service and the time it has operated since the moment it was put into service.

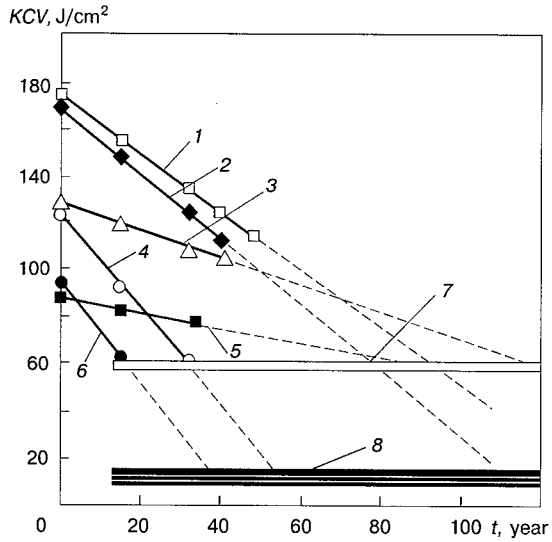

Figure 1. Change of impact toughness of steels with time: *1* — 09G2S; *2* — steel 20; *3* — 14KhGS; *4* — 19G; *5* — 17GS; *6* — 17G1S; *7, 8* — normal and critical *KCV* levels, respectively

As can be seen from Figure 1, the steel service life is not unlimited, although in individual cases it is more than 120 years.

Elaboration of the appropriate control standards based on the traditional approach is rather difficult in view of the need of allowing for a quite large number of factors influencing the conditions of the defect propagation and development, which does not seem possible. On the other hand, practical activity is making this task ever more urgent. Its solution should envisage provision of long-term service and possibility of repairing a structure proceeding from its actual condition.

One of the ways of solving this problem is the use of a comparatively new method based on analysis of elastic waves generated in materials during their structure transformation under deformation. The method automatically provides 100 % control of the plants. It is not susceptible to the conditions of measurement shade, as the elastic wave generated during propagation of a defect, in any case reaches the acoustic sensor, no matter where it is mounted. The method can be successfully used to detect acoustic pulses and determine their co-ordinates.

More difficult is evaluation of the information received from the object together with the deformation waves. This means that forecasting the structure condition and evaluation of its residual life, are difficult. Difficulty of evaluation of the deformation waves is related to the lack of the general engineering understanding of the method metrology which is based on the quantum fracture mechanics. However, its current level of development does not allow such work to be performed, although it permits a large number of problems to be solved.

According to the forecast, it is anticipated that the theory of the new method for practical application, will be constructed only by the year 2010. So far provision of safe service of the structures

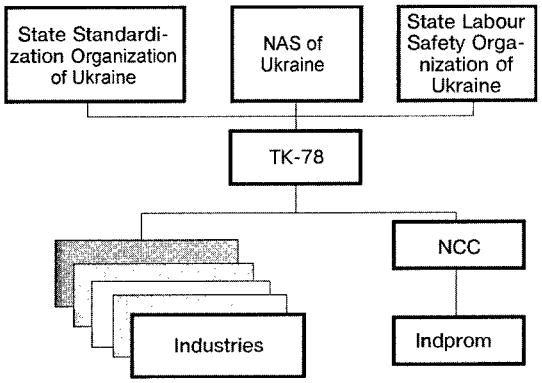

Figure 2. Block diagram of Technical Committee TK-78

requires the application of individual approaches using acoustic emission (AE) method.

The equipment applied for diagnostic purposes should be based on AE method. On the other hand, other data on the controlled plant should be also used. In other words, the so-called material state vector (MSV) should be formed, which determines the capabilities of the structures in service. The performance of the method and the used equipment is based on the correspondence between the AE events recorded by the equipment and those which run in the materials during their deformation. This constitutes the main feature and goal of the approach. Its partial solution and implementation of the investigation results into the actual commercial equipment took us 15 years.

The performed work permitted us to make the equipment a really diagnostic system, namely it began identifying and evaluating the events related to the processes of material fracture. Metrological certification of such instruments and their application procedures are based on a well-proven prototype. This way, commercial production of the equipment duplicates is ensured.

However, all the above-said is obviously insufficient for effective application of the equipment in practice. The following measures should be taken:

elaboration of codes and standards on the technical diagnostic procedure suitable for the method;

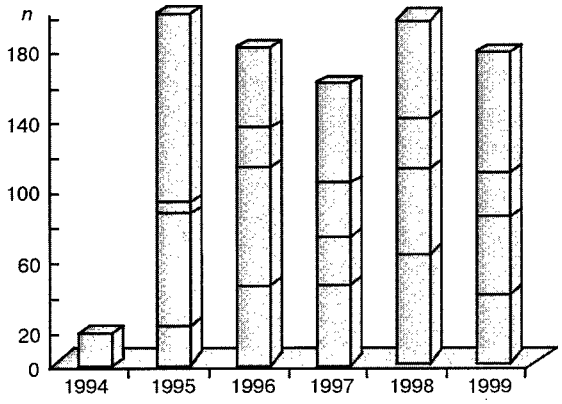

Figure 3. Chart of experts training (n — number of trained experts)

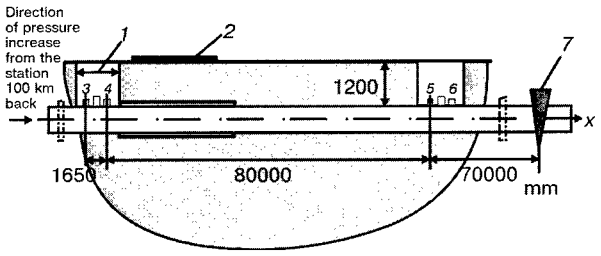

Figure 4. Tested section of 355 × 8 mm pipe of steel 20 of a product pipeline: *1* — 2500 mm wide test pit; *2* — car road; *3, 6* — AE transducers in zonal detection mode; *4, 5* — same, linear array; *7* — pressure regulation gate

training and certification of personnel performing control of the condition of structures in service with the aim of their mastering new control technologies;

certification of the units and laboratories performing technical diagnostic.

In Ukraine this large scope of work is carried out by the Technical Committee on Technical Diagnostic and NDT which is stationed at the E.O. Paton Electric Welding Institute. The Committee was set up by the National Academy of Sciences of Ukraine, State Standardization and State Labour Safety Organizations (Figure 2).

The Committee developed a number of measures which will permit solving the problem of ensuring safe service of structures. The greatest achievement in the sequence of these measures was development of a package of state standards which regulate the following aspects of the inspectors' actions when performing work on evaluation of the structure condition:

technical diagnostic (requirements to personnel and procedure of their certification);

pressure vessels and pipelines (general technical requirements);

requirements to laboratories and procedure of their accreditation;

requirements to personnel training and certification centers as well as the procedure of their accreditation;

boilers, pressure vessels and pipelines (AE method of control).

The Committee includes the National Certification Center (NCC) which performs training and certification of specialists (Figure 3), as well as

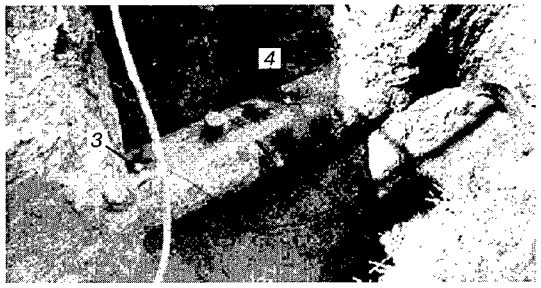

Figure 5. Arrangement of AE transducers on a pipe of a product pipeline

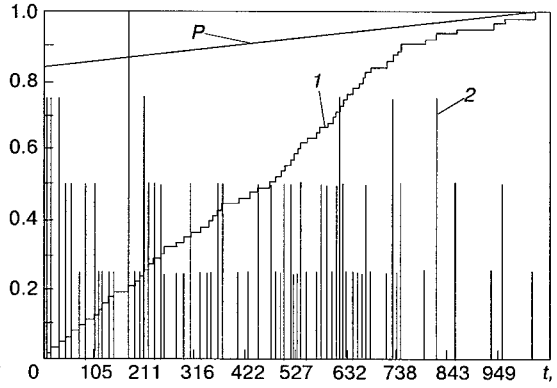

Figure 6. Change of MSV parameters in the zone of control of transducer *3*: *1* — total value of AE pulse amplitudes; *2* — AE pulses distribution in time; *P* — internal pressure

Cluster	*X, mm*	*S(X), mm*	*N*
1	79875	0	1
2	71418	988.7501	2
3	62509	278.9233	4
4	53083	0	1
5	38689	0	1
6	32581	0	1
7	17694	0	1
8	9989	0	1

Note: Here *X* is the distance from transducer *4* to the center of AE source cluster; *S(X)* is the error of determination of AE information cluster co-ordinates; *N* is the total number of AE events in the cluster.

assessment of the technical expertise of the diagnostic laboratories. More than 900 specialists have been trained during the period of the Committee functioning. Note that NCC attention is focused on practical introduction into diagnostic control of the methods which evaluate the actual residual life of the structures, allow reliable enough tracing of the changes in the structure of materials during their deformation under working loads. Diagnostic systems of EMA2, EMA3 and EMA3M type developed to the level of effective application, primarily belong to the equipment implementing these methods. They permit sufficiently reliable evaluation of the structure condition during operation, giving timely warning about development of dangerous zones.

Diagnostic systems which can operate in the mode of continuous monitoring of structures are becoming especially important. They permit taking the structures out of the critical condition, controlling the process of operation in the pre- and critical conditions.

The PWI is actively introducing the developed procedure and equipment in the industrial facilities of Ukraine, Russia and Poland. Over the last 10 years they have been applied for testing more than 700 structures of the petrochemical and processing industry, structures of gas and petroleum product lines and power generation industry.

Note that performance of inspection and diagnostic work with the application of EMA type equipment does not require removing from the structure the insulation, foundations, supports or other obstacles which usually hinder performance of control operations with the traditional methods. In order to conduct 100 % analysis of the item material condition, it is sufficient to make small shafts for mounting acoustic sensors.

As a second example of EMA3 equipment application, let us consider control of an underground part of a product line of 355 mm diameter (Figure 4). Steel with ultimate strength of 470 MPa and yield point of 290 MPa was selected for making the pipe. In order to evaluate the condition of the pipeline material, the acoustic transducers were mounted at 80 m distance from each other in the bared sections of the pipes. Transducers *3* and *6* operated in the mode of zonal detection, controlling the pipe surface at 100 m distance to the left and to the right of the transducer, respectively. Transducers *4* and *5* operated in the mode of linear detection with 80 m base.

Figure 5 shows transducers *3* and *4* mounted on the pipe surface.

The Table gives information on AE clusters in the pipe section 0 to 80 m long. One can see that diagnostic information is uniformly enough distributed along the pipe length.

Figure 6 gives information on the pipe MSV changing its parameters in time in the control zone at pressure rise from 4.3 up to 5.2 MPa.

In our opinion, the experience of Ukraine can be used in development of the technology of safe service of structures, provision of the conditions of effective operation of equipment and solving the most important task of to-day, namely protection of the environment.

DEVELOPMENT OF NON-DESTRUCTIVE TESTING OF CRITICAL METAL STRUCTURES

B.E. PATON and **V.A. TROITSKY**
The E.O. Paton Electric Welding Institute, NASU, Kyiv, Ukraine

ABSTRACT

The paper presents some recent developments in the field of non-destructive testing, promising directions of NDT as a basis for technical diagnostics of metal structures which have been in service for a long time, new technological capabilities in computerisation of the NDT process. The role of Ukrainian Society of NDT and Technical Diagnostics is shown.

Key words: *non-destructive testing, technical diagnostics, metal structures, defects, ultrasonic testing, computerisation.*

Potential scope of application and organisation of NDT activity in Ukraine. In Ukraine great importance is traditionally attached to application of the methods of NDT of quality in all the major industries.

In the industrial complex of FSU technical inspection was organised by industries. Each ministry had its own research institutes. As a rule, one of them was entrusted by the Ministry to set up an NDT department, as the leading one for this industry, which provided scientific and technological guidance in solving NDT problems, developed industry codes, supervised NDT performance in the enterprises.

Many of the enterprises have still preserved central factory laboratories, one of the functions of which is organisation (performance) of NDT. The majority of industrial institutes are now located outside Ukraine. Therefore, development of the specific procedures and equipment for NDT is currently conducted by the institutes of the National Academy of Sciences of Ukraine, higher educational establishments, laboratories of the major industrial associations and private companies.

Since the main producers of flaw detection equipment, like some industry institutes, are now outside the country, new companies appeared which deliver and produce flaw detectors, thickness gauges and other instruments required for NDT performance.

The role of the Ukrainian Society for Non-destructive Testing and Technical Diagnostics (US NDTTD) has become more important, the Society annually holding about five subject- or industry-oriented conferences in Ukraine. Subject-oriented seminars in Slavskoye, Yalta, Ivano-Frankovsk, Kiev and Dnepropetrovsk have become a tradition. The 3rd Scientific-Technical Conference on Technical Diagnostics and NDT in Ukraine was held in May, 2000 in Dnepropetrovsk.

US NDTTD is one of the founders of the European Federation of Non-destructive Testing (EF NDT). A number of bilateral agreements on Cooperation have been signed with similar societies in Russia, Belarus, Khorvatia, Poland, Czechia, Canada, Germany, Great Britain, Denmark, Italy, USA, etc. The Society participates in the meetings of the working groups of the Federation, in preparation of the World NDT Congress to be held in October, 2000.

Six accredited certification centers are currently operating in Ukraine (in Kiev, Kharkov, Dnepropetrovsk, Zaporozhje, Lvov and Ivano-Frankovsk) performing certification of NDT personnel. The most well-known of them is the NDT Certification Center at the E.O. Paton Electric Welding Institute which was the first to be granted (already in 1990) a licence by the USSR National Certification Committee (NCC) for certification of NDT experts.

NCC of Ukraine is active in EF NDT working group on improvement of the main European standard EN 473 as regards certification of NDT personnel.

Some recent developments in NDT. In the field of acoustic methods of NDT, automated units for ultrasonic testing (UT) of the quality of longitudinal welds on large-diameter pipes with a separate recording of defects in the weld and the HAZ have been developed and introduced in the pipe and metallurgical works. The speed of control with such units is up to 20 m/min. Control is performed by 6 to 8 probes. Each channel has a module of automatic marking of the defective sections. The following system permits the distance between the probes and the weld axis to be maintained with the accuracy of up to 2 mm. Ultrasonic waves are applied to the metal by means of a local pool. Application of different probes allows the kind and orientation of the defects to be determined and

control validity to be improved. NK-18 type unit performs automatic UT (AUT) of pipes of 478 to 1020 mm diameter and 8 to 32 mm wall thickness in the production flow and in the pipe bases. The unit offers a number of indubitable advantages over the foreign analogues in terms of technology, for instance, accuracy of following the axis of a weld of a complex geometry, couplant consumption, etc. The most significant advantage, however, is separate recording of the defects of the weld metal and the HAZ.

A pilot automated unit of NK-143 type was developed for AUT of flash-butt welded joints with difficult-to-reveal defects of the type of sticking, oxide films, etc. The unit operation is based on the procedure of statistical processing of ultrasonic information with adaptive selection of the rejection threshold. In this case, the rejection level corresponding to the anomalies of a butt welded joint is determined statistically by recording all the signals reflected from the weld, without application of the traditional calibration by reference blocks.

In order to detect low-reflectivity defects against the background of structural noise in the items, mathematical models of wave field and algorithms of defect detection and identification in automated control were developed. These developments formed a basis for creation of a multi-channel NK-164 type unit controlled by a microcomputer according to a program providing selection of the main parameters of the system (quantity and sequence of channels switching on, delay and duration of gates for each channel, echo-pulse gains, etc.). The same program processes the UT results, namely calculates the adaptive detection threshold, determines the conditional dimensions, location and kind of defects. All the required information is displayed and stored on floppy magnetic discs.

The reactors of a nuclear power station (NPP) are maintained in the operable condition by conducting periodic preventive repair operations, based on the results of NDT and technical diagnostics. The effectiveness of the preventive measures obviously greatly depends on the accuracy and validity of the data derived in NDT.

The PWI developed N193 system for AUT of circumferential welds of the piping of NPP primary circuit. In this system an eight-channel acoustic module is displaced by an easily detachable two-coordinate scanning mechanism, with up to 25 m/min speed. The system of control, processing, recording and displaying of UT data is implemented in AWS-350 industrial computer and 20 MHz ADC of «Advantech» company.

H193 system provides remote control of circumferential welded joints and determines the defect properties. The results of its operation on the piping of the main circulating pump of RBMK-1000 reactor of the Chernobyl NPP confirmed the technological effectiveness of the system.

The versatility of the developed flaw detection equipment allowed it to used as a basis for creation of equipment for AUT of the weld and the base metal of the posts of the upper circuit of process channels of RBMK-1000 reactor and other NPP equipment.

In order to perform fast control of the quality of welded joints of metal structures in the field, the PWI developed a portable flaw detector based on samarium-cobalt permanent magnets of EM-2 type, designed for continuous magnetisation of extended butt welded joints and sections of items of ferromagnetic materials in site and under the conditions when power supply is difficult or undesirable. EM-2 device is made in the form of a magnetic wheel pair with a common magnetic axle which carries a handle of a nonmagnetic material, thus allowing the item to be magnetised in any position in space. The device is safe in operation, does not need power supply, is reliably held on the controlled plant by the strength of the permanent magnet field to prevent its random separation from the plant. On the other hand, it is easy to take off from the surface being controlled by turning the handle by 180° relative to the magnetic axle. This device served as a basis for setting up the production of portable flaw detectors of MAGEKS type for magnetic particle inspection in the field.

Over the last years procedures have been developed for NDT of various coatings, ceramic, composite and non-metallic materials. The procedures for determination of defects location in welded joints of polyethylene pipes became the most widely accepted of these developments. Defects of the type of cracks, lacks-of-penetration, blowholes, pores and lacks-of-fusion are found in polyethylene due to UT application. Features of UT of welded joints of polyethylene pipes with application of echo-pulse and echo-mirror methods, as well as the diffracted wave method were studied. Comparative analysis of UT results and the data of destructive tests confirmed the high validity of detection of different types of defects in polyethylene.

Promising trends of NDT as a basis for technical diagnostics of metal structures operating for a long time. One of the quickly developing areas is computerisation of the NDT process and improvement of the flaw detection technology. Computer processing allows visualisation of control results, an essential improvement of the validity of the test results, processing of large data bulks, and development of fundamentally new NDT technologies. The advantages of such flaw detectors over other samples of similar equipment are as follows:

ability to memorise the shape of the acoustic signal, its spectral analysis with a high-resolution separation of the received signals;

statistical processing of information in the practically real time with plotting of appropriate graphs;

application of the method of synthesised focal aperture (SuperSAFT);

implementation of the method of defect sizing by the time interval between the acoustic waves diffracted at its edges in probing with a wide beam (TOFD method), etc.

In the latter case defect orientation, damping in the material, and quality of acoustic contact influence the control results much less than with the echo-pulse and other regular methods. The TOFD method enables detection and evaluation of parameters of defects in the joints made by flash-butt welding, electron beam and other welding processes in which flaw detection is difficult. Such flaw detectors were used for investigation of ceramic materials, plastics and composites. Ceramics has been widely used lately as an alternative material due to its low specific weight, high corrosion- and wear resistance.

A not less important issue has lately been assessment of pre-defect condition of the material, the data on which in the case when the discontinuity is not yet in place, allow the necessary measures to be taken which prevent the defect formation, as well as forecasting the item performance. The pre-defect condition of the material can be forecast based on evaluation of the spatial distribution and measurement of some physico-mechanical characteristics (PMC) of the material, which determine its strength properties.

The ultrasonic probing method is the one of the most acceptable (due to its high penetrability) for evaluation of metallic materials PMC, as a number of parameters of the probing ultrasonic field (speed, dispersion, amplitude, direction of polarisation vector) depend on the material PMC. About 90 % of the studies on PMC evaluation by the ultrasonic methods are based on the fact that the speed of ultrasound depends on PMC. The method of PMC evaluation by acoustic means, unlike the method of acoustic emission which registers discontinuities in the material structure, is a passive method, not requiring any external loading. Change of the material acoustic properties is an indication of structural changes, requiring early detection in critical objects.

Quite often, assessment of the strength and other physical properties of the metal is successfully performed also by magnetic properties [1] of a magnetised material (coercive force, residual induction, magnetic permeability, etc.), for instance, sorting out of parts after quenching, and of components after long-term service.

A passive magnetic method of evaluation of metal structure PMC emerged recently, not requiring the application of any special external test impact on the metal or magnetisation devices. This is the method of the so-called magnetic memory (MMM) based on analysis [2, 3] of scattered magnetic field distribution over the surface of the metal structure, representing its loading history and service features. The magnetic fields on the metal structure surface result from irreversible inner structural changes in the direction of the action of the principal working loads. This phenomenon is attributable to the presence of the magnetic field in each microelement of the structure. Chaotically located domain magnetic fields, under the impact of inner structural mechanical displacements in the metal, for instance in the bending zone, lead to magnetic particle ordering and to the appearance of a magnetic field on the metal surface, respectively. Naturally, the more intensive and the longer the metal structure loading, the greater the magnetic field on the surface and the more probable the development of a crack. MMM has found an effective application for evaluation of the pre-fracture condition of turbine blades, railway rails, etc. A program on MMM introduction in the facilities of Gosnadzorokhrantrud of Ukraine (Labour Safety Inspection) has been prepared and is being implemented now.

In practice, unfortunately, quite often we have to deal with a great number of the already formed defects, whose propagation and merging is to be followed. Computerisation of NDT processes allows defect detection to be performed in the most heavily loaded sections of the structure which can have a multitude of different defects in its bulk at the same time.

Illustrations of new technological capabilities in computerisation of NDT processes. Based on an order from the Ministry of Power Generation and Electrification of Ukraine, an ultrasonic computerised P-scan system was used to perform expert evaluation of the condition of the metal of critical components of power generation equipment after their examination with manual ultrasonic flaw detectors, and a comparative experimental study of the traditional technological procedures for compliance with the requirements of the current industrial standards was performed. Such a revision was used to study the difficult-to-evaluate pitting corrosion of the metal of pipelines, steam piping bends, welded joints on backing rings. It was possible to resolve a great number of fundamentally new problems related, for instance, to in-pipe diagnostics of the main pipelines, due to the ability to perform analysis of these data on different sensitivity levels, three-dimensional form of presentation of information on the defects, implementation of the TOFD, SuperSAFT methods, and viewing the entire defect

Customer, city	*Term of work performance*	*Objects of control*	*Purpose of NDT*
Kremenchug petroleum processing plant, Kremenchug	March–July 1994	Rectification columns, pipelines, separators, heat-exchanger cases	Accurate sizing of defects in welds and base metal
Ladyzhin thermal power plant, Ladyzhin	August–September 1994	Bends of feed water pipeline	Determination of the degree of corrosion damage of base metal
Khmelnitsk NPP, Neteshin	March–June 1995	Piping of primary circuit of reactor No. 1	Accurate sizing of defects
Kremenchug petroleum processing plant, Kremenchug	July–October 1995	Rectification columns, pipelines, separators, heat-exchanger cases	Detection of cold cracks (hydrogen-induced cracking) in welds and base metal
Chernobyl NPP, Slavutich	August–November 1995	Piping of primary circuit of reactor No. 2	Detection of defects in welds
Ukrtatnafta (Kremenchug petroleum processing plant), Kremenchug	May–October 1996	Rectification columns, pipelines, separators, heat-exchanger cases	Detection of defects in welds and base metal
Dashava-Kiev gas pipeline	1997	River crossing section	Separation of the zones of corrosion damage and metal delamination
Kherson petroleum processing plant, Kherson	October–December 1996	Reactor of coke-making plant	Generation of the pattern of corrosion damage of base metal
The same	May–July 1997	Rectification columns, pipelines, separators, heat-exchanger cases	Detection of cracking in welds
Ukrtatnafta (Kremenchug petroleum processing plant), Kremenchug	August–November 1997	The same	Detection of defects in welds and base metal
«Diascan» TDC, Lukhovitsy	1998	Oil pipelines with anomalies found by in-pipe inspection gear	Detection of anomalies in oil pipelines by TOFD and SuperSAFT methods

field. In-pipe diagnostics so far has achieved real success only in profilemetry, in detection of anomalies of pipeline geometry, and determination of metal losses of corrosion origin.

The PWI and «Diascan» TDC (Russia) applied expert UT for determination of the type and accurate dimensions of the anomalies found by in-pipe inspection gear. For this purpose, in the anomaly zones found by the gear, the pipeline is uncovered, cleaned from the insulation and UT is performed over the metal surface with a computerised P-scan flaw detector. So, in 1998 UT was performed in 18 pits of the «Druzhba» oil pipeline of 1020 to 1220 mm diameter and 12 mm pipe wall thickness in which the magnetic gear of «British Gas» company found 29 defects of the size of 40 to 90 % of the pipe wall thickness.

The TOFD diffracted wave method and the SuperSAFT synthesised focusing aperture method were used to determine the defect type and height.

By UT results all the studied welds were divided into four groups, depending on the degree of criticality and urgency of repair.

The first group included four welds which required urgent repair. These welds had flat-bottomed defects more than 5 mm high. Three other welds were classified in the second group and repaired in the second run. Four welds with minor defects by height and length which are currently being monitored, were listed in the third group. The fourth group included seven welds erroneously indicated by the gear, in which the defects were not confirmed by any of the above UT methods.

It was found that false indications from the magnetic gear were due to various deviations in the weld shape (edge misalignment, difference in thickness and ovality of pipes, shrinkage, etc.). Comparative analysis showed a 75 % coincidence of UT data with the defects detected by the magnetic gear. Metallographic examination confirmed the UT results, the error of defect height determination not exceeding ±1 mm.

Thus, the possibility is shown of accurate enough determination of the dimensions, type and height of the defects in welds of line pipelines after their diagnostics with magnetic gear.

Table shows ten more cases of UT of critical objects performed with the computerised UT flaw detector. In each of them original results were derived, this being impossible with the application of the traditional UT procedures and means.

Figure 1 gives a print-out of the results of control of a welded joint of a frame element 8 mm thick on a 125 mm section, which clearly shows that part of the reflectors are weld defects and lie in its central part. They are located in the middle and lower part of the weld section by the depth. The other part of the reflection is caused by defects in the base metal. They are located outside the weld zone and approximately parallel to its center

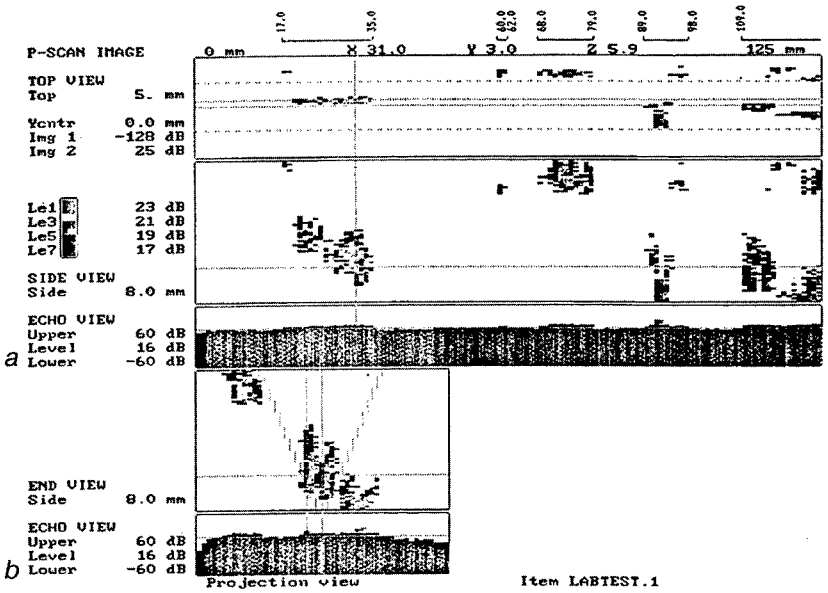

Figure 1. Location of reflectors in the welded joint zone: *a* — recording of echo-signals along the weld; *b* — recording of echo-signals across the weld

line. These reflections are located closest to the external surface across the metal section.

An illustration of the thickness control results representation is a map of corrosion failure of a shell of an underground tank (Figure 2, *a*), which shows the nature of fracture, presence of individual pits, their dimensions and orientation. The section profile of the area with the most intensive fractures allows evaluation of the residual thickness in individual points of the tank shell and detection of the places where the formation of a through-thickness defect is the most probable.

A similar kind of data presentation is also used in expert statement on the defects nature with the aim of prevention of an erroneous interpretation of reflections from metal delamination as an indication of pitting.

Figure 2, *b* is a print-out of the results of control of pipe metal thickness in the fly-over of Dashava-Kiev gas pipeline, which, by the estimate of many flaw detection experts, was regarded to be in a critical condition. The reflections from the closest rolled-out inclusions and delamination were identified as deep corrosion damage from the inside. In the print-out, however, one can see that all the reflectors are located only in the middle part of the metal cross-section, their reflecting surface is flat, this being characteristic for delamination and not for corrosion pits. The differences in the nature of reflectors for the sections with corrosion damage and delamination, are clearly visible in the plots of thickness distribution (Figure 3).

In the case of corrosion failure, the plot of thickness distribution is characterised by a smooth curve indicating the presence of reflectors in the entire thickness range (Figure 3, *a*). In the case of delamination, such a plot has two clearly defined peaks (Figure 3, *b*): one corresponds to the nominal thickness of the metal and the other to the depth of the delamination location. Thus, the earlier

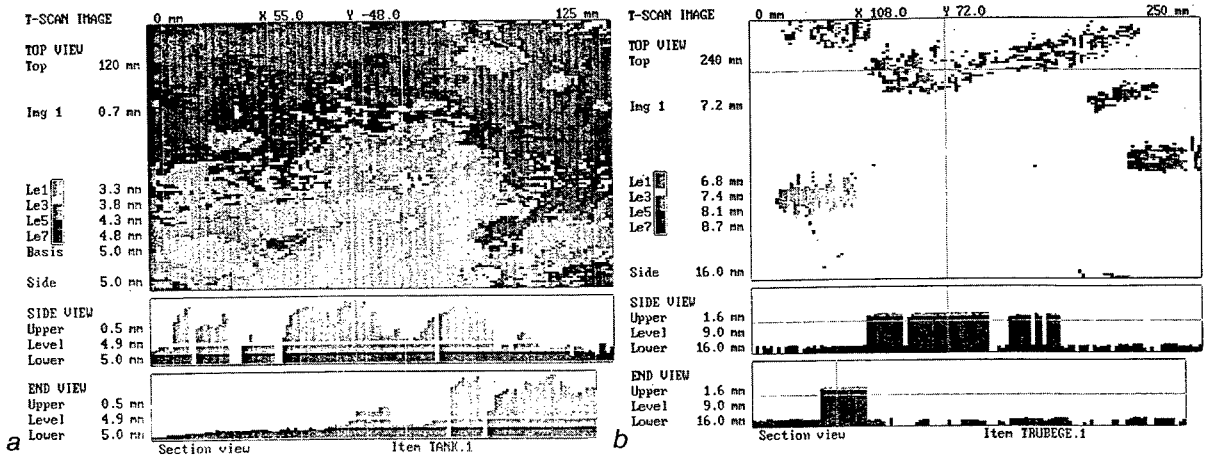

Figure 2. Maps of thickness of metal with corrosion damage (*a*) and delamination (*b*)

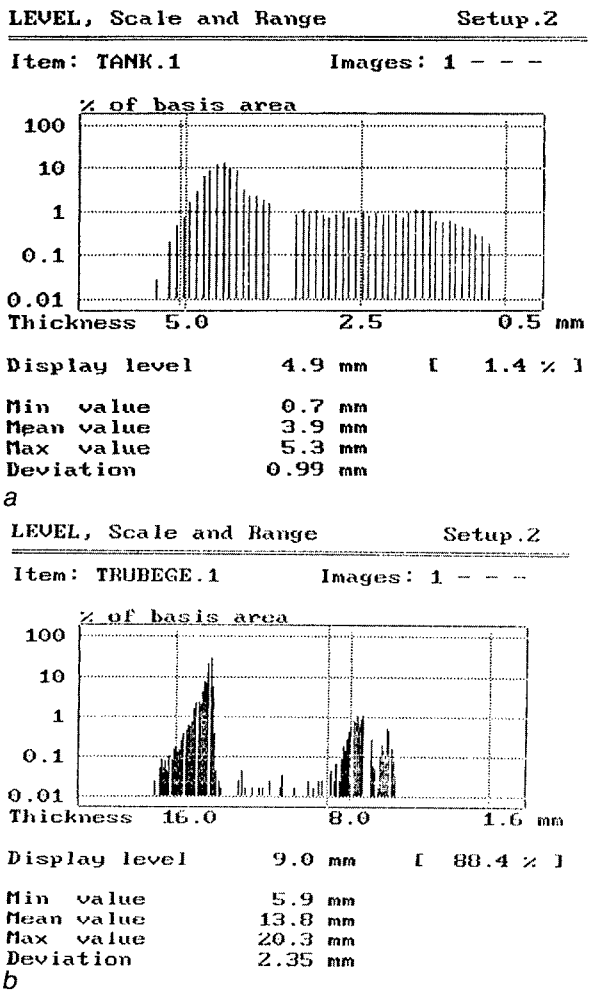

Figure 3. Plots of thickness distribution in the case of corrosion damage (*a*) and delamination (*b*)

taken decision on interrupting the pipeline operation, turned out to be wrong.

The three-dimensional form of presentation of information on the defects (see Figure 1) allows in a number of cases avoiding coarse errors in assessment of the defect level in an object. For instance, when a weld on a backing ring is controlled, signals created by reflections from the backing ring edges are recorded, which can have a considerable amplitude and can be erroneously interpreted as an inadmissible defect. The print-out shows a string of defects located along the welded joint boundary. One can see that these reflectors are shifted from the center line of the weld and are located as though above the pipe internal surface. Such a pattern is characteristic of signals from the backing ring edge, as in this case the acoustic wave propagates farther, not only in the welded joint metal, but also in the ring metal. On the other hand, the reflector which is located on the weld center line, is a defect of the root part and is the only one taken into account in assessment of the joint quality.

It is known that in a number of cases the echo-signal amplitude does not provide an unambiguous estimate of the defect size. This is an especially frequent case in detection of extended defects of a small height or round-shaped ones, which have a low reflectivity. Figure 4 gives a print-out of the results derived in examination of a section of a steam cooler collector pipe with internal corrosion damage in the form of fine defects located at different height. In this case, the surface of the metal on the walls of a loose corrosion defect had an irregular structure, causing a strong diffusion scattering of the acoustic energy. Therefore, the amplitudes of echo signals from the defects had a small value, while the defect was classified as an admissible one by the regular UT technology, although

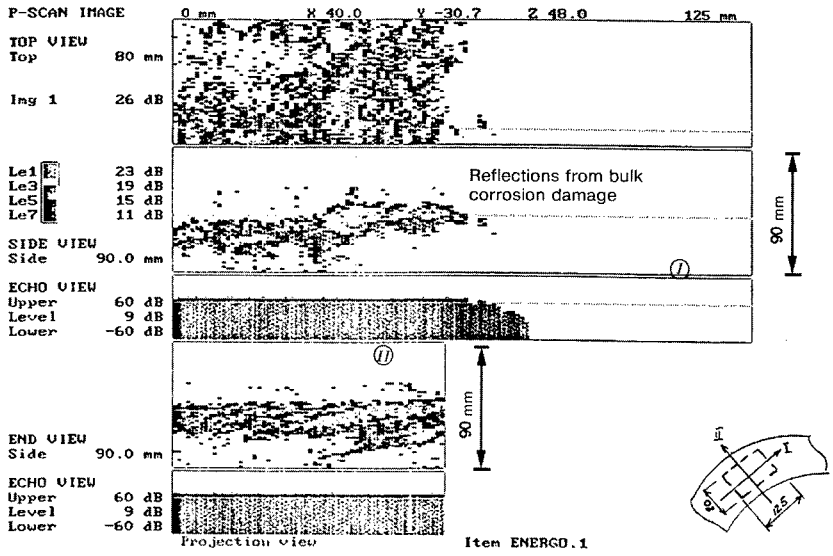

Figure 4. Corrosion damage inside the metal

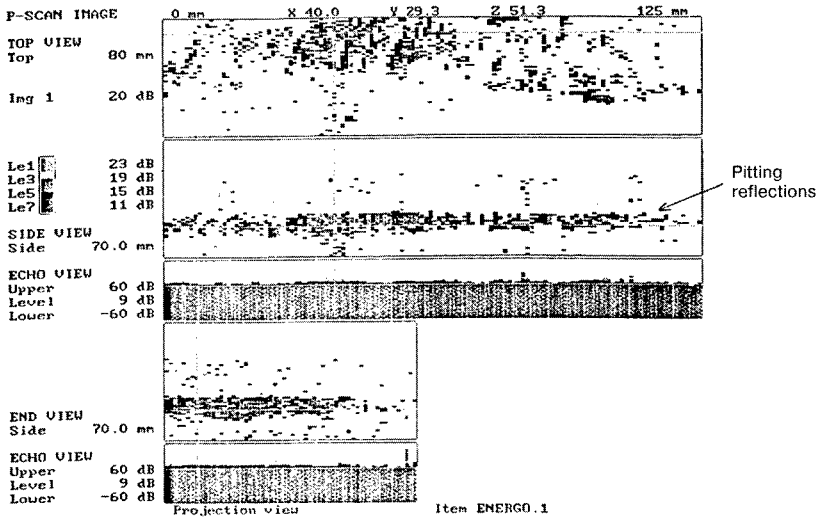

Figure 5. Case of weak pitting corrosion coming to the metal surface

the actual total degree of the metal loosening was significant.

In expert estimation of similar patterns not only the echo-signal amplitudes, but also the nature of the defect distribution in the pipe metal, are taken into account. One can see from the print-out that the reflectors do not lie in one plane, which would be characteristic in the case of weak pitting corrosion recorded in another section (Figure 5), but take up a rather wide zone (see Figure 4) across the wall section. The strongest reflectors are located at a small depth. All this is indicative of the presence of a defect zone in which in different points of the surface, the corrosion proceeds with different speed, which happens, for instance, at cavitation fracture.

Thus, use of information on all the reflectors location, alongside with the amplitude characteristics of defects, enables a more correct assessment of the condition of the metal of the object in the studied zone. With the regular UT technology, the pipe with fine defects was regarded to be acceptable, whereas after generation of the patterns given in Figures 4 and 5, it was removed from service.

The computerised systems, due to processing of a large volume of information, provide a more valid estimate of the defect level in the object, compared to the regular control means. Information on the location, dimensions and types of a large number of fine defects, allows the experience of qualified experts to be used for evaluation of the condition of critical objects.

As computerised UT systems become more widely accepted, the currently valid UT standards, taking into account only the defect amplitude characteristics, should be revised. The future standards, besides these parameters, will also include statistical estimates, as well as the indications of relative locations of the defects, and density of fine reflector distribution.

REFERENCES

1. Troitsky, V.A., Radko, V.P., Demidko, V.G. *et al.* (1986) *Non-destructive testing of the quality of welded structures*. Kyiv: Tekhnika.
2. Troitsky, V.A. (1997) *Brief guide on quality control of welded joints*. Kyiv: PWI.
3. Dubov, A.A. (1999) Diagnostics of fatigue damage of rails using the metal magnetic memory. *V Mire Nerazrushayushchego Kontrolya*, **5**, 22 – 23.

WEAR AND RELIABILITY OF STEEL STRUCTURES

A.V. PERELMUTER
UkrNIIProektstalkonstruktsiya, Kyiv, Ukraine

ABSTRACT

General principles of wear of steel structures are considered. Possible decisions which may be made after assessment of technical state of structures are indicated. Data on the accident rate of basic load-carrying structures are given. It is noted that in the majority of cases the accident rate is not related to the safety factor. In-service monitoring of the technical state of an object is considered to be very important. The necessity of developing regulatory and methodological documents for specification, assessment and maintenance of a certain level of safety of load-carrying structures is substantiated.

Key words: *steel structures, wear, reliability, check, repair, regulatory documents, safety.*

Evolution of technical state of structures. Physical wear of structures and their loading change with time. So do possible estimates of the technical state of objects. Figure 1 schematically shows the process of exhaustion of serviceability of a structure in the form of a function characterizing, e.g. its strength.

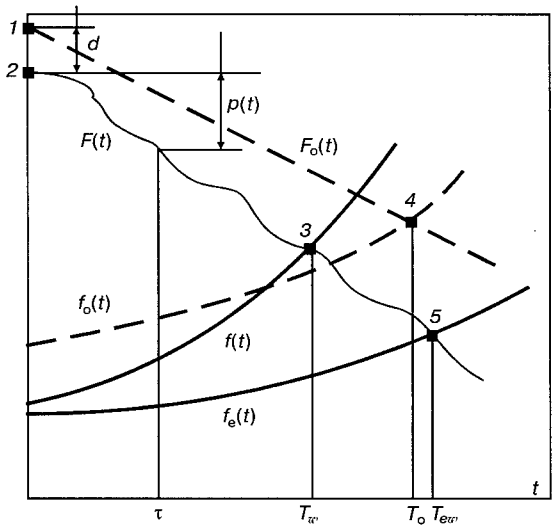

Figure 1. Changes in serviceability of an object: F_0 — predicted curve (most often it is assumed that load-carrying capacity is decreased following a linear dependence); F — actual decrease in load-carrying capacity; f_0 — predicted curve of demand for load-carrying capacity, allowing for rise in production (e.g. allowing for a required increase in a rated load capacity of cranes); f and f_e — curves of actual changes in demand for load-carrying capacity at actual changes in production with and without allowance for limitations on service conditions; $p(t) = F(t) - F(0)$ — damage evolution process; *1* — serviceable (designed) order corresponding to the zero time reference; *2* — actual initial state, allowing for a possible existence of defects $d = F(0) - F_0(0)$; *3* — point of intersection of curves $F(t)$ and $f(t)$, which characterizes the time moment T_w at which serviceability is exhausted; *4* — point characterizing service life predicted by design, T_0; *5* — point of intersection of curves $F(t)$ and $f_e(t)$, characterizing the time moment T_{ew}, at which serviceability turns out to be exhausted in the case of limitations on utilization of the object

Technical state of an object varies during operation, and this state should be assessed by regular inspections. In a general case, possible decisions which may be made after such inspections are reduced to the following actions: continuation of operation; operation with a limitation of the term of further service life and/or methods of utilization of a structure; reinforcement, repair, reconditioning of service properties; dismantling and replacement.

The corresponding scheme of actions is shown in Figure 2. A specialist who makes decisions chooses this or that variant on the basis of how critical the object is and how much it will cost to ensure its reliability.

The statement fixed in standards [1], which accepts only a serviceable state to be achieved after repair (overhaul, reconstruction), is of a cardinal importance. This problem is particularly pressing for the cases where a structure was designed and fabricated following the standards which were in force earlier and are no longer valid. It is often absolutely impossible to bring such a structure to the serviceable state (the simplest example is when a modular system is changed).

Accident rate of basic load-carrying structures. Statistics of failures should be used as the basis for investigations aimed at ensuring reliability of construction objects. However, considerable discrepancies are noted between such statistical data and basic theoretical developments associated with reliability. In this respect, the most theoretically elaborated area is that which considers the concept of reliability as function of the safety factor for strength. In this case the «safety factor» and «strength» concepts are treated in a very generalized sense. On the face of it, this approach seems reasonable. But the in-depth analysis shows that failure of a structure can be caused by very many factors (insufficient knowledge of service condi-

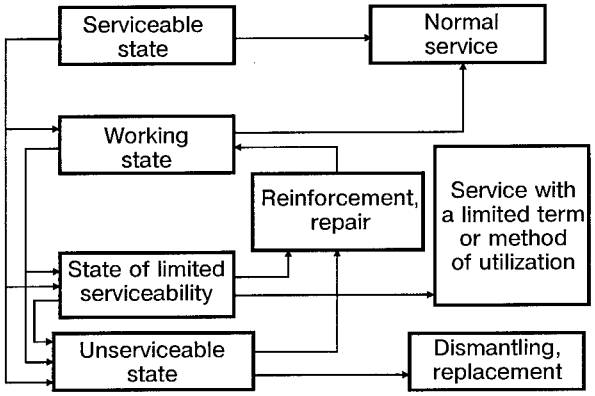

Figure 2. Schematic of possible actions to be made after assessment of technical state

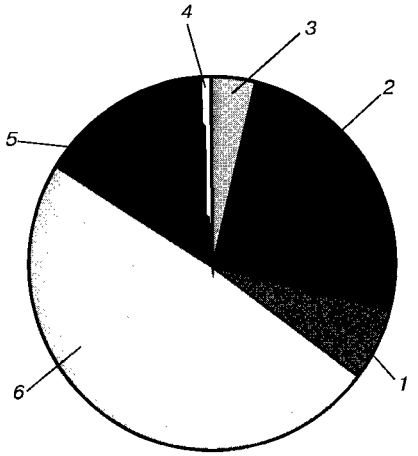

Figure 3. Causes of accidents at steel structures: *1* — low quality of materials (6.3 %); *2* — poor design, design errors (25.1 %); *3* — insufficiently elaborated design specifications (4.2 %); *4* — other causes and their combinations (0.4 %); *5* — improper maintenance (preventive maintenance) and repair (15.7 %); *6* — manufacture and erection defects (48.3 %)

tions of a structure, design, manufacture or erection errors, violation of service regulations), in addition to the case of exceeding an accidental value of load-carrying capacity by an accidental load (insufficient safety factor). In such cases it is unreasonable to choose as a measure of increasing reliability only an increase in the safety factor. The alternative methods for increasing reliability should also be taken into account. They include improvement of design of a structure, development of repairable designs, monitoring of a current state of a structure, improvement of service conditions and many others intended for increase in adaptability of a structure with random properties to uncertain service conditions. Therefore, the aspects to be considered should include not only technical problems, but also those related to ergonomics, i.e. interaction between a man (designer, builder, service operator) and a structure during the entire lifetime of this structure.

Validity of the above-said is confirmed by causes of failures of steel structures, the data on which are available in publications [2 – 6], including both general-application buildings and special structural objects (Figure 3). It can be seen from this Figure that no more than 29.3 % of cases at the best can be classed with causes which the classical areas of investigation of reliability are associated with (positions *2* and *3*). At the same time, as reported in certificates of assessment of a technical state of structures in operation, the dominating defects include substantial corrosion wear or damage of elements caused by striking by a transport vehicle or improper positioning of loads. Almost all of them are not related to the safety factor.

In consideration of causes of accidents, it is necessary to take into account the certain trend to overestimation (position *2*). This is associated with the fact that, compared with other participants in the construction process, designers are in a less favourable situation, especially in the cases where the cause of an accident is not evident and the immediate attempts to establish it fail. A specific manufacture or erection defect in a collapsed structure (e.g. a defective weld or lack of the required number of bolts) is hard to detect in a heap of metal scrap. At the same time, a design according to which a structure was built can be studied in detail and comprehensively analysed. The presence of even insignificant errors, which might not lead to the accident, will always be detected by experts and fixed in the accident investigation act.

Fortunately, full collapses of structures are rare occasions. However, the enormous number of unserviceable states of individual structural members of buildings and engineering structures are reported, where the catastrophic fracture did not occur only due to a favourable concurrence of circumstances or other random factors.

The extremely large data arrays, including results of inspection of existing structures, are available. These are the sources that may provide abundant information to study processes associated with failure of structures and develop precautions to extend their failure-free operation and longevity. Thus, UkrNIIProektstalkonstruktsiya conducted investigations to generalize data on damage of coverings on industrial buildings used in different industries (Table 1).

It can be seen from the investigation data that the relative quantity of trusses with defects and damage is rather large and varies insignificantly from industry to industry.

The main type of defects revealed was a general distortion of bars (64.2 %). The data on deflection of truss elements in excess of specifications, in absolute and relative values, as compared with a permissible value of $w/L = 1/750$, are given in Figure 4.

The accident rate was studied on 151 objects using data from accident investigation acts and reports of special post-accident inspections. In these objects 1318 trusses collapsed and 513 were tem-

Table 1

Industry	Q-ty of objects	Q-ty of trusses		
		Total, pcs.	With defects and damage	
			Pcs.	%
Machine building	15	1074	419	39.0
Ferrous metallurgy	18	1170	463	39.6
Non-ferrous metallurgy	4	336	117	34.8
Ship building	6	243	101	41.5
Power engineering	3	262	84	32.1
Total	46	3085	1184	38.4

Table 2

Service life, years	Q-ty of girders		
	Inspected, pcs	Damaged	
		Pcs.	%
1 – 3	29	4	14
4 – 6	70	12	17
10 – 12	105	64	61
20 – 22	62	45	73

porarily removed from service (until a decision is made on the possibility of their further utilization).

Similar data were accumulated also on other structural members, for example, on welded crane-runaway girders, where the main type of damage is cracking of belt welds in the top chord [7]. Here the dependence of the quantity of this type of damage upon the time of operation is obvious (Table 2). It should be taken into account that among the undamaged girders, which were in use for over 5 years, there were some which had been subjected to repair (sometimes more than once).

Defects and different types of damage may be formed both at the stage of manufacture and erection of a structure, and during operation. As a rule, the former further develop at the stage of operation, summing up with damage which is characteristic only of the stage of operation. Characteristic data on changes taking place during the operation process are shown in Figures 5 and 6, where the revealed defects and damage are indicated in relative (compared with specified) values.

Growth of relative deviations with time has been reported. It is true not only for the above defects, but also for all other controlled parameters of structural design.

A very characteristic damage is wear of crane rails, which leads to considerable expenses in the case of replacement of rails and rollers of travelling cranes, especially the cranes with a very heavy-duty operation. According to [8], consumption of metal in replacement of rails at some facilities after 2 – 3 years of operation can be comparable with the mass of metal of crane girders, whereas the initial mass of the rails is only 10 – 15 % of that of the girders.

It should be noted that many of defects detected by inspections are very dangerous, so that they may be a direct cause of a catastrophic fracture. Unfortunately, we have to state that the majority of defects are the result of a very negligent treatment of structures by attending personnel. Often are the cases of loading the covering trusses (e.g. in repair of travelling cranes) with undesigned weights, cutting out of elements which seem to be «in the way», overloading of structures with industrial dust, etc.

Principles of wear. Attempts were made to study principles of wear of buildings and structures. The generalized data on ratio Z of the mass of steel consumed for repair to the initial mass of a metal structure are given in [9]. These are the results of inspection of 100 spans of 20 shop buildings constructed in different years at the Magnitogorsk Metallurgical Works (MMW), Chelyabinsk Metallurgical Works (ChMW) and other factories in the Urals (Figure 7). One can easily notice a difference between buildings in which the crane trestle is separated from other structures (light circles) and buildings with the combined framework (dark squares).

The value of Z is a certain generalized indication of wear for steel structures at objects of approximately similar application. It is far from being versatile and does not solve the problem of assessment of different types of objects. The common indication of wear can be the cost of repair-reconditioning operations related to the initial cost of an object, although it includes a hindering factor — inflation

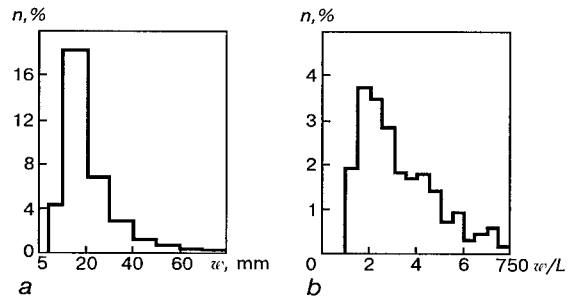

Figure 4. Distribution of absolute w (a) and relative w/L (b) deflections of truss elements (n — frequency of cases)

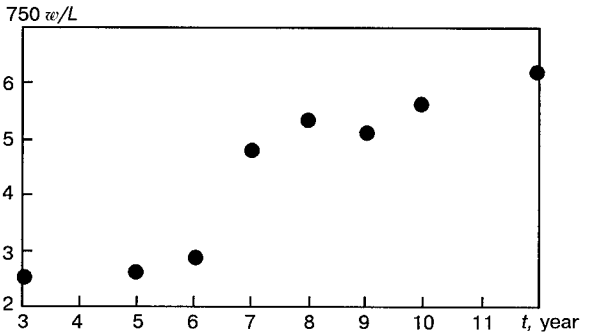

Figure 5. Relative deflections versus time of operation

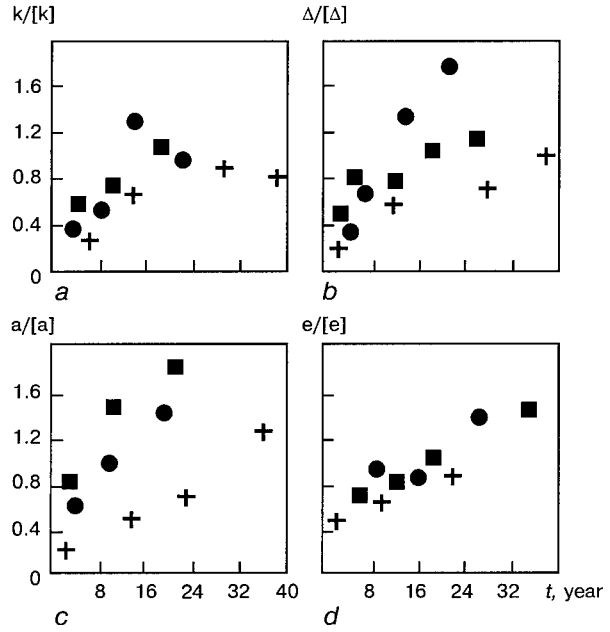

Figure 6. Degradation of the state of crane tracks: *a* — longitudinal slopes; *b* — difference in marks in cross members; *c* — narrowing and expansion of the gauge line; *d* — rail eccentricity (● — superheavy-duty; ■ — heavy-duty and × — moderate-duty of operation)

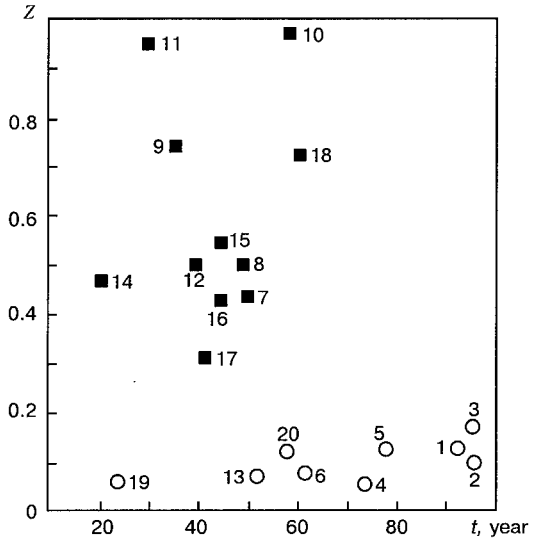

Figure 7. Wear of buildings in metallurgical industry (year of construction is given in brackets): *1* — open-hearth plant, Lieva (1900); *2* — wheel rolling mill shop, Vyksun (1898); *3* — rolling mill shop, Verkhnyaya Salda (1899); *4* — rolling mill shop, Zlatoust (1915); *5* — open-hearth plant, Verkh-Iset (1912); *6* — open-hearth plant, MMW (1930); *7* — reduction shop No. 3, MMW (1941); *8* — stripping department, MMW (1942); *9* — mould shop, MMW (1954); *10* — reduction shop No. 2, MMW (1933); *11* — slabbing, MMW (1959); *12* — plate rolling mill shop No. 2, MMW (1951); *13* — forge shop, MMW (1939); *14* — reduction shop No. 3, ChMW (1968); *15* — open-hearth plant No. 2, ChMW (1945); *16* — open-hearth plant No. 1, ChMW (1942); *17* — open-hearth plant No. 1, MMW (1952); *18* — rail-beam shop, Nizhnij Tagil (1932); *19* — heat treatment shop, ChMW (1965); *20* — open-hearth plant, Nizhnij Tagil (1944)

processes, which do not allow correct comparison of funds spent some time ago and current costs.

Nevertheless, this comparison can be made on the basis of a proper correction of total costs. This makes the use of this indication justifiable. Note that if the cost of repair-reconditioning operations is compared with the cost of a new object of a similar application, physical wear may be complemented by moral wear (in this case the cost of repair should include the cost of bringing the object to the level meeting up-to-date requirements).

Dependence of the cost of repair upon the extent of physical wear was investigated by an example of residential buildings. Processing of statistical data (Figure 8, squares) confirms existence of the smoothing dependence of a logarithmic type — $F = 21.628 \ln(S) - 32.45$, which can be regarded as sufficiently versatile.

Since the non-repairable defects (e.g. changes in rheological properties of materials) are also accumulated during operation, the cost of repair-reconditioning operations will include only part of wear which can be repaired (removed). Total wear in this case will be represented as follows:

$$U = C_{rep}/C_{init} + kt,$$

where C_{rep} is the cost of repair, C_{init} is the initial cost and k is the coefficient of growth of non-repairable wear. Values of the k coefficient were determined in [10] based on this representation and considering that by the end of the service life the non-repairable wear will amount to 35 – 40 %. Principles of changes in wear during the lifetime were determined for metal structures of industrial buildings with superheavy- and heavy-duty operational conditions (Figure 9).

Effect of in-service monitoring of technical state on reliability. As the level of damage of a structure tends to increase with time (real calendar time or conditional rated time), the importance of in-service monitoring of the technical state of an object drastically grows. An increase in the quantity of checks of a structure leads to an increase in its reliability. However, this increase involves growth of costs. Therefore, it is necessary to find a certain compromise between attempts to increase reliability and attempts to reduce the costs of maintenance. The problem of this type was solved by an example of damage of the type of fatigue cracks [11].

Analysis is based on two estimates. One refers to kinetics of propagation of a fatigue crack and estimation of residual strength of a damaged structure, and the other is related to estimation of pro-babability of detection of a crack of a certain length.

The probability of detecting a defect (event D) which has a characteristic parameter d (e.g. length of a crack) is determined by the following condition:

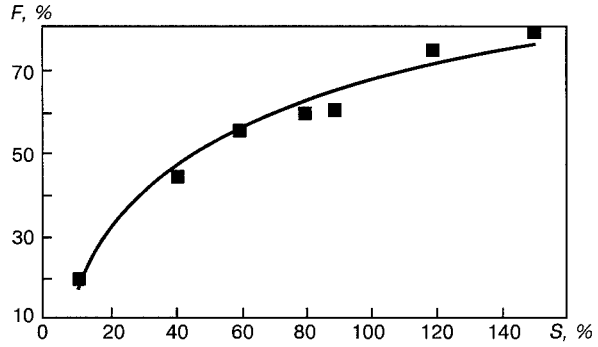

Figure 8. Cost of repair S versus wear F

$$P(D \mid d) = 1 - \exp[-(d/\beta)^{\alpha}],$$

where α and β are the parameters which are associated with the methods of diagnostics. The probability that the value of parameter d will be determined from a range of x to $x + dx$ by inspection is equal to

$$P(x < d < x + dx \mid D) = \{P(D \mid x < d < x + dx)\, P(x < d < x + dx)\}/P(d),$$

where $P(x < d < x + dx)$ is the probability that a defect has the corresponding dimensions (even if it is not detected) and $P(d)$ is the absolute probability of detecting defects with any value of d. In terms of densities of probabilities, this can be written as follows:

$$f(d \mid D) = k_1 f(d)\, P(D \mid d) = f(d) P(D \mid d)/P(D). \quad (1)$$

The density of probability of non-detecting is as follows:

$$f(d \mid \overline{D}) = k_2 f(d)\, x1 - P(D \mid d). \quad (2)$$

Their sum is

$$f(d \mid D)/k_1 + f(d \mid \overline{D})/k_2 = f(d),$$
$$1/k_1 + 1/k_2 = 1.$$

From (1) and (2) we obtain that

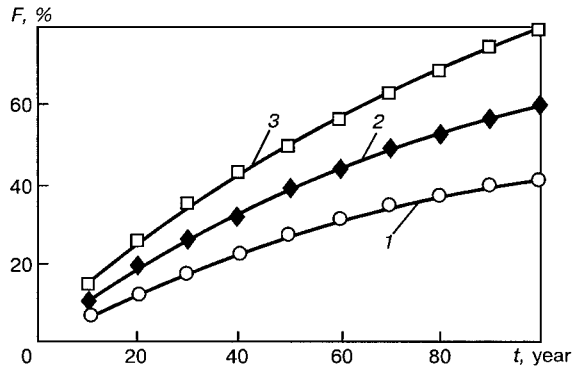

Figure 9. Changes in general wear of metal structures of industrial buildings in medium- (*1*), heavy- (*2*) and superheavy-duty (*3*) operation

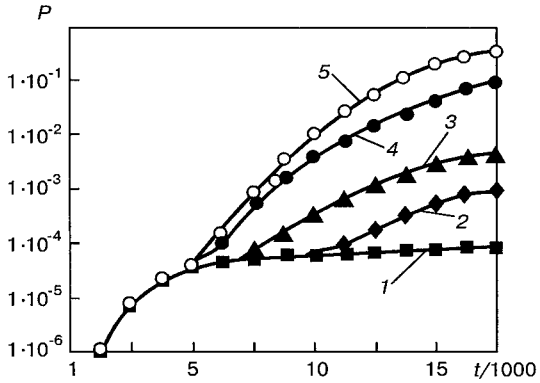

Figure 10. Dependence of probability P of the first failure upon the time of operation t and quantity of inspections N: *1* — 49; *2* — 24; *3* — 14; *4* — 5 and *5* — 0 inspections

$$f(d) = f(d \mid D)/([k_1 P(D \mid d)]),$$

$$f(d \mid \overline{D}) = [k_1/(1 - k_1)][f(d \mid D)/P(D \mid d)] \times [1 - P(D \mid d)].$$

Residual strength of a structure containing a crack was estimated by using the following approximate expression:

$$R(t) = R_0 \left\{1 - (1 - \xi)\sqrt{\frac{a(t) - a_0}{a_s - t_0}}\right\},$$

where $R(t)$ is the residual strength t hours after initiation of the crack with an initial size of a_0; ξR_0 is the residual strength at a maximum permissible size of the crack equal to a_s and $a(t)$ is the size of the crack at a time moment of t.

In [11], the curve of the probability of failure at the absence of inspections ($N = 0$) consists of two regions with different characteristics (Figure 10). The intensity of failures in the first region is determined by the probability of exceeding the value of tensile strength by a load, since even if the crack is initiated at the initial time moment ($t = 0$), it will take some time for it to propagate to reach a dangerous limit. In the second region the intensity of failures is determined more by the presence of cracks and probable exceeding the level of residual strength ξR_0 by a load. Therefore, inspections in this region have a fundamental effect on reliability. It can be well seen from Figure 10 which shows the data on the effect of the quantity of inspections N on the probability of failure.

Figure 10 shows that, in addition to a conclusion of the benefits from conducting inspections in a later time period (naturally, with the persisting acceptable level of risk), it can also be concluded that there is a certain «saturation limit» for the quantity of inspections. In this case almost all damages are revealed on time, so the second part of the curve is just a continuation of the first part.

Safety of construction objects. Building standards and regulations, with very rare exceptions, do not allow for any cases of occurrence of

technogenic accidents and catastrophes (accident effects of a natural character are considered at least to some extent). This is attributable, on the one hand, to a widespread opinion that structures become substantially more costly if they are designed with allowance for accident-inducing loads, and, on the other hand, to a naive but traditional belief that, since there should be no accidents at all, it is not worthwhile speaking of them. In the building practice the optimal strategy seems to be that which develops such precautions which could convert a catastrophic fracture into a small accident with consequences that are rather easy to remedy. An example of such developments is building of a rampart around an oil tank to prevent excessive overflow of oil products in the case of complete fracture of the tank. Such precautions have a relatively low cost, while the imaginary saving on these precautions may lead to enormous environmental, social and material losses.

It seems absolutely necessary to develop a system of regulatory and methodological documents to specify, assess and maintain a certain level of safety of load-carrying structures, bearing in mind that a probable violation of the safety level is associated not only (and even not so much) with deviations in strength of a material or intensity of a load, which are traditionally allowed for in structural design, but with such factors as:

violation of the design specifications and regulations of manufacture, erection, transportation, storage and conservation;

violation of the operation and repair rules;

mistakes of personnel;

critical failures of technospheres;

unfavourable natural factors (earthquake, tornado, meteorites, flood, karst falls, etc.);

absence or inefficiency of protection precautions.

This requires an exact formulation of requirements to safety of buildings and structures, allowing for indications of permissible risk by critical failures, requirements for availability of protection means, monitoring systems, etc.

These requirements may be included into special standards (e.g. there is a special system of standards on labour safety) or into other specifications for an object. But in the cases it is very important to note that the point is safety. Otherwise there will be a collision of designations, since the relationship of safety requirements with the necessity to ensure strength of a building or structure, which is absolutely obvious for a specialist, is not enough for substantiation of the use of special legal acts for safety assurance and often leads to legal confusions.

REFERENCES

1. (1995) *DBN 362–92. Assessment of technical state of steel structures of industrial buildings and constructions in operation.* Kyiv: Ukrarkhbudinform.
2. Belyaev, B.I., Kornienko, V.S. (1968) *Causes of accidents of steel structures and methods for their removal.* Moscow: Strojizdat.
3. Dobromyslov, A.N. (1990) Analysis of accidents of industrial building and engineering structures. *Prom. Stroitelstvo*, **9**, 9 – 10.
4. Krylov, I.I., Shevtsov, Yu.P. (1983) Classification of causes of failures of steel structures of industrial buildings and constructions. *Izv. Vuzov, Stroitelstvo i Arkhitektura*, **11**, 16 – 19.
5. Sakhnovsky, M.M., Titov, A.M. (1969) *Lessons from accidents of steel structures.* Kyiv: Budivelnyk.
6. Perelmuter, A.V. (1999) *Selected problems of reliability and safety of building structures.* Kyiv: UkrNII-Proektstalkonstruktsiya.
7. Kikin, A.I., Vasiliev, A.A., Koshutin, B.N. *et al.* (1984) *Extension of service life of metal structures of industrial buildings.* Moscow: Strojizdat.
8. Saburov, V.F. (1985) On the problem of improvement of grades of crane rails. In: *Transact. on Investigations on Building Mechanics and Building Structures.* Chelyabinsk: ChPI.
9. Shishov, K.A. (1985) Principles of theory of operation of industrial building structures. *Ibid.*
10. Egleskaln, Yu.S. (1974) *Investigation into physical wear of metal structures of industrial buildings.* Cand. Techn. Sci. Thesis. Moscow: V.V. Kujbyshev MISI.
11. Yang, J.-N. (1977) Optimal periodic proof test based on cost effective and reliability criteria. *AIAA J.*, **3**, 402 – 409.

ELECTRIC-ARC WELDING UNDER FORCED CONDITIONS

S.P. RAGUNOVICH, V.A. TSYGANOV and **V.K. SHELEG**
R&D Institute for Welding and Coating with Experimental Production, Minsk, Belarus

ABSTRACT

Described is the approach to investigation of relationship between volt-ampere dynamic characteristics of a heat source and peculiarities of formation of the weld pool which determine the quality of welding. The concept of computer diagnostics and monitoring of the arc welding process, based on the finite number of statistical moments of the arc power, is presented. The quantitative indication of the welded joint quality is suggested.

Key words: *welding, heat input, welding conditions, heat source, weld pool, weld quality.*

One of the ways of improving the quality of welded joints in critical structures is to decrease welding heat input, which leads to reduction of time during which the metal dwells within the unfavourable temperature range and to elimination of development of stresses and strains [1 – 3]. This is achieved by an increase in the concentration of energy of a heat source resulting from the use of forced welding conditions [4, 5]. The latter provide for an increase in efficiency of the welding process with no increase in thermal power of the heat source through using the rational diagrams of interaction of the plasma flow with the molten metal of the weld pool. The application of new heat sources to control both thermal power and force effect on the molten metal is one of the most important tasks ensuring advancement of the welding industry [6].

Peculiarities of the weld pool formation in welding under forced conditions. Welding under forced conditions using the concentrated heat sources is characterized by the presence of a deep crater in the weld pool and S-shaped front wall of the molten metal surface [5]. The effect of forcing is achieved as a result of high rates of ablation of the melting front due to an increased pressure within the active arc spot and velocity of movement of the plasma flow along the melting front.

The molten metal along the axial line of the melting front is pressed out from the active spot zone due to variation in the character of distribution of pressure of the plasma flow along the melting front. In cutting, a dominant factor is formation of a high-velocity boundary layer, whose parameters are determined by the gas-kinetic component of the plasma flow. In this case, the direction of the velocity vector of the boundary layer should correspond mainly to profile of the surface of the melting front.

In welding under forced conditions, the molten metal should be contained within the weld pool. In a case where the boundary layer moves mostly along the melting front deep into the welding crater, the molten metal layer will increase in thickness with depth to the crater cavity due to the metal coming from the above regions. This will lead to screening the melting front by the molten metal and decrease in the penetration depth for a given thermal power of the heat source. Therefore, in welding under forced conditions the most rational diagram is that causing the molten metal to move not to the depth of the crater, but along its lateral surfaces in parallel with the surface of the plates joined. This can be achieved by decreasing the gas-kinetic component of the plasma flow pressure on retention of a high pressure gradient in a direction parallel with the surface of the plates joined. In this case, however, with distance from the weld pool axis the volume of the moving molten metal also increases as a result of the metal coming from regions located closer to the axial line. Therefore, this should cause increase either in thickness of the molten metal layer or in rate of ablation. In this connection, the hypothesis which is based on a determining role of metal transfer over the melting front surface, resulting from the formation of the boundary molten metal layer and the plasma flow, and which provides for high gas-kinetic parameters of the latter, does not correspond to the description of the welding process under forced conditions.

At the same time, it should be noted that an increase in the gas-kinetic energy of the plasma flow leads to deterioration in the hydrodynamic situation in the weld pool and is associated with formation of some defects characteristic of welding under forced conditions, such as coarse-ripple surface of the weld, non-uniform penetration depth, periodic chain of course pores, molten metal spitting and tunnel effect in the weld root [5].

The purpose of this investigation was to reveal conditions of formation and development of the weld pool under the forced process parameters.

Assuming that the melting front has the cylindrical shape, in welding under forced conditions the average ablation rate in the first approximation can be determined from the following expression:

$$v_{ab.av} = \frac{\pi H_{weld}}{4\, l_{cr}}\, v_w, \qquad (1)$$

where H_{weld} is the average weld width; l_{cr} is the average length of the crater and v_w is the welding speed.

It follows from expression (1) that the wider the weld and the shorter the length of the crater, the higher the pressure gradient on the surface of the active spot to achieve the required average ablation rate. It can be supposed that the determining role in forcing the fusion welding process is played both by size of the active arc spot and by character of distribution of the plasma flow pressure over its surface. In this case the degree of the concentration of energy of the heat source should correspond to the penetration depth at a preset speed of the process. An increase in the penetration depth at a constant speed should be associated with growth of size of the active arc spot and, accordingly, with a decrease in the concentration of energy of the heat source at its increased thermal power. Widening of the range of thickness of materials welded and degree of forcing the process parameters requires development of new non-traditional heat sources.

Low-amperage constricted arc. The low-amperage constricted arc is characterized by a decrease in the gas-dynamic effect of the plasma flow on retention of the thermal power of the arc, which is achieved by proper selection of geometrical parameters of the arc chamber, torch nozzle and system of stabilization of the plasma flow.

As to its technological properties, the low-amperage arc takes an intermediate position between the arc that burns freely in the argon atmosphere and the constricted arc. Regulation of the gas flow rate allows rigidity of the arc to be varied over wide ranges, as the arc can be «soft» (like in oxygen flame) or «hard» (like in plasma cutting). Under «soft» burning conditions the flame is capable not only of propagating over the surface of a workpiece, but also of affecting the molten metal as a factor that stabilizes disturbances formed in the weld pool.

Technological peculiarities of the welding process using the low-amperage constricted arc are as follows: welding at a decreased current (20 – 180 A); self-adjusting stability of the weld pool in welding with the penetrating arc; decreased heat input into the torch of a simplified design; possibility of cladding and surface melting at a decreased heat input; position butt welding of pipelines without programming of the process parameters in different spatial positions; decreased requirements to skills of welding operators; welding with the penetrating arc in a manual mode.

Stability of the weld pool in welding under forced conditions. For the liquid–gas interface of an arbitrary shape the pressure is determined from an equation given in [7]:

$$\left[P_g - P_l - \sigma\,(K_x + K_y)\right] n_i = \left(T_{ik}^{(g)} - T_{ik}^{(l)}\right) n_k + \frac{\partial \sigma}{\partial x_i}, \qquad (2)$$

where $P_g = P_g\,(z,\ x,\ y)$ and $P_l = P_l\,(z,\ x,\ y)$ are the pressures of gas and liquid at points on the surface; σ is the surface tension coefficient at the liquid–gas interface; K_x, K_y are the surface curvatures; n is the single normal vector directed into the bulk of the gas; and $T_{ik}^{(g)}$ and $T_{ik}^{(l)}$ are the viscous stresses in gas and liquid, respectively, at the interface. The second term in the right part of equation (2) is the force gradient caused by a variation in the surface tension coefficient. If we ignore evaporation at the interface between the phases, the first term in the right part of equation (2) will be close to zero, as with the plasma (gas) flow, having kinematic viscosity ν_g and density ρ_g, blowing over the surface of the liquid with viscosity ν_l and density ρ_l without slipping, the relationship that usually holds is as follows:

$$u_0' << u' = u << u_0,$$

where u_0', u_0, u' and u are the velocities of the liquid and gas, respectively, in the flow core and at the interface.

Assuming in (2) the value of σ to be gradient-free, and setting the $\left(T_{ik}^{(g)} - T_{ik}^{(l)}\right) n_k$ term to be equal to zero, the initial equation of the force balance on the weld pool surface, called the Laplace formula, will be written as follows:

$$P_g - P_l = \sigma\,(K_x + K_y). \qquad (3)$$

In equation (3) the pressure of gas and liquid at the interface and the surface curvature along the main axes are the functions of coordinates of the surface points and process parameters.

Consider the process of a stationary interaction of the weld pool and the gas (plasma) flow in welding with through penetration. Figure 1 schematically shows the weld pool in the form of a section along its longitudinal axis. The *ABO* line is the melting front of the metal and the *CDE* line is the solidification front. The gas flow rate ahead of the weld pool crater is designated as u_0, while inside the crater it varies and is designated as u. The metal melts along the *ABO* line under the

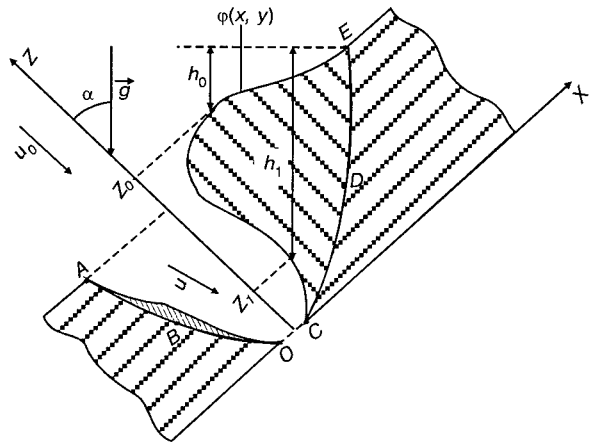

Figure 1. Schematic of the weld pool in its upper position with an inclination angle of $\alpha = 45°$

effect of the high-temperature gas flow and is transferred over the crater walls to the tailing portion of the weld pool to form a droplet with the surface described by a certain function of $Z = \varphi(x, y)$. The point on the droplet surface in the gravitation force field can be characterized by level h with respect to the highest point on the liquid surface. In particular, this level is a function of the weld pool inclination angle α.

While moving deep into the weld pool, the gas changes its thermodynamic and kinetic parameters under conditions of heat exchange with the metal, causes the melt to accelerate and imparts to it the kinetic energy sufficient to transfer the molten metal to the tailing portion of the weld pool. Upon passing through the crater, the gas goes out through a hole of through penetration (Figure 1) with the OC size.

Based on the fact that welding is performed in the mode of through penetration, it can be assumed that density of the gas is constant $\rho_g(z) = \rho_g = \text{const}$. Then, at a constant volume rate of the gas flow, G, and constant density, an additional equation can be easily derived from the equation of continuity to calculate the cross section area of the gas channel, F:

$$\frac{dG}{G} = \frac{d\rho}{\rho} = -\frac{dF}{F} - \frac{du}{u} = 0; \quad \frac{dF}{F} = -\frac{du}{u}.$$

Assuming the gas and liquid to be ideal and incompressible, their flow can be described by the gas heat content equation and the generalized Bernoulli's equation. After transformation of the equations, it was concluded that the gas channel of the penetration zone of the weld pool at constant values of the gas flow rate and density works simultaneously in four modes of the nozzle associated with internal effects (geometrical, thermal, mechanical and friction).

[8] gives an analytical expression of the thermal nozzle. The energy balance equation in its final form is as follows:

$$-\rho_g\left[c_p(T - T_0) + \frac{u^2 - u_0^2}{2}\right] \rho_l g(h - h_0) = \quad (4)$$
$$= \sigma(K_x + K_y - K_{x0} - K_{y0}).$$

Solution of the system of equations obtained in [8] yielded determination of u, T and P as functions of coordinate z and finding a function of $Z = \varphi(x, y)$ of the melt surface shape.

The energy balance equation (4) in a dimensionless form is as follows:

$$\frac{1}{\text{Ec}}\overline{\Delta T} - \frac{1}{2}(\bar{u}^2 - 1) + \frac{1}{\text{Ar}}(\bar{h} - h_0) = \quad (5)$$
$$= \frac{1}{\text{We}}(\overline{K}_x + \overline{K}_y - \overline{K}_{x0} - \overline{K}_{y0}),$$

where the dimensionless values are written with an overscribed bar; $\text{Ec} = u_0^2/c_p \Delta T_0$ is the Ekkert number; $\text{Ar} = \rho_g u_0^2/\rho_l g \delta$ is the Archemedes number and $\text{We} = \rho_g \delta u_0^2/\sigma$ is the Weber number.

Equation (5) contains four terms. The first and second terms are of auxiliary character, as compared with the third and fourth terms. This can have the following explanation. In welding with non-through penetration, the gas flow changes its direction to the opposite, but before it decelerates. A decrease in the rate is accompanied by growth of the static pressure and temperature. This leads, firstly, to an increase in the intensity of phase transition of the metal from the liquid to gaseous state, secondly, to excess of the thermal energy of the gas–liquid mixture at the interface over the energy of the surface forces and, thirdly, to local stabilization of the interface in the lower portion of the weld pool in the form of a gas cavity in the bulk of the weld, which is described in [9].

In the case under consideration the surface tension coefficient is also susceptible to changes, and approximation (3) of equation (2) is unacceptable. For welding with through penetration, based on an insignificant variation in enthalpy, equation (5) takes the following form:

$$\frac{1}{\text{Ar}}(\bar{h} - \bar{h}_0) = \frac{1}{\text{We}}(\overline{K}_x + \overline{K}_y - \overline{K}_{x0} - \overline{K}_{y0}), \quad (6)$$

which is acceptable for the welding processes which are close to the isothermal ones. In this case the Ar and We numbers are of primary importance. Consider now stability of the weld pool from this point of view.

As it is known from the theory of stability [10], destabilization of a droplet in the gas flow occurs at $\text{We} \geq 2\pi$ and $\text{Bo} = \rho_l g \delta^2/\sigma \geq 4\pi^2$. Therefore, based on reverse conditions and equation (6), it will hold

$$\text{We} < 2\pi; \quad \text{Bo} < 4\pi^2; \quad \text{Ar} > 1/2\pi, \quad (7)$$

where Bo is the Boltzmann number.

Figure 2 shows regions of stability of the molten metal of the weld pool corresponding to inequalities (7). It can be seen that stability is provided by certain relationships between inertia forces of gas, gravitation and surface forces. The inertia forces of the gas should be higher than the gravitation forces in the liquid, but should not exceed capillary forces.The optimal thickness of the metal, δ_d, comparable with size of a droplet in the weld pool is found from the condition of equality of three components of the process:

$$\delta_d = 2\pi \sqrt{\frac{\sigma}{\rho_l g}}. \quad (8)$$

For example, for steel with $\delta_d \sim 0.02$ m, the characteristic rate of the gas flow in this case should be $u_0 \sim 120$ m/s for argon. Note that relationship (8) determines the length of a capillary-gravitation wave on the surface of the liquid, at which its propagation velocity is minimum. It should be noted that in inequality (7) the Bo number was estimated at a value of acceleration g, with which in the case of a stable mode the interface should move toward the liquid phase.

For the weld pool to be stable, in addition to meeting conditions (7), it is also required that disturbance exceeding some critical value last shorter than time τ_*, during which its amplitude grows to a value comparable with size of the droplet. τ_* is usually assumed to be as follows:

$$\tau_* = \frac{\delta}{u_0}\left(\frac{\rho_l}{\rho_g}\right)^{1/2}, \quad (9)$$

which characterizes the rate of growth of the disturbance amplitude caused by the Rayleigh-Taylor instability. The full time of development of the instability, $\tau_0 = \tau_* + \tau_d$, includes also a period of natural oscillations of the droplet, τ_d, which can be estimated from the following formula:

$$\tau_d = \frac{1}{6}\sqrt{\frac{\pi \rho_l \delta^3}{\sigma}}. \quad (10)$$

Analysis of the experimental data [10] and comparing them with calculations using equations (9) and (10) allow a conclusion on orders of magnitudes of the time of beginning of the instability, τ_0, and the time of induction, τ_*. In the instability mode determined mainly from the We number (vibratory mode), the experimental and theoretical estimates are close and yield relationship $\tau_0/\tau_* \sim 2-3$.

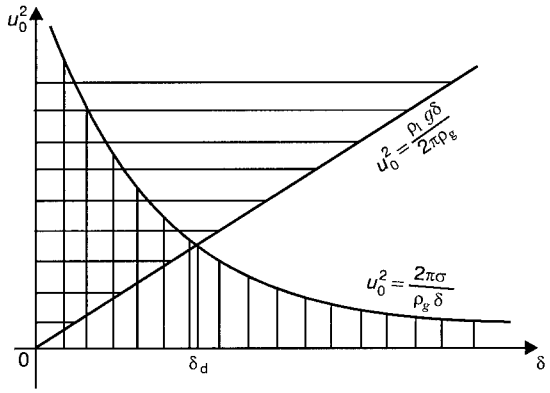

Figure 2. Regions of stability in accordance with inequalities (7)

REFERENCES

1. (1974) *Technology of electric fusion welding of metals and alloys*. Ed. by B.E. Paton. Moscow: Mashinostroyeniye.
2. (1978) *Welding in machine building*. Refer. Book. Ed. by A.I. Akulov. Moscow: Mashinostroyeniye.
3. (1991) *Welding and weldable materials*. Ed. by V.N. Volchenko. Moscow: Mashinostroyeniye.
4. Sheleg, V.K., Ragunovich, S.P., Denisov, L.S. (1998) Decreasing heat input is a way of increase efficiency and quality of welding processes in the 21st century. In: *Proc. of Int. Conf. on Welding and Related Technologies for the 21st century*. Kyiv: PWI.
5. Ragunovich, S.P. (1998) Welding using the low-amperage constricted arc under forced conditions. In: *Republican Interdepartmental Transactions*. Minsk.
6. Paton, B.E. (1998) Advances of welding at the transition of the centuries. In: *Proc. of Int. Conf. on Welding and Related Technologies for the 21st century*. Kyiv: PWI.
7. Landau, L.D., Lifshyts, E.M. (1988) *Hydrodynamics*. Moscow: Nauka.
8. Ragunovich, S.P., Tsyganov, V.A. (1999) Investigation of stability of the weld pool in arc welding. In: *2nd Int. Assembly on Machine Building'99*, Sofia, Bulgaria, Sept. 16 – 18, 1999. Sofia.
9. Tsyganov, V.A., Ragunovich, S.P., Andrushkevich, A.A. (1998) The problem of criterial investigation of stability of the weld pool. In: *Republican Interdepartmental Transactions*. Minsk.
10. Nigmatulin, R.I. (1987) *Dynamics of multiple-phase environments*. Moscow: Nauka.

STRUCTURE AND PROPERTIES OF E911 STEEL WELDED JOINTS

H. CERJAK and **E. LETOFSKY**
Technical University, Graz, Austria

ABSTRACT

Weldability and creep rupture strength of a new low-carbon chromium steel of the ferritic class at elevated temperatures were investigated. Compared to the known P91 steel, the new steel is further alloyed with tungsten. Investigations demonstrated that E911 steel is not inferior to P91 steel in weldability, while the creep rupture values of E911 steel welded joint are higher than those of P91 welded joint.

Key words: *ferritic stainless steels, E911 steel, weldability, creep strength, microstructure.*

Chromium low-carbon steels of ferritic class (9 to 12 % Cr) developed more than 40 years ago, are characterised by a high creep resistance at the temperatures up to 600 °C and higher. Due to higher thermal conductivity, low coefficient of thermal expansion, and high resistance to thermal shock, these steels offer certain advantages over austenitic steels [1, 2].

In 1975 a new modified grade of 9 % Cr steel has been developed in the US under the leadership of ORNL. In ASTM A335 standard it is designated as P91 (German designation is X10CrMoVNb9.1). Further work was performed to develop steels with a higher creep resistance, compared to the P91 steel. Within the framework of the European COST 501 programme — «Development of Materials for Advanced Steam Cycles» — a new tungsten-modified chromium E911 steel was developed designed for advanced fossil-fired power plants.

For acceptance in practice, investigation of weldability of the newly developed steels and their long-time behaviour are very important aspects. Paper [3] gives the data on creep resistance at different temperatures for samples of P91 steel and samples cut out of this steel welded joint across the weld (Figure 1). It can be observed that the welded samples failed in the HAZ at lower stresses than those of the base metal (P91 steel).

The goal of this study was characterisation of weldability of E911 steel, determination of creep rupture strength (creep resistance) of individual HAZ metal zones and detection of weak zones in the welded joints, as well as comparison of the main properties of the above steel with those of P91 steel.

Production of welded samples. Pipes of E911 steel with 336 mm outside diameter and 62 mm wall thickness, manufactured by Mannesmann Rohrenwerke Plant were used for investigations. Two welding processes were applied, namely submerged-arc welding (SAW) and shielded metal-arc welding (SMAW). Pre-tests of welding consumables of different manufacturers demonstrated that only the consumables of Bohler-Thyssen Welding company led to good impact toughness of the sample metal for both welding processes. Chemical analysis of E911 steel and weld metal is given in Table 1.

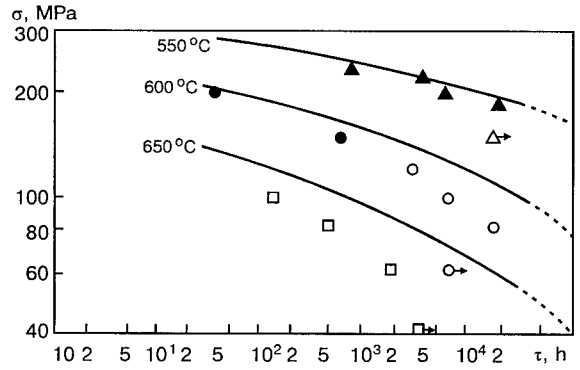

Figure 1. Creep rupture strength of P91 base material and cross-weld sample [3]: solid line — P91 base material; ●, ▲ — fracture in the base metal; ○, □ — fracture in the HAZ

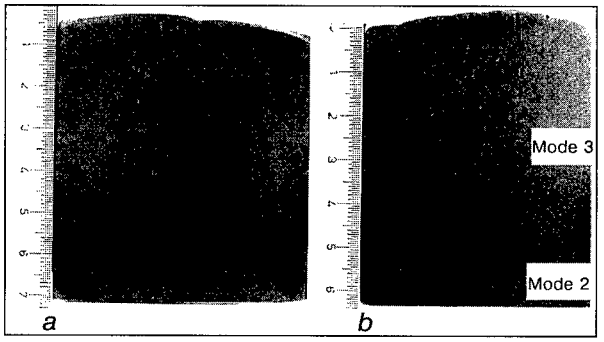

Figure 2. Macrostructure of the weld cross-section: *a* — SAW; *b* — SMAW

Table 1. Chemical composition of E911 steel and deposited weld metal

Material	Weight fraction, %									
	C	*Si*	*Mn*	*Cr*	*Ni*	*Mo*	*W*	*V*	*Nb*	*N*
E911	0.110	0.18	0.40	8.61	0.21	0.92	0.99	0.19	0.089	0.065
MTS 911	0.092	0.34	0.65	9.20	0.78	0.91	0.84	0.22	0.045	0.041
MTS 911/Marathon 543	0.089	0.29	0.51	8.69	0.73	0.90	1.25	0.20	0.030	0.051

The influence of heat input and welding process on the HAZ metal properties was studied in the following modes:

1. Downhand SAW with the heat input of 13 kJ/cm; Thermanit MTS 911 welding wire; Marathon 543 flux; welding current of 350 – 370 A; voltage of 29 – 30 V; welding speed of 50 cm/min.

2. Vertical SMAW with the heat input of 40 kJ/cm; Thermanit MTS 911 welding wire; welding current of 110 – 130 A; voltage of 25 – 28 V; welding speed of 3 cm/min.

3. Downhand SMAW with the heat input of 9.5 kJ/cm; Thermanit MTS 911 welding wire; welding current of 150 – 160 A; voltage of 27 – 30 V; welding speed of 25 cm/min.

Figure 2 is the macrostructure of the cross-section of samples welded by the above processes. The first sample was produced by SAW in mode 1. Half of the thickness of the second sample was welded by SMAW in mode 2 and the second half in mode 3.

Thermocouples were placed in the samples at different distances from the weld, which were used to record the thermal cycles during welding for further simulation of heating and cooling of the metal of the weld and the HAZ. To make the welding process similar to the regular workshop conditions, welding was interrupted over the weekend without maintaining pre-heat of the item being welded. After welding the welded samples were allowed to cool naturally to ambient temperature prior to post-weld heat treatment at the temperature of (770 ± 10) °C with 2 hours holding time.

Heat-affected zone simulation. Depending on the initial condition, different microstructures appear in the HAZ metal, showing different properties [4]. Simulation of weld thermal cycles is the most powerful method for investigation of the regularities of phase and structural transformations in the HAZ metal. Compared to investigation of the metal structures in real welded joints, simulation permits avoiding the errors caused by random factors.

Gleeble 1500 machine was used for simulation. The weld thermal cycles which are needed as input for the simulation process were calculated from Rosenthal's solution of Fourier's heat conduction equation in a simplified version derived by N.N. Rykalin [5]. The following characteristics were used for calculations: cooling time in the temperature range between 800 and 500 °C — $t_{8/5}$; peak heating temperature T_p, preheat temperature T_{pr}, and plate thickness δ.

Based on measurements during the welding process, weld thermal cycles were calculated for SAW process with a heat input of 13 kJ/cm and T_{pr} = 200 °C, and for manual SMAW process at q = 9.5 kJ/cm and T_{pr} = 180 °C. Cooling time $t_{8/5}$ in the first case was 12.19 s and 7.55 s in the second case. Single weld thermal cycles, with peak heating temperatures ranging from 700 to 1300 °C were simulated, with cooling times $t_{8/5}$ between 6 and 160 s. Standard post-weld heat treatment

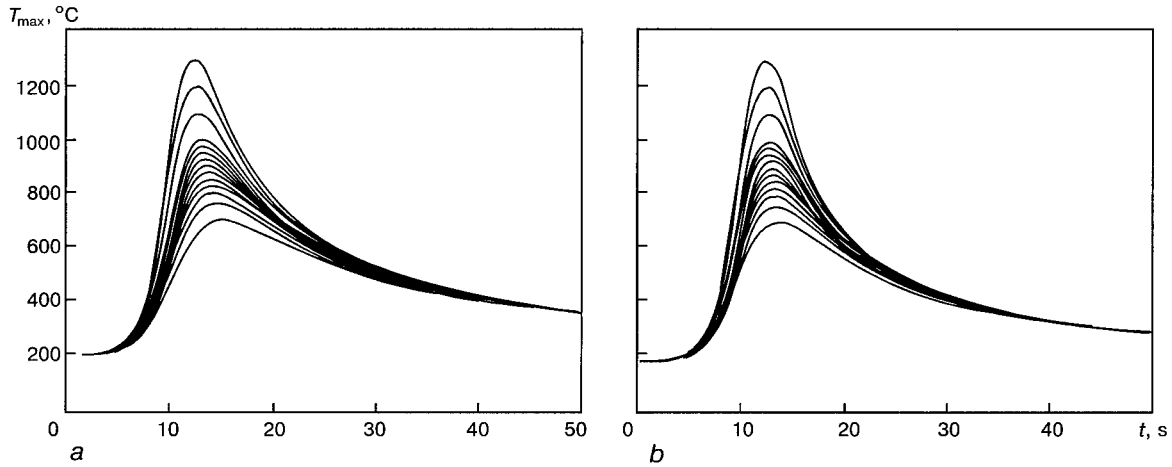

Figure 3. Thermal cycles calculated for various peak temperatures T_{max} (700 – 1300 °C) for both investigated welding processes; *a* — SAW (q = 13.0 kJ/cm; T_{pr} = 200 °C; $t_{8/5}$ = 12.19 s; δ = 62 mm); *b* — SMAW (q = 9.5 kJ/cm; T_{pr} = 180 °C; $t_{8/5}$ = = 7.55 s; δ = 62 mm)

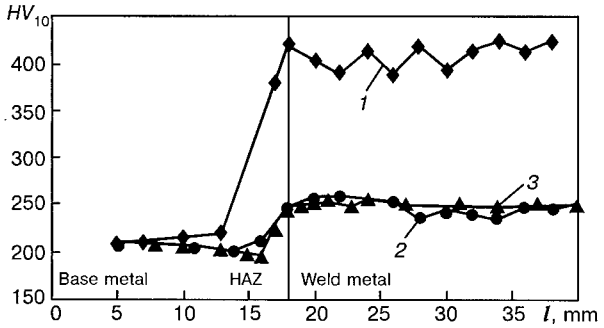

Figure 4. HV_{10} hardness of the weld and the transition zone of P91 [1] and E911 steel joints: *1* — as-welded P91 steel; *2* — same, after heat treatment (750 °C, 2 h); *3* — E911 steel after welding and heat treatment (760 °C, 2 h)

was performed at 760 °C for 2 hours. Multipass welding was also simulated by applying double thermal cycles, namely the first with a peak temperature of 1300 °C, cooling to 250 °C and then a second thermal cycle up to 900 °C.

Investigation of the properties of the actual and simulated HAZ. Standard tests of E911 steel welded joints were performed. Their creep rupture strength was also studied. The proposed model was verified by studying the influence of peak welding temperature T_p; heat input characterised by cooling time $t_{8/5}$; multipass welding (double thermal cycles); applied welding processes on the hardness, toughness, structure, and creep rupture strength of HAZ metal.

Results of standard testing of welded joints. Visual examination, ultrasonic and liquid penetrant testing of welds showed no recordable indications. All welded samples passed the side bend tests reaching 180° bending angle; only in SAW weld metal small pores were detected, which, however, did not cause any cracking. Transverse tensile tests of cross-weld samples were conducted. The ultimate strength of the samples welded by the first variant of technology was 669/671, by the second variant — 671/671, by the third — 677/677 N/mm^2. All the samples failed in the base metal. The results of ISO V-impact tests of welded samples are given in Table 2.

Table 2. ISO V-impact toughness tests of welded samples (mean values)

Welding process	*Heat input, kJ/cm*	*Impact toughness, J, at T, °C*		
		20	*50*	*80*
Submerged-arc welding	13.0	63	89	121
Shielded metal-arc welding	9.5	49	76	87
Shielded metal-arc welding	40.0	69	114	111

Hardness measurement yielded the following results: for base metal HV_{10} 200 – 216; for HAZ HV_{10} 211 – 220 (first and second variant); for HAZ in the root weld area HV_{10} 230 – 240; for weld metal HV_{10} 230 – 240 (for all welding processes).

All the above tests fulfilled the applicable standard requirements for E911 steel welded joints.

Experience showed that the weldability of E911 steel practically does not differ from that of P91 pipe steel. Long interruptions of welding and preheat, and sample temperature lowering to room temperature prior to post-weld heat treatment showed no detrimental effects on the welded joint quality. All this is highly important in fabrication of welded structures of E911 steel under workshop conditions and is one of its greatest advantages compared to X20CrMoV12.1 pipe steel.

Hardness. In hardness testing of P91 steel welded joints it was noted that the HAZ metal develops a soft zone after post-weld heat treatment. The metal hardness in the zone is by approximately HV_{10} 20 lower than that of the base metal (Figure 4). The hardness profile of the metal of the zones of E911 steel welded joint is similar to that of P91 steel (Figure 4).

To define the zone in which maximum HAZ softening occurs, simulation data were used, which are given in Figure 3. Simulation was performed for two heat input values. The derived results are presented in Figure 5. The thermal cycles with peak temperatures up to about 875 °C practically do not influence the hardness of E911 steel base metal.

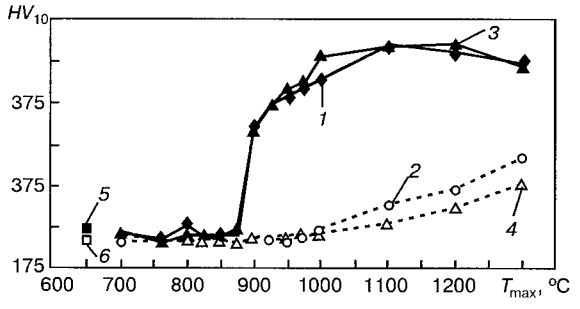

Figure 5. Hardness of E911 steel samples with simulation of thermal cycle of welding and heat treatment: *1* — SMAW; *2* — same, with heat treatment (760 °C, 2 h); *3* — SAW; *4* — same, with heat treatment (760 °C, 2 h); *5* — base metal hardness; *6* — same, with heat treatment (760 °C, 2 h)

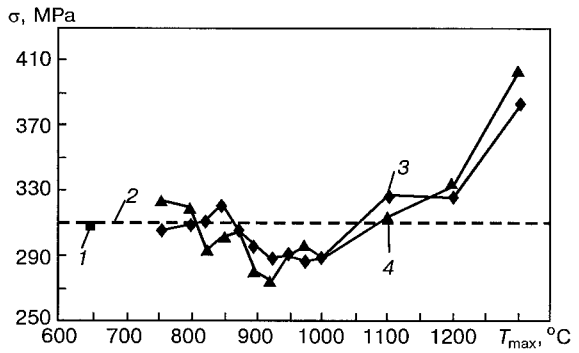

Figure 6. Results of creep tests of E911 steel samples simulating various HAZ zones: *1* — base material; *2* — same, with heat treatment (760 °C, 2 h); *3* — SMAW; *4* — SAW

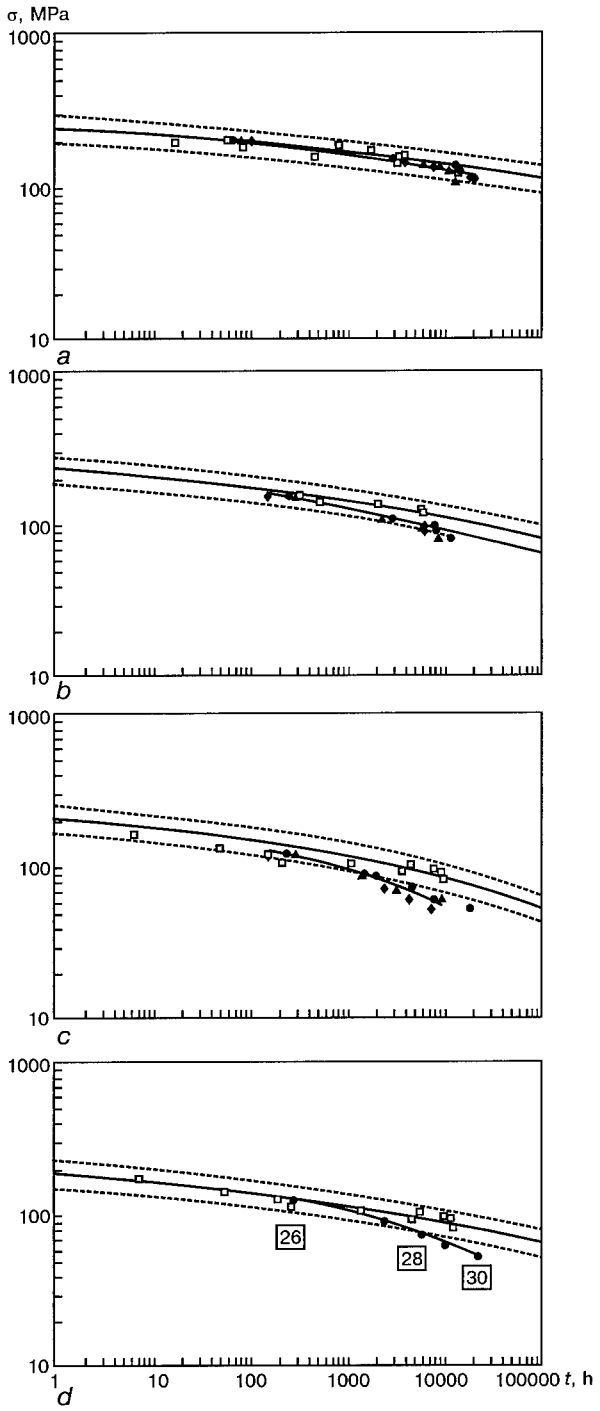

Figure 7. Creep rupture strength of E911 steel welded joint at different temperatures: *a* — 600; *b* — 625; *c* — 650 °C; *d* — same, after 16567 h of testing (points designated by numbers correspond to sample numbers in Figure 8); ❐ — base material; ▲ — SAW with heat treatment (770 °C, 2 h); ● — vertical SMAW with heat treatment (770 °C, 2 h); ◆ — same, in the horizontal position; dashed lines indicate the range of values for the base material; solid lines are for the welded joint

Minimum hardness was observed in the temperature range between 875 and 1000 °C. The hardness in this region is lower by about HV_{10} 10. The beginning of $\alpha \rightarrow \gamma$ transformation as a function of the thermal cycles can be observed by the hardness

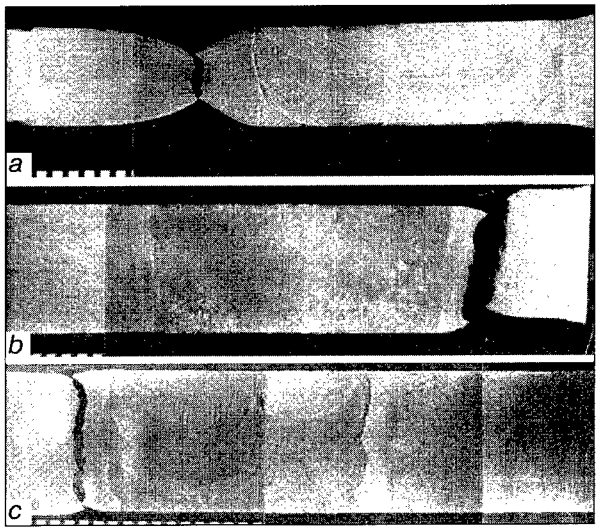

Figure 8. Fracture location in E911 steel samples welded by vertical SMAW process, after creep rupture tests at 650 °C: *a* — sample 26 (σ = 117 MPa; τ = 217); *b* — sample 28 (σ = = 70 MPa; τ = 4295); *c* — sample 30 (σ = 52 MPa; τ = 16567 h)

increase in as-welded condition. After heat treatment the hardening effect disappears.

Creep tests of samples simulating various zones of the HAZ. The purpose of the tests was to investigate the influence of the HAZ metal softening on creep resistance of E911 welded samples after heat treatment (760 °C, 2 h). Testing was performed at 600 °C with a constant strain rate $\varepsilon = 1 \cdot 10^{-5}$ s^{-1}. This test method was first applied on this type of steel in [6].

The results of these tests are shown in Figure 6. Under these conditions the maximum creep rupture value is 310 MPa for the base metal. For heating temperatures in the range of 850 – 1050 °C, the most significant decrease in creep resistance is found, whose minimal value (275 MPa) was recorded at 925 °C.

Creep tests performed on E911 steel welded samples at 600 °C have reached 20000 h, at 625 °C — 11000 h and at 650 °C — 16500 h duration time so far. The results of these experiments and E911 base metal tests are presented in Figure 7. Depending on testing temperature and stress, there is a tendency for the fracture location to shift from the base metal towards the soft zone in the HAZ. In the SAW samples the fracture is located in the weld, in which pores were detected as mentioned above.

The data of creep tests of the samples at 650 °C with testing time of 16567 h is shown in Figure 8, *c*. At high stress levels the fracture is located in

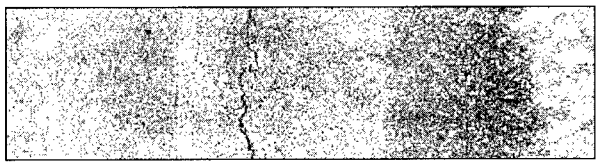

Figure 9. Macrostructure of the cross-section of sample 28 (left side)

the base metal (Figure 8, *a*). As the applied stress decreases, the fracture location shifts into the HAZ (Figure 8, *b, c*). Study of the microstructure of the sample given in Figure 8, *b*, showed (Figure 9) micropores and cracks in the HAZ zone (left side of the sample in Figure 8 , *b*) heated in the range of A_{c1} to A_{c3} temperatures.

Energy-Filtering Transmission Electron Microscopy (EFTEM). The EFTEM method [7] allows identifying different precipitates in the metal of the weld and the HAZ. Samples cut out of a welded joint of cast G-X12 steel similar to E911, were used for electron microscopy investigations. The weld metal structure is similar to that of the base material. The soft zone in the HAZ shows in the post-weld heat treated condition an annealed martensitic structure. After short testing times Laves phase developed in the weld and the soft zone of the HAZ, and after 12000 h duration time the appearance of a new so-called modified *Z*-phase was recorded [8]. With longer duration times a coarsening and coagulation of the Laves and *Z*-phases could be observed. Precipitates of chromium and vanadium carbides of $M_{23}C_6$ and MC type, respectively, which were also detected, did not coarsen. Appearance of the Cr- and V-rich *Z*-phase was accompanied by a decrease of carbide content. Creep resistance decrease with long duration of testing (> 10000 h) is probably due to the observed microstructural changes.

Similar electron microscopy investigations of E911 steel welded joints are now in progress. It is anticipated that they will demonstrate the same nature of microstructural changes in creep rupture tests.

In conclusion it should be noted that the new chromium E911 steel additionally alloyed with tungsten, has satisfactory weldability compared to the known P91 steel [1, 6], although in the HAZ metal a drop in the creep resistance can be observed.

Depending on testing temperature and stress, there is a tendency of the fracture location shifting. While at high stresses the fracture location was in the base metal, at their lowering it was found in a soft zone of the HAZ. At 600 °C and testing duration of 20000 h, the measured creep rupture values of the welded joint and the base metal were on the same level. At 625 and 650 °C the creep rupture values for the welded joint were below those of E911 base metal by 20 %. However, the drop in creep rupture values in E911 steel welded joints starts at higher temperatures than in P91 steel welded joints.

REFERENCES

1. Bendick, W., Cerjak, H., Niederhoff, K., *et al.* (1992) In: *Proc. of Int. Conf. on Trends in Welding Science and Technology*. ASM.
2. Blum, R., Hald, J., Lund, E. (1991) In: *Proc. of VGB-TB Int. Conf. on Werkstoffe in der Schweisstechnik im Kraftwerk*.
3. Bendick, W., Haarmann, K., Wellnitz, G. *et al.* (1993) Eigenschaften der 9- bis 12-%-Chromstahle und ihr Verhalten unter Zeitstandbeanspruchung. *VGB Kraftwerkstechnik*, **73**, Heft 1.
4. Easterling, K. (1983) Introduction to the physical metallurgy of welding. In: *Butterworths Monographs in Metals*.
5. Rykalin, N.N. (1957) *Berechnung der Waermevorgaenge beim Schweissen*. Berlin: VEB Verlag Technik.
6. Bruehl, F. (1989) *Verhalten des 9%-Chromstahles X10 CrMoVNb 9.1 und seiner Schweissverbindungen im Kurz- und Langzeitversuch.* Doctoral Thesis. Graz: TU-Graz.
7. Warbichler, P., Hofer, F., Hofer, P. *et al.* (1998) On the application of energy-filtering TEM in materials science. *Micron*, **1**, 63 – 72.
8. Strang, A., Vodarek, V. (1996) Z-phase formation in martensitic 12CrMoVNb steel. *Mat. Sci. and Techn.*, **12**, 552 – 556.

PROBLEMS OF CERTIFICATION OF WELDING FABRICATION IN MACHINE-BUILDING BRANCHES OF RUSSIA

V.V. SMIRNOV and **O.A.TSUKUROV**
Institute of Welding, St.-Petersburg, Russia

ABSTRACT

The state-of-the-art in certification of welding fabrication in the machine-building industry branches of Russia is analyzed and evaluated. The ways of an integrated solution of problems existing in the field of certification are suggested.

Key words: *production quality, certification (production, products, quality systems), certification systems, quality, special processes.*

During the period of formation of the market relations in Russia, the improvement of the quality of products, including weldments, is of a special importance, thus promoting the more complete meeting the customer requirements, the growth of the national resources, and also a successful competition of the Russian manufacturers at the domestic and international markets.

The production quality means the presence of certificates of conformity of products to the established functional requirements and/or standards of safety, as well as certificates for the quality system (QS) or fabrication facility, registered in the authorized systems of certification, for example, in the System of GOST R, at the customer's disposal.

At present, more than 1000 bodies (centers) on certification are accredited in the System of certification GOST R, including 46 bodies on QS certification, more than 2000 test centers and laboratories, about 100 system of a voluntary certification, 15 systems of a mandatory certification and more than 40 systems of certification of similar products and services [1 – 3].

Most manufacturers of different branches of a machine-building complex certify their products either in specialized industry systems of certification, or in systems of certification of groups of similar products, or in accordance with rules or procedures of certification of definite kinds of the products.

However, there are no systems and rules until now to certify the welding fabrication items, which do not belong to a potentially dangerous nomenclature. This led to the fact that the works on certification of welded structures are accomplished by non-specialized bodies and not taking into account the specifics of the technology of welding according to the rules (programs), which are not regulated at the all-system level within the scope of the System of certification GOST R. In addition, in the Register of personnel of Gosstandart the training and attestation of experts on certification of the products and QS of the welding fabrications are not organized properly. Therefore, the certification is often made by experts of other specialty with inviting consultants in the field of welding.

The absence of the system, rules and procedure, and also experts of the required specialization is especially negative in certification of products according to the schemes which envisage the assessment of status of the production system or its separate elements (analysis of status of production, certification of production or certification of the QS of the enterprise).

Certified and constantly improving QS of the enterprise or a certified production are the main guarantee of the stability of the product quality and serve an important confirmation of the competitiveness of the enterprise, an element of the industrial efficiency and a basis of the stable export of the products.

The QS on the basis of international standards (IS) ISO series 9000 found the widest application in the industrialized countries of the world.

The Gosstandart of Russia has accepted ISO standards, which define the requirements to the models of the quality assurance (ISO 9001, ISO 9002 and ISO 9003), as the national standards.

Russian standards GOST R ISO 9001, ISO 9002 and ISO 9003, harmonized with the international standards, regulate, by the idea of the developers, requirements to the models of QS of the enterprises, not depending on a definite branch of the industry, a sector of production and the products. However, these standards cannot be used to a full extent for the development and next certification of the QS

of the enterprises which have special technological processes, including welding [4]. This is due to an imperfection of the standard base of the Russian system of certification with respect to welding processes (fabrication). There are no groups of standards similar to IS ISO 3834 (1 – 4) or European EN 729 (1 – 4) in the System of certification GOST R, which define the requirements to the QS in welding fabrication and used in the international practice in combination with IS ISO 9001, ISO 9002 or individually [5]. The same concerns the IS which regulate the additional requirements to the personnel qualification, attestation of welding technology, some types of inspection of welding, supervising and inspection personnel and also to the tests of the technological equipment [6, 7].

As a result it is difficult to create a comprehensive model of QS of enterprise or a scheme of certification for the welding fabrication which will correspond to the international criteria using the existing domestic standardizing base.

Therefore, audit and assessment of the status of elements of the production system during certification of the welding products remain only intentions for the welding fabrication in spite of their great importance.

To solve this problem, the Technical Committee on standardization «Welding and Related Processes» TK-364 of Gosstandart of Russia has a proposal to discuss the problem about the need in the development of an individual integral System of a voluntary certification in the welding industry as a constituent part (subsystem) of the System of certification GOST R. The proposed system should meet the requirements of Laws of Russian Federation «About the protection of rights of consumers», «About standardization», «About certification of products and services», standard-legal acts in the field of certification, basic documents of the System of certification GOST R, and also specifics of welding technologies, products and requirements of international documents (instructions, standards, manuals, etc.) of the quality assurance of welding fabrication products.

Taking into account the domestic and foreign experience in the creation of systems of certification of groups of similar products and also the practical aspects of development and certification of the QS for the conformity to the Russian standards of GOST R ISO 9001, ISO 9002, IS ISO 3834 (1 – 4) the accreditation field of the suggested system should cover in a general form two basic and interrelated trends:

certification of groups of similar products of the welding fabrication for the conformity to the requirements of domestic standards;

certification of production system or its separate elements, production QS (including the analysis of status of production), and also the welding and inspection personnel.

Certification of groups of similar products of welding industry (welded structures). The rules of certification of products in the System of GOST R are established in a general form by a document «Procedure of certification of products in Russian Federation» (with Amendment N.1; registration number 1139), and also rules (procedures) of certification of similar products [8 – 10].

However, to certify the welded structures it is rational to make the rules more precise taking into account the specifics of the welding fabrication and the types of similar products characterized by definite common features.

As is known, the welding products possess the following peculiar features:

variety of nomenclature, groups and types;

different series production systems (from single and small production to mass production);

manufacture of products by the enterprises of different branches of the machine-building with different technical level of manufacture;

high requirements to the quality of welded joints and, as a consequence, the need in high skill of the welding and inspection personnel, as also in certified technological processes of welding, technological and test equipment.

Taking into account the above-mentioned features of the welded structures it is rational to work out several rules (procedures) of certification for each definite group of the similar products. These rules and the group of participants in certification will become a basis of the developing system of certification of a group of similar products of the welding industry.

The rules of certification of groups of similar products include:

purpose and field of their application;

list of the quality characteristics which provide the functional purpose of the product and its safety;

list of standardized documentation used in certification and test methods;

schemes of certification used in the system;

description of the structure of the system of certification of similar products;

procedure of conductance of works for certification of products in the system;

procedure of inspection of certified products, consideration of appeals, rules of storage and registration of certificates, etc.

Formation of systems of certification of groups of similar products is made taking into account the following:

presence of similar international system;

common character of the production method and fields of application of products;

common character of requirements to the products;

common character of methods of examination and testing;

common character of the field of spreading the standardized documentation.

In the system of certification of groups of similar products it is necessary to define the nomenclature of products subjected to the certification by referring to the codes of a classifier of products or a nomenclature of goods of foreign activity and also by indication of corresponding standards and documents suitable for them.

The quantity of rules (procedures) in the system of certification of the single products is determined usually both by a quantity of the group of the similar products proper and by the variety of schemes of certification of the products oriented to the inspection of the status of the production in several directions, requirements of standards ISO to welding concerning the attestation of the technology, equipment and personnel, requirements of standards of GOST and ISO to the test laboratories and bodies on certification.

In our case they are:

general rules of conductance of works on certification in the system of certification of similar products of the welding industry;

rules of certification of definite types of welded structures;

procedure of analyzing the status of welding fabrication;

typical programs of analyzing the status of welding fabrication;

procedure of conductance of works on certification of welding fabrication;

procedure of conductance of works on certification of QS of welding fabrication;

rules of certification of welding consumables;

rules of certification of welding equipment and auxiliaries;

procedure of attestation of personnel of welding industry;

procedure of testing welded structures;

procedure of inspection of bodies of certification;

procedure of inspection of certified products, QS, fabrication, personnel, etc.

Certification of a production system. During certification of products by a body of the certification, the production system is subjected to audit in one of three directions to assess the conditions for assurance of stable output of products with preset requirements [10, 11]: analysis of production status; production certification and certification of the QS of the enterprise.

To understand the place of the welding fabrication in audit and assessment of the production system, we shall describe each of the directions in detail.

Analysis of the production status. This analysis is used to confirm the presence of the necessary conditions for assurance of conformity of the output products to the established requirements.

The production status is evaluated by experts of the bodies of certification in accordance with recommendations on certification R50.3.004–99 «System of certification GOST R. Analysis of the production status in certification of products».

Recommendations contain the procedures of certification, rules for taking decisions and formulation of work results obtained from the analysis of the production status during mandatory and voluntary certification of products.

Scope and composition of all the audits during the analysis of the production status correspond partially to the requirements of 2 from 20 elements of the QS model according to GOST R ISO 9001, ISO 9002, namely: control of processes, inspection and testing.

The analysis of the production status is used in a domestic practice of certification of the products only due to the fact that the majority of enterprises are not yet ready to the creation and certification of the QS for conformity to the requirements of GOST R ISO 9001, ISO 9002.

However, in creation of the certification system in the welding fabrication it is rational to preserve the procedures of audit and assessment of the production status, adding them with requirements to the personnel qualification and also to the attestation of the welding technology and equipment.

Certification of production. This certification is aimed at the evaluation of its conformity to the requirements of the QS elements, which guarantee the stability of the quality characteristics and safety of the products inspected during certification.

The works on certification and inspection are performed in accordance with the requirements of standards of GOST R 40.004–96 «System of certification GOST R. Register of the quality systems. Procedure of conductance of production certification», GOST R 40.005–96 «System of certification GOST R. Register of quality systems. Inspection of quality and production systems», PR 50.3.001.

Certification is performed by the body on certification of production or the QS in cases when the certification of products is made by the scheme 5 (in accordance with certification ISO) and when there is no QS at the enterprise or when the manufacturer requires the certificate of production without certification of the products.

During certification of production, 10 from 20 elements of the QS model according to GOST R ISO 9001, ISO 9002 are checked. This provides a larger range of true data about the conditions of production than during the production status analyzing.

Only the experts on certification of productions or QS are admitted for the production certification.

After completion of the certification the Technical Center of Register of QS (TC RQS) issues the certificate to the enterprise about the conformity of production on the basis of an act of the commission of experts.

In foreign practice there are no schemes of certification of products using the certification of production, no analysis of the production status, because all the guarantees of stability of the production system are provided only by the certification of the QS. And, therefore, the certificate of production is not valid for the foreign partners as a document which guarantees the quality of products.

In certification of production as well as in certification of the QS of the enterprise, the scope and composition of audit by the element of «control of processes» (unlike the analysis of the production status) correspond completely to the element 4.9 of GOST R ISO 9001, ISO 9002 and contain requirements to «special processes», including welding.

However, to develop the required technical documentation for the mentioned element of the QS of welding fabrication (procedures of attestation of welding technology and personnel, method of technology testing, working instructions, etc.) is very difficult at present due to imperfection of the domestic standardizing base.

Certification of the quality systems. Certification of the QS is organized and carried out to convince consumers of products, management of enterprises-manufacturers and other interested parties of a feasibility of a manufacturer to provide consumers with products which correspond to the established requirements [12].

The certification of the QS is an action of third party which proves that the QS identified in appropriate way corresponds to a selected model of system of the quality assurance according to GOST R ISO 9001, ISO 9002 or another standardizing documents defined by an applicant [13].

It is evident that, first, the QS of the enterprises for the conformity to requirements of the definite standardized documents should be developed and implemented. And only then, it is possible to perform the certification of this system.

The development of QS in accordance with requirements of standards of GOST R ISO 9001, ISO 9002 and next certification of the functioning system, as a rule, does not encounter great problems if it does not concern the welding fabrication. Usually, the developer of the system has all necessary standard information, which corresponds to standards ISO series 9000, in its disposal and follows their requirements.

In case of development of QS in the system of GOST R for the enterprises dealing with welding, the developers encounter difficulties because of absence of standard documentation in this system, which regulate requirements to the welding processes in the aspect of the quality assurance. Therefore, it is necessary to develop standards for the suggested system of certification, within the scope of which the activity on certification of the welding fabrication QS will be realized. It is necessary to develop standards on which both the creation and subsequent certification of QS taking into account the Russian and international standards will be based. Moreover, the standard GOST R 40.001–95 recommends to establish requirements to QS in the certification system using in this case the IS ISO series 9000 and other international, regional and national documents.

Development of the standardized documentation for the creation and certification of QS in the welding fabrication should be made, in our opinion, in two variants.

According to the first variant it is necessary to develop a number of standards for the existing standards using the model of the quality assurance of GOST R ISO 9001, ISO 9002 for element 4.9. «Control of processes» (chapter «Special processes»). They will regulate both the requirements to the qualification of the welding technology, welding and inspection personnel and also the rules for conductance of their attestation, and also requirements to tests of technological equipment.

On the basis of these standards it would be feasible:

to develop the documented procedures, which will guarantee the conductance of welding processes under the controllable conditions by a qualified personnel and by using the certified technological equipment;

to make current records about the attestation of the qualified personnel, procedures of the process and equipment (record of quality).

Then, the certification of the QS and subsequent inspection can be performed in accordance with the requirements of the existing standards.

Certification should be made only by a body of the QS certification with experts on QS certification. On completion of certification, the certificate of QS conformity to the requirements of one of standards of GOST R ISO 9001, ISO 9002 will be issued to the enterprises on the basis of an act of commission of exports of TC RQS.

According to the second variant (not depending on the realization of the first variant) it is rational to use the basic standards from a complex of existing international standards ISO on assurance of quality in welding by their direct use, giving them status of national (similar to standards of GOST R ISO 9001, ISO 9002, GOST R ISO 14.001, ISO 14.004, ISO 14.010, etc.).

The basic standards of ISO on the quality assurance in welding are as follows:

ISO 3834 (1 – 4) «Quality requirements for welding-fusion welding of metallic materials (1 – 4 parts)»;

ISO 9956 (1 – 13) «Technical requirements and attestation of welding technology (1 – 13 parts)»;

ISO 9606 (1 – 5) «Attestation of welders; fusion welding (1 – 5 parts)»;

ISO 14731 «Supervision of welding jobs. Tasks and responsibility».

This list can be added by IS which are used in the development of elements of the QS according to ISO 3834 (1 – 4): «Analysis of agreement», «Inspection of structures», «Production and test equipment», «Filler materials», «Quality control and other tests», «Reports (records) on quality», etc.

Certification of personnel. At present in Russia there is no system of certification of personnel of enterprises, organizations and institutions in its international meaning, and, moreover, the law of Russian Federation «About certification of products and services» does not mention the certification of the personnel in general [14].

The mandatory certification of authorized persons, specialists and workers to obtain the permission to work was carried out only at the enterprises, organizations and objects, being within the jurisdiction of Gosgortekhnadzor, Gosatomnadzor, Gosstroy of Russian Federation and some other federal bodies.

Attestation has a private character and it is performed according to branch and departmental rules and rates (rather strict) and intended only for workers and specialists who is working at the supervised objects and having a professional education, practical experience in a specialty and, as a rule, high skill.

Similar attestation of the personnel at the objects of an increased danger also exists in the international practice, including that in the field of welding and related processes.

In our case we mean the system of certification of the personnel in the Russian Federation as a constituent part of the National System of certification GOST R (including welding personnel). The need in creation of this system was caused by an objective state of the Russian economy to assure the conformity of the qualitative level of the personnel to the requirements specified by the international markets of labour and also to harmonize the national system of certification with requirements of IS EN series 45000, ISO, IEC.

The certification and recognition (including mutual recognition) of qualification of personnel of the Russian enterprises at the international level would be useful, because at present in Russia the foreign certification of the personnel is not accepted and accreditation of foreign bodies on certification of personnel is not made.

In Russia the works on the creation of the system of certification of the personnel are carried out by the Ministry of labour and social development, as well as by Gosstandart on the instructions of the government of the Russian Federation since 1997 in accordance with the statement of April 29, 1997 No.219 «About the development of system of certification of personnel in the Russian Federation». These works were directly authorized by the Ministry of labour and social development in Russia. The management and coordination of works on attestation and certification of the system experts, as well as the certification of the personnel proper were entrusted to the Register of system of certification of personnel of Gosstandart. At present the system of certification of the personnel is at the stage of its establishment. Thus, in accordance with the order of Gosstandart No.428 of 13.10.1999 an expert commission has been created for the certification of the system experts and the procedure of conductance of works on certification of the experts is developed.

To certify specialists of the welding industry within the scope of the system of the personnel certification it is necessary to develop a number of standardized documents, which will regulate requirements to the qualification of specialists of different levels and to their certification and also to the bodies on certification of welding supervision and inspection personnel.

Realization of politics of Register of Gosstandart and central body of the system as well as certification of the personnel will be carried out in regions by the bodies of certification organized within the scope of the system. One of these bodies can be organized on the base of the Russian-German Educational Center on training and attestation of welders and specialists of the welding industry of the Institute of Welding of Russia.

Organizing of certification system in welding industry. Organizational structure of the certification system in the welding industry is presented in Figure 1.

Structure of the system of certification of similar products of the welding fabrication is given in Figure 2.

The National Body on Certification (Gosstandart of Russia) will realize its activity on the basis of rights, commitments and responsibility envisaged by existing laws of the Russian Federation and, as a Federal Body of an executive power it will realize the preparation and conductance of works on a mandatory and voluntary certification.

The Central Body of the system (CBS) will fulfil its functions in accordance with article 10 of Law of Russian Federation «About certification of products and services» and on the basis of status

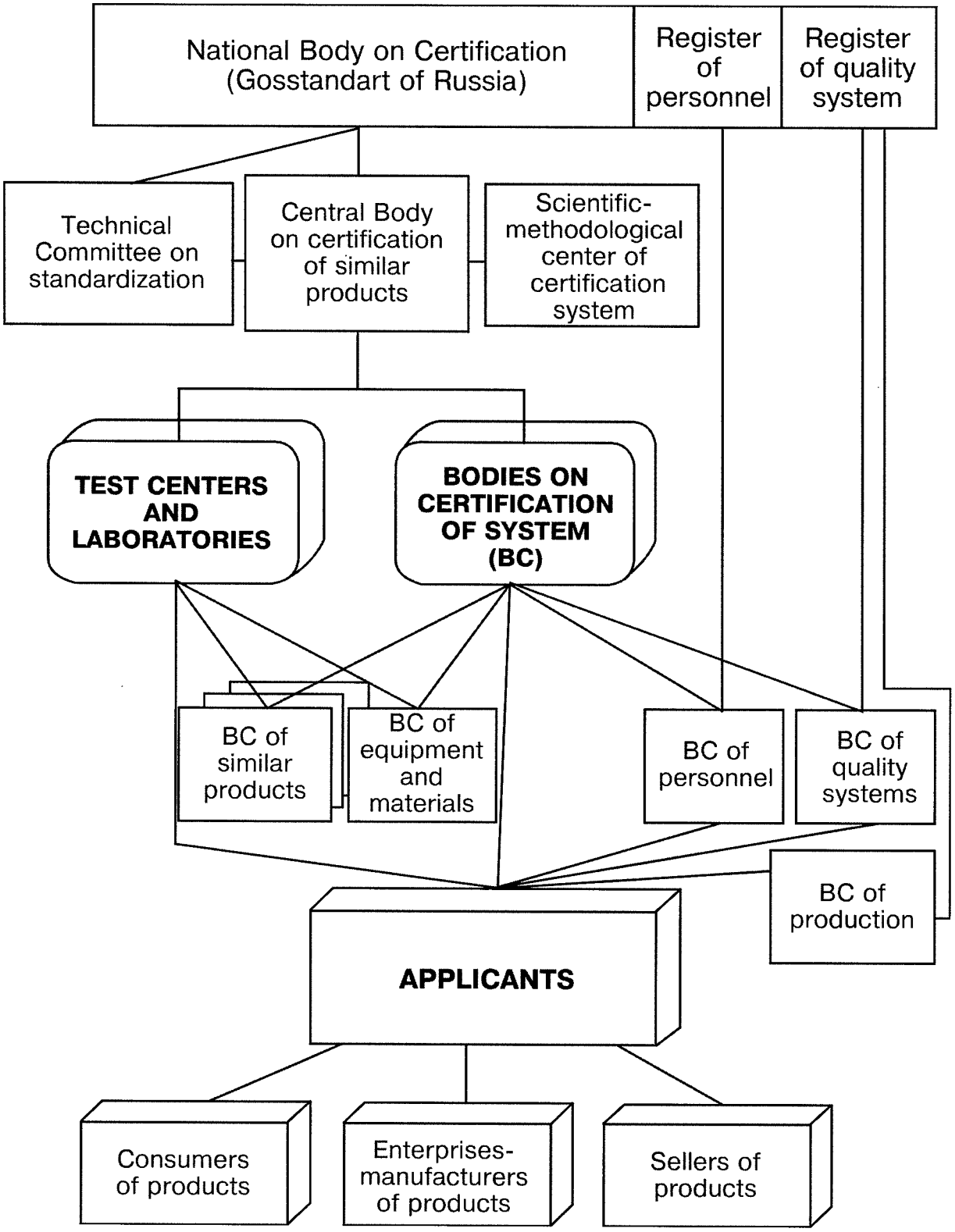

Figure 1. Organizational structure of system of certification of welding fabrication

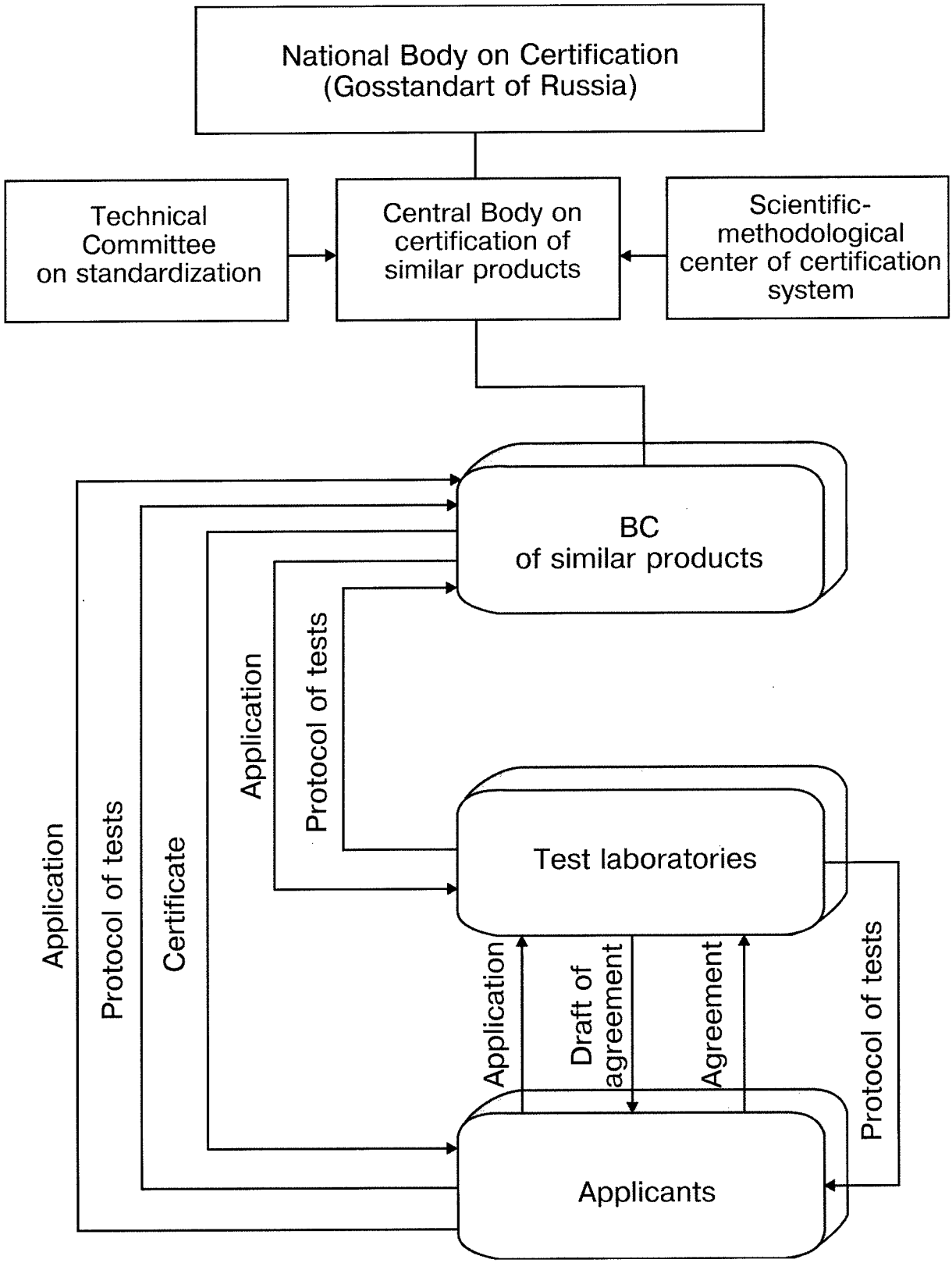

Figure 2. Organizational structure of system of certification of similar products of welding industry

of CBS. The CBS will be accredited by Gosstandart and will have a status of an independent and technically competent body on tests and certification of a wide assortment of products of the Russian and foreign manufacturers.

The functions of the CBS in certification of the QS and fabrication will be fulfilled by TC RQS, while in certification of the personnel these functions will be fulfilled by the Ministry of labour and social development of Russia.

Technical Committee on standardization «Welding and Related Processes» TK-364 will realize, by the proposal of CBS, management and coordination of the development of basic standardized documents of the system of certification in the welding industry.

Scientific-methodological center of the system of certification will realize the development of organizing-methodological documents of the system, render methodical assistance to the participants of the system, collect and analyze information about the results of activity on certification in the system and submit it to the central body.

The requirements to the bodies on certification of products, QS and productions have been established by the GOST R 51000.5–96 «General requirements to the bodies on certification of products and services».

The right for the conductance of works in System of GOST R are given to the accredited bodies on certification and test laboratories (centres), which received the license from Gosstandart of Russia. Functions, fulfilled by bodies on certification and test laboratories (centres), are regulated by the «Rules on conductance of certification in the Russian Federation» [8].

The work in the certification bodies is fulfilled by the specialists with an obligatory participation of experts on certification, who passed attestation in the Register of system of certification of personnel of Gosstandart.

At present, as to the field of welding fabrication, only one body on certification of materials and equipment for welding industry and welded structures is functioning in the System of certification GOST R on the base of the Institute of Welding. It is envisaged for the system of certification being formed to organize the additional body (bodies) on certification of similar products; bodies on certification of QS and productions; bodies on certification of welding and inspection personnel.

Requirements to the test laboratories (centres) are established in GOST R 51.000.3–96 «General requirements to test laboratories». As participants, the system can include the as-attested test laboratories of regional enterprises of the welding industry and also the territorial test laboratories and bodies of certification.

Applicants can be domestic or foreign organizations (enterprises), individual businessmen, who submitted the application for the certification.

It can be concluded that the development of the system of certification in the welding industry is not a simple, but a long organizing-technical process which requires great expenses. The start has been already made by the Technical Committee, Institute of Welding of Russia, and also by some enterprises dealing with welding technologies and which are interested in the manufacture of the competitive products.

REFERENCES

1. Alperin, L.N. (1999) Coordination of works on certification of the quality system in Russia. *Standarty i Kachestvo*, **12**, 56 – 59.
2. Rakhmanov, M.L. (1999) Organizing and standardized-legal assurance of works on certification of quality systems in Russia. *Ibid.*, **4**, 24 – 27.
3. Voronin, G.P. (1998) Solution of problems of quality in Russia is a deed of everyone. *Ibid.*, **10**, 6 – 10.
4. Smirnov, V.V., Tsukurov,. O.A. (1999) Problems of certification of welding fabrication at machine-building enterprises. In: *Collected papers of III Int. Conf. MET–99 on Welding Technologies, Equipment, Consumables, Related Technologies.* Riga.
5. (1994) *ISO 3834 (1 – 4 parts).* Quality requirements for welding-fusion welding of metallic materials.
6. von Hofe, D. (1998) Quality management with EN 729-an Overview (including the link to EN 287/288 and 719). In: *Proc. of Eurojoin.*
7. Tsukurov, O.A., Smirnov, V.V., Lanin, A.A. (1999) System of assurance of quality of welding fabrication in accordance with requirements of International and European standards. In: *Proc. of V Sci.-Tech. Seminar on Fuel-power Complex. Reliability, Life and Safety of Equipment. Materials and Resources-saving Technologies of the XXI century.* St.-Petersburg.
8. (1995) *Rules on conductance of certification in RF.* Moscow: Gosstandart Rosii.
9. (1998) System of certification GOST R. Rules on conductance of voluntary certification of products (works, services) for comformiy to the requirements of State standards. Vestnik Gosstandarta Rossii, 10, 41 – 54.
10. (1995) *Procedure of conductance of certification of products in the Russian Federation.* Moscow: Gosstandart.
11. (1999) *GOST R ROSS RU 0001.01.0001.* Statement about the system of certification. Approv. on 29.04.99.
12. (1996) *GOST R 40.003–96.* System of certification GOST R. Register of quality systems. Approv. on 01.01.96.
13. (1996) *GOST R 40.002–96.* System of certification GOST R. Register of quality systems. Basic statements. Approv. on 01.01.96.
14. Poshivalov, V.V., Churilin, V.S. (1998) About certification of personnel. *Standarty i Kachestvo*, **7**, 82 – 87.

MECHANICAL-CORROSION STRENGTH OF WELDED STRUCTURES

O.I. STEKLOV
Russian I.M. Gubkin State University of Oil and Gas, Moscow, Russia

ABSTRACT

State-of-the-art of the metal stock of welded structures under the conditions of their corrosion and ageing is considered. Specifics of a mechanical-corrosion strength of welded joints and approaches to the calculation of strength at stress corrosion are shown.

Key words: *welded structures, welded joints, mechanical-corrosion strength, electrochemical heterogeneity, residual welding stresses, stress corrosion.*

The mechanical-corrosion strength (MCS) means the resistance of materials and structures to fracture at a combined action of mechanical loads and corrosion-active media, including those with a sorption action at a dominating role of the energy of mechanical loads.

The most part of the large-sized constructions is the welded structures used under conditions of action of ecologically- and corrosion-hazardous technological and natural environments. Statistic processing and analysis of failures of welded structures show that the fracture is initiated mainly in the zone of welded joints and connections.

To evaluate the resistance of welded structures to fracture we have suggested and used the MCS model and algorithm of assessment of resistance of structures to fracture.

The principle of the model is as follows. The resistance R of metal structures to fracture and inverse value (susceptibility to fracture) are determined by three main conditions: material properties M; stress-strain state N and action of environment E, i.e. $R(\tau) \in M + N + E$. These conditions within the technological and service periods of « life cycle» of the structure are changed in time τ.

Depending on the definite conditions, different types of structure fracture are possible in the M–N–E system, i.e. from the mechanical fracture with a high rate of crack propagation to the fracture with relatively low rates in the form of a continuous corrosion. Each of the above conditions is interdependent.

The metal properties are determined from the initial parameters of metal M_i, their changing under the effect of technological treatment ΔM_t in the process of manufacture of structures and in service ΔM_s. Thus, $M(\tau) \in M_i \pm \Delta M_t \pm \Delta M_s$.

The first factor M_i depends on chemical composition of the material, its structure, phase composition, content and distribution of impurities and also on the technological heredity of production (it defines initial resistance of metal to the action of environment and loading under the given conditions); second and third factors depend on the degree of changing this resistance. Technological operations used in the process of structure manufacture (for example, welding) deteriorate the initial properties of the metal due to an additional heterogeneity caused by appearance of different types of non-homogeneity (macro- and microchemical, structural, elastic-plastic state, geometric, physical, electrochemical, etc.). The properties of material ΔM_s are changed greatly under the action of service environment, especially hydrogen-containing and hydrogen-evolving media.

The stress-strain state of the structure is determined by service loads: designed loads N_d, their deviation in service ΔN_s, technological stresses ΔN_t (assembly-erection, deformational, welding, etc.), i.e. $N(\tau) \in N_d \pm \Delta N_t \pm \Delta N_s$.

The stressed state is characterized by a value, sign, scheme rigidity, concentration, gradient, cyclicity of elastic and plastic deformations and stresses of I and II kind (σ_I and σ_{II}), reserve and concentration of a potential energy (W_I, W_{II}) of structure elements and the structure as a whole (for example, gas supply systems are characterized by a high reserve of a potential energy of the I kind).

The effect of service environment is determined by its initial properties E_i (chemical composition, concentration of active ions, pH, presence of impurities), which characterize both the technological media and transported products and also the effect of external factors (climatic conditions, properties of soils, etc.).

The degree of effect of environment depends on a number of the following factors: conditions of contact of medium with a material (temperature, pressure, flow rate, presence of hard particles, etc.) and the quality of protection (inhibition, protective coatings, electrochemical protection), on service changes and violation of design tasks (composition

of inner and external media, technological factors and environmental conditions). Thus, $E(\tau) \in E_i \pm \pm \Delta E_t \pm \Delta E_s$.

The corrosion action is complex, occurring under the definite temperature-time conditions in combination with sorption, erosion and cavitation phenomena. The resistance of metal structures to fracture (serviceability) is determined by a general structural formula

$$R(\tau) \in \begin{cases} M(\tau) \in M_i \pm \Delta M_t \pm M_s, \\ N(\tau) \in N_d \pm \Delta N_t \pm \Delta N_s, \\ E(\tau) \in E_i \pm \Delta E_t \pm \Delta E_s. \end{cases}$$

All kinds of corrosion failures of welded structures are caused practically by a stress corrosion (SC) as the load-carrying structures are used under the conditions of a complex stress-strain state (N_d, ΔN_t, ΔN_s) at the action of static and cyclic loads and also random loading.

Depending on the degree of effect of factors of M–N–E system the corrosion (anode), mechanical (deformational) and sorption (adsorption and absorption) processes are manifested in different degree and, respectively, the different types of corrosion-mechanical fractures are occurred: continuous and local corrosion, intensified by a mechano-chemical effect, cracking with a formation of cracks of an avalanche type under the action of static (corrosion cracking) and cyclic (corrosion fatigue) stresses.

At a complex action of aggressive environments the different mechanisms of stress corrosion fracture (SCF) are possible. Depending on the definite conditions one of the following processes can be decisive (the sequence of records reflects conditionally their importance) and, consequently, the fracture mechanism will be different: corrosion-mechano-sorption (c–m–s); mechano-corrosion-sorption (m–c–s); corrosion-sorption-mechanical (c–s–m); mechano-sorption-corrosion (m–s–c); sorption-mechano-corrosion (s-m-c); sorption-corrosion-mechanical (s–c–m). Effect of each process at different stages of cracking does not remain constant. Three main mechanisms: c–m–s, m–c–s, s–m–c are most practically important.

The stressed state promotes the corrosion process in metal due to the following factors:

increase in internal energy of metal, thus causing decrease in its thermodynamic stability;

violation of continuity and deterioration of protective properties of surface films under the action of deformation;

increase in degree of heterogeneity due to appearance of crystal lattice defects and new anodic phases under the action of deformation.

In general, the hazardous effect of stressed state on corrosion consists not much in increase in a continuous corrosion, but in changing its mode and transformation from a uniform corrosion to a local corrosion. Stresses intensify the local corrosion and have a negligible influence on the continuous corrosion.

Specifics of welded joints. Conditions of a spontaneous corrosion process are known: $\Delta S > 0$, $S \rightarrow \max$; $\Delta G < 0$, $G \rightarrow \min$ (S is the entropy of system, G is the Gibbs' isobar-isothermal potential) which characterize the thermodynamic and electrochemical instability of metal. The change of the electrochemical potential Δ_φ is associated with a Gibbs' potential by the relation $\Delta_\varphi = -\Delta G/n\mathrm{F}$ (n is the amount of gram-equivalent of substance; F is the Faraday's number). The change in the Gibbs' potential and, respectively, the electrochemical potential, caused by a physical-chemical effect of welding (PhChEW) is determined by the difference of potentials of the weld metal G_w, φ_w and parent metal G_m, φ_m, i.e.

$$\Delta G_w = G_w - G_m, \quad \Delta\varphi = \varphi_w - \varphi_m.$$

The effect of welding process is started at the technological stage of a «life cycle» of the structure in the form of action on the factors according to the scheme

$$\mathrm{PhChEW} \swarrow \begin{vmatrix} \Delta M_t\ (\Delta G_w) \\ \Delta N_t\ (\Delta G_{nd}) \end{vmatrix} \begin{vmatrix} \Delta G_{mw} \\ \Delta G_{fw} \end{vmatrix} \rightarrow \Delta G_w \rightarrow \Delta\varphi_w,$$

where ΔG_{mw}, ΔG_{fw}, ΔG_{nd} is the change of the Gibbs' potential under the action of the welding process in metal itself, in a surface film and, due to appearance of natural elastoplastic deformation, in the processes of melting, solidification, polymorphous transformation, decay of oversaturated solid solutions, ageing and recrystallization, deforming, respectively.

Coming from the above considerations, the welded joint is a complex physical-chemical, mechanical and electrochemical macro- and microheterogeneous system with typical types of inhomogeneity and their high gradient. The structural-chemical macro- and microheterogeneity (SChH) of metal and its surface are caused by the presence of typical HAZ (macroheterogeneity) and the presence of grains, their boundaries, phases, inclusions, clusters of dislocations (microheterogeneity) inside each zone. The heterogeneity of elastoplastic state (EPH) is caused by a non-uniform distribution of residual elastic and plastic deformations and their change in loading, while a geometric heterogeneity (GH) is caused by the presence of technological and design stress raisers in the joint and weld defects.

The heterogeneity of the mentioned types defines mechanical (MH), physical (PhH) and electrochemical (EChH) heterogeneity which are integral characteristics of properties of the welded joint, and different types of corrosion.

Thus, the effect of PhChEW on the structure resistance to fracture in reactive media can be presented in the form of a scheme

$$\text{PhChEW} \rightarrow \left| \begin{array}{c|c|c} \Delta M_t & \text{SChN} & \text{MH} \\ & \text{EPH} & \text{PhH} \\ \Delta N_t & \text{GH} & \text{EChH} \end{array} \right| \rightarrow R_w/R_m \le 1,$$

where R_w, R_m is the fracture resistance of welded joint metal and parent metal, respectively.

Among the complex of factors, influencing the MCS of welded joints and structures, we shall concentrate on the role of a macroelectrochemical heterogeneity of welded joints, effect of residual welding stresses and initial strength of materials being welded, steels of a ferritic-pearlitic class in particular.

Effect of macrostructural heterogeneity. The welded joint stipulates a localization of initiation and propagation of corrosion-mechanical fracture (CMF) due to inhomogeneity of metal properties, presence of initial stress raisers in the form of technological defects and design peculiarities of the joints, and also due to action of the residual stresses.

As the analysis of fractures of welded joints showed, the air-tightness of structures is disturbed due to propagation of corrosion defects, formed at the surface of the welded joint, inside of the metal; propagating of surface cracks occurred in the forming corrosion defect until formation of a through crack; growth of surface cracks (stress raisers) without large corrosion damages in the place of their initiation.

In the first case the service life of the structure is determined by a rate of formation of a corrosion defect Π(mm/year) which depends on maximum density of current i in accordance with the Faraday's law:

$$\Pi = \Pi_0 i_\Sigma,$$

where Π_0 is the electrochemical equivalent at i = = 1 A/mm^2, mm/year; $i_\Sigma = i_{ext} + i_{cor} + i_{m.ch}$ (i_{ext} is the density of the corrosion current determined by macroheterogeneity of the welded joint; i_{cor} is the density of corrosion current of autolysis of zones; $i_{m.ch}$ is the density of anodic current as a result of a mechano-chemical effect).

The procedure of Π determination includes, first, the determination of a section liable to greatest stress in the welded joint, which has a maximum current density, using a distribution of current density over the surface of non-homogeneous regions, and, secondly, the determination of constituents of maximum current density.

In the second case the service life of the joints consists of a duration of a stage of the corrosion defect formation until the moment of crack initiation in it and a stage of a stable crack propagation to critical sizes.

In the third case the assessment of the stage of initiation of the surface crack does not differ from the methods of its detection used in examination of fractures without a corrosion medium. The duration of the stage of a stable growth is determined the same as in the second case.

The influence of the corrosion-active media on the kinetics of fatigue fracture of welded elements from ferritic-pearlitic steels depends on two main factors: values pH and anode potential φ. The decrease in pH and decrease in an absolute value φ decrease the resistance of welded joints to the fatigue fracture.

The allowance for an effect of neutral corrosion environments, which are typical of ferritic-pearlitic steel structures, on the life of welded elements depends on the type of fracture. At alternating loads it is possible to distinguish two basic types of fractures: mechano-corrosion and corrosion-mechanical. In the first case, the mechanical factor was a cause of fracture. The presence of the medium does not change the essence of stages of fracture, and only intensifies the process of the crack growth. For CMF the first stage consists of a formation of a service stress raiser (corrosion defect) and initiation of a crack in it. The rate of growth of the corrosion defect v_c is calculated by formula

$$v_c = v_0 K_{i.c},$$

where v_0 is the rate of a uniform corrosion determined experimentally during examination of the object using relation $v_0 = (S_d - S_r)/t$; S_d, S_r are the design and real thickness of an element, respectively; t is the service duration); $K_{i.c}$ is the coefficient of intensification of corrosion at the expense of a mechano-chemical effect, which is calculated using a known relation

$$K_{i.c} = (K_{st}m + 1) \exp (K_n A^m),$$

where K_{st} is the mechano-static parameter (5 – 6 – for carbon steels, 6 – 7 – for low-alloyed steels); $K_n = V/\sqrt{3}RT$ (V – molar volume of steel); A and m are the parameters of a curve of a strain hardening.

The results of experimental study of effect of corrosion media on the characteristics of the fatigue fracture for steels of 17GS grade are given in Table. The decrease in pH and increase in an absolute value φ reduces the metal resistance to the fatigue fracture.

Residual welding stresses (RWS) are one of the main factors which determine a potential energy of the system (M–N–E) and energy conditions of the crack propagation.

Environments which cause the corrosion cracking and embrittlement of the material increase drastically the effect of residual stresses; the environments, which are neutral and plasticizing the material, change negligibly the role of residual stresses in the process of fracture as compared with an effect of the latter at the absence of the environment. The environments of the first group are most hazardous for a service strength of the structures.

Steel grade	*Type of medium*	φ, *mV*	*v, m/cycle in air*	*v, m/cycle in medium*	β_v
17 GS	Water solution with addition of caustic soda pH = 9.2 – 9.4	530 Weld	$1.0 \cdot 10^{-7}$	$4.1 \cdot 10^{-7}$	4.1
		580 HAZ	$1.6 \cdot 10^{-7}$	$7.5 \cdot 10^{-7}$	4.7
		490 PM	$1.3 \cdot 10^{-7}$	$4.3 \cdot 10^{-7}$	3.3
	Water solution with 3 % NaCl pH 6.5 – 7.0	530 Weld	$1.2 \cdot 10^{-7}$	$4.8 \cdot 10^{-7}$	4.2
		580 HAZ	$2.0 \cdot 10^{-7}$	$1.0 \cdot 10^{-6}$	5.2
		490 PM	$1.5 \cdot 10^{-7}$	$5.7 \cdot 10^{-7}$	3.8

Note. In manufacture of specimens a manual arc welding with 4 mm diameter UONI 13/45 electrodes was used; β_v is the coefficient of acceleration of fracture in medium.

The level, rigidity of the scheme and potential energy of the RWS have the effect on the resistance of the welded joints to the corrosion cracking.

It was established that the corrosion cracks are caused by the tensile components of stress, not depending on the method of loading. For all metals, the time before cracking is continuously decreased with the growth of the stress. The increase in stresses (both in σ_{ext} and σ_{nat}) promotes the weakening and damage of the protective films; causes the increase in concentration of elastoplastic deformations in microcracks and in the tip of the propagating crack, and also intensifies the mechanical and (associated with strain concentration) corrosion and sorption processes. At the same time, in most cases a threshold of minimum stresses σ_{thr} is observed on the curves of a corrosion cracking $\tau = f(\sigma)$, below which the cracking is not propagated during a long time or does not occur at all. The level of threshold stresses depends on a definite system *M–N–E*. The threshold of minimum stresses is observed in loading both at an external load and also RWS. The approximate values σ_{thr} for welded joints of steel of St.3 (rimmed) grade in alkali $\approx \sigma_y$, in nitrites $\sigma_{thr} \approx 0.5\,\sigma_y$, of steel grade 12Kh18N10T in boiling chlorides $\approx (0.4 - 0.6)\sigma_{0.2}$, titanium alloys in methanolbromic media $\approx (0.3 - 0.4)\sigma_{0.2}$, in acid media $\approx (0.5 - 1.0)\sigma_{0.2}$, aluminium alloys in sea water $\approx (0.5 - 0.8)\sigma_{0.2}$.

In accordance with a kinetic theory of strength of solid bodies the time τ before fracture of the material is determined by the expression of type $\tau = A\exp(-\alpha\sigma)$, where A and α are the constants, σ are acting tensile stresses. For a case when the material is subjected to corrosion cracking (typical brittle fracture), the law of superposition is justified, i.e. summation of stresses from external load and residual stresses. In accordance with a kinetic theory of strength and a law of superposition the life at the presence of residual stresses during corrosion cracking is determined by the expression

$$\tau = A \exp [-B(\sigma - \sigma_{thr})] = A \exp [-B(\sigma_{ext} + \sigma_{res} - \sigma_{thr})]$$

at $\sigma_{ext} + \sigma_{res} > \sigma_{thr}$, where σ_{ext}, σ_{res} are the stresses from external load and natural stresses, respectively; A(s) and B(MPa) are the coefficients which depend on properties of metal, medium and stressed state. The established relationship may serve a basis for calculation of strength and service life of the structure by a threshold stresses. The examples of calculations are given in works [1 – 3].

The propagation of avalanche cracks is determined by a potential energy of the first kind W_I. The most hazardous is an elastic energy of RWS, concentrated mainly in the zone of plastic deformations of the welded joints, whose metal is characterized by the highest inhomogeneity and, due to this, subjected to the corrosion action to the greatest extent.

Thus, the RWS are the potential source of initiating the fracture and propagation of cracks both under the conditions of static and cyclic loading over the whole trajectory of the propagating crack.

It was established that RWS in a reactive region can decrease greatly the fatigue limit of the welded element under the action of external load being transverse with respect to the weld. The adequate effect of RWS on the propagation of surface cracks directed along the weld is shown: in the region of low rates of the fracture propagation (near-threshold region) the tensile RWS accelerate the growth of surface cracks, while the compressive RWS delay their growth. For the through cracks an opposite tendency is observed: compressive stresses accelerate and the tensile stresses delay the propagation of the fatigue fracture. The main laws of RWS redistribution in the process of growth of a surface macrocrack are established. It is shown that during the crack propagation in the region of its tip the sign of the RWS is not changed even in that case when the crack tip is located in the region of the compressive RWS.

The effect of strength of materials being welded. Let us consider the case related to the gas pipelines. With increase in strength of the used materials the hazard of SCF was increased drastically. For example, during recent years the SCF becomes the main type of failures of the main gas pipelines (MGP). The fracture occurs mainly in the zone of welded joints, probably, by a corrosion-mechano-sorption mechanism (c–m–s).

At present, due to SCF, about 75 % failures of MGP was caused by corrosion, and during recent three years more than a half of total failures was

observed in gas pipelines of 1220 – 1420 mm diameter.

Failures caused by SCF are typical of the third (17G1SU grade) and fourth (16G2SFB) generations of pipe steels with a controllable rolling, as with an increase in a specific strength of the material, its sensitivity to the stress raisers, technological actions and reactive media is increased greatly.

The basic dependence of design strength S_d, i.e. resistance of structure to fracture under the action of external loads, on material strength S_m of a definite class has an extreme nature. Structures from materials of a low and medium strength are characterized by a proportional relation between S_m and S_d. An abrupt decrease in S_d with an increase in S_m due to a high increase in effect of stress raisers and technological factors in the structure manufacture on these characteristics is possible for the high-strength materials.

This tendency is intensified under conditions of stress corrosion which is manifested in an abrupt decrease in critical coefficients of intensity of stresses at corrosion cracking K_{1scc}.

Extremum of relationship $n_c = f(S_m)$ is determined by the M–N–E system and for various different classes of materials.

It seems to us that from the positions of MCS of oil and gas constructions the strength characteristics of steels of oil and gas assortment should be limited by the level of approximately 700 MPa.

The application of steels with an increased strength for the construction of large-diameter gas pipelines led to a significant increase in an elastic energy, stored in the pipe metal. As the statistics shows there is a real correlation between the dynamics of changing the strength of pipe steels, increase in reserve of elastic energy and the decrease in time before cracking the MGP at an incubation period of cracking of pipelines made of advanced steels, which amounts to about 10 years.

At the conditions of a critical combination of factors of M–N–E system all the pipe steels are susceptible to a stress corrosion in different ways. Thus, for the low-alloyed as-normalized steels the time of fracture, caused by SCF, coincides with the beginning of a period of an accelerated degradation of material properties caused by the processes of «ageing». For steels of the fourth generation the time before cracking does not coincide neither with a period of so-called extra-operation, nor with a period of «ageing». And here, each of failures of the MGP, caused by SCF, should be considered as a critical event. The difference in behaviour of the steel groups considered indicates that, probably, different mechanisms are responsible for the cracking in these steels.

The susceptibility of pipe metal to the cracking is determined by a total contribution of all kinds of heredity, acquired at the stages of manufacture of a rolled sheet and pipe, during assembly-welding-erection works, during construction of the pipeline, and also changes in structure and properties of metal, which are accumulated in it in the course of a long-time action of loads and corrosion media. In this case the metallurgical heredity is one of the causes of the metal cracking. As to the process of stress corrosion (especially for steels of the fourth generation), in parallel with peculiarities of the structure as steel purity by non-metallic inclusions, their shape and size, the role of factors of higher scale level, the role of a fine structure forming in metal of the pipeline at all stages of its service cycle in particular, is very important. And namely this can explain the high susceptibility of steels of a controllable rolling to stress corrosion, which, as compared with ordinary steels, are superior to latter, including contamination by non-metallic inclusions. In this connection, special investigations, directed to the optimizing the metal structure at the controllable rolling, should be carried out.

It should be noted that none of the characteristics of service properties, rated by existing standards for steel and pipes, gives a possibility to judge about the pipe metal resistance to SCF. This conclusion, from the one hand, proves that the susceptibility of steels to cracking is put even at the stage of designing (as in standards the requirements to the corrosion resistance are not specified), and from the other hand, it shows the impossibility of traditional methods of the quality control of pipe products to reveal those structural mechanisms which control the SCF process. Therefore, a number of service criteria should be supplemented with criteria of resistance to SCF. It is know that the large-diameter gas pipelines accumulate a large amount of a potential energy, which increases drastically the hazard of avalanche fractures. At the same time, in a practice of examination of causes of stress-corrosion fractures this factor was not paid a necessary attention. It is considered that during developing CMF the decisive role belongs to stresses, and the value of elastic energy of metal deformation depends completely on these stresses. However, the comparison of the given data shows that these concepts are not always equivalent in their effect. It was established, that the susceptibility to cracking and time before fracture almost in all cases correlate with a level of a potential energy stored in the pipeline, while such correlation is not very clear when the stress values are used.

In connection with above circumstances and high ecological hazard in case of a failure of oil and gas constructions, it is necessary to develop and keep scientifically-grounded requirements to the selection of materials, technology of manufacture (welding especially), integral protection (electrochemical, coatings, inhibition), technical

diagnostics in the course of designing, construction and service of the equipment made from steels of the fourth and next generations.

In general, the creation of the new fifth generation of steels of the oil and gas assortment should envisage a complex alloying, increased purity of metal with a globulization of impurities, optimizing of a controllable rolling with guaranteed service and technological properties including cold resistance, MCS and weldability.

Concerning the problem of hydrosulphuric cracking, the problem of selection of structural materials has been solved mainly as a result of purposeful research works and experience in implementation of the Orenburg GKM.

The present steels for the oil and gas equipment possess a complex inhomogeneous structure, whose corrosion properties are determined not much by the properties of the steel matrix, but by the ratio of phases in alloy, size of the structure grain, especially by the structure of a carbide phase, internal structural stresses, degree of dispersity of structure, its banding. Therefore, the measures directed to the increase in steel resistance to a hydrogen embrittlement should be assigned taking into account a definite structure of steel and required service characteristics of the pipe. On the basis of the requirements specified to the alloying and structure of metals, a number of grades of domestic steels, resistant to the hydrosulphuric corrosion cracking (20YuCh, 09Kh12NABCh, 14G2AF, 10G2F, 09KhG2NABCh, 10S2F, 09G2FB), has been developed and implemented.

The similar approach is necessary for the solution of the SCF problem in selection and improvement of materials for the advanced MGP. The application of the new structural materials with a high specific strength requires a serious approach.

Peculiarities in MCS determination. When calculating MCS the acting loads in the structure elements are compared with design loads (allowable) taking into account the safety factor and effect of environment. Coming from the design loads and service conditions the executive elements of the structure are determined.

When calculating MCS it is necessary to take into account the type of failure and justification of a design criterion on limiting state; justification of design scheme for determination of loads depending on the stress-strain state of the structure elements; justification of allowable values of design criteria taking into account the technical effect in manufacture of structures and service conditions.

With a specific action of the aggressive environments the area of design sections of the structure elements is decreased, for example, at a continuous corrosion; strength and deformational characteristics of metal due to sorption processes are deteriorated, for example, in hydrogenation, intercrystalline corrosion, effect of a corrosion medium and ionizing radiation.

Depending on the system M–N–E a loss in a load-carrying ability of the structure is feasible due to decrease in area of the structure element section at a continuous stress corrosion; local, intercrystalline, knife, pitting corrosion; crack formation with appearance of cracks of avalanche types without decrease or a minimum decrease in area of the working sections of the structure elements at a long-time static and cyclic loading.

In evaluation of MCS the following criteria are used:

force — allowable stresses (by yield strength, critical — threshold);

coefficients of stress intensity, amplitude of force characteristics (at cyclic loading);

deformational — plastic deformations, intensity of deformation, opening and length of crack;

time — fatigue life, number of cycles before fracture, rate of fracture propagation.

When calculating the elements of the welded structures operating in aggressive media it is necessary to take into account the effect of physical-chemical action of welding on the metal, quality of welded joint and its structure, influence of aggressive media, dominating type of failures (continuous and intercrystalline corrosion, corrosion cracking).

Calculation can be made by a load-carrying ability from the conditions of strength and a local damage, and also combination of these limiting states.

For cases of a continuous corrosion the method of calculation by allowable tensile stress taking into account the change in metal properties under the action of the welding process and medium can be used. The calculated level of stresses in welded joints is as follows:

$$\sigma_d \le [\sigma_j'']^c = \sigma_{all}[k_{wm}]_\sigma\,[k_w^c]_\sigma/k_{eff}^c,$$

where σ_{all}, $[\sigma_j'']^c$ are the allowable stresses of parent metal in initial state and metal of welded joint at corrosion, respectively; $[k_{wm}]_\sigma$ is the coefficient of reducing the strength of welded joint as compared with parent metal in initial state; $[k_w^c]_\sigma$ is the coefficient which characterizes the decrease in strength of welded joint after the action of the corrosion medium; k_{eff}^c is the effective coefficient of concentration in corrosion. When calculating the executive elements an allowance for a general corrosion is envisaged. To determine the equivalent stress an energy theory can be used.

In case of hazard of a corrosion cracking the structures should be designed by the value of an allowable stress $[\sigma_j'']^c$ for the given medium or by the value of critical stresses σ_{cr} which cause the initiation and propagation of the crack, or by a

limiting allowable depth of a corrosion crack or defect of the crack type. The design stresses are determined coming from the most strict condition.

The calculation by an allowable stress $[\sigma_{cr}'']^c$ determined for the given medium in accordance with given models is necessary, but it is not a sufficient condition of the structure strength if $\sigma_{cr} < [\sigma_{cr}'']^c$.

In turn, it is necessary to take into attention two limiting stressed states depending on the kinetics of a corrosion cracking.

1. Limiting stressed state which causes initiation and beginning of a subcritical growth of the crack. It is characterized by the value of threshold stresses σ_{thr}, σ_{cr}'', corresponding to a limiting coefficient of stress intensity K_{1scc} in material with initial defects.

2. Limiting stressed state which corresponds to transition of a subcritical growth of the crack into an avalanche mechanical fracture characterized by an appropriate critical stress σ_{cr} and intensity coefficient K_{1c} associated with it. The conditions of strength

in the first case

$$\sigma_d \le \sigma_{thr}(\sigma_{cr}^c),\ K_{1c} \le K_{1scc},$$

in the second case

$$\sigma_d \le \sigma_{cr},\ K_1 \le K_{1c}.$$

When selecting the allowable limiting stressed state (from the conditions of prevention of crack or fracture formation) it is necessary to come from the requirements specified to the structure, preset service and kinetics of propagation of the corrosion crack for the given metal-medium pair.

In case $t_{in} \approx t_{pr}$, i.e. small period of a subcritical growth of the crack, the calculation should be made using the first condition (crack prevention). In case of a long phase of a subcritical growth of the crack the calculation should be made using both the first condition (σ_{thr}, σ_{cr}^c, K_{1scc}) and the second condition (σ_{cr}, K_{1c}) taking into account the preset service life of the structure.

In case of a hazard of corrosion cracking the RWS should be taken into account in calculations, as here, the principle of superposition is valid. Therefore, it is necessary to keep the condition

$$\sigma_{ext} + \sigma_{res} \le \sigma_{thr},\ \text{i. e. } \sigma_{res} \le \sigma_{thr} - \sigma_{ext}.$$

Hence, it follows that to increase the serviceability of the structure it is necessary to take measures to decrease the residual stresses.

As is known, the calculations made using the methods of fracture mechanics are based on two basic fundamental relationships:

for static loading

$$K = \sigma \sqrt{(Ml)},$$

for dynamic loading

$$\Delta K = \Delta\sigma \sqrt{(Ml)},$$

where K is the coefficient of stress intensity, which integrally allows for a stress-strain state in the vicinity of a stress raiser (defect); σ is the acting stress in the structure; l is the size (length, depth) of crack (defect); M is the geometric factor which takes into account the type of the structure, trajectory of the defect, etc.; ΔK, $\Delta\sigma$ is the range of K and σ at cyclic loading.

The fatigue life is evaluated using a kinetic relation

$$K = f(l),$$
$$K = f(dl/d\tau),$$
$$K(\Delta) = f(dl/dN),$$

where $dl/d\tau$, dl/dN are the rates of defect propagation per unit of time and per cycle.

When evaluating the serviceability of the structure it is necessary to determine the critical values K_c, l_{cr}, σ_f, $v_{cr} = dl/dN$, N_{cr} with allowance for a reserve for stresses, length of crack, number of cycles n_σ, n_l, n_N.

It is assumed that $n_\sigma = \sigma_f/\sigma = 1.75 - 2.50$; $n_l = l_{cr}/l_d = 3 - 6$ (where the primary value corresponds to the end of structure service with a crack, the second value – the beginning of service); $n_N = N_{cr}/N_l \approx 10$ (n_N is high due to a high scattering of values of fatigue life).

For the pipeline elements the following types of calculation on the basis of fracture mechanics can be taken:

calculation for static strength using a critical coefficient of stress intensity K_{1c} and critical deformation criteria;

calculation for fatigue life by the rate of the crack growth at cyclic loadings ($1{\cdot}10^2 \le N \le 1{\cdot}10^6$) in accordance with a Paris relation $dl/dN = c_\Delta K^m$ or its modification.

At the present time the methods of a model, functional and test diagnostics have been developed which make it possible to assess the corrosion strength and corrosion mechanical strength of materials and structures taking into account their stress-strain state and service conditions. Standardized materials of assessment of resistance of metals and their welded joints to the corrosion fracture are developed (GOST 26294–84).

One of the main problem is the updating of test methods and standardized documents on the basis of advances in the field of MCS.

REFERENCES

1. Steklov, O.I. (1976) *Strength of welded structures in aggressive media*. Moscow: Mashinostroyeniye.
2. Romaniv, O.N., Nikiforchiv, G.M. (1986) *Mechanics of corrosion fracture of structural materials*. Moscow: Metallurgia.
3. Steklov, O.I. (1990) *Resistance of materials and structures to stress corrosion*. Moscow: Mashinostroyeniye.

STRENGTH AND LIFE OF WELDED JOINTS IN NUCLEAR POWER REACTOR STRUCTURES

K.V. FROLOV and **N.A. MAKHUTOV**
IMASh, Russian Academy of Sciences, Moscow, Russia

ABSTRACT

Features of design, technological solutions, welding defects and their influence on generation of the stressed-strained states in load-carrying structures of water-water power reactors are considered. Given are the results of experimental and design analysis of the fields of stresses which induce various limit states during the regular and emergency operation of NPP. Interaction of the academic, research, design, technological organisations and branch research institutes in solving the problems of strength and life of welded joints, is shown.

Key words: *strength, reactor, life, welded joints.*

For more than 40 years IMASh of the Russian Academy of Sciences together with the leading research and design organisations of former Soviet Union, Russia, Ukraine, Czechia, Slovakia, Bulgaria, Hungary, Finland, has conducted fundamental research on the problems of strength and life of welded joints applied in nuclear power reactors of WWER and BN type [1 – 10]. Important investigations have also been carried out for the nuclear steam plants for transport applications and heating nuclear power plants (HNPP) in Nizhny Novgorod, Voronezh.

The characteristic operational conditions, modes and theoretical coefficients of stress concentration α_σ are given in Tables 1 – 3 [2].

At the strength margins for σ_y in the range of 1.6 to 2.0, local stresses in the concentration zones can reach the values close to σ_y or exceed them by 1.5 to 2.0 times [2].

The load-carrying elements of WWER type reactors are made of low-alloyed Cr–Ni–Mo–V steels with a higher heat and radiation resistance with the yield point from 440 up to 540 MPa, ultimate strength from 550 up to 650 MPa.

The following types of welded joints are widely used in fabrication of reactor units:

with butt welds on the cases, covers, bottoms, and branch pipes;

with fillet and slot welds on the straight and inclined branch pipes and on the sleeves.

The majority of the reactor units have anti-corrosion cladding of austenitic steel. Typical welded joints and cladding [4] are shown in Figure 1. It indicates the points of experimental measurement of local stresses. Figure 2 shows the zone of an inclined branch-pipe, the model of his zone and the schematic of strain gauges location for stress measurement [4].

Selection of structural materials, welding and cladding technologies for the load-carrying elements of WWER primary circuit is based on a number of technical requirements to strength, adaptability to fabrication and resistance to service factors impact. They are as follows:

preservation of the specified level of mechanical properties (characteristics of strength and ductility) in a broad range of service temperatures (from 20 up to 350 °C for WWER and HNPP and up to 650 °C for BN);

production of stable mechanical properties when the element wall thickness is varied from 10 – 20 up to 200 – 500 mm for the accepted modes of rolling, forging and heat-treatment;

weldability of steels of the specified class in a broad range of thicknesses and possibility of production of dissimilar steel welded joints (for instance, of pearlitic and austenitic classes);

Table 1

Power, MW	*Pressure, MPa*	*Temperature, °C*		*Case dimensions, mm*			*Pin diameter, mm*	*Cover thickness, mm*
		inlet	*outlet*	*wall thickness*	*diameter*	*height*		
210	10.0	250	275	100 – 180	4000	12200	130	500 (flat)
365	10.5	250	280	120 – 180	4000	14100	130	500 (flat)
440	12.5	270	300	140 – 190	3900	14300	140	210
1000	16.0	290	325	200 – 285	4535	13500	170	236

Table 2

Modes	*Number of repeats*
Hydraulic strength testing	20 – 30
Start-up and shut-down with heating and cooling	130 – 375
Power change from 50 up to 100 % (step-like)	150 – 200
Power change by 25 %	up to 10000
Power adjustment by 10 % relative to rated value	up to 2000
Operation of emergency protection	150 – 600
Switching off of the main circulation pumps	600 – 800
Planned shut-down without cooling and subsequent start-up	500
Operation of the system of automatic cooling and protection	up to 1 – 5

resistance to radioactive irradiation (predominantly neutron and γ-irradiation), leading to a considerable change of the physico-mechanical properties;

resistance to corrosion and erosion damage in the heat-transfer agent flows and in the zones of stagnation;

resistance to repeated elastic, elasto-plastic deformation and change of shape in the zones of increased local stresses induced by thermal and mechanical loads;

strength and fatigue life (in the time and cyclic variants) under the impact of low-frequency (due to the change of operational modes) and high-frequency (due to the mechanical and hydrodynamic vibrations) non-stationary stress amplitudes;

resistance to brittle fracture allowing for the initial technological and developing service defects of the type of cracks;

cracking resistance under the impact of the above cyclic (low- and high-frequency) stresses;

control of the metal condition in service (by mechanical testing of the reference-samples, non-destructive testing of potentially the most damaged surface and subsurface layers of the base and the clad metal);

resistance to contact impacts (in the zones of the main joint of the reactor casing, supporting sides, threaded joints);

resistance to creep and one-sided accumulation of cyclic deformations for provision of the specified

Table 3

Reactor case elements	α_σ
Brach-pipe zone	1.5 – 2.9
Zone of transition to the flange	1.2 – 1.4
Zone of bottom connection	1.6 – 1.7
Straight and inclined holes in the cover	1.8 – 3.4
Threaded part of the pin	3.2 – 5.0

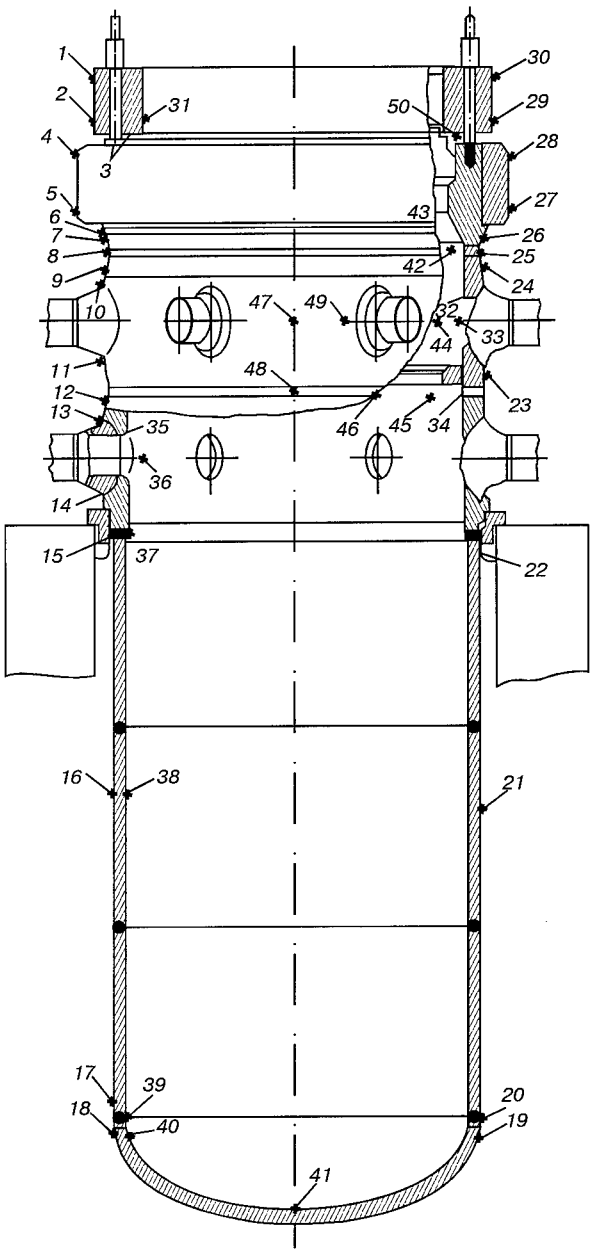

Figure 1. Welds in the active zone and measurement points (indicated by numbers) on WWER-210 case

relative position of the mating elements (main casing joint, protection control system components).

Many of the above requirements to the structural materials and the technologies of welding, cladding and heat-treatment were the basis for elaboration of the special technical conditions for delivery of materials, development of the technology of fabrication and control of the reactor load-carrying elements and components. A broad range of characteristics of material physico-mechanical properties is used in calculation of stresses, strength and life of nuclear reactors, including resistance to radiation damage (so-called radiation resistance coefficients, A_f). The above characteristics are determined by standardised or unified procedures.

The main problem in nuclear reactor design, still remains to be the strength of the load-carrying elements in terms of limit and admissible stresses. Solving the problems of the theory of elasticity, theory of vibrations, theory of plasticity and shell theory was reduced to determination of the static and dynamic nominal and local stresses σ^e induced by service loads P^e and cross-sectional dimensions S. Such characteristics of mechanical properties M as the modulus of elasticity E, yield point σ_y, ultimate strength σ_t and long-term strength σ_τ were used as criterial parameters of deformability and strength of structural materials in design of the first reactors:

$$\sigma^e = f(P^e, S, E, \alpha, \mu) \le \left\{\frac{\sigma_y}{n_y}, \frac{\sigma_t}{n_t}, \frac{\sigma_\tau}{n_\tau}\right\}, \quad (1)$$

where n_y, n_t, n_τ are the appropriate margins, which are equal to 1.5 to 3.0.

For welded joints S, σ_y, σ_t, σ_τ values corresponding to various zones of welded joints, are introduced into calculations. The task of the designers and the technologists was provision of equivalent strength of the welded joint and the base metal.

For power reactors of the first generation investigations of their fatigue and fatigue life were conducted in 1950s. Stresses σ^e and number of loading cycles N^e were considered to be the main parameters of operational loading of machines. Cyclic strength conditions were defined in addition to equation (1)

$$\sigma_a^e = f(P^e, N^e) \le \left\{\frac{\sigma_{-1}}{n_\sigma (K_\sigma \bar{\sigma}_a^e \varepsilon_\sigma) + \psi_\sigma \bar{\sigma}_m^e}\right\}, \quad (2)$$

where σ_a^e, σ_m^e are the amplitude and mean cycle stress ($\bar{\sigma} = \sigma/\sigma_{-1}$), respectively; σ_{-1} is the endurance limit of the structural material; K_σ, ε_σ, ψ_σ are the characteristics of material sensitivity to stress concentration, absolute dimensions and asymmetry of the cycle.

The strength and fatigue life of load-carrying welded components were calculated from equations (1), (2).

In the first stage of calculation and investigation of welded joint strength, the endurance limit was assumed for the respective welded joint σ_{-1c}, concentration factor $K_{\sigma c}$ allowed for the features of the welded joint geometry, and $\varepsilon_{\sigma c}$ value for the cross-section dimensions. Residual stresses in the welded joint were not directly introduced into σ_a^e and σ_m^e values.

With such a definition of the problem, experimental investigation of the local maximal service stresses σ_{max}^e from which σ_a^e and σ_m^e values are determined, was extremely important. IMASh, EDB GP and NIKIET developed the methods of stress simulation, namely photoelasticity, method of optically active stickers and strain measurement models of low-modulus materials [1, 2, 4, 10]. These investigations permitted equation (1) to be used for strength analysis in terms of local stresses. Here n_y value could be lowered to 1, i.e. a requirement on limitation of the possibility of plastic deformation development could be introduced.

In view of extremely large dimensions of the load-carrying element cross-section (diameters of up to 5000 – 6000 mm and wall thickness up to 300 – 500 mm), great importance was attached to provision of resistance to brittle fracture as the most hazardous and catastrophic, already when designing the reactors of the first generations [1 – 4]. In addition to equations (1) and (2) two more criteria were introduced into the analytical substantiation of strength in 1950 – 1960s:

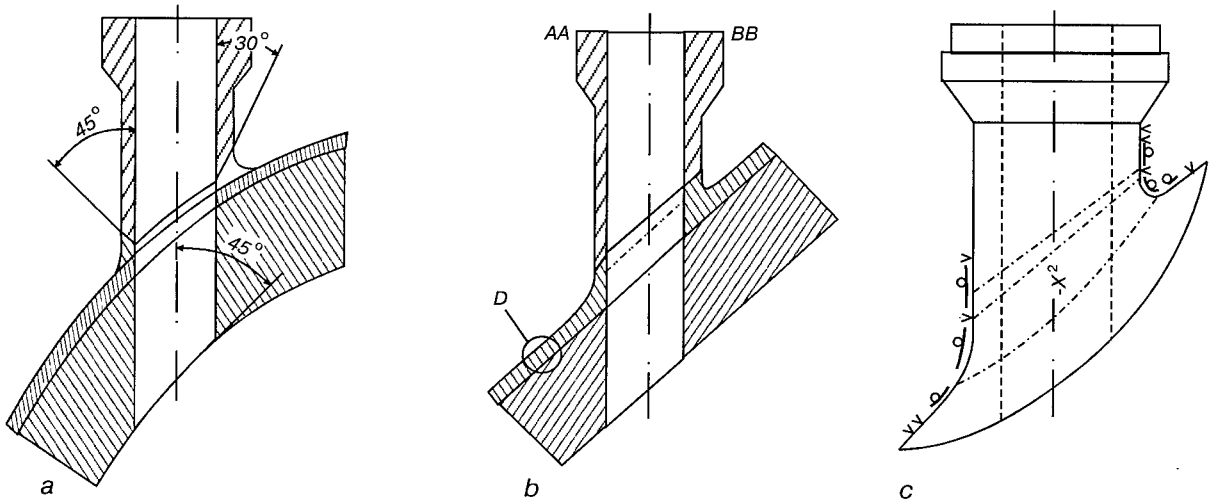

Figure 2. Zone of branch-pipe welding to the cover (*a*), schematics of simulation (*b*) and strain measurement (*c*)

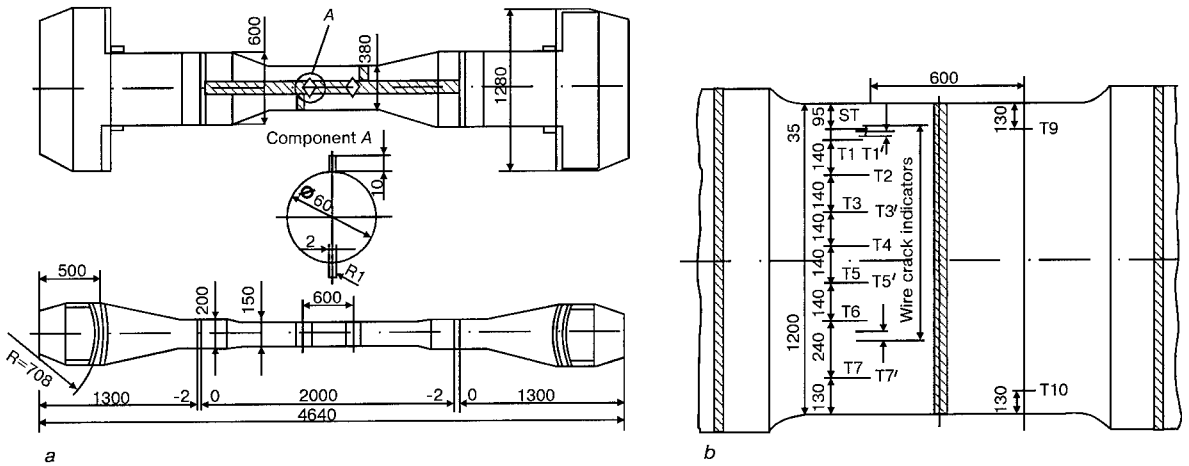

Figure 3. Large-sized samples of the base metal and welded joint metal for determination of brittle fracture resistance: *a* — in static tension; *b* — in tension with crack initiation under impact

$$\sigma^{e}_{max} = f(P^{e}, S) \le \frac{\sigma_{cr}}{n_{cr}},$$

$$T^{e}_{min} = f(S, M_w, P^{e}) \le T_{cr} + [\Delta T_{cr}],$$

where σ_{cr} is the resistance to brittle fracture in the base metal or in the welded joint; T^{e}_{min} is the minimal service temperature at the specified loading mode; T_{cr} is the critical brittleness temperature; $[\Delta T]$ is the margin on critical temperatures; M_w are the basic characteristics of mechanical properties of the base metal or the welded joint metal.

In order to derive experimental data on σ_{cr} and T_{cr} values for the base metal and the metal of the reactor welded joints, IMASh of the Russian Academy of Sciences, together with Krylov TsNII and Shkoda Enterprise conducted unique experiments beginning from 1960s [1 – 4], in machines with the limit forces of $1 \cdot 10^5 - 8 \cdot 10^7$ N (UME-10, ZDM-400, MUG-500, MUG-3000, ZZ-8000) in the two main modes:

static loading in the temperature range from −196 up to +100 °C and with cross-sectional dimensions from 4 up to $3 \cdot 10^7$ mm^2 (i.e. with about ten million times change);

static loading and dynamic crack initiation in the temperature range from −10 up to +100 °C.

Standard and non-standard cylindrical (2 to 100 mm diameter) and flat (153 to 25 × 100 mm section) samples of the base metal, metal of the welded joints and transition zones were subjected to tensile testing.

Testing for determination of the limit characteristics σ_{cr} and T_{cr} was conducted on samples with sharp notches of the base metal and the welded joint metal [1, 10]. Dimensions of the laboratory sample sections were varied from 1.5 × 14 up to 25 × 100 mm. Individual samples had the sections from 150 × 380 up to 250 × 1200 mm. In these samples the cracks were initiated both in the base metal and in the welded joint metal (Figure 3).

Power and exponential dependencies of the mechanical properties and critical stresses on temperatures T, cross-sectional dimensions S and crack sizes l were derived from the experimental results

$$\{\sigma_{cr}, \sigma_y, \sigma_t\} = f\{S, T, l, M_w\}. \quad (3)$$

It was shown that the residual stresses in welded joints are manifested only in the brittle states, when $T^{e}_{min} << T_{cr}$.

The methods of the standard [8] and more precise [3] evaluation of reactor structures resistance to brittle fracture were defined proceeding from the results of these tests.

In 1970 – 1980s the factors of intensity of stresses K_I (or strains K^{e}_{I}) were introduced into the equations for evaluation of brittle fracture resistance, based on the data of theoretical and experimental fracture mechanics investigations [2 – 4, 7, 10]

$$K^{e}_{I} = f\{P^{e}, T^{e}, S, l, M\} \le \frac{K_{Ic}}{n_K}, \quad (4)$$

where K_{Ic} is the critical value of stress intensity factor (fracture toughness) for the base metal and the metal of the welded joint; n_K is the fracture toughness margin ($n_y \le n_K \le n_t$).

In 1970 – 1980s testing of bimetal samples (samples with cladding) with different location of the initial defects (cracks) (Figure 4) was conducted for the clad cases of WWER and HNPP reactors. Samples of 20 to 150 mm thickness were tested by bending or off-center tension.

Processing of the results of testing in terms of breaking loads K^{*}_{c} and secant method (conditional values of K_Q) demonstrated [3] that a considerable lowering (compared to the base metal) of cracking resistance values K^{*}_{c} and K_Q by 2.7 to 2.3 times respectively, is found (Figure 5) at low temperatures in the clad samples with the surface semi-elliptical defect, shown in Figure 4, *d*. This is at-

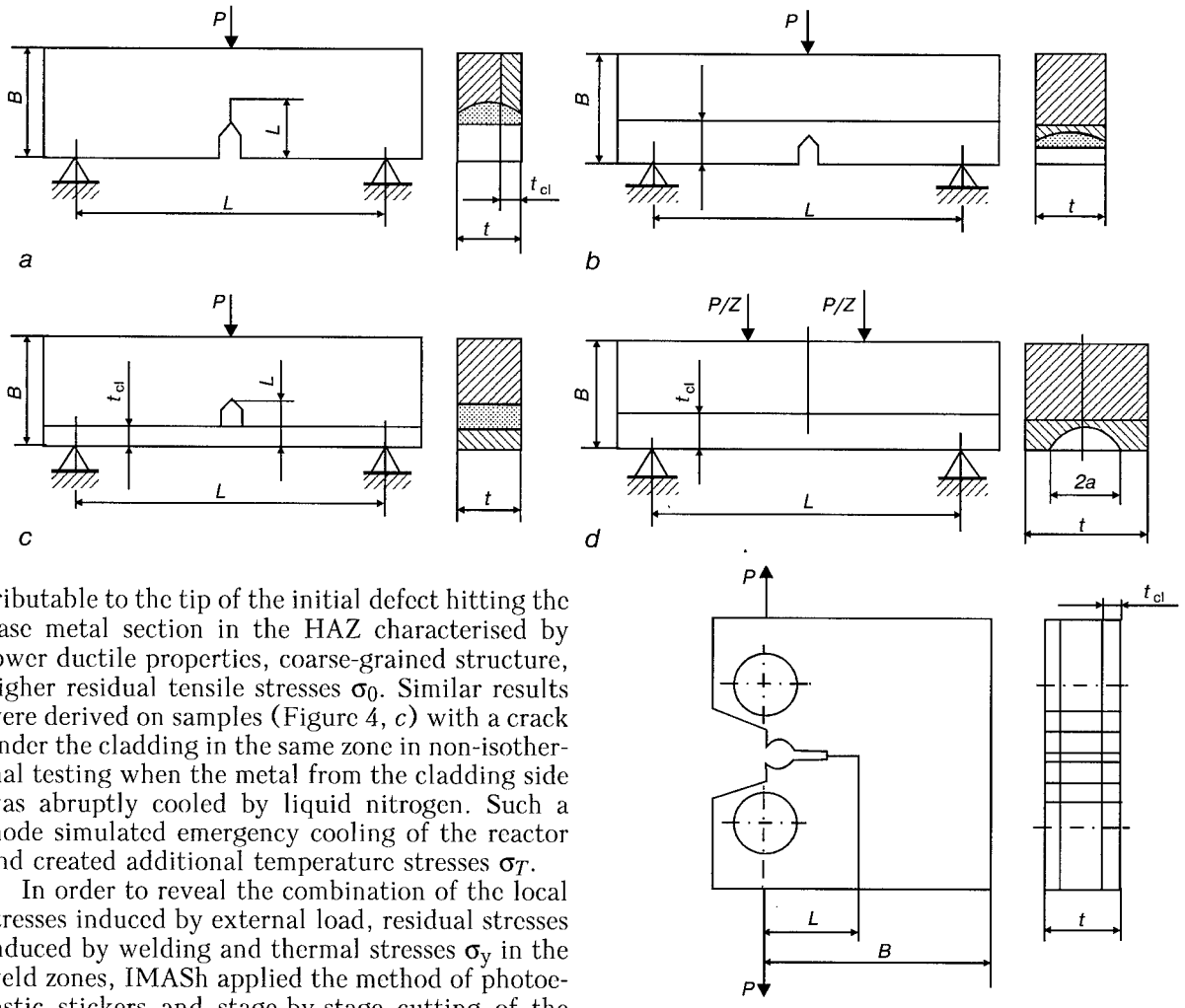

Figure 4. Samples with cladding (bimetal samples) for different kinds of testing

tributable to the tip of the initial defect hitting the base metal section in the HAZ characterised by lower ductile properties, coarse-grained structure, higher residual tensile stresses σ_0. Similar results were derived on samples (Figure 4, *c*) with a crack under the cladding in the same zone in non-isothermal testing when the metal from the cladding side was abruptly cooled by liquid nitrogen. Such a mode simulated emergency cooling of the reactor and created additional temperature stresses σ_T.

In order to reveal the combination of the local stresses induced by external load, residual stresses induced by welding and thermal stresses σ_y in the weld zones, IMASh applied the method of photoelastic stickers and stage-by-stage cutting of the cladding or the weld by electric erosion method. With such cutting the residual stresses are redistributed, this leading to a change in the stress intensity factors K_{I0} of the actual residual stresses σ_0. Dependence of K_{I0} on l is plotted by epures of the fields of local stresses and fracture mechanics equations, and σ_0 epure is determined by solving the inverse problem

$$\{K_{I0}, \sigma_0\} = f\{S, l, M_w\}. \quad (5)$$

Functional (5) is also derived by the X-ray method or method of holographic interferometry with drilling of small holes.

Values of K_I depending on external loads P^e and temperatures are determined by calculation (analytically or by FEM) or experimentally on models or full-scale elements by the methods of photo-elastic stickers and holographic interefometry

$$K_I = \{K_{IP}, K_{I0}, K_n\}. \quad (6)$$

For the region of brittle states, functional (6) can be replaced by a sum of the appropriate values; non-linear fracture mechanics criteria should be applied in the elasto-plastic region [3, 5, 10]. In this case conditional stress intensity factors are used

$$K_I^* = \{K_I^e\} = f\left\{K_I, \frac{\sigma^e}{\sigma_y}, M_w\right\}.$$

The results of fundamental research of radiation damage from neutron flows F, conducted during 1960–1980s in IAE, TsNII KM «Prometey», PO Shkoda were of principal importance for the reactor structures in the region of the active zone (primarily for the reactor cases and their welded joints) [1 – 3, 8 – 10]. This permitted the power and exponential equations to be written in the standard [8] and precised [2, 3] variants

$$\{\sigma_y, \sigma_t, KCV, K_{Ic}, T_{cr}\} = f\{F, T^e, \tau^e, A_c\}, \quad (7)$$

where A_c are the coefficients of sensitivity to damage from integral flows (fluences) F.

In this case rise of critical temperatures T_{cr} with the increase of F by the power function (with 0.33 to 0.50 power index) is regarded to be most im-

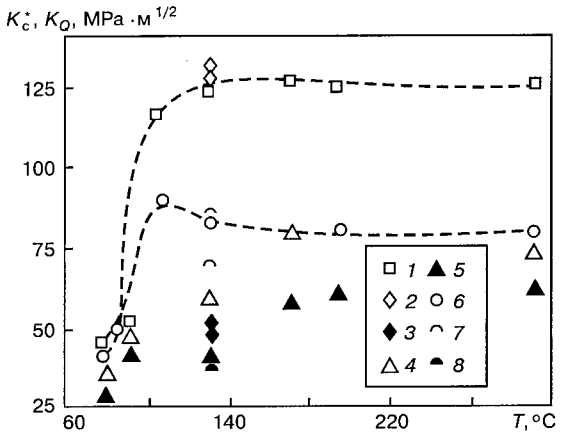

Figure 5. Temperature dependence of fracture toughness of 15Kh2MFA steel without cladding and with cladding with different types of defects: *1 – 5* — K_c^*, *6 – 8* — K_Q; *2, 3, 7, 8* — surface semi-elliptical; *4* — subsurface through-thickness; *5* — through-thickness under the cladding; *1, 6* — edge

portant. For the metal of the welds A_c value can turn out to be 1.5 to 2.0 times higher than for the base metal, in the case of determination [2, 3, 8] of lowering of the life after irradiation by equations (3) and (4), (7).

In view of the cyclic nature of thermomechanical loading of the load-carrying elements of nuclear reactors due to the features of the loading modes and structural shape (Tables 1 – 3), IMASh in 1960 – 1980s conducted systematic studies of low-cycle fatigue [2, 3, 5, 6].

Creation of non-elastic cyclic deformation regions in the zones of stress concentration, necessitated the transition from calculations in terms of local stresses to calculations in terms of local strains

$$\left\{\sigma^e, e^e, N^e\right\} = f(P^e, N^e, T^e, m) \le$$

$$\le \left\{\left[\left(\frac{\sigma_c}{n_\sigma}\right)\left(\frac{e_c}{n_e}\right)\left(\frac{N_c}{n_N}\right)\right] f(\sigma_y, \psi_c, m_p, m_e)\right\}, \quad (8)$$

where σ_c, e_c, N_c are the stresses, strains and cycle number, respectively; $\left(\sigma_c = S,\ e_c = \ln\frac{1}{1-\psi_c}\right)$; m is the characteristic of strengthening in the elasto-plastic field; ψ_c is the reduction in area at one-time fracture; m_p, m_e are the characteristics of the curve of low-cycle fatigue.

Methods of photo-elastic stickers, moire, small-base grids and small-base strain measurement were developed in order to determine σ^e, e^e, σ_c, e_c in the welded joints.

For the welded joints the characteristics of mechanical properties M_w incorporated into equation (8) can be determined [5, 6] through distributions of the local properties of various zones of the welded joint, allowing for the coefficients of contact strengthening χ_{ci}

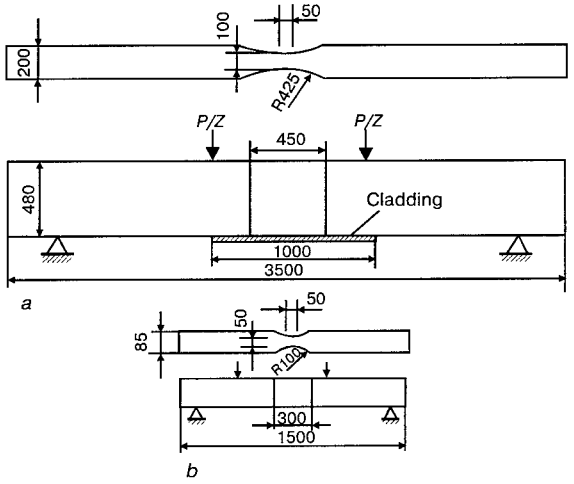

Figure 6. Geometry of samples with cladding (*a*) and base metal samples (*b*) for bend testing

$$\{M_{ci}\} = f\{(M_{ci}, \chi_{ci}, N)\}.$$

In order to address the new tasks of BN reactor design, IMASh, TsNII KM «Prometey», TsNII-TMASh, NIKIET performed investigations on determination of creep, high-temperature (up to 500 – 650 °C) short-term, long-term and cyclic strength, also in programmed loading modes. In strength and life analysis, equations (8) were complemented by equations of long-term (by duration of operation τ^e) strength $\sigma^\tau_{l.s}$:

$$\left\{\sigma^e, e^e, \tau^e, N^e\right\} = f(P^e, \tau^e, N^e, T^e) \le$$

$$\le \left\{\left(\frac{\sigma^\tau_{l.s}}{n_\tau}\right), f(m_\tau)\right\},$$

where n_τ is the time limit τ; m_τ is the characteristic of long-term strength curve.

Measurement of local stresses and strains was performed by the high-temperature strain measurement and moire methods on samples, models and full-scale structures [5, 9, 10].

Fundamentally important for the piping, inner components and pumps of nuclear reactors were the investigations performed in IMASh, PWI and IPP of the diagrams of cyclic deformation and fa-

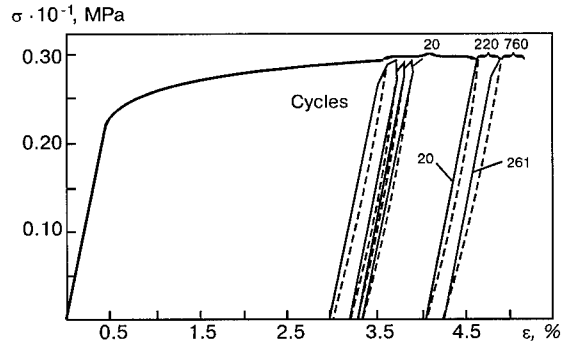

Figure 7. Diagrams of deformation in bending of a clad sample: ——— — loading; - - - - - - - - — load

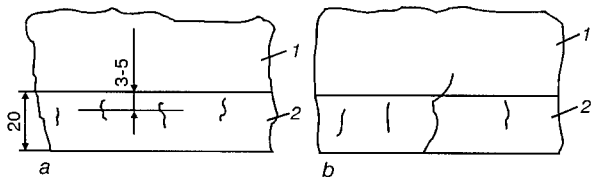

Figure 8. Schematic of initial (*a*) and subsequent (*b*) crack propagation in the cladding: *1* — base metal; *2* — cladding

tigue life in bicyclic loading modes when the life by the base number of cycles N^e decreased with the increase of the ratio of the frequencies and amplitudes of the high-frequency part of the spectrum [3, 4, 8]:

$$N_c = f\left\{\frac{\sigma_{at}}{\sigma_a}, \frac{f_t}{f}, t_c, \tau_c\right\}.$$

The influence of amplitudes σ_{at} and frequencies f_t of the high-frequency part of the loading spectrum is described by the power functions [2, 8].

For integral evaluation of the cladding effect at low-cycle loading Krylov TsNII and IMASh performed [2] unique experiments with loading by bending, on base metal samples of 50 × 100 mm cross-section and 1500 mm length and on clad samples of 100 × 500 mm cross-section, 3500 mm length (Figure 6).

A one-sided accumulation of plastic deformations was found at cyclic elasto-plastic bending (Figure 7). Cracks initiated in the cladding at 3 – 5 mm distance from the fusion zone at the fatigue life of approximately 0.5 of that of the base metal (Figure 8). Further on, these cracks ran through the cladding, changing their direction in the transition zone, thus leading to the final quasibrittle fracture through the base metal.

For the most complex modes of thermomechanical loading (operation of emergency protection, earthquakes) for the case of welded joints and cladding, IMASh together with EDB GP performed in 1970 – 1980s analytical studies (by the FEM) of local stresses and strains with introduction of appropriate characteristics of mechanical properties M_w. These calculations showed the important role of the cladding and the relatively small proportion (up to 0.1) of additionally accumulated cyclic damage from powerful seismic impacts [3].

The final stage of substantiation of the strength and life of all the pilot samples of the reactors, are the model and full-scale strain, temperature and vibration measurement studies [2 – 5, 9, 10]. Such investigations were conducted in the most complete manner in the 5th reactor of NPP in the city of Kozloduy, Bulgaria, when about 1000 initial sensors were used in total on all the elements of the primary circuit.

Only such a combination of the standard calculation procedures, more accurate calculations and experimental investigations on samples, models and full-scale tests enables a well-grounded evaluation of the strength and life of welded joints and the reactors as a whole. The same information is also used as the initial data for evaluation of NPP viability and safety [2, 3, 5, 8 – 10].

REFERENCES

1. (1968) *Investigations of the stresses and strength of the reactor case*. Ed. by S.V. Serensen, Ya. Nemets, N.I. Prigorovsky. Moscow: Atomizdat.
2. Makhutov, N.A., Stekolnikov, V.V., Frolov, K.V. *et al.* (1987) *Structures and methods of design of water-water power reactors*. Moscow: Nauka.
3. Makhutov, N.A., Frolov, K.V., Stekolnikov, V.V. *et al.* (1988) *Strength and life of water-water power reactors*. Moscow: Nauka.
4. Makhutov, N.A, Frolov, K.V., Stekolnikov, V.V. (1990) *Experimental investigations of the strains and stresses in water-water power reactors*. Moscow: Nauka.
5. (1997) *Problems of fracture, life and safety of engineering systems*. Krasnoyarsk: SO RAN.
6. Trufyakov, V.I., Makhutov, N.A. (1979) Strength of welded joints at alternating loads. In: *Welding in mechanical engineering*. Refer. Book. Moscow: Mashinostroyeniye.
7. Makhutov, N.A. (1988) Features of temperature dependencies of crack resistance of structural steels. In: *Fracture mechanics and strength of materials*. Refer. Book. Kyiv: Naukova Dumka.
8. (1989) *Codes of strength analysis of the equipment and piping of nuclear power plants*. Moscow: Energoatomizdat.
9. Frolov, K.V., Makhutov, N.A., Khurshudov, G.Kh. (1999) *Problems of life and safety of power equipment*. Moscow: IMASh RAN.
10. Frolov, K.V., Makhutov, N.A., Protsenko, A.N. *et al.* (1988) *Safety of Russia. Functioning and development of complex economic, engineering, power, transportation, communication systems and service lines*. Moscow: Znaniye.

RECENT DEVELOPMENTS OF STEEL AND WELDING MATERIALS CAPABLE OF IMPROVING STRUCTURAL INTEGRITY

Yu. FUJITA[1] and **N. YURIOKA**[2]
[1]Japan Welding Engineering Society, Tokyo, Japan
[2]Nippon Steel Corporation, Chiba, Japan

ABSTRACT

A number of problems associated with the creation of high-reliability engineering structures is considered. They include the peculiarities of application of structural materials of the new generation which is characterized by a high strength, corrosion resistance, high-temperature and heat resistance. The ways of development of materials for their welding are defined. It is shown that a simultaneous development of steels and welding consumables is a very important link in the process of improvement of reliability of welded joints from the point of view of resistance to tough and brittle fracture, fatigue, corrosion and/or creep.

Key words: *steel, thermomechanical treatment, welding consumables, weldability.*

Structural reliability of a welded steel structure is influenced by some of the base metal properties; they are the resistance to strain aging embrittlement, the capability of plastic deformation absorption, the resistance to general corrosion, and the ability of arresting a running brittle crack. However, the overall integrity of a welded steel structure is governed, in many cases, by the performance of welded joints which occupy only a small fraction of a whole structure. The performances of the welded joints mean their soundness and their resistance to joint deficiency. In an engineering term, they include the suitable joint strength relative to the base metal strength, toughness, freedom from weld defects, corrosion resistance, fatigue resistance, creep resistance and others. This report introduces several newly developed structural steels and welding materials with desired performances, i.e. improved reliability of their welded structures.

Weldable steels and welding materials. Weldability of steels means how reliably welded joints perform during their service. Therefore, the weldability includes toughness, fatigue resistance, corrosion resistance, creep resistance and other performances of welded joints. However, it means in a narrow sense to obtain welds not intolerably hardened and free from cracks. «Weldable» is used in this section as the narrow meaning.

The maximum hardness of a HAZ has been limited to not higher than *HV* 350. This limitation presumably stemmed from the experience that toe cracking, one type of cold cracking, was avoided in HAZ when HAZ hardness was lower than *HV* 350. In HAZ of off-shore structure steels, the HAZ hardness limitation was *HV* 325 or *HV* 300 for a certain safety margin. This limitation is a rather stringent requirement for heavy off-shore structure steels because they include hardenable elements to a considerable extent.

It has been considered that HAZ hardness is directly to the likelihood of sulfide stress corrosion cracking (SSCC) in steel HAZ during service under wet sour gas or H_2S solutions. The hardness of HAZ was limited to *HV* 248 in pipelines for sour gas service. Recently, a further severe hardness limitation was demanded. A Thermo-Mechanical Control Process (TMCP) strengthens steel thermomechanically and can reduce hardenable alloy elements. Therefore, it is essential to employ TMCP to produce steels, for which the HAZ hardness limitation is required, such as off-shore structure steels and sour gas service line-pipe steels. Meanwhile, the seam weld metal of submerged arc welding (SAW) pipes is heat-affected by circumferential welding (girth welding) and is hardened. HAZ of the seam weld metal is also required to satisfy the hardness limitation. Then, the SAW welding materials of low hardenability was developed for pipe seam welding [1].

HAZ hardness increases as a weld length shortens. A tack weld is always short, and thus HAZ hardness of a tack weld tends to increase. According to the Japan Maritime Association rule, a short bead shorter than 50 mm, but not shorter than 10 mm is allowed for the TMCP steels while a bead shorter than 50 mm is not allowed in the conventional steels. In fact, a longer tack weld is troublesome in shipbuilding. In this sense, the TMCP steel is very beneficial. A lot of tack welds and jig welds are made in welding construction of ships, buildings and bridges. Those welds are generally short, resulting in high HAZ harnesses and the high

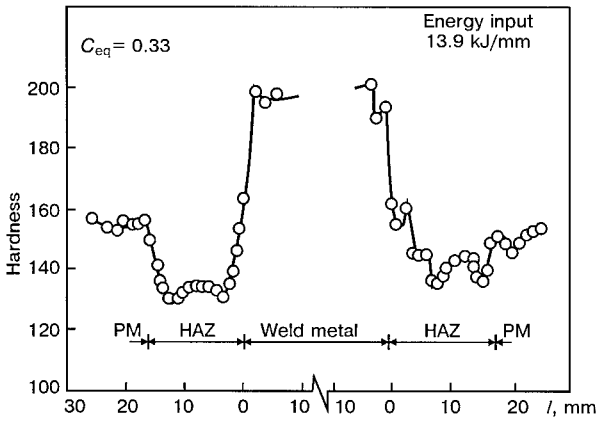

Figure 1. Distribution of hardness in welded joint (arc welding at high energy input) of ship hull of 25 mm thick steel produced using TMCP; l is the distance from fusion line

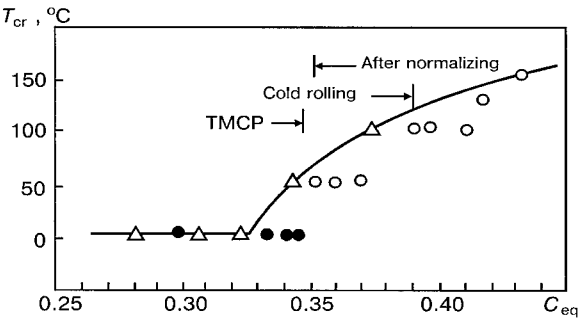

Figure 2. Critical temperature of preheating to prevent cold cracking at different carbon equivalent (test for crack formation at rigid fixture of a joint with Y-shaped groove, sheet thickness is 25 – 38 mm)

likelihood of cold cracking. To make matters worse, the welding control and inspection are, in general, not severe for tack welds and jig welds. From a fail-safe viewpoint, the TMCP steel is thus beneficial.

In shipbuilding, a very high heat input is generally used in welding to increase the production efficiency. The TMCP steel, which contains less alloy elements than the conventional steels, tends to soften in HAZ when welding with a high heat input. In ordered to acquire the overall joint strength, weld materials with higher strength are used as shown in Figure 1. This is a typical case of weld overmatching.

Cold cracking is caused by hydrogen which is generated from the dissolution of water existing in welding materials and atmospheric moisture under welding arc. Preheating is conducted to avoid cold cracking because preheating facilitates the effusion of hydrogen from a weld to atmosphere after the completion of welding.

Figure 2 shows the necessary preheating temperature to prevent cold cracking (root cracking) in small cracking tests [2]. It is seen that the TMCP steel needs lower preheat temperatures than the conventional steels do. Preheating is, in fact, unnecessary in shipbuilding of YS 360 MPa high-strength steels because steel plates for ships are not thick. However, steel plates for off-shore structures is much thicker than ship plates and preheating of high temperatures was required when the conventional normalized steels were used. The TMCP steel is characterized by low carbon equivalent. After the development of TMCP off-shore structure steels, it became possible to weld very thick plates of YS 360 MPa without preheating.

High strength steels of the TS 780 MPa grade were used for the Akashi Bridge, the world-longest span suspension bridge. Preheating of 100 °C is necessary for the conventional quenched-and-tempered TS 780 MPa steels of 38 mm thickness. Recently, the Cu-precipitated TS 780 MPa steel was developed. This steel was produced by direct quench (DQ), one type of TMCP, in which copper is in satisfactorily solid-solution and the temper treatment after DQ facilitates precipitation of solid-solution copper so that the steel can be strengthened. Actually, the Cu-precipitated TS 780 MPa TMCP steels were used to the upper decks of the Akashi Bridge and they were welded in preheating of 50 °C [3]. This Cu-precipitated steel originated in ASTM A710 which had been developed by INCO Co. in U.S.[4]. 2000 tons of YS 560 MPa A710 pipes were used for the Shell Oil Auger platform in the Gulf of Mexico mainly because of their excellent girth weldability [5].

Flux cored wires are increasingly used as gas shielded welding materials, mainly because of their high deposition rate. There are two types of flux cored wires: a plate folded type and a seamless wire type. The dehydrogen treatment at high temperatures is possible when producing the seamless type of flux cored wire, and thus this wire is characterized by the very low hydrogen potential. For instance, the weld metal hydrogen content is reduced to as low as 1.5 ml/100 g in a basic flux wire of a seamless type. Furthermore, this type of wire is little moistened during storage because the seamless tube wire has no opening. Welding construction of heavy TS 490 MPa grade steels without preheating is possible when using the seamless type flux cored welding materials [6].

Tough steels and welding materials. Japanese shipbuilders have employed high heat input welding to raise the productivity in welding fabrication. High heat input welding forms coarse-grained HAZ, resulting in the degradation of HAZ toughness. A specific precipitate TiN was found to effectively prevent grain coarsening through its pinning effect. For a long time, the TiN steels have been used as shipbuilding steels for high heat input welding. HAZ toughness tends to degrade with increasing carbon equivalent of steels. Therefore, the employment of TMCP along with the use of TiN is beneficial in improving HAZ toughness because it can produce low carbon equivalent steels.

The Ti and B bearing welding material had been known to provide very fine microstructures and thus high toughness with weld metal. The mechanism of the grain refinement was clarified in 1981. It is that titanium oxides in the Ti–B weld metal act as nuclei of intragranular accicular ferrite of a very fine grain [7]. This weld material has been used especially in high heat input welding. Heavy welded structures are often subjected to post weld heat treatment (PWHT) in order to reduce welding residual stresses. The Ti–B welding material provided satisfactorily high toughness as welded condition but not after PWHT. Recently, the welding material of 0.05C–1.3Mn–2.25Ni–Ti–B was developed which is preferably tough not only in as-welded condition but also in as-PWHT condition [8].

Oxides in steels had been considered as harmful inclusions. However, some oxides such as REM oxy-sulfide [9] and Ti_2O_3 [10] were discovered to have a capability of nucleating fine intragranular ferrite in the same manner as the Ti–B weld metal does. Unlike TiN precipitates, oxides are stable in high temperatures and never dissolve at the HAZ fusion line where the temperature rises close to the melting point of the steel. The HAZ toughness requirements are more stringent to off-shore structure steels than shipbuilding steels. The titanium oxides (Ti_2O_3) dispersed steels were used for an oil production platform in North Sea because of satisfactorily high toughness of their HAZ even made by high heat input welding.

The minimum necessary crack tip opening displacement (CTOD) was demanded to the welds of off-shore structures. However, a significant problem arose concerning the assurance of minimum CTOD values. Figure 3 shows the scatter of CTOD values at the fusion line HAZ of an off-shore structure steel whose toughness was already recognized to be very high with respect to Charpy testing. This scattering of a quite wide range was not unusual. This is because CTOD, which represents a property of brittle fracture initiation, is determined by toughness at an extremely localized area. Therefore, the elimination of localized brittle zones is essential. The intensive researches revealed that the localized brittleness is attributed to a small hard spot, that is, a martensite-austenite (MA) constituent which appears at the specific area of HAZ. It was found that the occurrence of brittle MA constituents is enhanced by the elements such as C, Nb, V and Mo and that Si and Al retard the decomposition of MA constituents during welding. Then, off-shore structure steels which can assure high critical CTOD at their HAZ was developed by TMCP together with a careful control of C, Nb, V, Mo, Si and Al to a minimum necessary level [11].

After a steam leakage incident caused by the rupture of a reactor coolant tube in a steam generator vessel in the Mihama NPS in Japan in 1992, most of steam generators were replaced by new

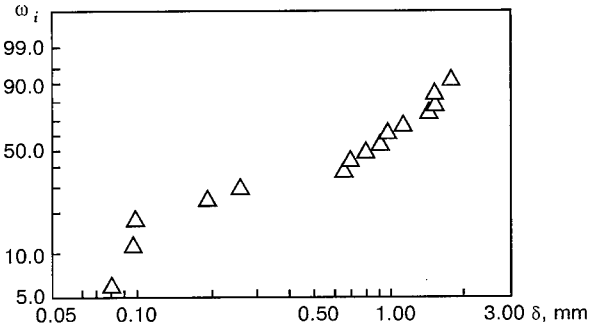

Figure 3. Value of CTOD in HAZ of ordinary steel welded by submerged arc welding (5 kJ/mm); ω_i – accumulated frequency; δ – critical value of CTOD

ones. Electron beam welding was first used for butt welding of ASME SA533 Gr.B Cl.2 steels in the new steam generators. To improve toughness of the electron beam weld metal, that is a remelting product of base steels, phosphorus was reduced as low as possible. The objective of the phosphorus reduction was to minimize the solidification segregation of phosphorus which is very detrimental to weld metal toughness.

Capability of arresting a running crack is required to the steels and/or their HAZ for specific steel structures whose structural integrity of a high degree is required such as LNG and LPG storage tanks. The fine grain Al-killed steels had been used to LPG tanks, while the 3.5 % Ni steels of a quenched and tempered (QT) type had been used to LPG tanks with a higher margin of safety. The control rolled and direct quench-temper (CR-DQT) process, one type of TMCP, facilitates grain refining and solid solution treatment of hardenable alloy elements. 1.5 to 2.5 % Ni steels produced by CR-DQT succeeded to satisfy the crack arrest property, K_{ca} requirement of 200 MPa $\sqrt{m}$ at −100 °C at the base steels.

For LNG tanks, whose arrest capability is required at −196 °C, 9 % Ni QT steels had been used. The employment of TMCP (CR-DQT, or CR-two stage DQ-T) markedly promotes the grain refining and the stabilization of residual austenite, resulting in satisfactory arrest capability not only in base steels but also in its HAZ. The TMCP 9 % Ni steel of the 50 mm thickness was used for a large LNG tank of a 200,000 kl capacity.

Recently, a new type of crack arrest steel was developed [12]. This steel is characterized by extremely fine grain microstructures at the plate surface. In brittle steels, a running brittle crack never forms shear lips of the ductile fracture fashion at the plate surfaces. The newly developed steel facilitates the shear lip formation at the plate surfaces and high arrest capability results. Fine grains at the plate surfaces are accomplished by hot rolling a plate at the time of increasing temperature, while the conventional hot rolling is conducted during decreasing temperatures. This steel is called SUF, i.e. surface layer with ultra-fine grain and is desired

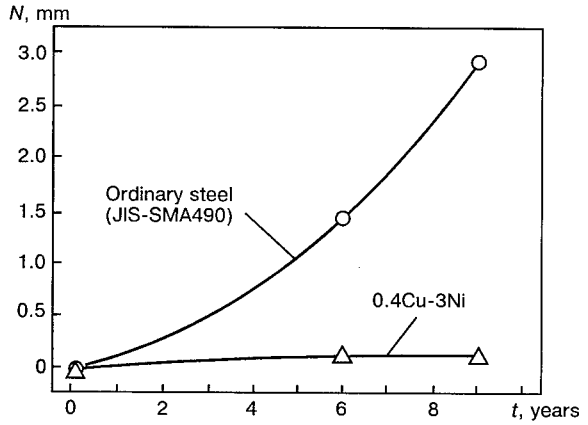

Figure 4. Change of penetration in steels used in near-shore conditions (atmosphere of coastline — 1.3 mg/dm^2/day); N — mean value of penetration; t — period of action

to be used for oil storage tanks in which a brittle crack must be arrested until the crack becomes catastrophically long.

The fatigue strength increases as the steel strength increases, provided welded joints are smoothly ground or machined. However, some discontinuity or notch concentration unavoidably exists at welded joints. In this case, fatigue strengths are governed by a notch concentration factor at welds rather than by the steel strength. A metallurgical factor contributes only to the fatigue crack initiation stage among the whole stage of fatigue crack initiation and propagation. When some discontinuities already exist in welds, fatigue cracks are ready to propagate and therefore, metallurgical microstructures have no effects on the fatigue strengths. In other words, it is a difficult task to develop a fatigue resistant steel metallurgically.

For ships and bridges generally subjected to cyclic loading during their service, the careful structural design is essential so that stresses do not exceed the fatigue threshold level, and concurrently smooth welds should be made during fabrication.

Corrosion-resistant steels. The weathering steel was first born as the COR-TEN steel in 1933 in U.S. Cu, Cr, and Ni are contained in this steel, forming the stable rust layer on their surfaces to prevent rust from growing into the inner base steels. Later, a modified weathering steel was developed by adding P and Cr to the COR-TEN type of steel. According to Japan Bridge Construction Association rule, the weathering steels are allowed to be used without painting, provided the service site is at some distances from the sea coast, i.e. under the condition that air-born salinity is less than 0.05 mg/dm^2/day. Recently, the 0.4Cu–3Ni weathering steel was developed [13]. This steel forms very stable rust under the coastline condition of high air-born salinity as shown in Figure 4.

The advantage of Zn-coated structures has emerged from an economical view point of the longer structural life and completely maintenance-free service. In the construction of Zn-coated structures, dip coating of zinc is conducted after welding fabrication. Therefore, liquid zinc embrittlement is likely to occur at grain-coarsened HAZ. The steel resistant to the liquid zinc embrittlement was developed in Japan. The chemical composition of this steel is controlled so that soft ferrite microstructures can remain along the grain boundaries of the coarsened HAZ [14]. The liquid zinc embrittlement is enhanced by the thermal distortion caused by hot dipping of zinc. It is important to take measures to minimize the thermal distortion in addition to the use of the zinc embrittlement resistant steel [15].

Corrosion of steel structures becomes harsh on coastal area and off-shore. It is considered that Cu- and P-bearing steels are effective at the splash zones while Cr-bearing steels are corrosion resistant in the sea. However, there is no carbon steel satisfactorily resistant to marine corrosion. Heavy painting and/or cathodic protection is needed for steel structures under marine environments. Recently, Ti-clad steels were used around the piers of the Trans Tokyo Bay Bridge, aiming the maintenance-free structure for a hundred year service life. The Ti-clad steels (with 1 mm thick titanium and 4 mm thick steel) were made by hot rolling two titanium plates and one steel plate with copper foil inserted between the titanium plates and steel plate. The Ti-clad steel plates were warped around the piers by welding the steel parts of the clad plate with piers [16]. The Ti-clad steels are very prospective for the construction of highly corrosion resistant structures under marine environments.

SSCC is caused by hydrogen entered from wet H_2S environments. SSCC occurs at the hardened HAZ because SSCC is one type of hydrogen induced cracking. Hardness increases especially at pipe-girth weld HAZ due to high speed welding, i.e. low heat input welding. Therefore, all the line-pipe steels for sour gas (wet H_2S) service are produced by TMCP which makes it possible to produce less hardenable steels.

Low alloy steel line-pipes are used for the transportation of processed gas and oil. However, unprocessed gas and oil must be transported in the deep sea, and stainless steels or high alloy line pipes are used. The duplex stainless steel (25Cr–9Ni–3Mo–2W–0.3N) was developed as weldable steels but they are expensive. Recently, the super 13Cr stainless steel (12Cr–6Ni–2.5Mo–Ti) of an economic type was developed in which a carbon content is reduced to 0.007 % from 0.02 % in the conventional 13Cr stainless steel for drilling pipes in order to improve the girth weldability [17].

The reduction of HAZ hardness is effective to prevent SSCC and the TMCP steels are extensively used as descried above. On the other hand, the

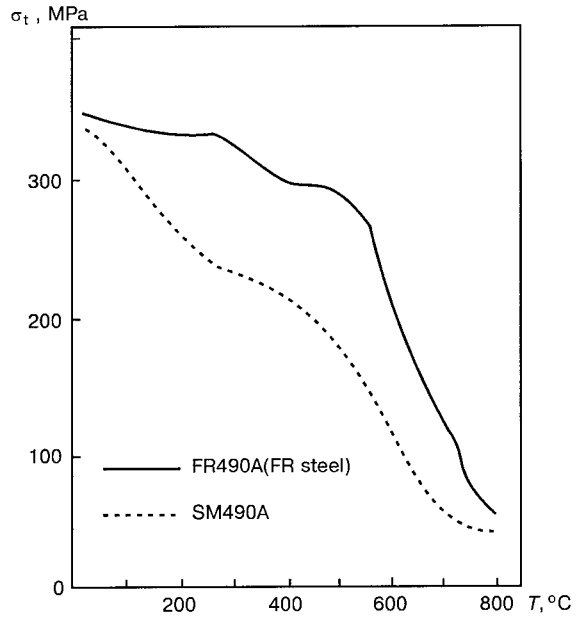

Figure 5. Ultimate strength of heat-resistant and ordinary steel at high temperatures

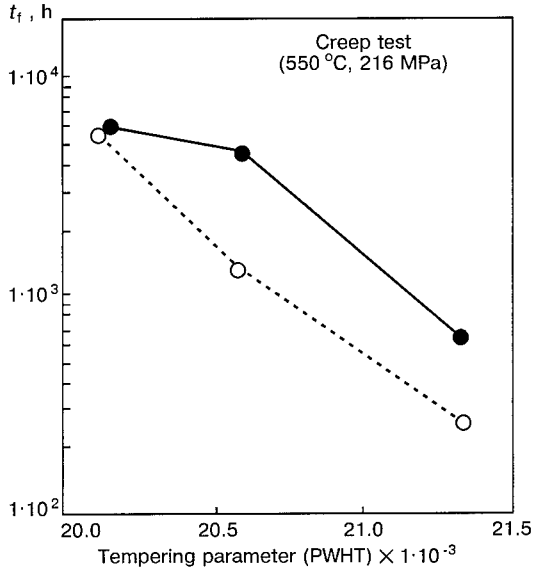

Figure 6. Duration of fracture t_f at creep of ordinary hardened-tempered steel and steel hardened from a cementation heating

occurrence of stress oriented hydrogen induced cracking (SOHIC) at the softened HAZ became a serious problem, but there is no metallurgical countermeasure against SOHIC.

In alkaline environments, stress corrosion cracking (SCC) is dominant. It is reported that there are no clear relationships between SCC susceptibility and steel microstructures. A survey on the amine acid gas absorbers revealed that no SCC was found in the absorbers on which PWHT had been conducted [18]. The major cause of SCC is not the hoop stress due to operating pressure but welding residual stresses. Carbon steels of the A516 grade are mostly used for the absorbers and PWHT must be employed. Stainless steels or clad stainless steel are recommended for severer corrosion environments.

High-temperature steels and welding materials. The Japan Ministry of Construction rule regulates that the temperature of steels in steel structures be 350 °C or less on the occasion of fire because the yield strengths of ordinary steels at 350 °C reduce down to a level of two-thirds of those at the room temperature. Figure 5 shows the temperature dependence of the yield strength of the fire-resistant steel and the conventional structural steel with the same strength at the room temperature. This result implies that no fire-protection coverings or the significant reduction of its use is allowed to the buildings made of the fire-resistant steel as long as the steel temperature does not exceed 600 °C. The high yield strengths at high temperatures are attained through precipitation hardening by the addition of Mo together with Nb or V [19]. The use of fire-resistant steels was not realized until a full menu of welding materials suitable for them had been developed for the whole welding process including SMAW, SAW and GMAW.

Cr–Mo steels are widely used as creep resistant steels. The modified 2.25Cr–1Mo–V steel has been developed which contains vanadium to raise the creep rupture strength at 482 °C [20]. A normalized (N) process or a conventional quenched-and-tempered (Q-T) process was employed to produce Cr–Mo steels, but recently the TMCP (DQ-T) process has replaced the conventional processes. Figure 6 shows the effect of DQ on the creep rupture time, indicating that DQ provides the Cr–Mo steels (2.25Cr–1Mo–0.25V–Nb–Ti) highly resistant to the softening during PWHT as well as to the creep rupture [21]. This improvement is attributed to the promotion of the refinement of austenite grains and the precipitation hardening. DQ-T was also employed to produce the 9 % Cr heat-resistant ferritic steels [22].

Austenitic stainless steels are used to boiler tubes for the steam temperatures over 570 °C. However, austenitic stainless steels have such shortcomings as higher thermal expansion rate, less thermal conductivity and higher susceptibility to SCC than ferritic steels. The modified ferritic 9Cr–1Mo steel with Nb and V exhibited higher creep rupture strengths at the temperatures up to 627 °C than austenitic SUS304 stainless steels. This steel is standardized as ASME T91/P91. The 9Cr–0.5Mo–0.5Mn–1.8W–Nb–V steel was newly developed by replacing 0.5 % Mo by W, Nb and V [23]. The permissible stress of this steel at the temperatures over 640 °C is 1.4 times higher than that of the modified 9Cr–1Mo steel.

Welding materials for boiler tubes are generally designed to be strength-overmatching against base steels so that creep rupture never occurs in the weld metal. For instance, a composition systme of 9Cr–0.5Mo–1.5Mn–0.6Ni–1.5W–Nb–V was used as

SAW welding materials for the 9Cr–0.5Mo–0.5Mn–1.8W–Nb–V steel tubes [24].

Earthquake-resistant steel. High-rise buildings in the earthquake prone areas must be designed to be earthquake-resistant. A concept of the earthquake resistance of buildings is that all the beam members should uniformly deform in a plastic manner to absorb earthquake energies while column members should remain in an elastic deformation condition.

Japan Industrial Standard (JIS) stipulated the SN400 (TS 400 MPa) and SN490 (TS 490 MPa) steels for buildings, specifying the low yield ratio (YR) and the narrow range of yield strengths. Accelerated cooling in TMCP facilitates the grain refining. However, the uniform fine-grain microstructures result in the increase in YR. In order to reduce YR, a mixed microstructure of soft ferrite and hard low-temperature-transformation products is desired. To obtain this kind of microstructure, a modified accelerated cooling process was introduced where the finishing temperature of hot rolling is raised and the start temperature of accelerated cooling is reduced to less than the transition temperature, A_{r3} [25]. In the high-strength steel of a TS 590 MPa grade, the low YR was attained by the employment of DQ-L-T where DQ is followed by the L-treatment conducted between the A_{c3} and A_{c1} transition temperatures.

The weld metal should be strength-overmatching so that distortion never concentrates in the weld metal of beam connection joints on a occasion of a major earthquake. However, the strength of the weld metal tends to decrease because the inter-pass temperature during welding construction tend to be very high due to the short weld length in building welded joints. The welding materials for buildings were developed which can guarantee the strength and toughness of the weld metal under the welding condition of the inter-pass temperature as high as 300 °C.

CONCLUSION

A number of new steels have been developed and they have made it possible to manufacture the welded structures for the severer use than before. The welding materials suitable for newly developed steels were also developed together with the steel development. It is obvious that the structural integrity of almost all the welded structures is governed by the performance of welds including weld heat-affected-zones of steels and weld metals. The cooperative development of steels and welding materials has been and will be important to improve the reliability of welded joints with regard to ductile fracture, brittle fracture, fatigue, corrosion, and/or creep.

REFERENCES

1. Shinada, K., Horii, Y., Yurioka, N. (1992) *Welding J.*, **71**, 253.
2. Kobayashi, E. (1985) *Proc. of Symp. on Welding Metallurgy of TMCP steels*. JWS.
3. Okamura, Y., Tanaka, M., Okushima, M. *et al.* (1994) Current advances in materials & processes. *ISIJ*, **7**, 523.
4. Jesseman, R. J., Murphy, G. J. (1983) *HSLA Steels, Technology and Applications*.
5. Irving, B. (1995) *Welding J.*, **4**, 39.
6. Miura, T., Katoh, T., Kamada M. (1999) *IIW Doc. IX-1959–99*.
7. Watanbe, I., Kojima, T. (1981) *J. JWS*, **50**, 778.
8. Kojima, K. *et al.* (1999) In: *Proc. of the 18th Int. Conf. on Off-shore Mechanics and Arctic Engineering*, Canada, St. John's, July. Newfoundland.
9. Funakoshi, T. *et al.* (1977) *Tetsu-to-Hagane*, **2**, 105.
10. Homma, H., Ohkita, S., Matsuda, S. *et al.* (1987) *Welding J.*, **10**, 301.
11. Arimochi, K. (1989) *Transact. of JWS*, **20**, 7.
12. Ishikawa, K., Hagiwara, Y., Aihara, S. (1996) *J. Soc. Naval Architects of Japan*, **177**, 259.
13. Kihira, H. *et al.* (2000) *Zairyo-to-Kankyo*, **49**, 30.
14. Kanaya, K., Takeda, T., Inoue, T. (1986) *Testsu-to-Hagane*, **72**, 1532.
15. Abe, H. *et al.* (1995) *IIW Doc.-IX-571–95*.
16. Kagaya, Y. *et al.* (1991) *Transact. of Japan Soc. Civil Engineers*, **435**, 79.
17. Ueda, M. *et al.* (1996) In: *Paper Corrosion/96 NACE Int. Anual Conf.*
18. Richert, J. P. *et al.* (1988) *Materials Performance*.
19. Kamata, Y. *et al.* (1991) *Technical Report of Sumitomo Metals*, **7**, 23.
20. Ishiguro, T., Ohnishi, K., Watanabe, J. (1986) *Tetsu-to-Hagane*, **72**, 70.
21. Shimoura, J. *et al.* (1988) In: *Proc. of 6th Int. Conf. on Pressure Vessel Technology*. Beijing.
22. Tsuchida, Y., Okamoto, K., Tokunaga, T. (1995) *Iron Steel Inst. of Japan*, **35**, 309.
23. Naoi, H. *et al.* (1991) *Seitetsu Kenkyu*, **340**, 302.
24. Morimoto, H. (1999) *Development of welding materials for W-bearing 9Cr creep resistant steels*. Doctoral thesis to Osaka University.
25. Ohashi, M. *et al.* (1989) *Seitetsu Kenkyu*, **344**, 17.

DEVELOPMENT OF TWO WIRES TIG WELDING WITH ELECTROMAGNETICALLY CONTROLLED MOLTEN POOL PROCESS

Yu. FUJITA[1], **Yu. MANABE**[2], **S. ZENITANI**[2] and **S. URAKAWA**[2]
[1]JWES, Tokyo, Japan
[2]Mitsubishi Heavy Industries, Hiroshima–Tokyo, Japan

ABSTRACT

In horizontal position, welding bead has an inclination to become hanging bead by gravity, and this problem makes horizontal welding difficult for high-deposition rate welding. To solve this problem, authors proposed a new concept of welding process, so-called electromagnetically controlled molten pool (ECMP) welding process. In this process the molten metal flow and bead shape are controlled by using upward electromagnetic force.

Key words: *arc welding, welding pool, filler wires, weld formation, electromagnetic control.*

The TIG welding process with ECMP using two filler wires simultaneously is proposed. For this purpose, two filler wire feeders are connected in series to a wire heating power source, and one wire is inserted at front position, and another is inserted at rear position of the arc. Wire heating current flows in the molten pool and improves the shape of weld bead. Also, the wire current increases wire deposition rate by Joule heating. In the test, stable welding was possible under high-deposition rate such as 100 – 150 g/min, and the bead shape was improved remarkably in proportion to the magnetic flux density. V-groove joint weld was done for stainless clad steel, and good penetration, smooth bead shape, sound weld joint property were obtained under high deposition rate welding conditions such as 100 g/min. After these basic tests, this welding process with ECMP was applied to a huge steel structure, and practicability of this process was proved by successful result.

In the horizontal welding of the large steel structures, such as steel stacks, bridges and ships, molten metal flows in an unexpected direction due to gravity, resulting in formation of irregular bead such as undercut and overlap bead, which sometimes causes welding defects such as lack of fusion at the next pass in case of multi-layer welding [1].

Under these circumstances, welding heat input and deposition rate are limited and inefficient welding work becomes unavoidable. Welding condition is also limited. These become serious problems in the practical application.

To solve these problems, authors had developed a new welding method called Electromagnetically Controlled Molten Pool Welding Process (hereafter referred to as ECMP method), where the current path inside the molten pool is controlled by electrified filler wire and magnetic field given to create an upward electromagnetic force, thus the flow of molten metal and the bead shape can be controlled, which prevents droplet of molten metal [2].

In this report, the results of examination of the high deposition rate (100 g/min; approximately 3 times of that of the conventional TIG Hot Wire welding process) of the same level as that of the flat welding as well as the method of increasing the upward electromagnetic force holding the molten metal are shown to promote further efficiency of the horizontal position TIG welding. That is, two filler wires connected linearly to the wire heating power source are inserted into the front and the rear of the arc respectively, thus allowing the welding under the external magnetic field given perpendicularly to the base metal. This is called Two Wire TIG Welding process with ECMP in horizontal position (hereafter referred to as Two Wires ECMP method).

This method is presented and a prototype equipment using this method is fabricated experimentally. Moreover, wire melting and welding phenomena under this method are examined and the results of its practicability verification through the application test to huge steel structures are reported.

This research is targeted mainly the horizontal TIG welding of the stainless steel and stainless clad steel that require quality joints.

Principle of Two Wires ECMP method is shown in Figure 1, *a*. This Figure shows details of the welding torch vicinity arrangement, external magnetic field given to the molten pool, one-directional current element and direction of electromagnetic force generated in the molten pool.

Two filler wires are inserted into the front and the rear of the molten pool. These filler wires are connected to the plus and minus of the wire power

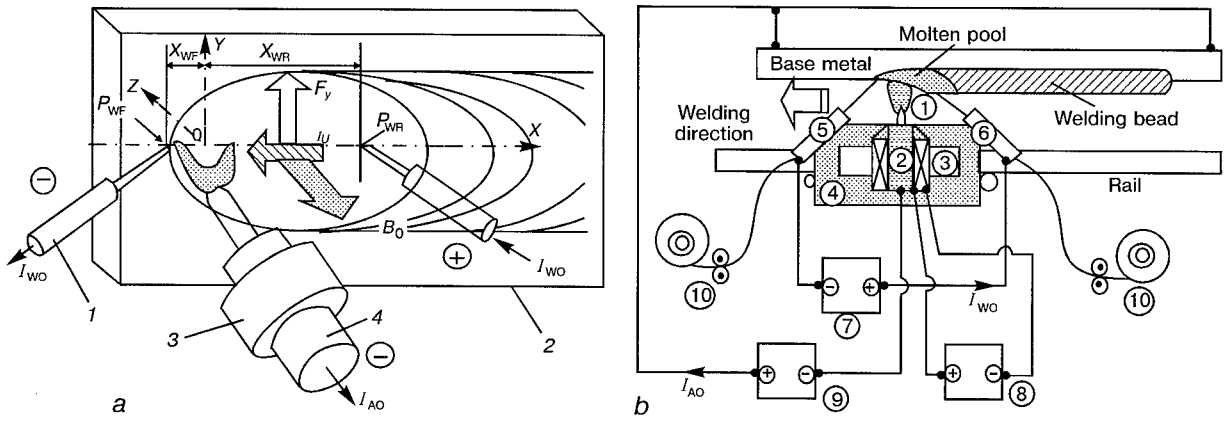

Figure 1. Schematic diagram of Two Wires TIG welding process with ECMP: *a* — weld area, position of welding torch, magnetic coil and filler wires (*1, 2* — front and rear wires, respectively, *3* — reel; *4* — torch); *b* — scheme of process of horizontal Two Wires TIG welding with ECMP (*1* — arc; *2* — TIG welding torch; *3* — magnetizing coil; *4* — carriage; *5, 6* — front and rear wires; *7* — wire heat source; *8* — device for magnetizing; *9* — welding power source; *10* — wire feeding mechanism)

source respectively, then electrified. At this point, a current path is formed between the wire insertion points in the molten pool. Here, a magnetic field acting perpendicularly to the base metal surface being given, an upward electromagnetic force is generated inside the molten pool, thus droplets of any beads can be prevented. In addition, the deposition rate can be increased by Joule heating the two filler wires through electrification against resistance.

Figure 1, *b* shows the experimental apparatus configuration for the Two Wires ECMP method. This equipment consists of the wire power source to electrify the filler wires, and the excitation equipment to give a magnetic field in the direction of base metal thickness to the molten pool.

For TIG welding, DC power source of 800 A rated capacity is used and the polarity of torch minus is applied. Grounding cables are connected to the ends of base metal to prevent the uneven distribution of the arc current and the associated magnetic arc blow.

For the wire heating power source, DC power source of 300 A rated capacity is used. This is connected linearly to the filler wires inserted into the front and the rear of the arc in the molten pool. Where, the front wire is connected to the plus while the rear wire is connected to the minus, creating the wire current flowing longitudinally across the molten pool.

The excitation power source of the magnetized coil can generate both alternate (AC) and direct currents (DC). DC is applied in this case.

For TIG welding torch, the water cooling type of 500 A rated is used. The magnetized coil is arranged coaxial to the welding torch as shown in Figure 1, *a*. As to the dimensions and magnetic flux distribution characteristics, the magnetized coil of the same characteristics as shown in the previous report [2] is used. In the area of high current density distribution in the molten pool (the area of 10 mm from the arc point), almost constant magnetic flux density distribution can be observed.

The welding torch, exciting coil and filler wire torch are mounted on the welding carriage. Welding is performed as this welding carriage is travelled.

As for specimen, commercial austenite stainless steel (JIS SUS304) of 10 mm thickness is used except for butt joint welding tests. For the butt joint welding test, the clad steel (12.5 mm of overall thickness) cladding 11 mm thick weatherproof steel SMA400AP with 1.5 mm thick austenite stainless steel (JIS SUS316L) is used in consideration of applying to the huge structures described afterwards. For the filler wires, 1.2 mm diameter austenite stainless (JIS SUS309MoL) solid wire is applied to every base metal.

Filler wire melting and bead formation phenomena. Figure 2 shows the welding phenomena when the external magnetic flux density B_0 and total wire feeding rate Σv_f are changed.

Welding bead appearances and cross sections are shown in Figure 2, *b* – *f*. Hatching section in Figure 2, *a* is an area where stable bead formation is possible, however, when Σv_f = 100 g/min is constant, the bead shapes show significant vertical asymmetry due to dripping at B_0 = 0 T (Figure 2, *b*). When the magnetic field of B_0 = 0.01 T (Figure 2, *c*) is given, the beads show favorable vertically symmetric shapes due to balancing between the push up effect of the upward electromagnetic force and the gravity.

When the magnetic flux density increases to B_0 = 0.015 T (Figure 2, *d*), molten metal is pushed upward due to excessive upward electromagnetic force and the contact angle at the top end of bead increases significantly. Shallow undercuts appear below the beads. In addition, bead bottom ends appear to be slightly snaking and the limit of magnetic flux density allowing stable bead formation becomes obvious. Moreover, when the magnetic flux density is increased as high as B_0 = 0.02 T (Figure 2, *f*), the molten metal at the bottom of bead splashes upward, causing a situation where bead formation is no longer possible.

Meanwhile, the lower limit of wire feeding rate is determined by arcing, this becomes 90 g/min

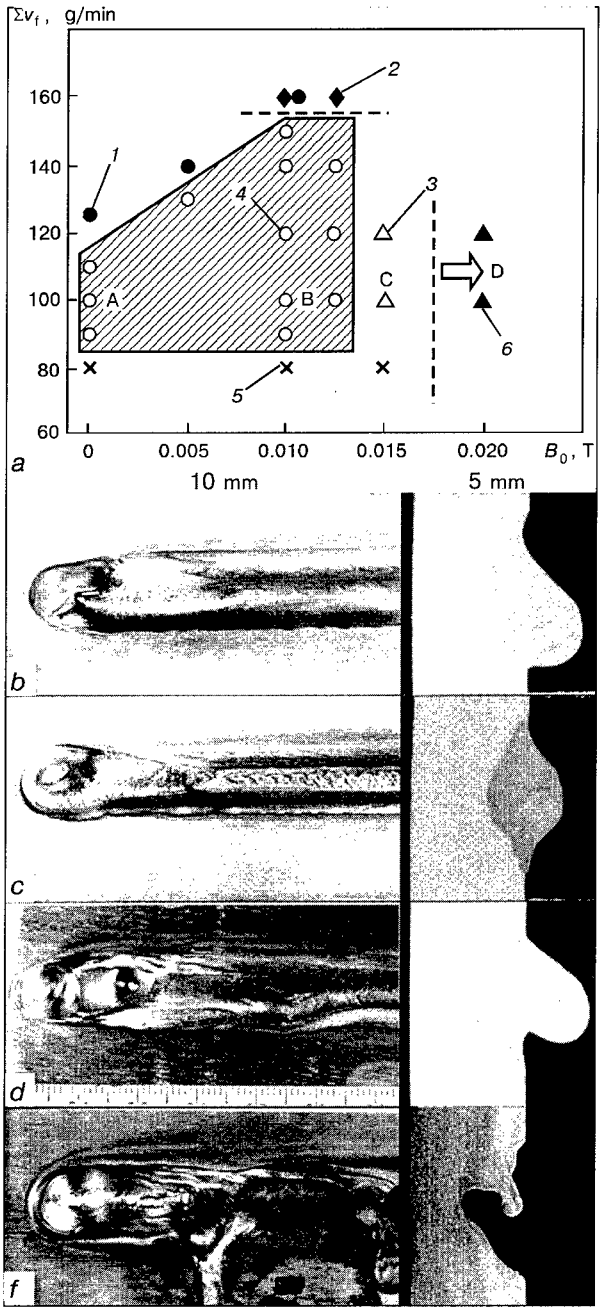

Figure 2. Effect of bead formation control during two wires bead-on plate welding with ECMP: two wires welding with ECMP at different wire feeding rates and density of a magnetic flux (I_{AO} = 500 A; I_{WO} = 120 A; v_w = 50 cm/min); *b* – *f* — appearance and cross section of weld beads at different density of a magnetic flow (I_{AO} = 500 A; I_{WO} = 120 A; Σv_f — 100 g/min): *1* — bead with droplets; *2* — unmelted rear wire; *3* — non-uniform bead; *4* — uniform bead; *5* — arc burning; *6* — metal spattering

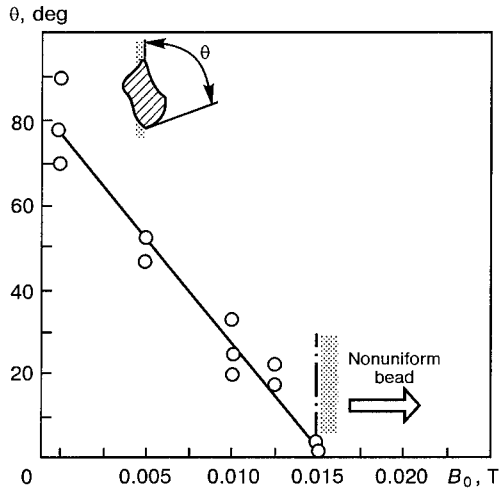

Figure 3. Contact angle θ of bead at different density of the magnetic flux B_0 (I_{AO} = 500 A; I_{WO} = 120 A); O — two wires (Σv_f = 100 g /min), welding speed is 50 cm/min

constant regardless of the magnetic field density. Upper limit of Σv_f is 110 g/min at B_0 = 0 T, above it, droplets are observed. On the other hand, at B_0 = 0.01 T, upper limit of Σv_f, enabling stable bead formation, increases up to 150 g/min because the upward electromagnetic force, which pushes up molten metal, increases as the magnetic flux density increases. At Σv_f = 160 g/min, molten metal droplets are observed and melting of the rear wire becomes unstable.

Effect on contact angle by magnetic flux density. As an index of improvement effect of buildup shape, Figure 3 shows the relation between magnetic flux density and contact angle, which poses a problem in welding quality of overlap bead, etc.

The contact angle decreases as the magnetic flux density increases. When the magnetic flux density B_0 = 0.01T, where welding bead formation is stable and the maximum shape improvement effects can be obtained, the contact angle decreases to approximately one thirds of that at B_0 = 0 T.

Based on the results of basic tests so far, aiming at practical application of this welding process to huge structures, horizontal multi-layer welding test is implemented using V-groove joint of stainless clad steel plate.

The joint geometry is shown in Figure 4, *a*. Macropictures of the surface of final layer, the back surface of first pass and the cross section are shown in Figure 4, *b* – *d*. As to the welding condition, for the first layer, arc current I_a = 320 A and total wire feeding rate v_f = 40 g/min are set to prevent excessive dilution. After the second pass, high deposition rate of v_f = 90 to 100 g/min at I_a = 450 to 500 A is applied.

Thanks to the above described bead shape control effects of electromagnetic force, stable work is ensured. Besides, favorable welding results without any shape deficiencies (lack of fusion) such as overlaps and undercuts are obtained.

Required man-hour can also be decreased by successfully reducing the multi-layer pass number eight for the conventional CO_2 welding process to five. Favorable results of sufficient strength and bending ductility are obtained even in the joint tensile test and the face and root bending tests.

Based on the results of basic tests so far, the method is applied to the block welding of huge steel structures composed of stainless clad steel of

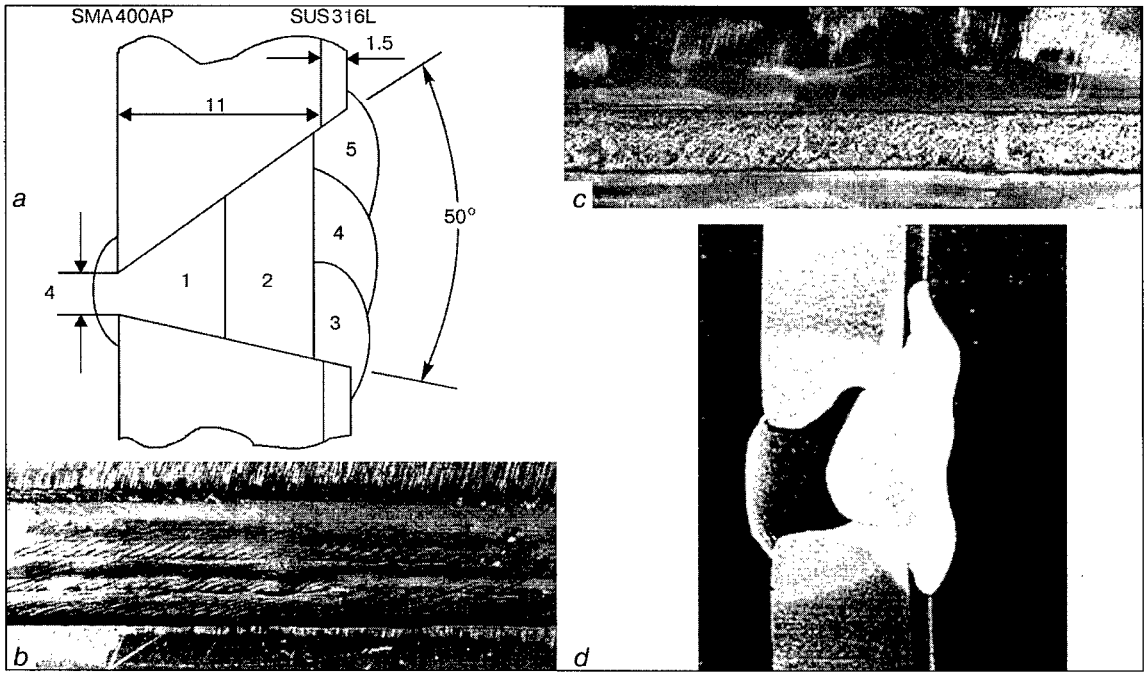

Figure 4. Results of two wires welding with ECMP of joints with V-groove: *a* — butt geometry and sequence of passes; *b* — cross section; *c* — surface of a last layer; *d* — reverse side of the first pass

the thickness and the groove shape as shown in Figure 4, *a*.

The single block is cylindrical with the diameter of 5 m and the height of 3 m. Circumferential in horizontal welding to joint blocks is implemented. The application situation is shown in Figure 5.

Similar to the joint welding test shown in Figure 4, high deposition rate of max. 100 g/min can be performed stably, and even in practical structures, this welding method enables approximately 3 times more efficient welding performance than the conventional TIG Hot Wire method.

CONCLUSIONS

In the horizontal welding process, molten metal flows in an unexpected direction due to gravity, causing welding defects and hindrance to welding efficiency. To cope with these problems, authors had previously presented the ECMP method which controls molten metal flow and bead shapes by electromagnetic force. In this research, the horizontal TIG welding using two wires ECMP method of even higher efficiency is promoted by doubling the wire application. Also, its practicability is evaluated through the application test to huge structures. Obtained results are summarized as follows.

1. The horizontal TIG welding method by electromagnetically controlled molten pool with two wires is presented. Bead shape improvement effects and deposition rate increasing effects, that are obtained using the current path control inside the molten pool by the electrification between two filler wires and the electromagnetic force generated by the magnetic field given, are verified to be significant.

2. In the joint welding of stainless clad steel, a favorable joint performance is verified to be obtainable by achieving approximately 3 times higher deposition rate welding than the conventional welding (TIG Hot Wire method).

3. This welding method is applied to the block welding (horizontal circumferential welding) of huge steel structures of stainless clad steel. Quality welding is verified at the same deposition rate as in the joint welding test; practicability of this method is proved.

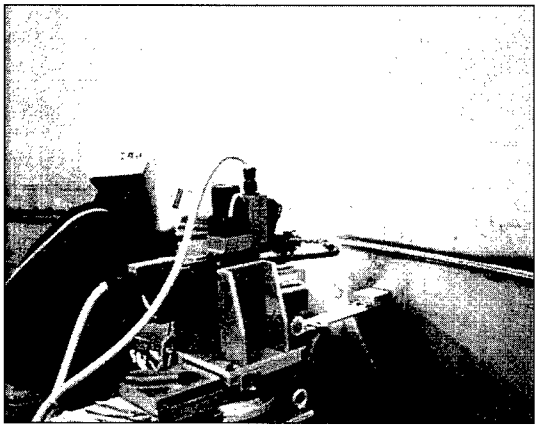

Figure 5. Detail of weld, arrangement of welding torch, magnetic coil and filler wire

REFERENCES

1. Wada, H. *et al.*(1998) Study on high efficiency by welding robot in construction site. *Industrial Management Practical Research Papers*, **5**, 78 – 87.
2. Manabe, Yu. *et al.* (1999) Basic concept possibility of electromagnetically controlled molten pool welding process. *J. of High Temperature Society*, **1**, 38 – 45.

INNOVATIONS IN JOINING TECHNOLOGY — PROCESSES AND PRODUCTS FOR THE FUTURE

D. VON HOFE and **K. MIDDELDORF**
DVS, Dusseldorf, Germany

ABSTRACT

Promising areas of development of different materials (steels, light metals and alloys, metal foams, composites, polymers) are considered. It is noted that in the future welding and related technologies will be the preferred methods, because of their high productivity, high degree of automation and simulation.

Key words: *welding, cutting, coating, joining, technology, materials, market of the future.*

People–Technology–Environment–Quality [1 – 6]. Society's increasing sensitisation to environmental questions is linked to people's concern about their own well-being and about that of future generations. People's wishes for safety and security apply to their environment in general and, specifically, to their local environment, e.g. to their place of residence and workplace. In this connection, general expectations are directed at technology with which, however, fears are also associated — this is applicable to joining technology as well. Whereas priority was, in the past, almost always given to technical questions (e.g. the improvement in the mechanical and technological properties of the joints), other main focal points have been added in recent years, such as:

- conservation of the environment;
- economical handling of energy;
- conservation of raw materials;
- improved benefits for the user.

Consideration is now also given to environmental influences resulting from the use of joining-technology processes as well as to possible health hazards caused by harmful substances. This is supplemented by approaches relating to achieving an ecological balance. Furthermore, products and processes are no longer assessed solely according to the aspects of their compatibility with the environment and their conservation of resources but instead also according to the more extensive approach with regard to their sustainability. Sustainable economic activity offers the prerequisite for economically successful actions. For all sectors of technology, this results in the following objective: to meet the customer demands while minimising the utilisation of personnel, material and energy and maximising the productivity and thus profitability — this with the best possible conservation of resources and the minimum environmental pollution.

In the fields of joining, cutting and coating (as in other sectors), the trend is emerging on the user side towards covering the requirements for devices, filler metals, consumables and miscellaneous accessories with the aid of system suppliers (so-called tool shops). This trend towards purchasing from one source will not only influence and change the current dealer system in an enduring way but will also lead to restructuring measures on the part of the manufacturers of these products.

In the concurring opinion of the American Welding Society and the DVS, the processes of joining, cutting and coating will, in the future as well, be the preferred methods for the successful processing of the widest possible variety of materials into marketable products. However, in future, welding-technology processes will ever less frequently be understood as an «obstacle» to a «rapid» and smooth fabrication process, but will instead also be increasingly included in the deliberations in all the phases relating to the design, development and fabrication of a product. This interdisciplinary approach will be pursued in a consistent manner and the «isolation» of the joining, cutting and coating processes in the overall manufacturing process, which can still often be found today, will soon be a thing of the past.

On the basis of these fundamental statements, it is possible to define the following theses.

Costs and Productivity. Cost-favourable joining-technology processes with increased productivity and further improvements in quality are becoming an integral part of the manufacturing processes. Optimum solutions can be achieved by means of the best possible combinations of the joining processes while making use of their respective strengths. They are pursuing a process of consistent automation. It will soon constitute the state of the art to use simulation techniques in order to model the processes. Simulation technology is thus becoming the key to the further development of the joining processes.

Technologies and Processes for the Markets of the Future. New technologies and simulation processes for the modelling of complete fabrication sequences as well as the utilisation of innovations from information and sensor technology lead to consistently open and compatible, user-friendly systems

(plug and play). The possibilities of the virtual world will play a decisive role in this respect. Product-development cycles will become even shorter. Joining, cutting and coating technology can then be defined as a kind of guiding technology. It will thus be possible not only to safeguard the current areas of application of joining technology but also to open up new promising fields.

Quality Standards. The manufacture of high-quality joints and coatings without the necessity of subsequent inspection as well as methods for the precise prediction of the service lives of structures and products will basically confer upon the products the image of being «safe» and «reliable».

Material Developments. For 2020, it is assumed that industry will, for various reasons, require alternatives to 95 % of the materials used in the fabrication process today. With regard to their development, greater attention must be paid to ensuring that they can be joined, cut and coated safely. Developments relating to the materials and in joining technology will reciprocally create innovative solutions. This connection is considered in Chapter 3 of this contribution.

Training and Advanced Training. Since the specialist competence of the employees in a company on the one hand and the economic viability of the production and the product quality on the other hand are inextricably linked to each other, even greater significance will be attached to the qualification of the personnel in future. Together with modern devices and installations as well as optimised design concepts, qualified personnel will become one of the crucial production factors.

The aspects of material developments, applications and joining technologies are to be dealt with in greater detail below.

Material Developments [7, 8]. New materials for innovative applications are undoubtedly one of the most strategically significant technological targets in our economy. New materials are an important building block for processes and products which conserve resources, the environment and energy. They provide impetus for innovations whose effects, on the one hand, extend into the living world and into people's everyday life and, on the other hand, relate to global competitiveness.

The main focal points with regard to the research into and development of materials are shifting ever further away from generating materials with the best possible properties, such as the highest strength, the greatest corrosion resistance, the highest toughness or the highest electrical conductivity. Instead, the trend is heading towards the «design material», i.e. towards the development of materials which can perform a certain task in an absolutely specific way while meeting the targets relating to economic viability. Nowadays, innovations in material development thus no longer necessarily entail just new but rather the best possible material solutions to a clearly outlined problem. Therefore, the multi-material design according to which the material suitable in each case is used at the correct position in the structure is increasingly taking effect with regard to the areas of application. In this respect, material developments must not be considered in an isolated way. Success with regard to the introduction of new materials can only arise in accord with their manufacture and processing and with new construction methods. Another factor relates to the requirements for their reutilisation. The necessary cost accounting must be carried out in such a way as to include all the follow-up costs which are incurred during the entire life cycle. In this respect, increasing significance is being attached to the further development of the process technology for the manufacture and processing of materials which are already being used as well.

One essential criterion for every newly developed material is its weldability.

This results in the following necessities:

- proof of the fundamental weldability of newly and further developed materials using conventional welding processes and/or new and alternative joining techniques;
- new or further development of suitable filler metals and consumables which are appropriate for the combination of the process, material and application purpose.

In this respect, material development encompasses all groups of materials, not only the metallic and non-metallic materials but also material compounds and composite materials. The current status of development in the following groups of materials is addressed below:

- metals – steels, light metals and metal foams, light-metal matrix composite materials;
- polymer materials and fibre-reinforced polymer materials;
- ceramics and nanomaterials.

Steels. Steel will remain the most important construction material in future as well. No less than half of the around 2,000 steel grades which have been registered in the meantime have come on to the market in the last five years. The principal areas of application in Germany are for processing in the first production stage (40 %), for vehicle construction and mechanical engineering (15 % and 10 %, respectively) as well as for the building trade and structural steel engineering (12 %). However, the economic significance of steel products is considerably greater because, as a rule, their proportion of the value added also increases along with the processing stages. Moreover, in many cases, central components which determine the efficiency of the entire installation are manufactured from steel. This applies to wideranging fields of power engineering, traffic technology and medical technology. For example, special emphasis is placed on the parameters of efficiency, emissions and power density in the construction of power stations and aircraft engines. The elevated-temperature strength of the moving blades in the first row of turbines (today, these moving blades are made of superal-

loys or special steels) is decisive for the efficiency of the turbines. The particular advantages of using steel are:

- reusability (recycling);
- design diversity, also taking account of aesthetic aspects;
- good processing possibilities.

As the knowledge in the fields of metallography and metallurgy as well as in material engineering has grown in the past decades, this has meant that assured knowlege about the steels is now available for practically all applications and stress types.

This is applicable with regard to:

- high-strength fine-grained structural steels for automobile construction;
- duplex and superduplex steels for apparatus and plant engineering;
- high-temperature steels for the construction of power stations;
- coated materials, sintered and foamed metal materials as well as materials for sandwich constructions.

It has been proven that the development of high-strength and high-temperature steels has also provided fundamental stimuli for welding technology. For example, economically viable gas-shielded metal-arc welding processes and submerged-arc welding processes with appropriate filler metals are being developed for high-strength fine-grained structural steels and high-temperature ferritic chrome steels.

Light Metals and Metal Foams. Light metals are becoming increasingly important all over the world as innovative materials with diverse applications and combinations in industrial production. Nowadays, light metals are being used for applications ranging from automobile and aircraft construction to medical technology.

Aluminium Alloys. Application possibilities of aluminium alloys are being investigated intensively in Germany as well. Examples of newly developed aluminium materials are the hardenable and weldable aluminium alloys on a magnesium-silicon or magnesium-lithium-scandium basis. This group also includes the aluminium-lithium-copper alloys which were recently developed for the construction of aircraft. The metal foams also fall into the category of the new metallic aluminium materials. For example, for the core of the aluminium foam sandwich (AFS), aluminium powder with a low melting point is mixed homogeneously with a titanium hybrid. The high strength of these foams and their low weight allow new construction concepts to be developed. In the search for appropriate joining techniques, the suitability of various processes is being investigated at the moment.

Even now, aluminium and its alloys are already playing a dominant role in the construction of rail vehicles – 80 % of all the carriages for passenger transport consist of this light metal which is also becoming ever more important for the construction of high-speed ferries.

With the introduction of aluminium alloys into large-scale series fabrication in various sectors, ever more stringent demands are being made on the welding processes as well. Here, increasing significance is being attached to MIG tandem welding as a high-productivity welding process with high welding speeds and high deposition rates. Because of its technical conditions, this process can be fully mechanised. Furthermore, friction stir welding will lead to a decisive extension to the processing range of aluminium alloys. Thus, aluminium alloys (even those which cannot be joined using conventional fusion welding processes) can be joined using friction stir welding.

Magnesium Alloys. Because of the growing significance of the environment, interest is centred on weight-saving and thus on increased fuel efficiency and lower emissions, especially in vehicle construction as well. This fact results in the need for materials which are as light as possible, such as the magnesium alloys. This material is being used to an increasing extent due to the development of high-purity magnesium alloys with greatly improved corrosion properties. Such high-purity alloys in particular have a high application potential in aviation and space travel (frequently together with appropriate coatings). It is also possible to manufacture alloys which contain yttrium and neodymium additives and whose strength and ductility behaviour is equivalent to that of high-strength aluminium alloys. Moreover, the wear resistance can be increased by adding hard ceramic particles. Thanks to the possibility of manufacturing high-quality series components in mass fabrication with optimised costs with the aid of the die-casting process, the automobile sector is one branch of industry where magnesium alloys are already being processed on a large scale or where this will be possible in future. Examples of applications are: gearboxes, rocker covers, instrument panels, steering wheels, carburettors and car wheel rims.

In any case, further research and development efforts are still necessary with regard to the weldability of magnesium alloys. However, it may be stated in general that, if attention is paid to the material-specific peculiarities, it should be possible to use not only the gas-shielded arc welding processes and plasma welding (TIG processes) but also laser-beam welding in order to manufacture joints with the same quality characteristics as those achieved when aluminium alloys are welded.

Titanium Alloys. Materials on a titanium basis with high temperature stability are manufactured, amongst other items, as alloys with 45 – 48 % aluminium and other metallic additives. In this case as well, the application development is concentrated on the system concept, i.e. the control over the entire process from the material generation and the fabrication technology (i.e. the joining technology as well) to the finished product. Initial parts such as engine valves and turbine engines and blades have already been manufactured from inter-

metallic titanium aluminides which have significant advantages in comparison with the materials used until now. They are only half as heavy as nickel and iron alloys and withstand higher temperatures than normal titanium alloys.

The plasma welding of titanium and the friction stir welding of titanium alloys are suitable joining processes for this group of materials. Titanium alloys, which are important for the aircraft industry, can be joined in a mechanised process by means of argon-shielded metal-arc welding.

Light-Metal Matrix Composite Materials. The specified groups of materials on an aluminium, magnesium and titanium basis are also extremely important as a matrix material for corresponding composite materials. Fibre-reinforced and particle-reinforced composite materials are the starting point for extending the utilisation potential into areas where priority is given to reducing the weight of components.

Development objectives for such composite materials are, for example:

- increasing the yield strength and tensile strength at room temperature and at elevated temperatures while maintaining the ductility;
- increasing the creep resistance at elevated temperatures;
- increasing the fatigue strength at elevated temperatures;
- improving the thermal fatigue resistance.

It is obvious that these composite materials necessitate correspondingly adapted joining technologies which are, in most cases, still in the development phase. However, it is already emerging that TIG welding and gas-shielded metal-arc welding appear to be suitable processes for the joining of light-metal matrix composite materials.

Polymer Materials and Fibre-Reinforced Polymers [7 – 14]. Because of their versatility, additional areas of application are constantly becoming accessible to the polymer materials. Germany accounts for approximately 10 % of the world-wide production of plastics of around 140 million tonnes and is thus by far the largest single producer within Europe. Until now, the synthesis of new monomers (i.e. of new building blocks for new types of polymers) has been regarded as the motor of development. However, an evident change is emerging at the moment. This change is characterised by the combination of known monomers in order to form new so-called polymer blends (as it were, alloys of different polymers) and material compounds with fibre or particle reinforcement which can be used in order to achieve certain properties in a targeted way. For the future, it is expected that these mateirals will increasingly be tailored to specified applications and will therefore compete not only with glass or metals (as was the case until now) but instead with other polymers to a greater extent.

In the case of the high-performance polymer materials, Germany has a 15 % share of the world market and thus occupies a good starting position at least in Europe which reaches 33 % in total. The market leader is the USA with 36 %, followed by Japan with 31 %.

The «intelligent» materials, which are extremely light as well, include the fibre-reinforced polymers. However, since they exhibit hardly any dead weight, disturbing vibrations often occur in the case of lightweight structures. So-called adaptive structures which detect mechanical changes and actively react to them should provide a remedy here. Such intelligent fibre-reinforced composite materials should muffle engine noise, make lenses more precise and recognise damage such as cracks in components.

As a rule, glass fibres and carbon fibres are used for reinforcement purposes. Because of their potential for lightweight construction, fibre- reinforced polymers are today already used in aircraft construction and, to an increasing extent, in the construction of road and rail vehicles as well.

The application possibilities not only of the polymer materials but also of the fibre-reinforced polymers necessitate suitable joining techniques. Until now, ultrasonic welding has been put to widespread use not only for semi-finished products and moulded parts made of thermoplastics but also for fibre-reinforced polymers. One new aspect is the attempt to weld thermoplastics by means of the targeted input of energy using microwaves.

The development of the welding of polymers is closely connected with the development of the polyvinyl chloride (PVC) material. The development of the polymers setting in according to that has given rise to a series of new problems associated with the welding of series parts and has thus exerted an enduring influence on the development of the most important welding processes. It is primarily the following welding processes which are used for the welding of polymers in pipeline and tank construction and in apparatus and plant engineering:

- hot-gas welding;
- heated-tool welding;
- hot-gas extrusion welding.

Ultrasonic welding, vibration welding, rotational welding and high-frequency welding are also used in series fabrication. In recent times, infrared welding and laser welding have also become established as supplementary processes.

Ceramic Materials and Nanomaterials [7, 15 – 18]. The world market for base materials for high-performance ceramic materials is registering a continuous rise in production figures. Whereas the turnover was still only DM 2 billion in 1990, the market volume had already grown to DM 3.2 bil-

lion in 1992. A turnover of just under DM 5 billion is already being expected for the present time. As in the case of the metals, the next stage of value added is many times higher. Therefore, a figure of DM 55 billion is being assumed at the moment. The growth predictions are for 7 – 10 % per year.

The world market for structural ceramics is shared as follows: Japan 41 %, the USA 32 % and Europe 25 % (two-fifths of which is accounted for by Germany).

The example of a ceramic valve illustrates that the design of a component can ultimately be less expensive than the successful development of the manufacturing process, including the finishing of the hard ceramic.

In the form of substrates, sensors, actuators and sound transformers, ceramic materials are being introduced (for example) into such growth-oriented fields of information technology, data processing, electronics as well as automobile and aircraft construction.

The application of ceramics in medicine, which has grown sharply in the past years, should be mentioned as well. Examples of this are, amongst other items, ceramic hip-joint prostheses with outstanding tissue tolerance, tooth implants and bioactive, bone-friendly ceramics.

Ceramic materials are a good example of the need for parallel developments in joining technology. While it frequently used to be possible to apply a joining process without any major scope of development work for one group of materials and for various material thicknesses and dimensions, modern materials often require complicated testing and process adaptation not only to the special material but also to the material thickness, workpiece dimensions and operating conditions. A metal-ceramic joint which, for example, can be manufactured with certain dimensions and at operating temperatures below 100 °C using a specific process requires, in some circumstances solely because of the thermal expansion which cannot be adjusted completely to larger dimensions and higher temperatures, a totally different and, in part, specially adapted joining process. If this scope of work is not performed, it is not possible to achieve a joining result which is satisfactory with regard to technical and economic aspects. As one result of corresponding research and development work, a two-beam laser process provides good welding results in the case of an aluminium-dioxide ceramic. One CO_2 laser is used for heating purposes in the supply line and a downstream Nd:YAG laser welds the workpieces.

The future potential of material research is symbolised by the nanomaterials. Nanotechnology permits material development at the atomic and molecular level not only for the manufacture of composite materials with components in the nanometre range but also for the production of structures in this order of magnitude. Here, there is, above all, a demand for joining, cutting and coating processes which have no or only a minor influence on the complex material properties.

Design Concept for Lightweight Construction [1, 5, 8, 19, 20]. As already mentioned, some of the above material developments are directly related to the design concept for lightweight construction. A number of materials and new types of design concepts on the one hand and the existing possibilities in joining technology on the other hand are competing or cooperating with each other here. It is precisely this field which embodies the diverse possibilities resulting from the optimum combination of the material, the design appropriate for the material and the joining processes specifically adapted to the material. In many industries which are significant for the national economy (such as vehicle construction, shipbuilding, mechanical, apparatus and structural steel engineering as well as environmental technology), lightweight construction is leading to great weight savings and thus to associated advantages. The potential existing here is far from being exploited to the full and will, in future as well, make additional rewarding fields of activity accessible to research and development in the areas of material science and metallurgy as well as with regard to joining technology.

Lightweight-construction concepts are exploited in various areas of application. It is particularly the following materials which are used for lightweight construction in the road-vehicle industry: optimised steels, aluminium, magnesium as well as materials reinforced with glass and carbon fibre.

One well-known example of the successful implementation of this concept is the ultra-light steel auto body (ULSAB) which has been developed by the steel industry in international cooperation and with which a 25 % weight saving has been achieved in comparison with conventional steel auto bodies. The further development also involves doors, tail gates, suspensions, springs and shock absorbers (ULSAC – ultra-light steel auto closures and ULSAS – ultra-light steel auto suspension). Their consistent reduction is described by the ULSAB-AVC (advanced vehicle components) project. The all-embracing consideration of the entire vehicle and of the processes also incorporates the overall energy balances with extensive conservation of energy and resources as well as a complete recycling system.

Tailored blanks (i.e. laser-beam-welded sheet bars with locally optimised characteristics and a combination of sheet thicknesses, strengths and anti-corrosion protection appropriate for the stresses) also exert a crucial influence on the implementation of the lightweight concept in the construction of road vehicles.

It is precisely tailored blanks to which increasing importance is being attached in the construction of road vehicles. Whereas the demand for tailored blanks amounted to approx. 50,000 t in 1993, a demand of 450,000 t is being forecast for 2000.

In aircraft construction as well, the continuing compulsion to save fuel and to further decrease the emission of harmful substances is leading to intensive endeavours to reduce the structural weights by using lighter, high-strength materials. In this connection, it is interesting that the development in the aircraft industry is aimed more at welded structures in order to achieve material savings by avoiding riveted designs and the overlaps caused by these.

Developments and Further Developments in Welding Technology [14, 21 – 24]. At the same time as the new and further development of materials, the existing welding processes must be modified or optimised in a material-specific way or new types of welding processes must be developed. In addition to the further development of conventional processes such as manual metal-arc welding and gas-shielded arc welding, it is particularly in the field of laser-beam welding and cutting that substantial progress has been made. This is shown by their increasing acceptance in many fields of industrial and manual fabrication. Considerable advances have also been made with regard to adhesive bonding and mechanical joining. A material can only be used successfully if the joining technique is suitable. All the material developments prove emphatically that the development of materials is only half the job and that the integrated approach described at the beginning must instead be pursued in a consistent way.

It may be assumed that arc welding technology will be able to maintain its leading position in the near future. In this respect, processes and devices will be developed further. Resistance welding technology will also continue to be extremely important in its typical areas of application but will have to surrender market shares to alternative processes such as mechanical joining. Studies relating to the development of turnover in 1999 show that approx. 20 % of the total turnover from metal welding installations is accounted for by resistance welding installations. An increase of up to 15 % is expected by 2003. However, the processes will be supplemented by adhesive-bonding technologies and by mechanical joining processes such as clinching or double-bend joining.

For the joining of newly developed materials and combinations of materials, ever greater significance will be attached to the special welding processes such as friction welding and diffusion welding. In this respect, it will also be possible to increase the economic viability of these processes through the development of new process variants or the combination with upstream or downstream heat treatment or forming processes.

Current examples of the process development with regard to the special welding processes are linear friction welding and friction stir welding whose origin is to be sought in the friction welding process.

In the case of friction stir welding, the welding process (as with rotational friction welding) is carried out below the melting temperature of the materials to be joined, in the boundary area of the heterogeneous «solid-liquid» phase field, i.e. in the pasty state. Therefore, it is also characteristic of this process that the heat input into the material is limited to the direct vicinity of the weld. Using friction stir welding, it is no problem to manufacture longer, high-quality butt and lap welds. The process is also used in the vehicle industry in order to fabricate panels and profiles with large cross-sections and with weld lengths of up to 14 m.

While the friction stir welding process is already being put to more widespread use with aluminium and magnesium and their alloys (it can also be used for copper, titanium, zinc and lead), its utilisation possibilities with steel sheets have not yet been investigated comprehensively in spite of initial promising tests. However, interesting results may certainly be expected here in future.

The extent to which laser-beam welding has already been introduced into the operational fabrication process is shown by the example of laser-welded sandwich components made of steel for structural elements in shipbuilding. However, laser-beam-welded components made of steel are not used solely in shipbuilding but instead in a large number of other areas of daily life. Bridges, rail vehicles, shaft walls and shuttering, steel structures and tanks are just a few applications which can be mentioned in this context.

The manufacture of bottom plates in the tunnel area with different wall thicknesses can be cited as an example of the application of laser-beam welding in automobile construction.

In addition to the well-known and widely used CO_2 and Nd:YAG laser-beam sources, new welding applications are being opened up by diffusion-cooled CO2 lasers and diode-pumped multi-kW Nd:YAG lasers. Additional impetus for applications is to be expected in particular as a result of the further development of the high-power diode lasers. The introduction of scanner optics leads to so-called «remote welding systems» for three-dimensional structural elements with high productivity. The multi-spot technique in which it is possible to make efficient use of the expensively generated laser energy by means of a multi-beam distributor module can be used in order to manufacture welds in a particularly efficient way. As with all welding processes, the laser technology used will

basically be oriented towards the application requirements.

Electron-beam welding will be able to retain, and probably extend even further, its importance for the joining of highly reactive materials and of workpieces requiring particular cleanness.

The hybrid technologies constitute another promising development direction.

Hybrid technologies provide advantages by making use of synergetic effects resulting from the combination of two or more joining processes. One interesting hybrid joining process is, for example, gas-shielded metal-arc welding in combination with laser-beam welding. This combination of processes permits a higher welding speed although the laser-beam power is reduced by 40 %. It also allows the welding process to be adapted in a better way to conditions relating to fabrication technology and material science. The process is equally suitable for steel and other materials. Another example is the combination of the laser beam and the arc (as is used for the welding of aluminium profiles) where the laser welding process is supported by a microplasma welding system. Hybrid technologies are also used in order to join brittle materials such as ceramics and for glass.

The following tendencies are emerging with regard to the future of joining technology:

- established welding processes are being substituted in part or in full;
- the ongoing rapid development in the fields of microelectronics and microsystem technology is exerting a positive influence on the further development of the periphery of joining technology. Those areas concerned are, for example, sensors, actuators as well as process control and regulation;
- the progress in computer technology on both the hardware and software sides is opening up for simulation technology possibilities whose effects with regard to joining technology as a whole are, as yet, unforeseeable;
- the development of new materials and design concepts is creating the necessary prerequisites for additional innovative joining techniques and intelligent services;
- automation as a result of constant progress in robotics.

Below, a few welding processes are to be considered in greater detail with regard to future development trends and research necessities.

Arc Welding. In future, there will be a need, above all, for welding processes or process variants which permit further increases in productivity with an assured quality of the welded joints. The more frequent utilisation of new materials (especially of non-ferrous metals) necessitates the further development of the existing arc welding processes.

Existing arc welding processes can be developed further by means of electronic welding power sources, process analysis, process control and process optimisation. This also includes the dynamic simulation of the metal transfer on the basis of volume-of-fluid methods. Parameters for gas-shielded metal-arc welding processes can be generated using neural networks. The time required for the development work on new process variants will be shortened considerably by such procedures. An improvement in the reproducibility of the process parameters gives rise to an increase in the fabrication certainty and reduces the scrap by the post-weld machining times.

Resistance Pressure Welding (and Allied Processes). As has been the case until now, the resistance pressure welding processes in which the joint is manufactured with the effect of force and with conductive or inductive heating can fulfil with high productivity ever more stringent requirements resulting from new materials and joining parts with product-specific surface modifications. In this respect, special emphasis is placed on the following aspects:

- process regulation and quality assurance in the fabrication process (development of intelligent fabrication systems, amongst other items, on the basis of mathematical methods such as fuzzy logic, neural networks and numerical process simulation);
- measures in order to increase the electrode lives;
- process simulation (experimental and numerical);
- environmental compatibility and safety at work (e.g. susceptibility to electromagnetic interference).

Special Welding Processes. Special welding processes in which the joint is manufactured below the melting temperature by means of pressure and/or heat allow the manufacture of temperature-resistant, vibration-resistant, vacuum-tight and low-deformation joints for combinations of materials with different joining-part geometries for which other processes such as brazing and soldering, adhesive bonding, fusion welding or mechanical joining do not lead to the desired success. Furthermore, the special welding processes are characterised by low distortion, high repeat accuracy of the welding results, short cycle times and low environmental pollution.

The following aspects are being discussed in particular:

- joining of different metals which cannot be joined with each other by means of fusion welding;
- joining of components with extremely low material thicknesses or diameters and of components with extreme differences in thickness;
- manufacture of products in one operation from one material;
- joining processes with an extremely low welding temperature and a low thermal load.

Beam Welding Processes. If special emphasis is placed on precision and/or on difficult-to-weld materials where conventional welding processes often fail, it is possible, depending on the application, to use laser-beam or electron-beam welding. Even the vacuum in electron-beam welding, which is detrimental at first glance, can be used advantageously for high-quality joints or in the case of reactive metals. Furthermore, it is possible to drastically reduce non-productive times for the evacuation of the work chamber by using vacuum locks or jigs. Non-productive times are eliminated all together if the electron-beam welding process is performed out of vacuum.

Particular attention must be paid to the following points:

- improving the plant engineering and introducing new types of installations and installation concepts;
- improving the physical and mathematical models for the energy input into the workpiece so that the welding results can be predicted in a better way.

Due to the great variation range of the materials and material thicknesses which can be welded using the beam welding processes, an increasingly wide spectrum of application possibilities is available to the electron and laser beams.

The out-of-vacuum electron-beam welding installation which leads to the introduction of a new welding process is regarded as a new type of installation. Out-of-vacuum welding with the electron beam promises to revolutionise beam welding, particularly in the case of parts for lightweight construction.

Research projects dealing with the physical and mathematical understanding of the beam welding processes are contributing to the development of models which allow the welding result to be forecast on the basis of the welding parameters and material data. The objective is to develop knowledge-based systems and simulation programs which will make it possible to do without extensive test welds for the determination of welding parameters.

CONCLUSIONS

In future, joining technology in the all-embracing sense (i.e. welding and allied processes, including the cutting and coating processes) will, to an even greater extent, be the preferred technology for the fabrication of innovative products which are successful on the world markets. For this purpose, joining technologies will be included in all phases of product development and fabrication in a consistent way. Joining technology will have a guiding function. Joining technologies for the markets of the future are characterised by high productivity on the basis of consistent automation and the use of simulation processes.

REFERENCES

1. von Hofe, D. (1999.) *Modern Joining Technologies in the Metal Sector Paper presented at the IIW-Study Group RES «Welding Research Strategy and Collaboration»*. Lisboa.
2. Köhler, G., Reineck, H., Reichert, A. (1999) Qualitäts-, Umwelt- und Sicherheitsmanagement in der Fügetechnik unter den besonderen Bedingungen kleiner und mittelständischer Unternehmen. *DVS-Berichte Band 196*.
3. Sepold, G. *Probleme der Schweißtechnik an der Jahrtausendwende, Vortragsmanuskript*.
4. Eisenhauer, J. (1998) *Welding — Industry Vision Workshop Results Summary (DRAFT)*, Gaithersburg, Maryland, 1998, June 30 – July 1. U.S. Department of Energy, Office of Industrial Technologies and American Welding Society.
5. von Hofe, D. (1998) Trends in R&D Activities in Joining Technologies. In: *IIW Doc.-SG-GE-RES-119–98*.
6. Persson, K.-A. (1999) Welding and Cutting beyond the Year 2000. *Svetsaren*, **1 – 2**, 74.
7. Harig, H., Langenbach, C.J. (Hrsg.) (1999) Neue Materialien für innovative Produkte. *Springer-Verlag*.
8. (1997) Bundesministerium für Wirtschaft (Hrsg.). *Neue Technologien*.
9. (1999) RIFTEC — Robotic Friction Welding Application and Technology Centre, Friction Stir Welding. In: *GKSS*. TWI Workshop, May 3, 1999, Geesthacht.
10. (1999) N.N. Friction stir-Welding nun auch in der Massenproduktion von Aluminiumprofilen. *Schweißen & Prüftechnik*, **53**, 135.
11. Krohn, H., Singh, S. (1999) Schweißen von Magnesiumlegierungen für den Automobilbau. *DVS-Berichte Band 204*, 197ff.
12. Herold, H., Zahariev, S., Wohlfahrt, H. *et al. Aktuelle Untersuchungen zur Weiterentwicklung und Anwendung des WIG- und des WPL-Schweißens von Magnesiumlegierungen im Automobilbau Ebda*.
13. Cramer, H., Baum, L., Limley, P. *et al. Schweißen von Magnesiumstrukturen Ebda*.
14. Matthes, K.J. *et al.* (1999) Neues in der Schweißtechnik 1998. *Schweißen und Schneiden*, **6**, 340ff.
15. Svensson, L.-E., Elvander, J. (1999) Challenges for Welding consumables for the new Millenium. *Svetsaren*, **1 – 2**, 3.
16. Lehrheuer, W. (1999) Schweibtechnik im nächsten Jahrtausend — ein Ausblick auf die Entwicklung Jahrbuch Schweibtechnik 2000. *DVS-Verlag*, 5ff.
17. Wagner, J., Schlicker, U., Eifler, D. (1998) Bindungsbildung beim Ultraschallschweißen von Keramik mit Metall. *Schweißen & Schneiden*, **10**, 636ff.
18. Wagner, G., Roeder, E., Eifler, D. (1998) Bedeutung der Fügeflächentemperatur bei der Herstellung von Keramik. Metall-Verbunden durch Ultraschallschweiben. *DVS-Berichte Band 192*, 325ff.
19. Engl, B., Heller, T., Kawalla, R. (1999) Stand und Potential der Werkstoffentwicklung am Beispiel der Stähle für die Automobilindustrie. *Forum Thyssen-Krupp*, **1**, 20ff.
20. Prange, W., Stegemann-Auhage, T., Wonneberger, I., *et al. Anlagentechnik und Anwendungen für Tailored Blanks und Thyssen Engineered Blanks Ebda*.
21. Lugscheider, E., Kortenbruck, G. (1997) Stoffschlüssiges Fügen und thermisches Beschichten in der Produktion der Zukunft. *DVS-Verlag*.
22. (1999) Studiengesellschaft Stahlanwendung Forschungskolleg Stahlanwendung 99 Innovative Fügetechniken für Stahl. *Tagungsband 726*.
23. Emmelmann, C., Lunding, S. (1999) Schweissen mit Lasern hoher Strahlqualität. *DVS-Berichte Band 204*, 1ff.
24. Radaj, D. (1999) Schweißprozeßsimulation — Grundlagen und Anwendungen Fachbuchreihe Schweißtechnik. *DVS-Verlag*.

EFFECT OF SHIELDING GAS COMPOSITION ON CHARACTERISTICS OF HIGH-EFFICIENCY CONSUMABLE-ELECTRODE SHIELDED-GAS WELDING (MAG)

B. CZWORNOG
Institute of Welding, Glivice, Poland

ABSTRACT

The results of investigation of high-efficiency processes of welding in Ar–He–CO_2 and Ar–CO_2 mixtures at 450 A currents are given. The sizes of a cross-section of deposited beads, including the depth of penetration are evaluated. The chemical composition was determined, metallographic examinations, and also the tensile tests, impact bend and fracture toughness tests of metal deposited in shielding gas mixtures at 300, 350 and 400 A currents were performed. There were no significant differences in properties of the metal deposited in various mixtures. Good characteristics of properties of the deposited metal and welded joints obtained at currents up to 430 A using all compositions of shielding gas mixtures were confirmed.

Key words: *arc welding, consumable electrodes, shielding gases, carbon dioxide gas.*

New processes of metal-arc active gas (MAG) welding which have the common characteristics of a high level of the arc energy, permit achievement of electrode wire melting rate 2 to 3 times higher compared to the earlier used welding processes. The applications of these processes include fabrication of plate and tubular welded structures of a great thickness. The factors essentially limiting the introduction of advanced welding processes, are the economic characteristics of the process. For instance, the best known high-efficiency welding process called T.I.M.E. is based on the application of special equipment and expensive shielding gas consisting of four components. The results derived by various independent investigators point to the possibility of MIG/MAG welding with a higher parameter arc, when standard equipment and less complex gas mixtures are used. These results have been confirmed by investigations performed in the Institute of Welding in Glivice (Poland).

High-efficiency processes of MAG welding. The high-efficiency MAG welding processes which emerged in Europe in 1990s are those which were named in the organisations which had developed them (T.I.M.E., Rapid Melt, Linfast). The first of the above-listed was T.I.M.E. process developed at the start of 1980s in Canada. It is characterised by a high current density, greater electrode wire extension, use of a special mixture of gases for protection of the arc zone and of welding equipment providing high rates of electrode wire feed, and reliability. The shielding gas often contains 65 % Ar, 26.5 % He, 8 % CO_2 and 0.5 % O_2. As stated by the authors of [1], helium presence in the gas mixture increases the shielding gas ionisation potential and arc potential gradient, thus increasing the arc voltage. In this case, the level of the arc energy rises, resulting in higher pressure of the arc plasma flow, i.e. a deeper penetration of the base metal is ensured with stable dimensions of the weld cross-section.

Rapid Melt process also provides an increase of the electrode melting rate in welding of metal thicker than 10 mm. Use of this process is the most effective in mechanised work stations [2, 3]. The typical wire feed rate in this case is 25 to 35 m/min, while the melting rate is 10 to 20 kg/h of deposited metal. Ar + 8 % CO_2 mixture is recommended for use as the shielding gas. The authors of this process believe that such a composition of the shielding gas promotes achievement of the required metal transfer in the arc, good wetting of the base metal with the molten metal of the weld pool, as well as reduction of the amount of spatter and slag. Small additions of nitrogen oxide are recommended, which reduce the amount of evolving ozone.

One of the most recently introduced new high-efficiency MAG welding processes is Linfast [4] performed in the same modes as Rapid Melt. Its main advantage is the absence of disruptions of the stability of the high-energy arc running and use of specially developed gas mixtures of a new generation which promote a higher stability of arcing and quality of welded joints. In this case, use of a two-component mixture (Ar + CO_2) is also possible. Improvement of the penetration shape and appearance of welds produced at the wire feed rate of 15 to 20 m/min is provided by addition of 20 to 30 %

helium to the shielding gas composition. Use of gas mixtures called T.I.M.E. II, Corgon He25C or Corgon He25S enabled elimination of arcing instability in mechanised welding and the concurrent defects in welds. The composition of the above gas mixture grades was not published. It is only known that besides the already mentioned helium addition, these mixtures contain a relatively large amount of CO_2.

Thus, it can be stated that all the high-efficiency MAG welding processes are based on the same principles, whereas the differences between them are primarily in the composition of the recommended shielding gases, namely:

- two- and three-component mixtures, as well as mixtures of four components in which carbon dioxide or oxygen, and sometimes, both the gases, are the reactive elements, are used as the shielding gas. The base of the gas mixtures is argon, the volume fraction of which is between 60 and 96 %. The mixtures containing three or four components, include another inert gas, i.e. helium;
- helium addition to the shielding gas promotes a greater stiffness of the arc and its arcing stability [1, 4], better penetration and weld shape [4], this being the result of the arc voltage rising and increase of its energy. The stability of the process and the concurrent good weld properties are ensured by mixtures not containing any helium [2, 3];
- content of reactive components in the shielding gas in the majority of high-effeciency welding processes is lower (by approximately two times) than in the case of the traditional MAG welding.

Investigation of MAG welding processes with the use of various shielding gases. One of the main goals of investigations was determination of the influence of the shielding gas composition on the weld shape and dimensions, deposited metal characteristics and properties of welds made with higher welding parameters under the conditions close to those of welding productions of Polish enterprises. A semi-automatic machine fitted with a standard thyristor power source and wire feed mechanism providing up to 25 m/min feed rate, was used in this case. SG2 welding wire of 1.2 mm diameter and the following shielding mixtures were selected as the welding consumables:

60 % Ar + 30 % He + 10 % CO_2 (60/30/10),
75 % Ar + 15 % He + 10 % CO_2 (75/15/10),
90 % Ar + 10 % CO_2 (90/10).

Investigations included bead deposition on plates and measurement of their cross-section, recording and analysis of the regularities of welding current and arc voltage variation, determination of the properties of the deposited metal and welded joints.

Investigation of welding modes and deposited bead shape. Changes of welding current and arc voltage were recorded on magnetic discs by a special instrument and then processed in the computer. Within the modes characteristic for spray metal transfer, these changes differed from each other only slightly (irrespective of the shielding gas composition), although a certain disruption of the stability of the measured parameters was recorded when mixtures without helium were used.

Evaluation of the influence of the welding modes and shielding gas composition on the deposited bead dimensions was performed by measurement of the weld convexity height and width, as well as of penetration depth on macrosections. These investigation results show that the weld shape is influenced by the shielding gas composition. The width of the beads deposited in the mode of spray transfer in the mixtures containing helium, on average is by 2 mm smaller and the convexity height is approximately by 0.8 mm greater compared to the welds made in gas mixtures without helium. The influence of gas shielding on penetration depth is ambiguous; however, uniform penetration by depth was achieved in all the cases.

Investigation of the deposited metal. Plates were welded at 300, 350 and 400 A currents in 90/10, 75/15/10 and 60/30/10 shielding gases with SG2 wire to determine the deposited metal properties.

Investigations also included chemical analysis of the gases, metallographic examination, as well as tensile, impact bending and fracture toughness tests.

Chemical analysis of the samples permitted determination of the amount of alloying elements in the deposited metal, and of oxygen, nitrogen and hydrogen content with LECO instrument (Table 1).

As shown by composition analysis results, within the studied welding modes the increase of the arc energy does not influence the degree of alloying elements loss. The shielding gas composition does not make any significant influence on the process of alloying elements oxidation, either, this being probably related to the same content of CO_2 (10 %) in the shielding mixtures. Oxygen content in the deposited metal has a tendency to increase with the welding current, its content, however, not exceeding the undesirable level (400 ppm). In the studied range the welding parameters do not practically influence the nitrogen content in the metal.

Metallographic examination demonstrated the following:

- fine nonmetallic inclusions of about 1 μm are found in the deposited metal, which, as a rule, are complex oxysulphides uniformly distributed over the weld section;
- analysis of the multilayer weld structure revealed the presence in the joint of about 20 % of metal which had not undergone any structural changes and about 80 % of metal recrystallized

Table 1. Content of alloying elements and gases in the deposited metal

Sample number	Shielding gas	Current, A	Weight fraction of alloying elements and gases in the deposited metal					
			%			ppm (average value)		
			C	Mn	Si	O_2	N_2	H_2
1		300	0.090	1.11	0.67	289	71	1.15
2	60/30/10	350	0.095	1.10	0.66	297	68	1.12
3		400	0.090	1.10	0.62	329	132	0.37
4		300	0.095	1.14	0.67	246	74	0.36
5	75/15/10	350	0.095	1.09	0.64	249	105	0.33
6		400	0.085	1.15	0.60	323	71	0.20
7		300	0.090	1.08	0.66	314	66	0.57
8	90/10	350	0.095	1.05	0.59	271	64	0.30
9		400	0.095	1.15	0.66	329	60	0.41
16	90/10	400	0.100	1.10	0.62	–	–	–
17	60/30/10	400	0.100	1.18	0.63			

Note: Samples No.16 and 17 are designed for fracture toughness testing.

under the impact of the heat applied in deposition of subsequent beads. The metal which did not undergo changes mostly consists of complex ferrite structures with hypoeutectic ferrite precipitating along the primary austenite grain boundaries, platelike (Windmanstätten) and fine acicular ferrite. The total content of hypoeutectic ferrite was about 10 %, that of plate-like ferrite being about 15 %, and of acicular ferrite about 75 %. No significant influence of the welding mode or shielding gas composition on the content of the above ferrite structural components was found; the recrystallized metal in the majority of cases demonstrated a granular ferrite-pearlite structure, practically the same for all the samples welded in shielding mixtures, irrespective of the shielding medium composition.

Tensile, impact and fracture toughness testing. The results of tensile and impact toughness tests are given in Table 2. The differences between the values of yield point σ_y and ultimate tensile strength σ_t of the deposited metal samples produced in the studied gas mixtures, are practically insignificant. These testing results are ambiguous. In helium-containing mixtures, σ_y and σ_t values increased with the increase of the welding heat input, while in 90/10 mixture they decreased.

The results of fracture toughness testing (CTOD) indicate that the temperature at which the studied deposited metal (samples No.16 and 17) demonstrates brittle fracture susceptibility is below −20 °C. At this temperature the admissible length of the defect for the metal of sample No.16 should not exceed 4 to 5 mm, whereas for the metal of sample No.17 the admissible defect of this order is found at −40 °C. The brittle transition temperature at δ_c = 0.2 mm is in the range of -13 – -15 °C. Such a brittle transition temperature range of the deposited metal is characteristic for the wire-flux systems widely used in practical work in submerged-arc welding of low-alloyed steels and for wire-gas systems in the traditional modes. In coated-electrode arc welding, however, generation of similar results depends on introduction of alloying elements into the coating composition or application of heat treatment. The CTOD testing re-

Table 2. Mechanical properties of the deposited metal

Shielding gas	Current, A	Yield point, σ_y, MPa	Ultimate tensile strength, σ_t, MPa	δ_5, %	Work of fracture, KV, J at T, °C			
					+20	−20	−40	−60
	300	437.2	581.9	26.2	175.6	102.6	71.6	51.5
60/30/10	350	436.3	586.0	26.0	157.5	73.1	58.8	27.0
	400	520.2	660.9	13.2	86.8	45.4	35.3	19.2
	300	462.9	580.5	30.3	195.7	107.9	104.1	39.7
75/15/10	350	459.4	583.2	26.6	168.7	116.7	61.9	39.2
	400	539.8	670.3	18.0	63.2	32.6	24.8	21.4
	300	528.5	615.2	25.5	140.2	94.1	76.5	26.0
90/10	350	473.0	598.2	24.8	158.9	117.6	56.5	40.2
	400	465.3	588.2	18.0	162.3	74.2	54.2	18.7

Table 3. Mechanical properties of welded joints

Sample designation	*Shielding gas*	σ_t, *MPa*	*Bend angle, deg*	*Work of fracture, KV, J, at T, °C*		
				+20	*–20*	*–40*
Z1	90/10	566.7	130	104.4	66.7	45.1
		559.1	130	90.2	55.9	26.5
				101.7	49.6	23.5
Z3	60/30/10	564.8	130	113.8	49.0	36.3
		573.5	130	128.5	59.8	23.5
				83.4	56.9	42.2

sults are preferable in evaluation of the deposited metal produced in welding in helium-containing mixtures.

Investigation of welded joints. Butt joints of 20 mm 18G2A steel were studied. Plates with Y-shaped edges (50° groove angle) were assembled without a gap and welded in the studied gas mixtures at 430 A current. The heat input in welding was 28 kJ/cm. The welded plates were subjected to X-ray inspection, and then samples for mechanical testing were cut out of them. The testing results are given in Table 3.

As shown by the testing results, the mechanical properties of welded joints practically do not depend on the composition of the shielding gas which in our experiments was the only varying parameter. It follows from these results that under the production conditions not only Ar + 30 % He + 10 % CO_2 mixture, but also Ar + 10 % CO_2 mixture as a less expensive gas providing good properties of the metal of the welds and the welded joints, can be used for arc protection.

CONCLUSIONS

At up to 450 A current, the MAG welding process runs in a stable manner and does not practically depend on the composition of the studied shielding gas, namely Ar–CO_2 or Ar–He–CO_2. The shape and dimensions of the beads, as well as the mechanical properties of the deposited metal and welded joints are independent of the composition of the studied gas mixtures. Helium addition does not make any essential influence on the nature of the welding process and its results. Use of a simple and inexpensive Ar–CO_2 mixture provides a high brittle fracture resistance in the weld metal, which is indicated by the results of impact bend and CTOD testing. This is the result of a relatively low content of nonmetalic inclusions in the welds and a favourable structure with prevailing acicular ferrite, as well as sections of fine-grained pearlite and ferrite structures in the zones exposed to the heat applied when filling the multipass weld groves.

REFERENCES

1. Church, J., Imaizimi, H. (1990) Welding characteristics of a new welding process. T.I.M.E.-process. *IIW Doc.-XII-1199–90.*
2. Bengtsson, P. (1992) High speed welding with A400 HSW robot system and the rapid arc and rapid melt processes. *Svetsaren*, **2**, 26 – 29.
3. (1993) *Facts about: rapid arc, rapid melt high-productivity MIG/MAG welding.* AGA.
4. Trube, S. (1997) High performance MAG welding with Linfast concept. *IIW Doc.-XII-1499–97.*

ENSURING OF SAFE OPERATION AND EXTENSION OF SERVICE LIFE OF MAIN PIPELINES

K.V. CHERNYAEV and **E.S. VASIN**
Open Joint-Stock Society of the Diagnostics Centre «Diascan», Lukhovitsy, Russia

ABSTRACT

The Joint-Stock Company Transneft developed and put into operation the system for ensuring safe operation and extension of service life of main pipelines. The system is based on integrated four-level diagnostic monitoring using in-pipe high-resolution diagnostic gears, allowing all types of defects which are the main causes of accidents to be revealed. Repair of pipelines is planned on the basis of estimation of an extent of danger of defects revealed. The composite-coupling technology is employed for selective repair of pipelines without any interruption of pumping. The system makes it possible to fundamentally decrease the rate of accidents at main oil pipelines and provides substantial cost effectiveness.

Key words: *main pipelines, in-pipe diagnostics, technical state, selective repair, monitoring.*

One of the basic requirements imposed on main pipelines is their reliability and safety during a long-time operation.

The Transneft system of main oil pipelines with a diameter from 530 to 1220 mm is an integrated underground engineering structure with a total length of 46800 km, which connects oil production regions with refinery centres and export terminals. It pumps through almost all oil produced in Russia.

At present the operating life of about half of all main oil pipelines has exceeded their assigned life of 33 years or is close to it (Figure 1).

In fact, the Transneft system of main oil pipelines, that lived through the running-in and stabilization periods, has come to the so-called «wearing life period», which is characterized by a general deterioration in its state and an increased risk of accidents. This is caused by a considerable operating life of pipelines, decrease in their load-carrying capacity due to strain ageing and accumulation of damages in the pipe metal and welds.

Analysis of causes of accidents shows that they are associated primarily with development of corrosion and fatigue damages, the initiation centres of which are various factory defects made in pipes during manufacture, construction-erection operations and, in particular, during welding.

Traditionally, the problem of prevention of accidents was solved first of all by overhaul of a linear part of a pipeline, by replacing all pipes or insulation coatings in large sections of pipes. In this case the information for selection of sections to be repaired was limited and included only the data of test pitting and results of measurement of electrochemical protection potential. By the beginning of the 1990s, under conditions of the «wearing life time» of main oil pipelines, the traditional methods exhausted their potential. The rate of accidents at the linear part of pipelines has been growing.

It should be noted that the rates of processes of accumulation and development of damages for different regions of oil pipelines can be substantially different. Therefore, to effectively prevent accidents at minimum associated costs, the pipeline should be restored only in those defective zones where a decrease in strength of the pipe reached a dangerous level, while the rest of the zones should be kept under control, i.e. repair should be made depending upon the actual state.

This idea was used as the basis for development by Transneft of a cardinally new system for ensuring safe operation and extension of service life of main pipelines.

The system includes the following subsystems:

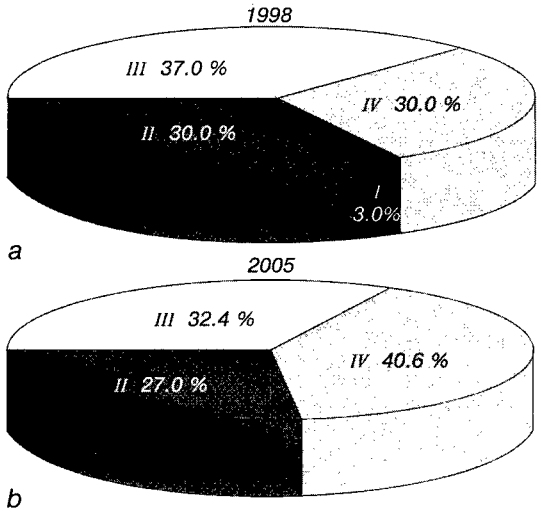

Figure 1. Operating life of the Transneft main oil pipelines: *I* – up to 10; *II* – from 10 to 20; *III* – from 20 to 33; *IV* – above the depreciation term of 33 years

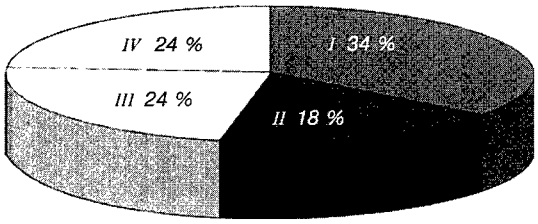

Figure 2. Classification of causes of accidents at the Transneft main oil pipelines in 1990 (0.27 acc./1000 km): *I* — corrosion; *II* — factory defects (delaminations, inclusions, longitudinal welds); *III* — erection-construction defects (dents, buckles, longitudinal welds); *IV* — mechanical damage

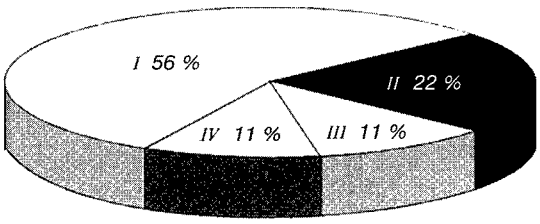

Figure 3. Classification of causes of accidents at the Transneft main oil pipelines in 1996 (0.19 acc./1000 km): *I* — defects in assembly circumferential welds; *II* — corrosion damage; *III* — defects in factory longitudinal welds; *IV* — incidental damage

receiving and processing of primary information on the state of a pipeline on the basis of the in-pipe diagnostics data;

evaluation of the technical state and defining of safe conditions for operation of the pipeline;

maintenance and restoration of serviceability of the pipeline;

monitoring of the technical state of the pipeline.

The system is based on a classical principle: detection of defects in the pipeline, evaluation of their state, repair of the most dangerous defects and monitoring of the rest of the defects. All this is done without interference into normal operation of the pipeline.

The cardinally new and key point of the developed system is the use of the in-pipe diagnostics. Diagnostic gears, which are made following the specialty specifications, are unique. They are utilized in oil pipelines of Russia and other CIS countries, featuring stable operation and giving qualitative test results. There are four types of gears. They differ in principles of operation, are characterized by a high resolution and allow the four-level diagnostic monitoring to detect such types of defects:

pipeline geometry defects (dents, buckles);

metal losses and delaminations;

cracks and crack-like defects in circumferential welds;

cracks and crack-like defects in longitudinal welds.

First of all, it is necessary to perform monitoring of level *I* — check the presence of dents and buckles that cause narrowing of the flow section of the pipeline. This is done using the profile metering gears. Profile metering of the main part of the oil pipeline system of Russia was completed in 1997. All narrowings that prevented passage of the gears were removed.

The choice of priority of other levels of monitoring was based on analysis of the accident rates at main oil pipelines to remove primarily the defects which caused the largest number of accidents (Figure 2). In 1990 it was corrosion. Therefore, diagnostics of the pipelines was started with using ultrasonic flaw detectors which enabled such defected to be detected.

At present the primary inspection of the Transneft main oil pipeline system using the ultrasonic flaw detecting gears of level *II* is coming to completion. The secondary inspection using this type of gears has been started in some regions.

Detection and removal of corrosion defects led to a substantial decrease in the total amount of accidents in 1996. At the same time, the structure of the accident events was changed (Figure 3). Accidents caused by defects in circumferential welds, constituting more than half of all accidents, came to the first place.

The in-pipe inspection of level *III* is performed currently to reveal these defects. This is done using the high-resolution magnetic gears. More than 4000 km of main oil pipelines have been already inspected using these gears.

The work on the manufacture of ultrasonic gears of level *IV*, intended for detection of crack-like defects in longitudinal welds, is at the final stage of performance. By putting these gears into operation, Transneft completes the formation of the integrated four-level diagnostic monitoring system for detection of all basic types of defects which may cause accidents in main oil pipelines.

The primary goal of using the in-pipe diagnostics is arrangement of monitoring of the technical state of the entire system of main oil pipelines in order to determine the rate of development of defects and choose the efficient strategy and tactics of repair, which eventually will make it possible to control the life of oil pipelines. Currently, monitoring is realized through periodic inspections of oil pipelines using ultrasonic gears of level *II* to detect metal losses.

Existing scientific procedures and devices fail to make it possible to precisely determine the rates of development of the corrosion processes. Because of many factors, such as differences in service durations and conditions, conditions and quality of construction operations, pipe materials, insulation coatings, etc., these processes occur non-uniformly in different regions of oil pipelines and develop with different intensities. As a result, some regions may be in a satisfactory state and some — in a state close to critical. It is impossible to detect these regions without the use of the in-pipe diag-

nostics. Therefore, the entire system of oil pipelines should be periodically inspected and the rate of the corrosion processes should be directly measured.

Analysis of the data of repeated inspections proves that the corrosion processes are developing both inside and outside of the pipelines. Moreover, they tend to develop non-uniformly along the length of the pipeline and at different rates.

Results of the repeated inspection of the entire system of oil pipelines using the ultrasonic gear allow the rate of corrosion to be estimated for each defect and in each location. In turn, this should enable the grounded decisions on assignment of regions and planning of terms for overhaul and selected repairs at minimum costs to be made, reliability and safety of operation to be improved, service life of main oil pipelines to be extended and, thus, their residual life to be controlled.

In future, it is advisable to apply this approach of repeated inspections to magnetic gears of level *III* (to detect abnormalities in circumferential welds) and ultrasonic gear of level *IV* (to detect cracks in longitudinal welds).

The efficient calculation method are needed to estimate the degree of danger of defects by the data obtained using the in-pipe gears. For this purpose, the full-scale tests were conducted to check static and cyclic strength of pipes with different defects, such as corrosion, scratches, dents, delaminations, cracks in the base and weld metal. The standard methods for calculation of strength of oil pipelines containing defects were developed on the basis of results of the above tests.

Diascan used these methods to determine the actual state of each investigated region of the pipelines without their stripping. Defects classified as dangerous are subject to repair within the shortest possible time. As to the rest of the defects, they should be kept under control.

The wide-scale in-pipe diagnostics in conjunction with estimation of strength of defective regions made it possible to come to selected repair as per actual state of oil pipelines.

At present, overhaul involving replacement of sections is made only in locations of the highest concentration of defects, which resulted in a multiple increase in its efficiency.

The new efficient technology for selected repair was developed for localized defects, which constitute 3/4 of their total amount. This technology had to meet a number of critical requirements: repair without interruption of pumping, full recovery of strength and service life of a repaired section, versatility in terms of repair of different types of defects, repair of the oil pipeline body avoiding welding, etc.

As shown by comparative analysis, among all other repair methods available in the world and in domestic practice, the composite-coupling technology meets these requirements to the highest extent

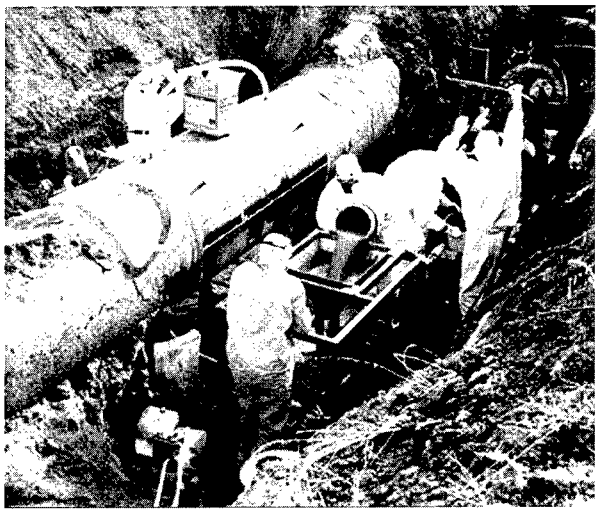

Figure 4. Filling the installed coupling with a composite compound

(Figure 4). It allows repair of different types of defects with widely differing geometrical parameters, including such dangerous defects as longitudinal cracks with a depth of up to 70 % of the pipe wall thickness, defects of metal losses deep up to 90 % and weld defects. Also, it can be applied to repair defects in the form of dents and buckles, as well as combined defects, such as a scratch in a dent.

The high potential of this technology of the combined-coupling repair is based on the fact that it can serve as the basic technology for further development of new types of repair (under the water, under winter and Arctic conditions, at increased humidity and temperature).

At present, the composite-coupling technology, optimized for conditions typical for Russia, is applied by Diascan to the Transneft system of main oil pipelines. The regulatory documents for its application are available. This technology has found its way into application. The work on installation of composite couplings is done by qualified specialists of ten repair departments of Diascan, which are equipped with all necessary materials and facilities.

Application of this system at Transneft for the first two levels of diagnostics resulted in a profit of $ 734 mln., which was gained during a period of 1994 – 1997. Cost effectiveness increased with an increase in the scope of application of the diagnostics and repair. This provided a decrease of more than 4 times in the accident rate at the linear part of the main oil pipelines.

The efficiency of the system for safe operation and extension of service life of main oil pipelines has been proved by its practical application by Transneft. The system is versatile and is worthy of being employed at any main gas and oil pipelines of Russia and throughout the world.

HEAT TREATMENT AND CLADDING USING A LIGHT BEAM HEATING

SHAN JIGUO, WU AIPING, ZHANG DI and REN JIALIE
University Thing-hua, China

ABSTRACT

The problems of heat treatment and cladding using a method of a light beam heating to improve the serviceability of components under the complex conditions of loading are considered. It was established that the use of a light beam source is an alternative to a laser source. It is shown that the light beam cladding of a composite powder of Ni–Cr–B–Si–WC system on steel 45 contributes to the increase in microhardness of coating almost by 2 times.

Key words: *cladding, light beam heating, surface modifying, microhardness, energy input.*

The application of a light beam as a heating source for different welding and allied processes has several advantages as compared with other high-concentration heating sources. Unlike the laser and electron beam, a light beam treatment does not require an expensive equipment and the efficiency factor of this process is much higher. Investigations carried out over the recent years confirmed the challenging future for using the light beam heating for hardening and cladding the different components [1 – 5].

The present paper describes the results of investigations of technological processes of a light beam heat treatment and cladding, structural transformations in as-treated and as-clad metals, and also properties of heat-treated and deposited layers.

A light beam installation of the SR-1 type [1], developed at the University Thing-hua, was used. It consists of three main parts: a power source, a radiator and optical systems (Figure 1). An arc xenon air-cooled lamp of 5 kW capacity serves a radiator. The power source with a falling external characteristic provides a flexible control of the lamp power within the ranges from 0.6 to 5.0 kW. An elliptic reflector with a $f_2/f_1 = 14$ ratio of focal distances was used as a primary optical system, while a lens with a 60 mm focal distance was used as a secondary optical system that provides a power density of up to $1 \cdot 10^4$ W/cm^2 at 5 mm diameter of a heat spot and allows the heat treatment and cladding of products to be performed with the high productivity.

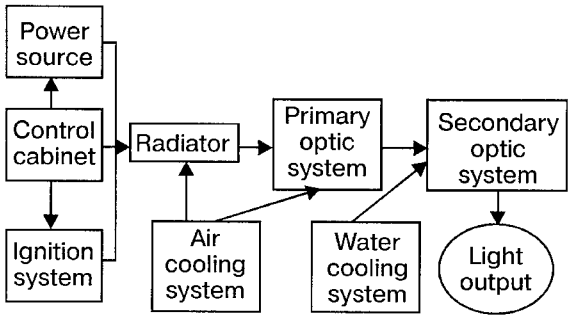

Figure 1. Schematic diagram of a light beam unit of SR-1 type

To determine the technological capabilities of a light beam the experiments were carried out on melting different alloys. It was established that the light beam heating ensures a reliable melting both of tin-based fusible alloys and also refractory nickel-based alloys (Table 1).

The grey cast iron specimens were light-beam treated with and without fusion of their surface. The initial microstructure of a grey iron is a flaky graphite and a pearlitic matrix.

At cast iron treatment with a surface fusion the effect of sizes of a spot of a focused light beam and energy input on structure and properties of the fused surface were studied. Using the metallographic sections the microstructure was examined, sizes of the fused zone were determined, microhardness of metal in its depth was measured. At 5 kW capacity of light beam and 10 mm size of the heat spot the reduction in an energy input from 7000 to 5000 J/mm leads to the decrease in a width of the zone fused from 12 to 10 mm and its depths from 1.0 to 0.5 mm.

Table 1. Values of temperature of melting different alloys and light beam power consumed for their melting

Alloy	*Melting temperature, °C*	*Power, kW*
Sn–Pb	183	1.1
Al–Si	570	1.3
Cu–Zn	790	2.7
Cu–Mn	890	2.7
Ni–Cr–B–Si	1050	4.5
Ni–Cr–Zr	1200	4.5

Figure 2. Microstructure of white cast iron treated with a light beam: *a* — surface zone (with fusion) (×500)(reduced by 0.75); *b* — the same (without fusion); *c* — boundary of a treated zone (without fusion) (×1500)(reduced by 0.80)

At high values of the energy input the metal of a surface layer has a purely-austenitic structure due to the carbon burning out, its hardness does not exceed $HV_{0.2}$ 350. The deeper layers have a structure which consists of a ledeburite and troostite. Microhardness of this zone reaches $HV_{0.2}$ 700. A ledeburite structure with graphite inclusions is formed at the boundary of the fused zone due to relatively low rates of cooling. Its microhardness is $HV_{0.2}$ 550.

At decrease in the energy input to 5000 J/mm the carbon burning out in a surface layer was not observed. The microstructure of this zone is a ledeburite and troostite, the microhardness of metal is $HV_{0.2}$ 850. It should be noted that the microhardness across the thickness of the fused layer in this case is higher than in treatment with an energy input 7000 J/mm. To improve the hardness and produce martensite in the fused layer the surface was treated at a lower energy input than 5000 J/mm. However, in the fused zone and HAZ the martensitic transformation was not also observed and the hardness was not increased.

At decrease in a heat spot to 5 mm and appropriate increase in a power density of the light beam, the cooling rate is increased and the structure of the cast iron fused layer is changed. Except the ledeburite, the martensite is appeared in the structure of metal of the fused zone and HAZ (Figure 2, *a*), thus contributing to the significant increase in their microhardness ($HV_{0.2}$ 900 in the fused zone and $HV_{0.2}$ 700 in HAZ, respectively).

The effect of technological parameters of the process on size, structure and microhardness of the hardened zone of cast iron after treatment with a light beam without fusion of the surface was investigated (Table 2). The results of experiments showed that at other conditions being equal the increase in power (or decrease in rate of displacement) of a light beam with respect to the workpiece leads to the increase in width and depth of the strengthened zone, however, the rigid conditions (high power and rate of displacement of the light beam) is more preferable, because in this case a high efficiency of the process and the microhardness of the treated layer are provided (Table 2, specimens No. 2 and 4).

The microstructure analysis revealed the pearlite-austenite-martensite phase transformation in the surface layer (Figure 2, *b*). At the boundary of the treated zone with a parent metal the martensitic transformation was not observed and the troostite and austenite are revealed in the metal structure (Figure 2, *c*). The decrease in an energy input leads to the refining of a martensitic structure of the surface layer and to the appropriate increase in microhardness.

The technological feasibility of using a light beam for cladding was investigated on 12.35 × 12.35 × 30.00 mm specimens from annealed steel 45. As surfacing materials, the mixtures of self-fluxing nickel powder of Ni–Cr–B–Si system (80

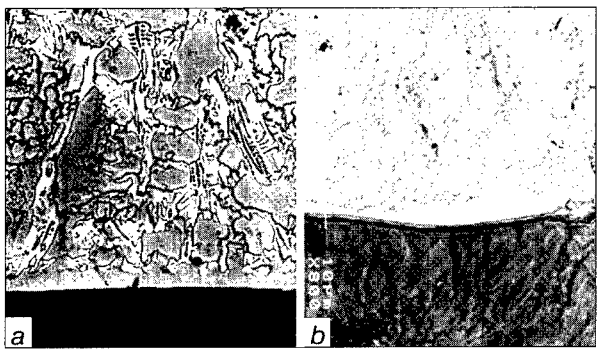

Figure 3. Microstructure of coating deposited on steel 45 using different surfacing mixtures: *a* — WC with a nickel cladding; *b* — the same, without nickel cladding (×800) (reduced by 0.75)

Table 2. Technological parameters of process of light beam treatment of grey cast iron without surface fusion, geometric sizes and microhardness of a zone treated

No. of specimen	*Speed of work-piece displacement, mm/s*	*Power of light beam, kW*	*Energy input, $1 \cdot 10^3$ J/mm*	*Width/depth of zone treated, mm*	*Microhardness, $HV_{0.2}$*
1	4.2	4	0.82	2.70/0.35	722
2	6.0	4	0.60	2.60/0.30	770
3	8.6	4	0.40	2.30/0.20	895
4	8.6	5	0.50	2.80/0.37	882
5	2.9	5	1.40	3.60/0.60	776

Table 3. Distribution of chemical elements in separate phases of the deposited and parent metal

Phase (area of element location)	*Elements, mass %*					
	C	*Si*	*Cr*	*Fe*	*W*	*Ni*
Flaky phase (deposited metal)	18.97	–	21.47	40.40	14.12	5.50
γ-phase (transition zone)	7.45	2.18	4.71	54.99	2.86	28.18
Matrix (parent metal)	22.16	1.88	0.18	75.19	–	0.16

mass %) and powder of tungsten carbide of conventional type and clad with nickel, were used. The chemical composition of nickel alloy is as follows, mass %: 0.7 C; 17.0 Fe; 18.0 Cr; 4.1 B; 4.0 Si; Ni – the rest.

Experiments showed that in cladding with a light beam at a large heat spot and argon shielding of the weld pool only, the good formation of the deposited bead is not ensured. When cladding is made in a quartz chamber filled with an argon, and also in case of decrease in a heat spot during cladding out of a chamber and argon shielding of the weld pool only (that simplifies significantly the technology) the formation of the deposited layer is noticeably improved. The deposited bead has a shape of a convex segment with a small angle of wetting at thickness of up to 1 mm and width of up to 10 mm, thus proving a rather high efficiency of the light beam cladding. The visual inspection did not reveal any surface defects in the deposited layer.

The examination of microstructure of the deposited layer showed that introduction of the tungsten carbide, clad with nickel, to the surfacing powder prevents the formation of such defects as flakes and non-metallic inclusions which are often observed in case of using a conventional tungsten carbide. This depends, probably, on the better wetting of a tungsten carbide, clad with nickel.

Independently of the condition of preparation of the tungsten carbide surface the microstructure of the deposited layer consists of a matrix (γ-phase), near the boundary of which the eutectics is revealed. In addition, a flaky phase was observed in its structure. Tungsten carbides clad with nickel are dissolved completely in the deposited layer (Figure 3, *a*), and their forming elements (tungsten and carbon) are either dissolved in γ-phase with its hardening or they form complex carbides with alloying elements of the nickel alloy. This is proved by tungsten appearance in γ-phase, and also by the increased content of carbon, chromium and iron in primary flaky phases (Table 3). Unlike the tungsten carbides clad with nickel, the carbides without cladding do not dissolve in the alloy matrix (Fi-gure 3, *b*). At the boundary of parent and deposited metals there is a noticeable transition zone whose width is approximately 0.025 mm.

X-ray microanalysis revealed an increased content of iron and carbon in the transition zone that was due to an additional fusion of the parent metal and its mixing with the deposited metal. The HAZ metal structure is sorbite-troostite without presence of the martensite. This is, probably, explained by a small rate of cooling because of a relatively low density of radiation.

The hardness of the deposited metal is rather high. At the same time high scattering of its values is observed. Thus, the mean value of hardness of the deposited metal which contains the tungsten carbides without nickel cladding is *HRC* 54 at mean square deviation 19.6306, while in case of using the tungsten carbides clad with nickel it is *HRC* 46 at mean square deviation 5.5136. Microhardness of the deposited metal is almost twice higher than that of the parent metal. Moreover, the introduction of tungsten carbides without nickel cladding leads to an abrupt variation of values of microhardness because of the formation of defects.

CONCLUSIONS

1. Treatment of surfaces of structural metallic materials with a light beam is very promising for improving the surface properties of the components.

2. Light beam cladding of a composite powder of Ni–Cr–B–Si–WC system on steel 45 promotes the increase in hardness almost by 2 times. It is recommended to use the particles of the tungsten carbides clad with nickel during the light beam cladding to prevent the formation of defects and to provide the best effect of hardening.

REFERENCES

1. Shan Jiguo, Zhen Thale (1999) Light beam surfacing of mixture of powders made from self-fluxing nickel alloy and tungsten carbide. *Avtomaticheskaya Svarka*, **4**, 56 – 58.
2. Arkhipov, V.E., Ablaev, A.A., Krasnov, T.L. *et al.* (1990) Structure and hardness of high-strength cast iron VCh50 in hardening with light beam. *Metallovedeniye i Term. Obrabotka Metallov*, **7**, 34 – 35.
3. Shan Jiguo, Ren Jialie, Xu Binshi (1998) Surface hardening with light beam. *China Surface Eng.*, **11**, 16 – 18.
4. Shan Jiguo, Ren Jialie (1999) Microstructure and hardness of strengthened layer in light beam hardening of alloying cast iron. *Applied Laser*, **19**, 265 – 268.
5. Suleimanov, V., Baizakov, A. (1999) Cladding of stainless steel on carbon steel. *J. de Physique*, **9**, 447 – 449.

ADVANCED EQUIPMENT FOR ELECTRON BEAM WELDING

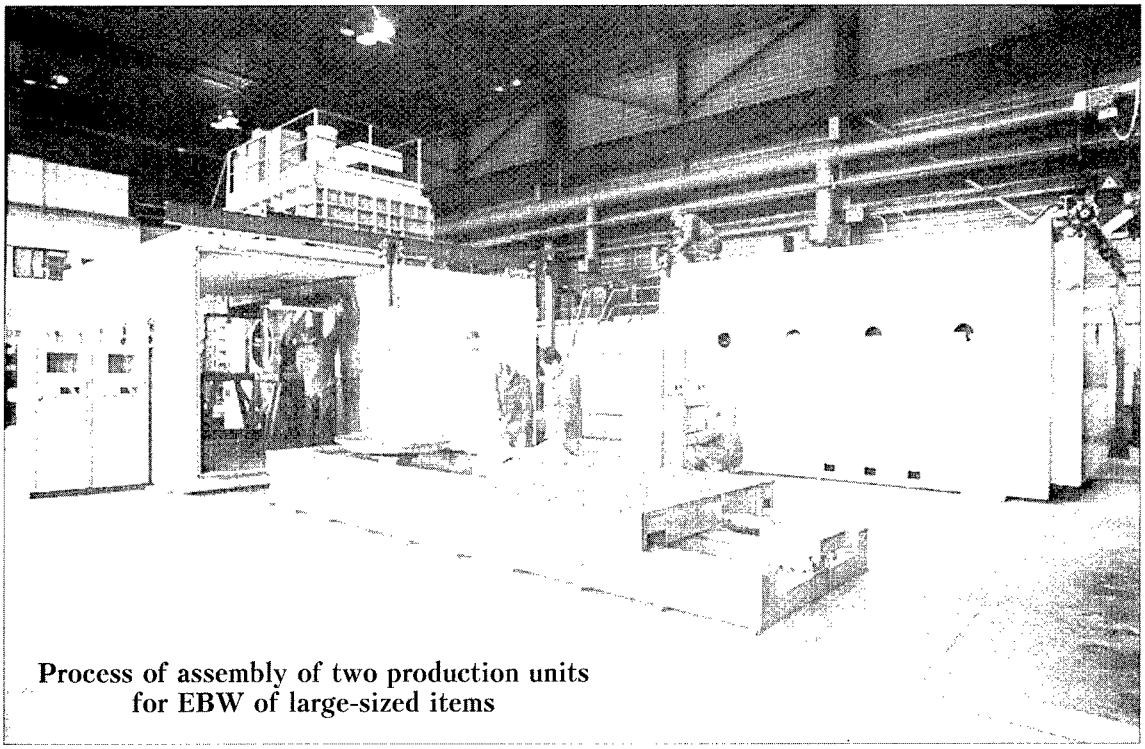

Process of assembly of two production units for EBW of large-sized items

More than ten units for EBW of small- and large-sized items have been exported over the last 3 years

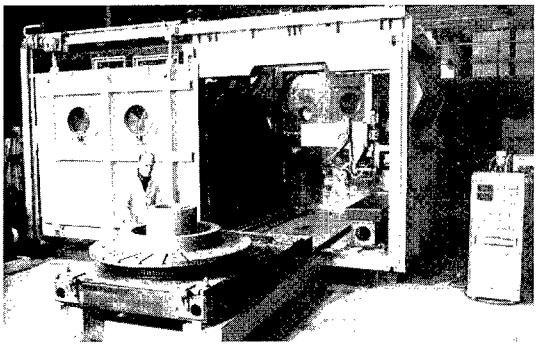

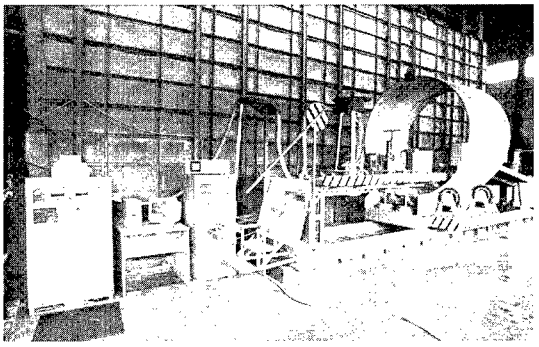

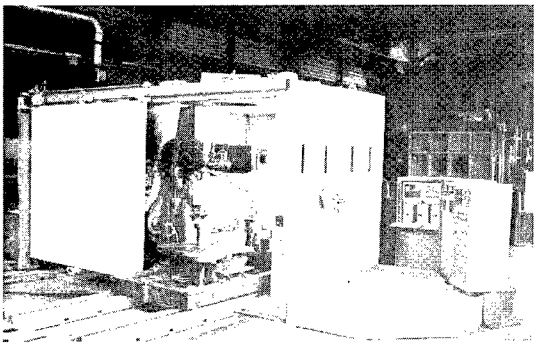

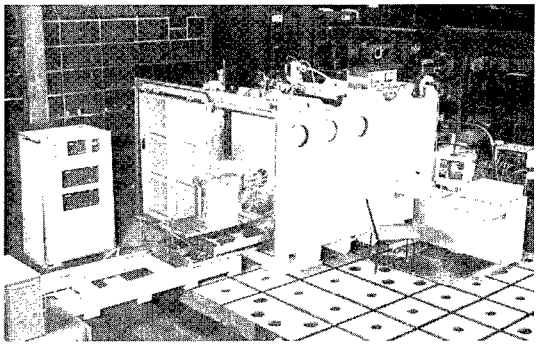

The E.O. Paton Electric Welding Institute. Tel./fax : (38044) 265 43 19, 220 94 54

SPACE TECHNOLOGY

- ✧ Development, testing and adaptation to on-board systems of processing equipment for use in space objects
- ✧ A package of engineering services in the field of electron beam technologies for space
- ✧ Development and testing of tools for performance of manual welding and other operations in raw space
- ✧ Design, fabrication and testing of transformable welding structures for space applications

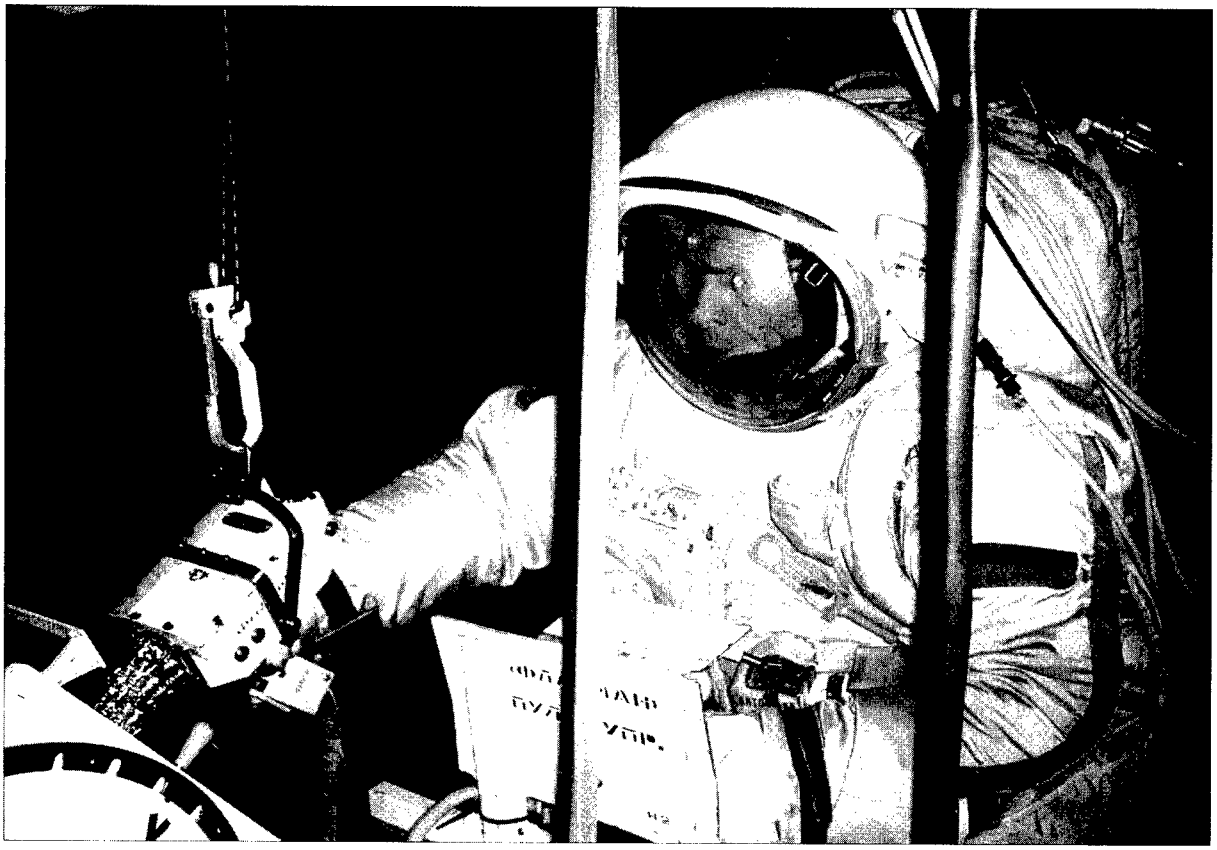

SPACE TECHNOLOGY DEPARTMENT OF THE
E.O. PATON ELECTRIC WELDING INSTITUTE
Tel.: (380 44) 227 67 57
Fax: (380 44) 220 91 15

UP-TO-DATE INVERTERS FOR ARC WELDING

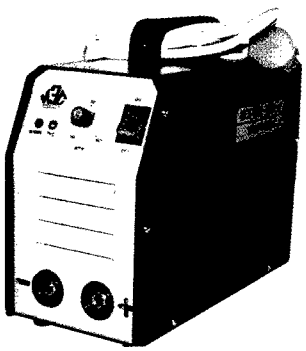

"KORAL-154/i" ARC WELDING SOURCE BASED ON HIGH-FREQUENCY TRANSISTORIZED INVERTER

1. Supply voltage (V, Hz).....220/50
2. Maximal input current (A).....18
3. Limits of welding current adjustment (A).....5–140
4. Open-circuit voltage (V).....55
5. Efficiency (%).....85
6. Power factor.....0.95
7. Duty cycle.....90A–100%, 120A–60%, 140A–35%
8. Overall dimensions (mm).....290x240x125
9. Weight (kg).....7.6

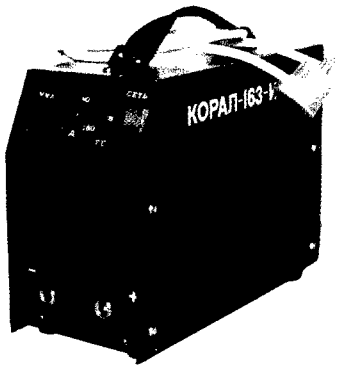

"KORAL-163/i" ARC WELDING SOURCE BASED ON HIGH-FREQUENCY TRANSISTORIZED INVERTER

1. Supply voltage (V, Hz).....220/50
2. Maximal input current (A).....20
3. Limits of welding current adjustment (A).....5–160
4. Open-circuit voltage (V).....75
5. Efficiency (%).....87
6. Power factor.....0.95
7. Duty cycle.....110A–100%, 130A–60%, 150A–35%
8. Overall dimensions (mm).....290x240x125
9. Weight (kg).....6.6

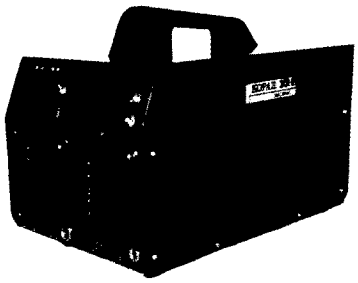

"KORAL-301/2" ARC WELDING SOURCE BASED ON HIGH-FREQUENCY TRANSISTORIZED INVERTER

1. Supply voltage (V, Hz).....220/50
2. Maximal input current (A).....35
3. Limits of welding current adjustment (A).....10–300
4. Open-circuit voltage (V).....55
5. Efficiency (%).....85
6. Power factor.....0.95
7. Duty cycle.....220A–100%, 250A–60%, 300A–35%
8. Overall dimensions (mm).....290x240x125
9. Weight (kg).....6.6

Koral-301 family of welding machines is a set of multifunctional transistorized inverters of a rearrangeable structure based on identical modules. The required circuitry of the source is selected depending on the technological (welding, cutting, surfacing) problem which is being addressed.

Machine type	Machine functional purpose
Koral-301/1	D.C. welding, 300 A mode
Koral-301/2	D.C. welding, 300 A mode, two-station mode, 2 x 150 A
Koral-301/3	D.C. welding, 300 A mode, two-station mode, 2 x 150 A
Koral-301/4	D.C. welding, 300 A mode, two-station mode, 2 x 150 A
Koral 301/5	D.C. and A.C. welding, 300 A mode
Koral 301/pa	D.C. and A.C. welding, 300 A mode, two-station D.C. mode, 2 x 150 A D.C. welding, 300 A mode, mechanized self-shielded wire and CO_2 welding[x)]

[x)] Feeding mechanism with a mechanical welding current modulator is used

Further information is available at the following addresses:
EPIS, Ltd.
E. O. Paton Electric Welding Institute, Kyiv, Ukraine
Tel.: (380 044) 261-51-02, Fax: (38044) 261-58-44

Research-Training Centre "Welding & Testing"

Research-Training Centre "Welding & Testing" at the N. E. Bauman Moscow State Technical University (MGTU) is one of the leading organizations of Russia in the field of welding fabrication and non-destructive testing.

R&T Centre "Welding & Testing" offers an entire cycle of works on welding and non-destructive testing, including development and manufacture of equipment, working out of regulatory documents, certification of equipment, training and attestation of specialists, assistance in starting up, maintenance and service, industrial inspection of objects, as well as development of welding and NDT software products. Our developments have found wide application both inside the country and abroad.

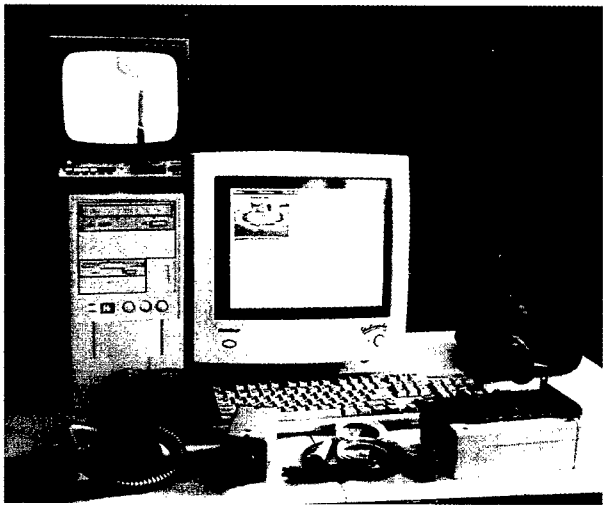

Computer system for of the fusion welding process control

This computer system was developed for use in combination with standard welding equipment (welding automatic devices, manipulators and robots). It allows improvement of welding quality, reduction in reject and improvement of welders' working conditions. The system provides visualization of the scene of welding, weld tracking, determination of welded joint geometry and control of weld formation using different fusion welding methods.

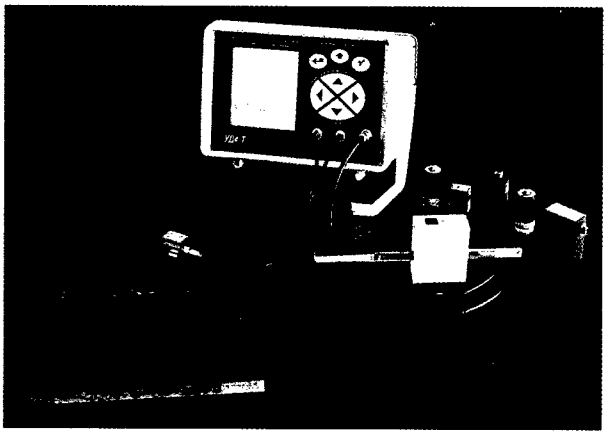

Ultrasonic tomography flaw detector UD4-T

Ultrasonic tomography flaw detector UD4-T is intended for NDT of materials, items and welded joints to check the presence of defects of the type of discontinuity or heterogeneity.

UD4-T is applied for:

- detection of defects
- measurement of coordinates of defects
- measurement of amplitudes of echo-signals
- measurement of equivalent surface areas of defects
- plotting of tomographic images of type B of defective regions in items tested
- evaluation of configuration and shape of defects detected
- accumulation and storing the test results to enter them into a computer data bank or print out in the form of a document